Molecular Portraits of Cancer Evolution and Ecology

Dhruva Biswas

University College London

and

The Francis Crick Institute

PhD Supervisor: Charles Swanton

A thesis submitted for the degree of

Doctor of Philosophy

University College London

August 2020

Declaration

I Dhruva Biswas confirm that the work presented in this thesis is my own. Where information has been derived from other sources, I confirm that this has been indicated in the thesis.

Abstract

Research on the molecular lesions that drive cancers holds the translational promise of unmasking distinct disease subtypes in otherwise pathologically identical patients. Yet clinical adoption is hindered by the reproducibility crisis for cancer biomarkers.

In this thesis, a novel metric uncovered transcriptional diversity within individual non-small cell lung cancers, driven by chromosomal instability. Existing prognostic biomarkers were confounded by tumour sampling bias, arising from this diversity, in ~50% of patients assessed.

An atlas of consistently expressed genes was derived to address this diagnostic challenge, yielding a clonal biomarker robust to sampling bias. This diagnostic based on cancer evolutionary principles maintained prognostic value in a meta-analysis of >900 patients, and over known risk factors in stage I disease, motivating further development as a clinical assay.

Next, *in situ* RNA profiles of immune, fibroblast and endothelial cell subsets were generated from cancerous and adjacent non-malignant lung tissue. The phenotypic adaptation of stromal cells in the tumour microenvironment undermined the performance of existing molecular signatures for cell-type enumeration. Transcriptome-wide analysis delineated ~10% of genes displaying cell-type-specific expression, paving the way for high-fidelity signatures for the accurate digital dissection of tumour ecology.

Lastly, the impact of branching, Darwinian evolution on the detection of epistatic interactions was evaluated in a pan-cancer analysis. The clonal status of driver genes was associated with the proportion of significant epistatic findings in 44-78% of the cancer-types assessed. Integrating the clonal architecture of tumours in future analyses could help decipher evolutionary dependencies.

This work provides pragmatic solutions for refining molecular portraits of cancer in the light of their evolutionary and ecological features, moving the needle for precision cancer diagnostics.

Impact Statement

Lung cancer is the leading cause of global cancer mortality. Surgical resection alone in non-small cell lung cancer is considered curative for the majority of patients with stage I disease. However, around a third of stage I cancers return after surgery. A genomic test to distinguish between high- and low-risk lung tumours could help identify patients that might receive benefit from adjuvant therapy. This has proved difficult, in part because cancer is an evolving disease, with a patchwork of different cells making up each individual tumour. With existing tests, sampling two sites of the same tumour could yield two completely different results depending on where the biopsy needle is placed. In this thesis, a novel genomic test was developed to solve this problem. Combining an understanding of cancer evolution with machine learning approaches, the test identified high-risk stage I patients that were missed using known risk factors, warranting further development as a clinical assay.

The licensing of immunotherapy drugs for lung cancer patients has given rise to another diagnostic challenge, as durable responses are only seen in ~20% of patients with advanced lung cancer. A molecular measure of immune infiltration within tumours could predict patient responses. Yet existing biomarkers fall short of clinical-grade accuracy. In this work, detailed molecular profiles of immune cells were generated from lung cancer patients. These profiles varied between cancerous and adjacent non-malignant lung tissue, which impacted the performance of some existing immune infiltration metrics. Moreover, discriminating molecular signals unique to each individual cell-type could be identified, paving the way for robust ecological biomarkers.

Computational approaches can illuminate core evolutionary dependencies between alterations in cancers. However, these methods may be biased to focus on ancestral events, occurring early in the life history of a tumour. This thesis confirmed that existing methods tended to overlook branching signals of on-going evolution. Addressing this bias could help define evolutionary bottlenecks that might be therapeutically targetable.

Overall, the results of this thesis demonstrate how an understanding of the evolutionary and ecological behaviours of lung tumours can be taken to the clinic.

Acknowledgements

I am enormously grateful to my primary supervisor, Prof Charlie Swanton, for funding, supporting, and mentoring my studies. Thank you Charlie for giving me the opportunity to train as a scientist within the fantastic environment of the Cancer Evolution & Genome Instability lab and the wider TRACERx consortium. I am also indebted to Prof Javier Herrero and the team at the Bill Lyons Informatics Centre for patiently dispensing bioinformatics knowledge over the past four years.

During my PhD I have had the good fortune to collaborate fruitfully with a number of scientists across London and around the globe. In particular, I am deeply appreciative of Dr Nicolai J Birkbak, Dr Nicholas L McGranahan, Dr Rachel Rosenthal, Dr Yin Wu, and Dr Mihaela Angelova for sharing their valuable time and expertise so generously. I am grateful to them and also Aśka Przewrocka and Lewis Au for help proofreading this thesis.

It has been my privilege to work between two world-class scientific laboratories, the UCL Cancer Institute and the Francis Crick Institute, an operation smoothly managed by Sharon Vanloo. Moreover, as a proud student of the UCL MBPhD programme, I am thankful for guidance from Prof Áine Burns, Carolyn Cohen, Prof Raymond MacAllister and Susan Beesley. I also owe a great deal to scientific mentors from my undergraduate medical studies, especially to the late, great Prof Roger Carpenter.

As in all things, I am grateful to my family for their patience, counselling, and fierce support. Instilling the value of education through example early in my life, and continuing to prescribe aphorisms as required:

उद्यमेन हि सिध्यन्ति कार्याणि न मनोरथैः ।

न हि सुप्तस्य सिंहस्य प्रविशन्ति मुखे मृगाः ।।

Table of Contents

Table of figures

List of tables

Abbreviations

APOBEC	apolipoprotein B mRNA editing enzyme catalytic polypeptide-like
AIC	akaike information criterion
ALL	acute lymphoblastic leukemia
AML	acute myeloid leukemia
BAF	b-allele frequency
BIC	bayesian information criterion
BLCA	bladder urothelial carcinoma
BRCA	breast invasive carcinoma
CCF	cancer cell fraction
CIN	chromosomal instability
CLL	chronic lymphocytic leukemia
CO	co-occurrence
COAD	colon adenocarcinoma
CPI	checkpoint inhibitor
DEG	differentially expressed gene
DLBLC	diffuse large b-cell lymphoma
DMSO	dimethyl sulfoxide
DNA	deoxyribonucleic acid
ECM	extracellular matrix
EDTA	ethylenediaminetetraacetic acid
EMDR	environment-mediated drug resistance
FACS	fluorescence-activated cell sorting
FBS	fetal bovine serum
GBM	glioblastoma
ICGC	international cancer genome consortium
IFN	interferon
IHC	immunohistochemistry
Indel	small insertion/deletion
ITH	intra-tumour heterogeneity
logR	log-ratio

LOH	loss-of-heterozygosity
LUAD	lung adenocarcinoma
LUSC	lung squamous cell carcinoma
ME	mutual exclusivity
MHC	major histocompatibility complex
MMR	mismatch repair
NGS	next-generation sequencing
NK	natural killer (cells)
NSCLC	non-small-cell lung cancer
ORACLE	outcome risk associated clonal lung expression
OS	overall survival
PBS	phosphate-buffered saline
PCA	principal component analysis
PCAWG	pan-cancer analysis of whole genomes
PFS	progression-free survival
READ	rectum adenocarcinoma
RNA	ribonucleic acid
RNA-ITH	transcriptomic intra-tumour heterogeneity
RPMI	roswell park memorial institute (culture medium)
RT-PCR	reverse transcription polymerase chain reaction
RTK	receptor tyrosine kinase
SCNA	somatic copy number aberration
scRNAseq	single-cell rna-seq
SKCM	skin cutaneous melanoma
SNP	single nucleotide polymorphism
SNV	single nucleotide variant
STAD	stomach adenocarcinoma
TCGA	the cancer genome atlas
TCR	t-cell receptor
TIL	tumour infiltrating lymphocyte
TMB	tumour mutational burden
TME	tumour micro-environment
TNF	tumour necrosis factor

TNM	tumour-node-metastasis
TPM	transcripts per million
UCEC	uterine corpus endometrial carcinoma
UMAP	uniform manifold approximation and projection
VAF	variant allele frequency
WES	whole exome sequencing
WGS	whole-genome sequencing
WHO	world health organization

Chapter 1. Introduction

1.1 Introduction

The transformation of normal healthy cells into malignant cancers involves the acquisition of somatic alterations, re-wiring the signalling pathways that govern cellular proliferation and homeostasis (Hahn and Weinberg, 2002). In the words of Peyton Rous, “tumours destroy man in a unique and appalling way, as flesh of his own flesh which has somehow been rendered proliferative, rampant, predatory and ungovernable” (Rous, 1967).

Over the past two decades, research on the molecular lesions that drive cancers has begun to translate into improved patient outcomes (Collins and Varmus, 2015). Yet there is a substantial disparity between the research and labour investment in molecular oncology over the last two decades and clinically validated molecular markers (Kumar-Sinha and Chinnaiyan, 2018). In the context of diagnostics, this mismatch has been referred to as the “cancer biomarker problem” (Sawyers, 2008).

In this chapter I give an overview of the current landscape for molecular biomarkers in oncology, and explore in detail the emerging evidence on the potential roles of two frontiers in the future development of molecular biomarkers: cancer evolution and ecology (Maley et al., 2017; Zahir et al., 2020).

1.2 Molecular portraits of cancer

Over the past two decades, oncological diagnosis in solid cancers has moved from a taxonomy based on tissue-type (lung cancer, breast cancer, etc) to a more precise approach integrating indicators of patient or tumour biology (biomarkers) (Sawyers, 2008). Prognostic biomarkers predict survival time from diagnosis to death, helping to stratify patients for surgical resection and (neo)adjuvant treatment. Alternatively, predictive biomarkers estimate the benefit for a specific therapy, helping choose between treatment options (Ballman, 2015).

In this section, I first outline the utility and limitations of tumour staging as a widely adopted prognostic biomarker. A brief history of molecular oncology is then provided, illustrating how technological advancements have led to an explosion in understanding of cancer as a genetic disease. Lastly, I give an overview of the promise and pitfalls of the emerging landscape of molecular biomarkers in the delivery of precision oncology.

1.2.1 Tumour stage is an imperfect predictor of survival risk

Tumour staging criteria capture the anatomic extent of disease at diagnosis. Classification is typically made according to the tumour-node-metastasis (“TNM”) scheme: T- primary tumour invasiveness and size, N – involvement of regional lymph nodes, M – presence of distant metastasis. TNM staging is prognostic, and is widely used as a biomarker to plan cancer treatment; to illustrate the scheme for non-small-cell lung cancer (NSCLC) is shown (Figure 1-1). Early-stage patients are considered low-risk, and surgical resection of the primary tumour is often curative. By contrast, late-stage patients are typically stratified for surgery and (neo)adjuvant chemotherapy, or palliative care in the presence of metastases in organs distant from the primary tumour (with the exception of a few cancer-types, such as advanced melanoma, where cures are now possible in stage IV disease).

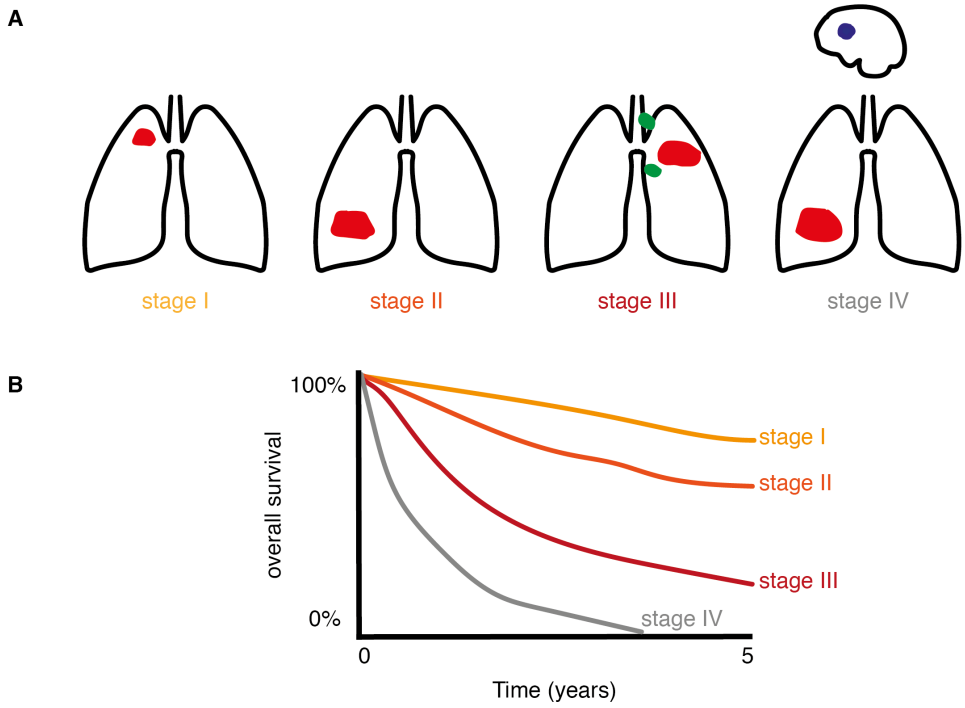

Figure 1-1 Tumour stage as an anatomical biomarker
The Tumour-Node-Metastasis (TNM) system for staging classifies cancer patients according to the anatomical extent of disease. A, The assessment of TNM stage is illustrated for four NSCLC patients, brief descriptions (with TNM breakdown) from left-right: stage I (T1N0M0) patient with small (<3cm) primary tumour; stage II (T2N0M0) patient with a larger (3-5cm) primary tumour; stage III (T2N2M0) patient with two ipsilateral lymph node metastases; stage IV (T2N0M1b) patient with a single extrathoracic metastasis to the brain. Colour scheme highlights primary tumour (red), lymph node metastasis (green), and distant metastasis (blue). B, Relationship between TNM stage and overall survival in NSCLC. Kaplan-Meier curve adapted from (Goldstraw et al., 2016).

While Denoix first proposed the TNM scheme in 1946 (Denoix, 1946), widespread adoption was not immediate. In lung cancer a practical TNM scheme was not available until 1974, when Mountain and colleagues assessed the “force of mortality” for TNM combinations using data from more than 2,000 lung cancer patients (Mountain et al., 1974). Moreover, TNM staging schemes are continually revised to provide greater specificity in classification. In Mountain’s original TNM scheme for lung cancer, the “T” descriptor classified patients as “T1” if the primary

tumour diameter was <3cm (Mountain et al., 1974). This was later updated and split into “T1a” (<2cm) and “T1b” (2-3cm) (Goldstraw et al., 2007), and recently further sub-divided into “T1a” (<1cm), “T1b” (1-2cm) and “T1c” (2-3cm) categories (Goldstraw et al., 2016). In melanoma, the anatomical metric itself was revised. Initially, the diameter of the melanoma was used to estimate prognosis (Lehman et al., 1966), but this measure was later found to be an unreliable predictor and replaced by “Breslow’s depth”, measured from the surface of the skin to the deepest component of the melanoma (Breslow, 1970).

In spite of these revisions, tumour stage is an imperfect predictor of survival risk, as patients with the same TNM class can have markedly different clinical outcomes. The heterogeneity of end results within stage groupings can confound patient stratification, resulting in under- or over-treatment. In lung cancer, surgical resection alone was considered curative for stage I patients (using TNM version 7 criteria), but approximately 30% of stage I patients died within 5 years of diagnosis (Goldstraw et al., 2007), indicating this patient sub-group may be under-treated. Indeed, a meta-analysis of 5 trials of adjuvant chemotherapy by the Lung Adjuvant Cisplatin Evaluation group suggested a lack of treatment benefit in stage IA lung cancer (Pignon et al., 2008). A sub-group analysis of an adjuvant chemotherapy trial found a marginal benefit from chemotherapy in stage IB lung tumours >4cm in diameter (Strauss et al., 2008). The TNM classification for lung cancer was revised accordingly for the 8th version (Goldstraw et al., 2016), yet under-treatment remains a substantial problem (Sangha et al., 2010; Vargas and Harris, 2016). Early-stage breast cancer patients face the opposite problem of over-treatment, as the marginal survival benefit afforded by chemotherapy is outweighed by substantial treatment morbidity (van’t Veer and Bernards, 2008). In a meta-analysis by the Early Breast Cancer Trialists’ Collaborative Group, the majority of patients with small (<2cm) node-negative estrogen receptor positive (ER+) breast tumours <2cm received adjuvant chemotherapy, despite a survival benefit of less than 4% over 10 years follow-up (Early Breast Cancer Trialists’ Collaborative Group, 2005).

Overall, there is a clinical need for novel biomarkers where current clinicopathological diagnoses fail to stratify patients with sufficient precision. Well-

developed and validated molecular assays could support personalized therapy decisions.

1.2.2 A brief history of molecular oncology

> *"The revolution in cancer research can be summed up in a single sentence: cancer is, in essence, a genetic disease."*
>
> Bert Vogelstein & Kenneth W Kinzler (Vogelstein and Kinzler, 2004)

Somatic mutations in cancer genes contribute to tumourigenesis (Vogelstein and Kinzler, 2004). Oncogenes are typically involved in processing extracellular growth-stimulatory signals, and are activated in tumours by gain-of-function mutations, yielding a constitutive proliferation signal. On the other hand, tumour suppressor genes constrain deleterious cell proliferation. Loss-of-function mutations in tumour suppressor genes liberate cancers from growth suppression; canonically, "two-hits" are required to inactivate a tumour suppressor gene (Knudson, 1971). Major categories of somatic mutations include point mutations, involving subtle intragenic changes affecting crucial amino acid residues that regulate the activity of the gene product, and somatic copy number aberrations (SCNAs), involving chromosomal gain or loss events.

As early as 1890, Boveri and von Hansemann described chromosomal abnormalities in their studies of dividing cancer cells, leading them to suggest that malignant behaviour may be driven by altered hereditary material (Boveri, 1914; von Hansemann, 1890). The first description of a genetic change leading to malignant transformation was provided almost a century later, with careful sleuthing identifying a HRASG12V point mutation as the oncogene activation event in human bladder cancer cells (Reddy et al., 1982; Tabin et al., 1982). This ushered in a new era of research aimed at uncovering the molecular determinants of cancer.

The discovery of cancer genes was a focus of early molecular studies (Futreal et al., 2004). Techniques used in the search for cancer genes included mutational screens that could either explore small sections of the genome at high-resolution, enabling the discovery of *BRAF* and *PIK3CA* as oncogenes in human cancer for

example (Davies et al., 2002; Samuels et al., 2004), or the entire genome at low-resolution, permitting the quantification of mutation rate (on average 90 out of >13000 protein-coding genes in a cohort of breast and colorectal tumours (Sjöblom et al., 2006; Wood et al., 2007)). By the mid-2000s, a draft census of the genes and pathways commonly altered in cancer had been assembled (Vogelstein and Kinzler, 2004).

The initial sequencing of the human genome in 2001 (Lander et al., 2001; Venter et al., 2001) was seen as another turning point for cancer research (Dulbecco, 1986). The advent of massively parallel “next-generation” sequencing (NGS) technologies for DNA and RNA sequencing provided high-throughput methods to survey entire cancer genomes and transcriptomes at single-base resolution (Bentley et al., 2008; Z. Wang et al., 2009). Indeed, by the end of the decade several proof-of-concept studies demonstrated the potential for NGS analyses in cancer research: identifying novel mutations and rearrangements at base-pair resolution (Campbell et al., 2008b; Ley et al., 2008); delineating mutational profiles of tobacco carcinogens and transcription-coupled DNA repair (Pleasance et al., 2010); establishing how the aberrant transcription of cancer driver pathways can be linked to the underlying somatic alterations (Jones et al., 2008).

Over the last decade, the coordinated sequencing of thousands of cancer genomes has led to an explosion in molecular knowledge about human cancers (Garraway and Lander, 2013). Much of this work has been undertaken by multi-centre consortium studies, including The Cancer Genome Atlas (TCGA) (Blum et al., 2018), the International Cancer Genome Consortium (ICGC) (The International Cancer Genome Consortium, 2010), and the Pan-Cancer Analysis of Whole Genomes (PCAWG) consortium (The ICGC/TCGA Pan-Cancer Analysis of Whole Genomes Consortium, 2020) (Figure 1-2). The availability of data from large-scale cancer genome projects was accompanied by the development of a slew of software tools, providing algorithms to detect somatic alterations in DNA and RNA sequences (Cieślik and Chinnaiyan, 2018; Ding et al., 2014). Making these datasets available to scientific community as rapidly as possible was a core principle of several consortia, accelerating the pace of cancer genomics research.

Importantly, these cancer NGS studies provided a wealth of data to develop molecular biomarkers.

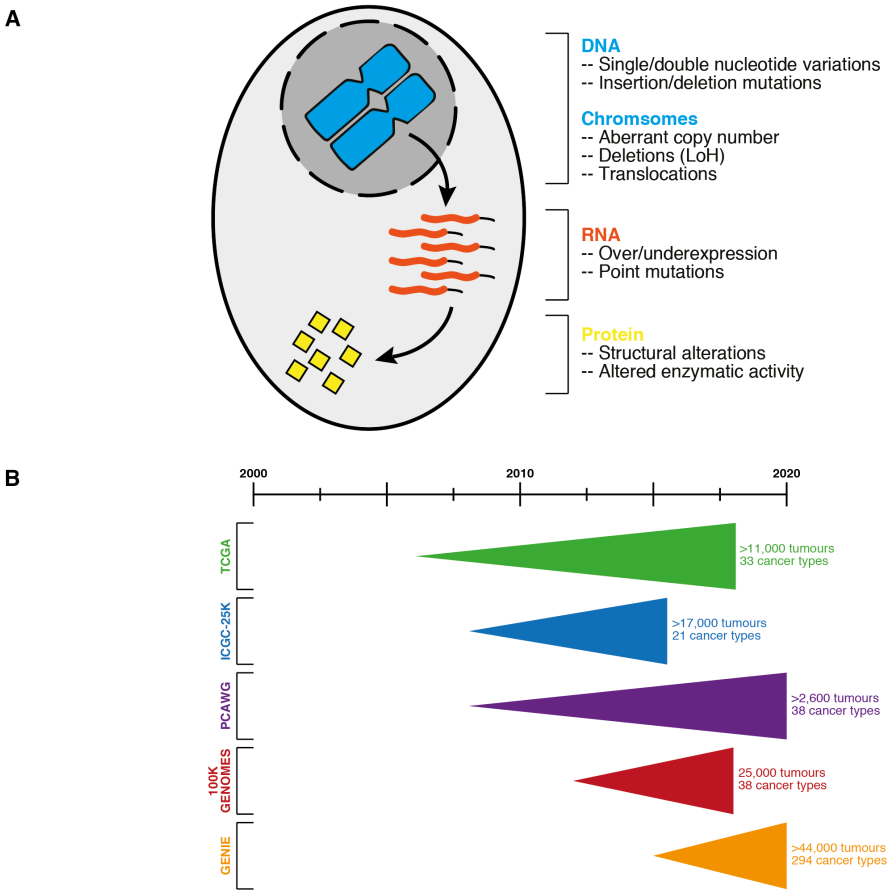

Figure 1-2 Charting the molecular landscape of cancer
A, Potential molecular markers of cancer highlighted on the central dogma of molecular biology. B, Timeline of large-scale cancer next-generation sequencing projects: The Cancer Genome Atlas (TCGA); the International Cancer Genome Consortium (ICGC) "25K initative" and Pan-Cancer Analysis of Whole Genomes (PCAWG) consortium; Genomics England 100,000 (100K) genomes project; Genomics Evidence Neoplasia Information Exchange (GENIE) project by the American Association for Cancer Research.

Major findings from cancer NGS studies include defining the frequency of somatic alterations. Contrary to the prior assumption that cancer genomes would harbor a uniform mutation rate, analysis of exome-sequencing data from TCGA revealed point mutation frequencies vary more than 1000x between cancer types, with the

average number of mutations per exome as low as one in pediatric cancers (rhabdoid tumour, median=0.1/Mb; medulloblastoma, median=0.3/Mb) to hundreds in melanoma and lung tumours (median=12.9/Mb) (Lawrence et al., 2014). A similar variation was found for SCNA burden between cancer types, with the average number of SCNA ranging from <10 in myeloproliferative disorders to >120 in dedifferentiated liopsarcoma (Beroukhim et al., 2010).

Defining a comprehensive catalogue of cancer genes is another key question for cancer genomics, particularly the distinction between “driver” mutations, that are causally implicated in oncogenesis and confer a growth advantage on the cancer cell, from “passenger” mutations, that do not contribute to cancer development and simply accumulate over the life history of a tumour (Stratton et al., 2009). Defining drivers as genes recurrently altered at a higher mutation frequency than background, Kandoth and colleagues detected 127 significantly mutated genes in a study of >3000 cancer exomes from TCGA (Kandoth et al., 2013). Subsequently, the PCAWG consortium has discovered driver events in the non-coding parts of the genome (Rheinbay et al., 2020). Amongst other applications, studying patterns of driver mutations can provide molecular evidence to underpin clinical understanding of disease. For example, TCGA studies have supported the distinction of oesophageal cancer as two disease subtypes (The Cancer Genome Atlas Research Network, 2017), shown colon and rectal tumours constitute a single type of cancer (The Cancer Genome Atlas Network, 2012), and found molecular similarities between breast and ovarian tumours (Cancer Genome Atlas Network, 2012; The Cancer Genome Atlas Research Network, 2011).

The genome-wide characterization of mutational processes can lead to the discovery of novel causative forces in cancer. Analysing >7000 tumours from TCGA, Alexandrov and colleagues deciphered 20 mutational signatures, many of which could be linked to established endogenous (e.g. DNA damage repair) or exogenous (e.g. smoking, ultraviolet light exposure) mutagens, while several had an unknown aetiology (Alexandrov et al., 2020). A recent *in vitro* study reported that exposing a cell line to aristolochic acid gave rise to the same mutational signature seen in renal and hepatic cancers in parts of the world where the

aristolochia plant grows (Kucab et al., 2019). This provides a framework for "molecular epidemiology", wherein linking mutational signatures to causal agents can inform public health initiatives (Nangalia and Campbell, 2019).

Analyses of cancer transcriptomes have revealed the prevalence of somatic alterations at the RNA level, such as TCGA analyses of alternative splicing (Kahles et al., 2018) or driver fusion events (Gao et al., 2018). A PCAWG study deciphered the genetic underpinning of RNA alterations in tumours, demonstrating SCNA as the main driving force (Calabrese et al., 2020).

1.2.3 The cancer biomarker problem

> *"The major cancer discovery in my lifetime is that cancer isn't one thing, but rather it's many things. … What we thought were maybe 10 or 15 unique diseases were really hundreds of diseases, and they each had their own epidemiology and risk factors, and would respond differently to therapies."*
>
> Ned Sharpless, Director of the US National Cancer Institute (Zaromytidou, 2020)

Molecular biomarkers are the foundation of improving diagnostic precision in cancer (Vargas and Harris, 2016). Proof-of-concept studies have shown molecular profiling can complement current histology-based classification, delineating cancers into prognostic risk groups (van 't Veer et al., 2002), or sensitivity to genome or immune targeted therapies (Paez et al., 2004; Taube et al., 2012). Yet, for successful translation to clinical practice, a biomarker must make a clinically informative distinction between patients, and perform reliably across independent patient cohorts. The slow progress towards developing prognostic or predictive indicators that fulfil these criteria has been referred to as the "cancer biomarker problem" (Sawyers, 2008).

1.2.3.1 Molecularly defined risk groups

Early genome-wide studies of cancer transcriptomes leveraged DNA microarray technology to uncover molecular heterogeneity in otherwise pathologically identical

patients. This transcriptional diversity could be used to recover established clinical classes, for example Golub and colleagues demonstrated that unsupervised clustering separated transcriptional profiles from acute leukemia patients into the known acute myeloid leukemia (AML) and acute lymphoblastic leukemia (ALL) subtypes of disease (Golub et al., 1999). A landmark analysis by Perou and colleagues revealed that breast cancer encompassed four transcriptional subtypes with distinct biological features (ER+; ER- basal-like; ER- Erb-B2+; ER- normal breast) (Perou et al., 2000), demonstrating the potential to discover novel molecular subtypes of disease. Similarly, Alizadeh and colleagues discovered two molecularly distinct forms of diffuse large B-cell lymphoma (DLBLC), corresponding to distinct stages of B-cell differentiation (Alizadeh et al., 2000). Importantly, the molecular classification of DLBLC patients associated with significantly different survival outcomes, independent of an established clinical risk factor (international prognostic indicator score), indicating the discovery of transcriptional subtypes with distinct clinical phenotypes could be applied to construct prognostic tests.

The clinical adoption of RNA-based prognostic tests (prognostic signatures) in breast cancer provides a model for the use of molecular diagnostics to improve patient outcomes. For example, the OncotypeDx test is a 21-gene RT-PCR assay developed to estimate recurrence-risk in ER+ breast cancer patients (Paik et al., 2004), that has been validated in prospective trials of >10,000 patients (Sparano et al., 2018). Other clinically approved prognostic signatures for breast cancer include the 70-gene MammaPrint test (van ’t Veer et al., 2002) and the 50-gene PAM50 assay (Parker et al., 2009). The uptake of these prognostic signatures by oncologists over the last decade has been associated with a steep and persistent decline in the use of systemic chemotherapy (Kurian et al., 2017), helping to reduce over-treatment in early-stage breast cancer (Katz et al., 2018).

However, there remains a general apprehension in the field about the utility of expression signatures as biomarkers. Meta-analyses of prognostic signatures have found their prognostic capacity can be explained by confounding due to a tumour’s subtype or clinicopathological profile (Tofigh et al., 2014), or have shown that carefully crafted signatures can be out-performed by randomly generated

signatures (Tang et al., 2017; Venet et al., 2011). These studies serve as examples of the prevailing sentiment of disappointment in current RNA-based biomarkers, and the need for stable and reproducible prognostic signatures to encourage clinical uptake.

1.2.3.2 Drugging molecular targets in the cancer genome

Genome-driven oncology holds the promise of leveraging the molecular characterization of cancers to establish targets that serve as predictive biomarkers for therapeutic intervention (Hyman et al., 2017). First-generation inhibitors of the *EGFR* gene (gefitinib and erlotinib) initially received clinical approval for use in NSCLC without restrictions. However, only a subset of NSCLC patients responded to these EGFR-inhibitors (EGFRi). A series of sequencing studies established that activating mutations (exon 19 deletion or L858R point mutation) in the EGFR gene predicted sensitivity to EGFR inhibition (Lynch et al., 2004; Paez et al., 2004; Pao et al., 2004). The approval of EGFR inhibitor usage was revised with *EGFR*-mutant as a predictive biomarker. Other early successes of drugs targeted to the cancer genome include trastuzumab for *HER2*-amplified breast tumours (Slamon et al., 2009), and imatinib for chronic myeloid leukemia patients with a BCR-ABL fusion (Druker et al., 2001).

A further accomplishment of the genome-driven oncology era is the rational design of strategies to overcome resistance to targeted drugs. On-target mutation is a common resistance mechanism in *EGFR*-mutant NSCLC patients receiving erlotinib or gefitinib therapy, with a substitution of threonine at the “gatekeeper” amino acid 790 to methionine (T790M) observed in >50% of patients after disease progression (Kobayashi, 2005). A third-generation EGFR inhibitor (osimertinib) was manufactured to selectively inhibit both sensitizing and resistance (T790M) mutations in *EGFR*. Compared to standard-of-care platinum therapy, osimertinib improved overall survival by 6 months in *EGFR*-mutant NSCLC patients that had progressed on erlotinib/gefitinib therapy (Mok et al., 2017). Osimertinib was also recently reported to out-perform erlotinib/gefitinib as first-line therapy for *EGFR*-mutant NSCLC patients (Ramalingam et al., 2020). An understanding of cancer

pathways provided a strategy to overcome signalling bypass resistance through combination therapy. For example, in *BRAF*-mutant colorectal cancers, inhibition of the MAPK pathway through doublet (BRAFi + MEKi) or triplet (BRAFi + MEKi + EGFRi) therapy lead to significantly more durable responses than mono-therapy (BRAFi only) (Kopetz et al., 2019).

Yet there is a general sentiment that, despite substantial research investments, molecular targeted agents have not yet realised the full promise of genome-driven oncology (Tannock and Hickman, 2016). This can be partly explained by the fact that most cancers lack mutations in readily “druggable” genes, such as kinase oncogene alterations, indicating that the early successes of single kinase inhibitor therapy may only benefit a small proportion of all cancer patients (Greenman et al., 2007). A retrospective cross-sectional study of US patients with cancer evaluated patient eligibility for 31 targeted drugs, estimating that in 2018 only 8.3% of metastatic cancer patients would have been eligible for genome-targeted therapy (Marquart et al., 2018). It is possible that innovative trial design may increase this proportion in the near future. The recently reported National Lung Matrix Trial screened >5000 patients with advanced NSCLC using NGS, finding that 36.7% of patients were molecularly eligible for entry into the umbrella trial testing 8 different targeted drugs (Middleton et al., 2020). However, a substantial increase in the number of cancer patients eligible for targeted drug therapies will likely require novel approaches to widen the druggable repertoire.

Synthetic lethality, in which the inhibition of one of a pair of genes is compatible with cell viability but the loss-of-function of both genes leads to cell death, may provide an alternative means to develop cancer-specific cytotoxic agents (Kaelin, 2005). For example, cancer cells harbouring mutations in *BRCA1*/*2* genes are defective in the homologous recombination pathway of DNA repair. Such *BRCA*-mutant cancer cells were found to be exquisitely sensitive to poly(adenosine diphosphate-ribose) polymerase inhibitors (PARPi) (Farmer et al., 2005). A number of clinical trials followed, demonstrating the clinical benefit of PARPi therapy in *BRCA*-mutant tumours of ovarian, breast, pancreatic, and prostate histologies (Audeh et al., 2010; Fong et al., 2009; Kaufman et al., 2015; Tutt et al., 2010).

Overall, the recent clinical approval of PARPi for *BRCA*-mutant cancers provides a proof-of-concept that synthetic lethal interactions can be translated into cancer therapies (Lord and Ashworth, 2017). This underscores the need to better understand epistatic interactions between cancer genes.

1.2.3.3 Sensitivity to immune checkpoint blockade

The normal function of immune checkpoint molecules involves regulating the amplitude of the immune response, to maintain peripheral self-tolerance and shield against tissue damage (Quezada and Peggs, 2013). For example, T-cells requires both antigen binding to the T-cell receptor (McIntyre and Allison, 1983) (signal 1) and CD28 co-stimulation (Harding et al., 1992) (signal 2) for licensing to specifically kill target cells. Some checkpoints operate centrally in lymphoid organs, such as the cytotoxic T lymphocyte antigen 4 (CTLA4) molecule that is involved in the co-stimulatory activation of naïve and memory T-cells. Others operate in peripheral tissues, including the programmed cell death 1 (PD1) molecule that limits T-cell activity, conferring an exhaustion phenotype in antigen-specific T-cells. Cancers leverage these checkpoints to co-opt immune inhibitory pathways. For example, temporary blockade of CTLA4 reduced tumour growth in murine models of cancer, suggesting a mechanism to “release the brakes” of the immune system to fight cancer (Leach et al., 1996).

Over the last decade, a molecular understanding of these immune evasion mechanisms has led to the development of checkpoint inhibitor (CPI) therapy. Phase III trials of a CTLA4-inhibitor (ipilimumab) reported it was the first ever drug to improve overall survival in patients with metastatic melanoma, with complete or partial responses recorded in 6-11% of patients (Hodi et al., 2010). Similarly, early phase I trials of drugs blocking the PD1/PDL1-axis showed responses in ~20% of patients with advanced NSCLC, melanoma, or renal cancer (Brahmer et al., 2012; Topalian et al., 2012). While a minority of patients exhibited remarkably durable responses to CPI, the large number of non-responders indicated a need for predictive biomarkers of CPI sensitivity (Nishino et al., 2017).

The inflamed tumour hypothesis suggests that checkpoint expression reflects the presence of anti-tumour immunity (exhausted tumour-specific T-cells), so should positively correlate with CPI response (Taube et al., 2012). In a multi-cancer phase I study of PDL1 inhibitor, immunohistochemical (IHC) staining for PDL1 in baseline samples revealed significantly higher expression levels in responders (Herbst et al., 2014), supporting the inflamed tumour hypothesis. Subsequently, a consistent positive association between PDL1 expression and objective response rate has been confirmed by a number of trials (Sacher and Gandhi, 2016). In particular, on the basis of the KEYNOTE trials (Garon et al., 2015; Herbst et al., 2016), a clinical assay of PDL1 expression received clinical approval for use in stratifying NSCLC patients for pembrolizumab therapy (a monoclonal anti-PD1 antibody).

Tumour mutation burden (TMB) is another biologically-motivated predictor of CPI sensitivity. The underlying hypothesis is that TMB generates somatic neo-epitopes, inducing a natural anti-tumour immune response that might be augmented by checkpoint blockade (Schumacher and Hacohen, 2016). Analyses of whole-exome sequencing (WES) data revealed that high mutational load correlated with sustained clinical benefit in two melanoma cohorts treated with a CTLA4-inhibitor (Snyder et al., 2014), and a NSCLC cohort treated with a PD1-inhibitor (Rizvi et al., 2015), providing proof-of-concept. An affordable clinical assay for TMB has been developed, estimating the genome-wide measure from targeted sequencing of ~3% of the coding genome (Frampton et al., 2016).

Remarkably, a trial of PD1-inhibitor therapy in Mismatch Repair (MMR) deficient tumours across 12 cancer types reported radiographic responses in 53% of patients (Le et al., 2017). This led to the clinical approval of PD1-inhibitor therapy as a “tissue agnostic” drug in all MMR deficient cancers, regardless of histology, exemplifying the potential utility of molecular markers to select cancer treatment.

Yet both checkpoint expression and TMB are imperfect biomarkers of CPI sensitivity, with clinical responses observed in biomarker-negative patients (PDL1 expression <1%, TMB) (Garon et al., 2015; Samstein et al., 2019). Additional

mechanism-driven biomarkers are required to advance the field of precision immune-oncology (Havel et al., 2019; Topalian et al., 2016).

1.2.3.4 Summary

Molecular biomarkers have substantial translational promise, with some startling clinical applications. However, these pale in comparison to the research and labour investment in molecular oncology over the last two decades (Kumar-Sinha and Chinnaiyan, 2018). Several limitations of existing molecular biomarkers have been described in this section.

In the remainder of this chapter, I will explore two frontiers for refining molecular biomarkers: evolutionary and ecological features of cancer (Maley et al., 2017).

1.3 Darwinian evolution in cancer

1.3.1 Intra-tumour heterogeneity as a substrate for evolution

Darwin's famous "I think" phylogenetic tree depicted the origin of many species from a single common ancestor. In 1976, Peter Nowell first proposed that the same, branching pattern of evolution might be observed in the genetic material of cancer cells (Nowell, 1976). He suggested "acquired genetic lability permits stepwise selection of variant sublines and underlies tumour progression". Within a decade, Gloria Heppner defined intra-tumour heterogeneity (ITH) as "tumour cell differences [that] are believed to be due to differences in cell lineage (ie due to presence of distinctly different subpopulations capable of breeding true)" (Heppner, 1984).

In the 1970s, several murine studies described extensive intra-tumoural phenotypic variation, and hinted at a genetic origin. Sectioning mouse sarcomas into four equal regions, Håkansson et al discovered the regions from some tumours differed significantly in sensitivity to cytostatic drugs (Håkansson and Tropé, 1974). Fidler et al observed large variation in metastatic potential between cell lines derived from a single murine melanoma, with the average number of pulmonary tumour metastases generated by intravenous injection ranging from 3.5 to more than 500 (Fidler and Kripke, 1977). In a similar experiment, Dexter et al found *in vitro* differences in morphology and growth patterns between cell lines isolated from a single murine mammary tumour (Dexter et al., 1978). Importantly, karyotypic analysis revealed very significant differences in the modal chromosome numbers of each cell line (range=39-130), and that the parental tumour contained the full spectrum of karyotypes observed, suggesting the inheritance of genotypic heterogeneity. Overall these murine studies helped provide evidence for intra-tumoural variation in genetic and phenotypic properties.

In a small cohort of chronic lymphocytic leukemia (CLL) patients (n=22), Campbell et al performed massively parallel pyro-sequencing of the *IGH* locus to delineate cancer phylogenies (Campbell et al., 2008a). This study demonstrated that NGS studies of single tumour biopsies represent a snapshot of cancer evolution,

permitting the timing of specific genomic aberrations (Figure 1-3). “Clonal” mutations are present in every cancer cell, so are thought to occur early in the life history of a tumour, forming the trunk of evolutionary tree. By contrast, “subclonal” mutations are present in a fraction of cancer cells, so form the branches of the tree.

The presence of Nowell’s “variant sublines” (Nowell, 1976), or malignant subclones, has since been demonstrated in multiple cancer-types. In a pan-cancer analysis of WES data from ~2,700 tumours across 9 TCGA cancer-types, McGranahan and colleagues discovered that cancer driver genes tended to be clonally mutated relative to other genes, for example *VHL* in kidney cancer, *CDKN2A* in lung cancer, and *TP53* across cancer-types (McGranahan et al., 2015). Recently, Dentro and colleagues found evidence of distinct subclonal expansions in 95% of samples from a pan-cancer whole-genome sequencing (WGS) dataset of >2,600 tumours from the PCAWG study (Dentro et al., 2020).

Yet single-region sampling is vulnerable to the “illusion of clonality”, wherein a somatic alteration appears to be present in every cell from one tumour biopsy, but may actually be absent in other regions of the same tumour (Figure 1-3). This can be overcome by multi-region sampling strategies. Bhandari and colleagues estimated that single-region sampling typically detected <50% of the cancer cell populations identified by multi-region sequencing in a prostate cancer dataset (Bhandari et al., 2018). In a cohort of patients with lung cancer, 76% of mutations classified as subclonal using multi-region WES could have appeared to be clonal if single-region sampling had been used (Jamal-Hanjani et al., 2017).

Both single- and multi-region sequencing approaches share the restrictions of single time-point analyses, such as limited resolution of early clonal events at tumour initiation (Greaves, 2015). To some extent, this can be addressed by innovative approaches to analysis. For example, the REVOLVER tool applied transfer learning to multi-region WES data from a cohort of lung cancer patients, inferring that clonal *CDKN2A* mutations tend to precede clonal alterations in *TP53* (Caravagna et al., 2018). NGS profiling of pre-invasive lesions provides a definitive

molecular archaeology, revealing that 51% of mutations in lung adenocarcinoma (LUAD) precursor lesions were subclonal (X. Hu et al., 2019).

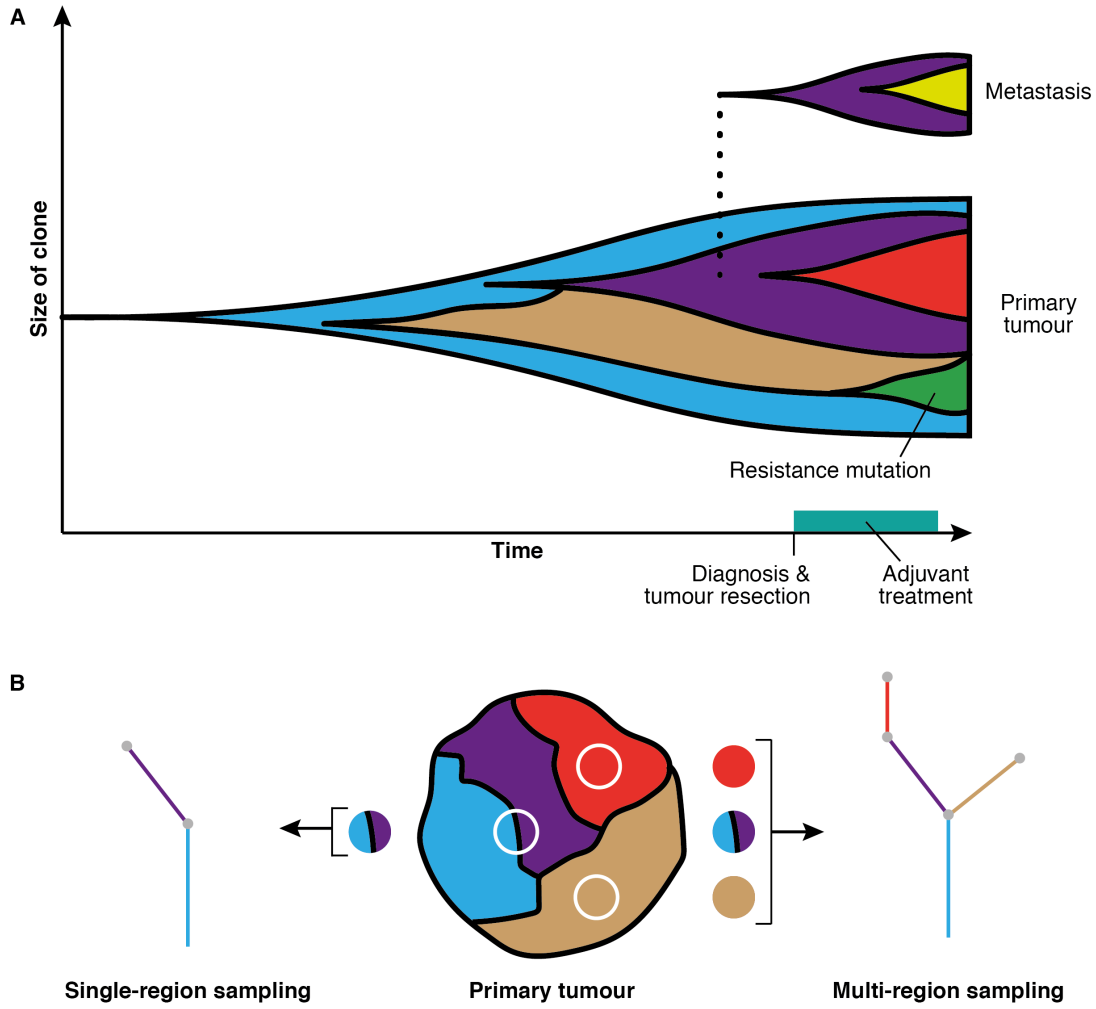

Figure 1-3 Sampling and reconstructing the life history of a tumour
A, Graphical representation of clonal evolution in the life history of a tumour. The founding clone (blue) gives rise to subclones (brown and purple). One subclone (purple) gives rise to disseminated disease ("metastasis"), prior to clinical detection and surgical resection of the primary tumour. The other subclone acquires a resistance mutation on-therapy, engendering a drug-resistant subclone (green). B, The impact of tissue sampling strategy on reconstruction of tumour phylogenies. The primary tumour from A is shown at the point of diagnosis and surgical resection (left); the tumour contains multiple spatially separated subclones, and three potential biopsy sites are indicated (white circles). Single-region sampling, and inferences about mutation clonality, allows

partial reconstruction of the tumour's phylogenetic tree (middle). However, single-region sampling under-samples the heterogeneity present in non-sampled parts of the tumour, and is also vulnerable to the "illusion of clonality". Multi-region sampling gives a broader view of heterogeneity across the entire tumour and, in this simplified example, permits reconstruction of the tumour's full phylogenetic tree.

1.3.2 Clonal diversity as a prognostic biomarker

Rare subclones, present at diagnosis, have been shown to harbour mechanisms of therapy resistance, and seed relapse in leukemias (Ding et al., 2012; Roche-Lestienne et al., 2003), colorectal cancer (Diaz Jr et al., 2012; Misale et al., 2012) and medulloblastoma (Morrissy et al., 2016). Evidence for a "lethal" subclone with metastatic potential has also been observed in multiple cancer-types (Kim et al., 2015; Yachida et al., 2010; Yates et al., 2015). Yet branching, Darwinian selection is not the only possible explanation for the co-existence of multiple subclones (Greaves, 2015). Williams and colleagues defined a "null model" of ITH, finding a power law for neutral evolution fitted 36% of ~900 cancers across 14 cancer-types (Williams et al., 2016). The authors suggested this might indicated a "big bang" architecture of neutral tumour evolution, with clonal selection complete in the first cancer cell, and the subsequent accumulation of passenger mutations engendering non-functional ITH.

Clonal diversity has also been linked with clinical outcomes. In CLL, Landau and colleagues linked the presence of subclonal driver events with poor survival outcome in a discovery cohort of 18 longitudinal samples, then validated this association in an validation cohort (n=149 samples), showing this evolutionary metric remained significant in multivariate analysis with established risk factors (Landau et al., 2013). Three separate pan-cancer analyses of 1,100-4,700 tumours from the TCGA study quantified ITH, using either PyClone (Andor et al., 2016; Morris et al., 2016) or mutant-allele tumour heterogeneity (MATH) scores (Noorbakhsh et al., 2018), and described significant survival associations in a subset of cancer-types. However, Reiter and colleagues conducted a meta-

analysis of several multi-region cancer datasets, concluding that subclonal driver mutations were non-functional and not prognostic (Reiter et al., 2019). Moreover, clinical development of ITH as a prognostic biomarker is complicated by the need for multi-region sequencing for accurate estimation (Abécassis et al., 2019), and the algorithmic challenges of subclonal reconstruction (Salcedo et al., 2020). In summary, multiple challenges must still be overcome for the direct usage of ITH as a prognostic biomarker

1.3.3 Mechanisms of cancer genome evolution

As part of his proposal that cancer is an evolutionary disease, Nowell speculated that “acquired genetic lability permit[ted] stepwise selection of variant sublines and underlies tumour progression” (Nowell, 1976). This “genetic lability” has been observed in across cancer-types, fuelling mutational diversification and ITH.

Genetic instability operating at the level of single nucleotide variations (SNVs) can drive subclonal diversification, shaping clinical outcomes. In gliomas, large increases in the number of somatic mutations was discovered after treatment with alkylating agents (temozolomide), and associated with the inactivation of a mismatch repair gene (*MSH6*) (Hunter et al., 2006). A similar branching pattern of evolution post- temozolomide treatment in glioblastomas was enriched in responders to PD1-inhibitor therapy (Zhao et al., 2019). The APOBEC (apolipoprotein B mRNA editing enzyme catalytic polypeptide-like) mutational signature was over-represented in subclonal mutations in treatment-naïve NSCLC tumours (de Bruin et al., 2014; Jamal-Hanjani et al., 2017), and was enriched in a treatment-resistant clone from a patient who died of metastatic disease. Thus the accelerated accumulation of SNV can underpin “micro-evolutionary” events in cancer genomes (McGranahan and Swanton, 2017).

Large-scale chromosomal alterations underlie “macro-evolution” in cancer (McGranahan and Swanton, 2017). Chromosomal instability (CIN), a dynamic state involving SCNAs in whole or parts of chromosomes, leads to inter-cellular variability in chromosomal number and structure (McGranahan et al., 2012). CIN is

caused by mechanisms including defective mitotic checkpoints, impaired non-homologous end joining, and telomere dysfunction (Maser and DePinho, 2002). Karyotypic diversity provides a substrate for Darwinian tumour evolution, allowing the emergence of rare cells with increased fitness (for example, amplifications in core proliferation genes (Endesfelder et al., 2014)), and convergence on favourable karyotypes (Laughney et al., 2015). In NGS studies, CIN has consistently associated with poor prognosis (McGranahan et al., 2012). Carter and colleagues developed an RNA-measure of CIN, identifying 70 genes with expression associated with aneuploidy (Carter et al., 2006). This "CIN70" signature included regulators of replication and chromosome segregation (*AURKA, AURKB, NEK2, H2AFX, CDC20, ZWINT, CCNB1, CCNB2*), and correlated with survival in several datasets. Recently, a WES-based measure of CIN was developed using a multi-region dataset of patients with NSCLC, quantifying the extent of spatially separated SCNA changes, and associated with worse disease-free survival (Jamal-Hanjani et al., 2017). In bacteria, high levels of genetic instability can lead to "mutational meltdown" (Lynch et al., 1993). Along the same lines, applying the CIN70 signature to >2000 tumours, Birkbak and colleagues observed that the quartile of tumours with highest CIN paradoxically had improved survival outcomes compared to the second-highest quartile (Birkbak et al., 2011).

Overall, micro- and macro-evolutionary mechanisms have been observed to foster ITH and increase proliferation advantage across several cancer-types. CIN also holds promise as a prognostic biomarker, if a robust metric can be derived and clinically validated (McGranahan and Swanton, 2017). Bakhoum and colleagues have also suggested CIN as a predictive marker for therapy response, stratifying low-CIN tumours with low adaptability for genome-targeted drugs, and applying cytotoxic therapies to high-CIN tumours that tend towards genomic catastrophe (Bakhoum and Landau, 2017).

1.3.4 Evolutionary constraints

> *"Throw up a handful of feathers, and all must fall to the ground according to definite laws. But how simple is this problem compared to the action and reaction of the innumerable plants and animals which have determined, in*

> *the course of centuries, the proportional numbers and kinds of trees now growing on the old Indian ruins."*
>
> Charles Darwin (Darwin, 1859)

In the belief that sequential selection "is not completely random", Nowell proposed that "certain similarities are acquired by different tumours as they progress" (Nowell, 1976). Yet mutations accumulate randomly, and can have variable fitness effects in different contexts (Sidow and Spies, 2015). Resolving evolutionary dependencies in cancer is an important frontier for precision oncology (Lipinski et al., 2016).

In cancer, parallel evolution is defined as recurrent alterations in the same driver gene in spatially separated regions of an individual tumour. Observations of parallel evolution suggest the existence of evolutionary constraints (McGranahan and Swanton, 2017). In a landmark multi-region study, Gerlinger and colleagues assessed genetic ITH in four renal tumours (Gerlinger et al., 2012). Multiple distinct and spatially separated mutations were observed in driver genes (*SETD2, PTEN,* and *KDM5C*) within a single tumour, suggesting convergent phenotypic evolution. Subsequently, in a larger cohort of patients with ccRCC (n=101), parallel evolution at the SNV-level was detected in 13% of tumours, typically involving *SETD2*, *BAP1*, and *PTEN* driver genes (Turajlic et al., 2018). Parallel evolution can also occur at the SCNA level. This phenomenon was observed in >60% of NSCLC tumours, including amplifications in *CDK4*, *FOXA1*, and *BCL11A* (Jamal-Hanjani et al., 2017). Parallel evolution has been reported in multiple other cancer-types, including glioma (Francis et al., 2014; Johnson et al., 2014), oesophageal adenocarcinoma (Murugaesu et al., 2015), and CLL (Yeh et al., 2017). Overall, this suggests a finite set of genetic routes for evolving tumours.

The evolutionary fitness of a new mutation may be influenced by the net effect of preceding mutations. In a study of patients with myeloproliferative neoplasms, Ortmann and colleagues established that the mutational order of *TET2* and *JAK2* mutations was associated with expansion of different cell-types, different expression profiles, and distinct clinical outcomes (Ortmann et al., 2015). A recent multi-region study of renal cancers discovered *PBRM1* mutations tended to

precede *SETD2* alterations (Mitchell et al., 2018). Such tendencies for driver mutations to be acquired in a particular order has also been identified in colorectal cancer (Cross et al., 2018; Sottoriva et al., 2015), and prostate cancer (Gerhauser et al., 2018).

The finding of parallel and ordered mutational events within cancer NGS datasets supports the existence of constraints to cancer evolution. In future, it is possible that this knowledge could be therapeutically exploited. Predicting the resistance genotype and the probability of disease progression (Lipinski et al., 2016), or targeting evolutionary constraints in a “checkmate” therapeutic strategy wherein an evolving tumour has no avenue of escape (McGranahan and Swanton, 2017).

1.4 Tumour sampling bias of molecular biomarkers

> *"… the most remarkable feature in the natural history of [the Galapagos] archipelago; it is that the different islands to a considerable extent are inhabited by a different set of beings … I never dreamed that islands, about fifty or sixty miles apart, and most of them in sight of each other, formed of precisely the same rocks, placed under a quite similar climate, rising to a nearly equal height, would have been differently tenanted; but we shall soon see that this is the case."*
>
> Charles Darwin (Darwin, 1845)

Studies of ITH reveal a similar pattern in cancer to Darwin's observations of species diversity in the Galapagos archipelago. This gives rise to the problem of tumour sampling bias. Single-site needle biopsy sampling is currently used as the standard protocol for diagnostic testing, regardless of the biomarker modality (genetic, transcriptomic, epigenetic or proteomic), typically sampling less than 1% of the primary tumour mass (Litchfield et al., 2020). Diagnostic biopsies can therefore be confounded by spatio-genomic heterogeneity within individual tumours, as molecular testing might yield completely different results depending on where the biopsy needle is placed (Boutros, 2015; Swanton, 2012; Yap et al., 2012). Moreover, the move to minimally invasive sampling techniques, which yield less biopsy tissue for diagnosis (McCall and Dry, 2019), indicates sampling bias will only become a larger problem in the future.

In this section I review the confounding effect of tumour sampling bias on the performance of molecular biomarkers. I will also highlight emerging solutions that could help clinicians better place – or go beyond – the biopsy needle.

1.4.1 Tumour sampling bias confounds molecular diagnostics

1.4.1.1 Prognostic biomarkers

Flow cytometry studies of intra-tumour variability provided early evidence that sampling bias could confound DNA-based prognostic biomarkers. Assessing DNA ploidy status as a potential prognostic factor, Petersen and colleagues obtained 6-10 spatially separated biopsies from each of a small series of colorectal tumours

(n=6 patients), discovering mixed populations of near-diploid and hyperploid cancer cells in 83% (5/6) of tumours (Petersen et al., 1979). This was the first report showing that such “mosaic” cellular composition may be a common phenomenon in cancers, leading the authors to suggest that a single biopsy may not be representative of the whole tumour. In a larger series of breast tumours (214 samples from n=44 patients), Beerman and colleagues estimated that only taking one sample would have wrongly classified a tumour as diploid in 30% of cases, writing that the underestimation of ITH may account for disagreement in the literature about the prognostic value of DNA ploidy (Beerman et al., 1991). A multi-cancer analysis (>1,400 samples from 140 tumours of breast, gastrointestinal and melanoma histologies) of several potential prognostic biomarkers measured by flow cytometry concluded that the intra-tumour variability observed was so high that all single-site testing should be abandoned, and that the use of molecular biomarkers would not be possible until the way the tumour is sampled or prepared for laboratory testing was changed (Barranco et al., 1994). The unexpected degree of intra-tumoural RNA variation, revealed by early multi-region transcriptomic profiling studies, suggested that ITH might also bias RNA-based prognostic biomarkers (Blackhall et al., 2004).

In recent years, multi-region studies have quantified tumour sampling bias for a number of state-of-the-art prognostic biomarkers. Boutros and colleagues examined the ITH of candidate DNA-based prognostic biomarkers in 5 prostate cancer patients, finding all yielded different predictions depending on which tumour region was analysed (Boutros et al., 2015); for example, *NKX3-1* was deleted in two of five regions from one tumour. In a small cohort of clear-cell renal carcinoma tumours (n=10 patients), Gerlinger and colleagues reported that 9p SCNA loss and BAP1 mutations were heterogeneous in all cases identified (Gerlinger et al., 2014). In the same cohort, Gulati and colleagues reported a similar result for an RNA-based prognostic measure, finding the “ccA” risk signature was heterogeneously expressed in 80% (8/10) of tumours (Gulati et al., 2014). Applying the OncotypeDx test to a large multi-region cohort of ER+ breast tumours (181 samples from 71 patients), Gyanchandani and colleagues found risk classification varied depending on biopsy site in 25% (18/71) of tumours (Gyanchandani et al., 2016). This

indicated that even clinically approved assays might be vulnerable to tumour sampling bias.

1.4.1.2 Predictive biomarkers for genome-targeted therapy

In describing cancer as a disease of clonal evolution, Nowell proposed “one could hope to eradicate the clone and effect a cure” by targeting a mutation arising occurring “at the time of the initial neoplastic change” (Nowell, 1976). Diagnostic samples can be used to identify mutations occurring early (clonal) or late (subclonal) in tumour evolution through analyses of mutation clonality. Clonal somatic alterations, which are present in every cancer cell, can then be prioritised for therapeutic targeting (Yap et al., 2012). However, this scheme could be undermined by genetic ITH, giving rise to sampling bias in predictive biomarkers for genome-targeted therapy.

Sampling bias could arise if the drug target itself is heterogeneously distributed through the primary tumour. An analysis of WES data from 9 TCGA cancer-types discovered that almost every gene linked with a targeted therapy approach was subclonally mutated in at least one tumour (McGranahan et al., 2015). Taking EGFRi in LUAD as a canonical example, 14% (3/21) of druggable mutations were subclonal in this analysis, in line with an earlier study describing ITH of *EGFR* exon-19 deletion in a multi-region set of clinical samples (Sakurada et al., 2008). Genetic ITH of the target may also be a concern for emerging “tissue-agnostic” drugs. For example, 5% (4/74) of patients recruited in the SUMMIT basket trial harboured subclonal *HER2* mutations, and none of these patients were responders to HER kinase inhibitor therapy (Hyman et al., 2018).

Pre-treatment samples could also contain a drug resistance mechanism as a minor subclone, evading detection in single-sample diagnostic testing, yet rapidly giving rise to primary resistance. Prior to first-generation EGFRi therapy (gefitinib/erlotinib), a subset of lung adenocarcinoma patients harboured on-target (*EGFR* T790M) or signalling bypass (MET amplifications) resistance mutations,

and this group of patients was significantly enriched in non-responders to therapy (Inukai et al., 2006; Turke et al., 2010).

1.4.1.3 Patient stratification for immunotherapy

ITH has also been reported in clinically-approved markers of CPI response. Topalian and colleagues quantified PDL1 expression (percentage positive tumour cells) by immunohistochemical analysis in pre-treatment samples (61 samples from 42 patients) as part of a multi-cancer phase I trial of PD1-inhibitor therapy. (Topalian et al., 2012). 75% (9/12) of patients with data available for multiple malignant samples exhibited variable PDL1 expression between biopsy sites. Heterogeneous expression of PDL1 might naturally be expected, as this checkpoint is reactively induced in cells neighbouring the site of a CD8+ T cell infiltrate, so would display lower expression in T-cell sparse tumour regions (Ribas and Hu-Lieskovan, 2016). McGranahan and colleagues have shown ITH of neoantigens is pervasive in NSCLC, and that response to CPI is better modelled by a combination of neoantigen burden and clonality than by either predictor alone (McGranahan et al., 2016). In a CTLA4-inhibitor trial in patients with melanoma, Riaz and colleagues corroborated the finding that an ITH-cutoff improved upon TMB-based prediction of response (Riaz et al., 2017). Lastly, RNA-based predictive biomarkers for CPI also exhibit substantial sampling bias. In a multi-region RNA-Seq dataset of NSCLC tumours, discordant rates were 33% and 44% for the IPRES and TIDE signatures respectively (Hugo et al., 2016; Jiang et al., 2018; Rosenthal et al., 2019).

1.4.2 Emerging tissue-based solutions

Overcoming ITH as a confounding factor for biomarker applications may improve the estimation of survival risk and CPI response. Sampling is effectively bypassed in melanoma, as the whole tumour is taken for clinical assessment (Breslow, 1970; Lehman et al., 1966). However, this is impractical for routine clinical use in most solid cancer-types. Here I discuss emerging approaches to address the sampling bias problem (Figure 1-4).

Pooling multiple biopsies for each tumour is a way to minimize artefacts from tumour heterogeneity. If multi-biopsy sampling is required, how many regions of an individual tumour should be sampled? Conducting bootstrap resampling in a multi-biopsy dataset of a DNA-based prognostic metric, Barranco and colleagues estimated that at least 3 sites should be biopsied per tumour to achieve a 90% probability for a stable prognostic read-out (Barranco et al., 1994). Similarly, Blackhall and colleagues ran a confidence interval analysis on a multi-region RNA dataset of NSCLC tumours, recommending that biopsies should be pooled from at least four biopsies per tumour (Blackhall et al., 2004). In a more recent empirical analysis, Turajlic and colleagues calculated ITH saturation gradients in a multi-region cohort of renal tumours, discovering that 2 biopsies would detect 50% of driver mutations, and 7 biopsies would recover 75% of drivers (Turajlic et al., 2018). Formal analyses, based on a mathematical model of tumour heterogeneity, might provide an alterative means to estimate the number of biopsies required for pooling (Opasic et al., 2019).

The entire tumour can be blended, then a single molecular test applied to a single aliquot of the homogenize mixture. Joung and colleagues provided proof-of-concept for this approach in a multi-cancer analysis of a small number of tumours (Joung et al., 2016). More recently, Litchfield and colleagues quantified the accuracy of the method on a larger scale (Litchfield et al., 2020). This elegant solution is caveated by the need for access to the bulk tumour, requiring modification of current pathology workflows, and the homegenization of tumour samples runs the risk of dilution of the individual test results (Fuhr et al., 1991).

An alternative method is to filter for genes that are stably expressed across all tumour regions, therefore allowing estimation of a whole tumour expression value from a single biopsy in routine clinical use. Obtaining RNA data for 33 biopsies from 11 patients with cervival cancer, Bachtiary and colleagues found that the 7.6% (1,536/20,000) of expressed genes with lowest transcriptomic ITH allowed estimation of a representative whole tumour expression value from a single biopsy (Bachtiary et al., 2006). The authors concluded that a useful prognostic marker should both correlate with patient outcome and be homogenously expressed, to

eliminate tumour sampling bias as a confounding variable. However, prior to this thesis, a practical implementation of this “clonal biomarker” solution was not available.

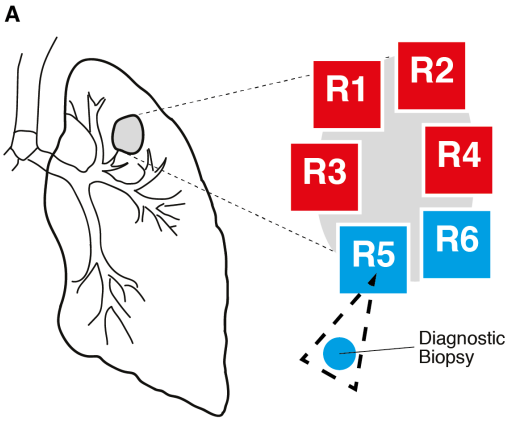

B

Strategy	Cost: Tissue requirement (# regions)	x	Cost: Biomarker technology (# tests)	=	Cost: Total
All	6		1		6
Some	4		1		4
Blend	6		1/6		1
Clonal	1		1		1

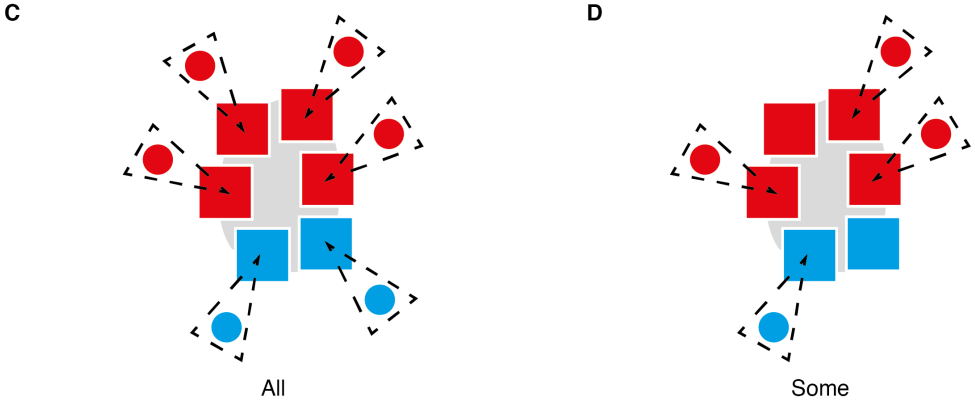

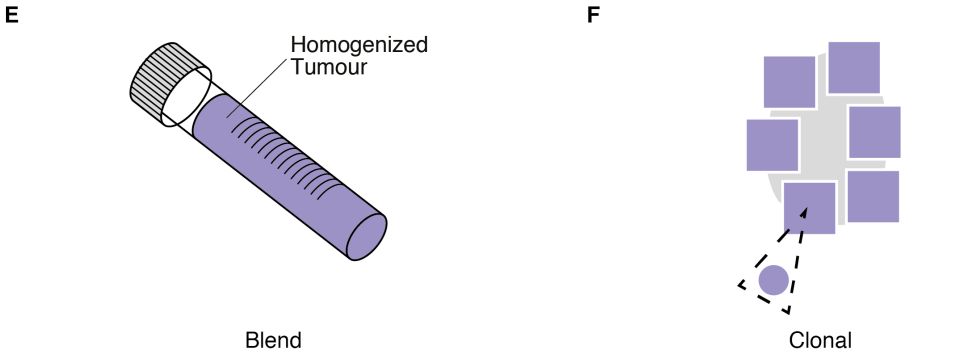

Figure 1-4 Emerging tissue-based solutions to the sampling bias problem

A, The sampling bias problem is illustrated for a lung tumour. Here, a prognostic biomarker classifiers tumour regions (R1-6) as high- (red) or low-risk (blue). It can be seen that the diagnostic biopsy (labelled triangle) samples from only one tumour region. Therefore the read-out of molecular risk for this patient will depend entirely on where the biopsy needle is placed. B, Four strategies to

mitigate sampling bias are tabulated, comparing their tissue and cost requirements. C, Sampling and testing "all" (n) tumour regions bypasses the sampling problem, however is the most expensive in terms of tissue and technology costs. D, A multi-biopsy strategy, sampling "some" regions (four regions have been suggested for lung cancer), brings down the cost while tending to capture intra-tumour variability. E, "Blend" the entire tumour, and apply one test to an aliquot from the homogenized mixture. This strategy has the same cost as testing a diagnostic biopsy, however requires pathology access to the full tumour. F, In theory, the "clonal" strategy is the most economical, providing a stable molecular read-out from a single diagnostic biopsy.

1.5 Cancer ecology

"Tumors: wounds that do not heal"

Harold Dvorak (Dvorak, 1986)

In the late 1950s, Burnet and Thomas proposed the cancer immunosurveillance hypothesis, suggesting that adaptive immunity inhibits cancer development (Burnet, 1957; Thomas, 1982). Confirming this hypothesis required the generation of immune-compromised *in vivo* models. In 2001, two studies demonstrated that interferon (IFN)-γ receptor-deficient or RAG2-deficient mice developed tumours more rapidly and with greater frequency than immunocompetent mice (Kaplan et al., 1998; Shankaran et al., 2001). Evidence that the tumour genome is antigenic was first provided by Boon and Schreiber in the 1980s, identifying neo-epitopes and suggesting that this could drive cancer immunity (Boon, 1983; Torre-Amione et al., 1990). Through the 1990s, the molecular identification of tumour neoantigens was performed by several groups (Monach et al., 1995; Topalian et al., 1992; van der Bruggen et al., 1991). The phases by which the tumour genome can elicit T-cell mediated clearance has been described as the "cancer immunity cycle" (Chen and Mellman, 2017). Within this scheme, tumours can be classified into one of three immune profiles: "immune desert", lacking T-cells in both parenchyma and stroma due to deficits in cancer antigen presentation or T-cell activation; "immune excluded", with stromal cells forming nests around cancer cells, preventing T-cell trafficking and infiltration; "immune inflamed", with T-cells in close proximity to tumour cells, capable of cancer cell recognition and killing. Immune evasion is now an established hallmark of cancer (Hanahan and Weinberg, 2011).

Stromal cells in the tumour microenvironment (TME) also have a role in sustaining and enabling the acquisition of cancer hallmarks (Hanahan and Coussens, 2012). In 1986, Dvorak summarised the generation of an activated TME, describing tumours as "wounds that do not heal" (Dvorak, 1986). The co-conspiratorial behaviour of stromal cells can shield cancer cells from cytotoxic and genome-targeted therapies.

In this section, I discuss the influence of the cellular components of the TME on clinical outcomes.

1.5.1 Immune contexture as a diagnostic scheme

To link the lymphoid and myeloid immune components of solid tumours with clinical outcomes, Fridman and colleagues provided the “immune contexture” framework (Fridman et al., 2017). This classifies tumours according to the density, composition, functional state and organization of immune infiltration. Here I give an overview of literature supporting the relevance of the immune contexture to cancer prognosis and sensitivity to immunotherapy.

1.5.1.1 Density

Extensive evidence links the density of tumour infiltrating lymphocytes (TILs) with patient survival (Figure 1-5). Classification of the presence of TILs in primary melanomas as “brisk”, “nonbrisk” or “absent” through histopathology review revealed the presence of TILs to be a significant prognostic factor independent of established risk factors (thickness and mitotic rate) (Clemente et al., 1996). Using IHC to stain and quantify subsets of TILs at higher granularity, Pagès et al reported high levels of effector memory (CD8+CD45R0+) T-cells was an independent predictor of overall survival in a large cohort of colorectal tumours (n=956) (Pagès et al., 2005). Further spatial classification of TILs revealed intra-epithelial, but not stromal, TIL density was associated with improved overall survival for CD8+ T-cells in oesophageal cancer (Schumacher et al., 2001) and for CD3+ T-cells in ovarian cancer (Zhang et al., 2003). Sato et al built on the latter result, noting that intra-epithelial CD8+ T-cells correlated with improved survival in ovarian cancer, but neither intra-epithelial nor stromal CD4+ TILs were prognostic (Sato et al., 2005). Examining cell-type ratios, they unearthed that intra-epithelial CD8+/CD4+ ratio had a significant association with improved prognosis, suggesting that the immune-suppressive effects of CD4+ TILs can limit the beneficial anti-tumour impact of CD8+ TILs, underlining the need for a nuanced understanding of the relationship between TIL density and prognosis. In addition, several authors have suggested

schemes to integrate TIL density with PDL1 expression to refine prediction of CPI sensitivity (Teng et al., 2015; Zhang and Chen, 2016).

1.5.1.2 Organisation

In a seminal paper, Galon and colleagues performed immunostaining of colorectal tumours (n=415), classifying the T-cells as located in the centre of tumours (CT) or at the invasive margin (IM) (Galon et al., 2006). Their analysis demonstrated that the density and location of immune cells in colorectal tumours associated with survival outcomes more strongly than TNM staging (Figure 1-5). Subsequent work developed the “immunoscore” as a diagnostic scheme incorporating the type, density, and location of immune cells (Galon et al., 2013). An international consortium is currently validating the IHC-based clinical assay (Galon et al., 2014). The binary CT/IM classification may be further refined in future. For example, a recent immunofluorescence analysis of kidney tumours, linked the organisation of stem-like CD8+ T-cells in intra-tumoural “antigen-presenting niches” to improved progression-free survival (Jansen et al., 2019).

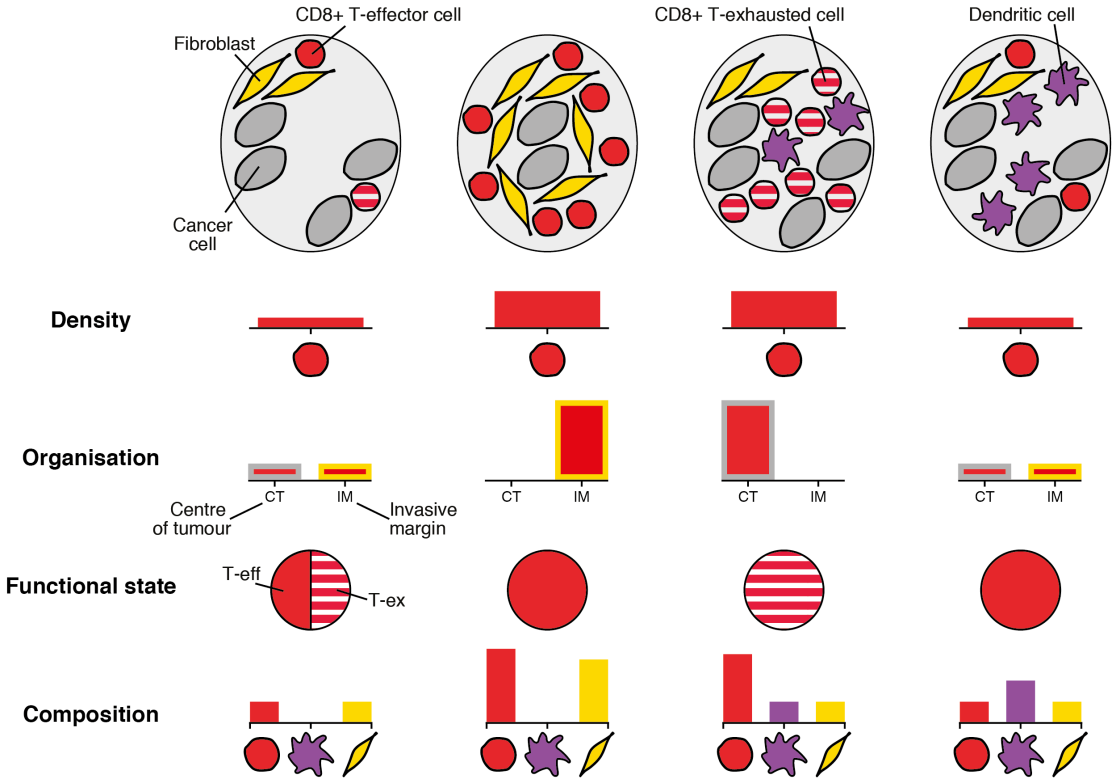

Figure 1-5 Immune contexture

The immune contexture provides a scheme to classify tumours according to the density, organisation, functional state, and composition of the TME. Here four tumours are shown to illustrate how this multi-dimensional scheme can provide a nuanced portrait of cancer ecology. Using density as a metric of CD8+ T-cell infiltration, the two central tumours appear identical. However, the integration of spatial information in the form of T-cell organisation reveals the left-middle tumour is immune excluded, with stromal nests shielding the cancer cells from T-cells, and might require the inhibition of fibroblast-secreted factors for effective immune clearance. By contrast, the right-middle tumour is immune inflamed, with T-cells in close proximity with cancer cells. Further classifying CD8+ T-cells as T-effector (PD1-low) or T-exhausted (PD1-high) shows that the middle-right tumour is infiltrated by checkpoint-expressing T-cells that might respond well to checkpoint blockade immunotherapy. Lastly, profiling the composition of other cells present in the TME, identifies that the left two tumours do not contain dendritic cells, and might require treatment using immune adjuvants to enhance the function of antigen-presenting cells.

1.5.1.3 Functional state

The characterization of T-cell "quality" reveals that only a subset of TILs is typically responsible for tumour recognition potential. RNA-Seq analysis of TILs sourced from NSCLC tumours (n=11) discovered that the subset of PD1-high TILs had higher T-cell receptor (TCR) clonality, and upregulated cell cycle and division pathways, suggesting antigenic stimulation (Thommen et al., 2018). The presence of the subset of PD1-high cells was strongly predictive for CPI response and survival in a small anti-PD1 treated cohort (n=21 stage IV NSCLC patients). Similarly, the presence of a subset of CD8+ T-cells, with a clonally expanded TCR repertoire and displaying an exhausted tissue-resident memory phenotype, was associated with overall survival in head and neck cancer (Duhen et al., 2018). A single-cell RNA-Seq (scRNAseq) study of >6,000 T-cells isolated from breast tumours verified significant heterogeneity in TIL population (Savas et al., 2018). Features of tissue-resident memory differentiation correlated better with improved survival than CD8 expression alone. Moreover, this signature was enriched in responders to PD1-inhibitor therapy in an external dataset of melanoma patients. Overall, these analyses highlight the importance of qualitative differences in CD8+ T-cell subsets for predicting clinical outcomes (Figure 1-5).

1.5.1.4 Composition

The cellular composition of the TME, beyond T-cells, influences the immune response and can shape clinical outcomes. For example, in NSCLC CD8+ T-cells, M1 macrophages and tertiary lymphoid structures, have been associated with good prognosis (Dieu-Nosjean et al., 2008; Goc et al., 2014; Ohri et al., 2009), whereas T-regs and M2 macrophages have been associated with poor survival outcomes (Hirayama et al., 2012; O'Callaghan et al., 2015). Moreover, a study of syngeneic hypermutated gliomas indicated resistance to CTLA4-inhibitor therapy was driven by macrophages (Aslan et al., 2020). In a PDL1-inhibitor trial of patients with metastatic urothelial cancer, non-responders were enriched for fibroblast-secreted TGF-β signalling, contributing to immune exclusion (Mariathasan et al., 2018). The

cellular composition of the TME can potentially be leveraged for the rational design of combination immunotherapies (Figure 1-5) (Smyth et al., 2016).

1.5.2 Environment-mediated drug resistance

The TME can play an active role in determining responses to genome-targeted therapies. Abnormal adhesion to the extracellular matrix (ECM) can re-wire signalling pathways within cancer cells, including response to drug therapy. In a cohort of patients with small-cell lung cancer (n=16), tumours with an extensive fibronectin matrix had significantly shorter overall survival, and adherence to the integrin ECM protein inhibited the apoptotic response of cancer cells to chemotherapy (Sethi et al., 1999). Similarly, ECM reorganisation and collagen VI over-expression was observed in cisplatin-resistant ovarian tumours (Sherman-Baust et al., 2003). An *in vitro* experiment of a breast cancer cell line co-cultured with fibroblasts demonstrated exceptional protection to dual targeted therapy (EGFRi + HERi), which was abrogated by the removal of the ECM component hyaluronic acid (Marusyk et al., 2016).

Factors secreted by stromal cells can underlie drug resistance. Screening 35 anti-cancer drugs against *in vitro* co-cultures, formed of 45 cancer cell lines with 23 stromal cell-types, revealed that 65% (15/23) of stromal cell-types were associated with environment-mediated drug resistance (EMDR) (Straussman et al., 2012). Focussing on resistance to BRAFi in a melanoma cancer cell line, Straussman and colleagues identified stromal HGF expression conferred resistance. In a similar screen of 41 kinase-addicted cancer cell lines, treated with targeted therapies, receptor tyrosine kinase (RTK) ligands (HGF, FGF, NRG1 and EGF) broadly rescued cell viability (Wilson et al., 2012). Drug-induced damage in stromal cells can trigger re-wiring of cancer cells. Treating primary prostate fibroblasts with genotoxic drugs, Sun and colleagues observed that WNT16B secretion was induced in response to DNA damage (Sun et al., 2012). Similarly in colorectal cancer, chemotherapy-treated fibroblasts secreted IL-17A, increasing the renewal and invasion of colorectal cancer stem cells (Lotti et al., 2013).

EMDR can also be driven by immune cell subsets. In a mouse model of gastrointestinal stromal tumours, a KIT inhibitor reduced tumour cell expression of Ido, inducing the activation of CD8+ T-cells and apoptosis of T-regs (Balachandran et al., 2011). In a cohort of patients with gastrointestinal stromal tumours (n=36), sensitive tumours had a greater ratio of intra-tumoural CD8+ T-cells to T-reg cells, and this correlated with IDO protein expression. In BRAF-mutant melanoma, treatment with BRAFi/MEKi induced macrophage proliferation and secretion of TNF (tumour necrosis factor)-α, fostering drug resistance (Smith et al., 2014).

Overall, multiple components of the TME can support the evolution of resistance mutations in drug-sensitive cancer cells, by providing a safe haven for the emergence of minimal residual disease during therapy (Meads et al., 2009).

1.5.3 Immunoediting

An evolving tumour has multiple roads to immune freedom. A previous section has mentioned microenvironmental mechanisms, including the induction of an exhausted T-cell phenotype, and the recruitment of stromal cells to exclude cytotoxic immune cells from the TME (1.5.1). Here, I discuss cell-intrinsic mechanisms of escape from immune-surveillance.

Robert Schreiber proposed the cancer immunoediting hypothesis to explain the dual role of the immune system, initially acting as an external tumour suppressor then actively sculpting the tumour to facilitate acquisition of the immune evasion hallmark (Schreiber et al., 2011). First the elimination phase, in which lymphocytes and IFN- γ collaborate to selectively destroy cancer cells, as an extrinsic mechanism of tumour suppression. Then the equilibrium phase, wherein cancer cells can survive under immune surveillance, but in a restricted capacity. And lastly the escape phase, involving the immune-mediated selection and outgrowth of tumour subclones with decreased immunogenicity, and an abrogation of the immune response.

Cancer NGS datasets have revealed signals of immunoediting in human tumours.

Rooney and colleagues developed a novel metric to quantify the depletion of neoantigens in a pan-cancer analysis of data from TCGA (Rooney et al., 2015). First they estimated the observed ratio (“O”) of neoantigens, by dividing the number of predicted MHC (major histocompatibility complex)-binding point mutations from the total number of non-synonymous point mutations. Then this was compared with an expected ratio (“E”), using a null model calculated from the rate of synonymous point mutations. Using this “O:E” metric, Rooney and colleagues detected neoantigen depletion in 35% (7/20) of the datasets assessed, with the most substantial depletion observed in colorectal cancer and clear-cell kidney cancer. In a separate analysis of TCGA data, Davoli and colleagues reported that high SCNA tumours had less neoantigen editing (increased O:E ratio), suggesting aneuploidy decreases immune selective pressure, possibly by decreasing the relative concentration of neoantigens and altering flux through the proteasome (Davoli et al., 2017). Applying the O:E metric to paired primary-metastasis samples from two patients with colorectal cancer, Angelova and colleagues observed that highly immune infiltrated metastatic samples tended to undergo neoantigen depletion (Angelova et al., 2018). Moreover, longitudinal sampling pre- and post-treatment has shown neoantigen loss under the selective pressure of immunotherapies, including adoptive T-cell treatment (Verdegaal et al., 2016) or CPI drugs (Anagnostou et al., 2017).

In future, classifying tumours according to the quality of individual neoantigens, or by immunoediting phase, might help reduce the risk of tumour escape by editing of vital immunogenic signals (McGranahan and Swanton, 2019; Schumacher and Schreiber, 2015).

1.6 Outline of the thesis

1.6.1 Summary of background information

Molecular biomarkers hold the translational promise of unmasking distinct disease subtypes beyond clinical descriptors such as tumour TNM staging. Recent examples include a TNM-“Biology” scheme for prognostication in lung cancer (Kratz et al., 2019), or a TNM-“Immune” classification incorporating the immunoscore into colorectal cancer diagnosis (Galon et al., 2014). Yet clinical adoption is hindered by the reproducibility crisis for cancer biomarkers (Sawyers, 2008).

Refining molecular biomarkers in the light of the evolutionary and ecological features of cancer (Maley et al., 2017) may help overcome these challenges (Figure 1-6). Specific knowledge gaps in the literature, which preclude this goal, include:

1) An understanding of the mechanisms underlying non-genetic ITH, specifically the link between genetic and transcriptional diversity within individual tumours;
2) A solution to the diagnostic challenge of tumour sampling bias that is compatible with existing pathology workflows;
3) A strategy to characterize the immune contexture of tumours with clinical-grade accuracy;
4) Approaches for the systematic discovery of evolutionary constraints, specifically whether mutational timing is considered in analyses of epistatic interactions between genes.

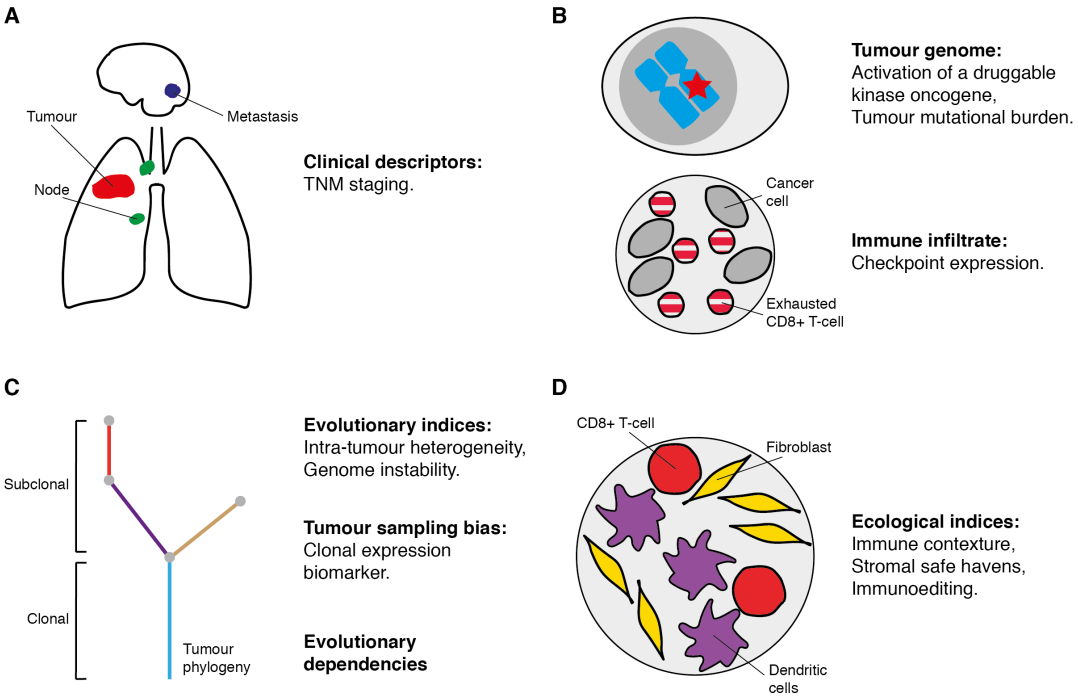

Figure 1-6 Cancer biomarkers: past, present and future

A, Traditional indicators of clinical outcomes include tumour staging, which was widely adopted in the 1940s, and still universal today despite being an imperfect predictor of survival risk (see 1.2.1). B, The advent of molecular oncology has moved the needle for cancer diagnostics, identifying novel markers of clinical outcomes encoded in the cancer genome or the tumour microenvironment. However, exciting research biomarkers typically fail to be clinically adopted (see 1.2.3). In this thesis, cancer evolutionary (C) and ecological (D) principles will be incorporated into existing approaches to molecular biomarker design.

1.6.2 Thesis aims

To pursue the hypothesis that integrating evolutionary and ecological features could improve the performance of molecular cancer diagnostics, four studies were conducted in this thesis:

1) The level of transcriptional diversity within individual NSCLC tumours was quantified, using a novel metric. This measure was related to mechanisms of cancer genome evolution, and sampling bias for existing prognostic biomarkers.
2) To address the sampling bias problem, a homogeneous expression biomarker was derived and validated.
3) Molecular profiles of stromal cell subsets were generated from patients with NSCLC. This dataset revealed phenotypic adaptation in the TME and paved the way for high-fidelity cell-type-specific signatures.
4) The impact of branching clonal architecture on the detection of epistatic interactions was assessed in a pan-cancer analysis

This work aims to provide pragmatic ways to refine molecular portraits of cancer, towards realising their full translational potential.

Chapter 2. Data & Methods

2.1 Introduction

Deciphering cancer genomes through an evolutionary or ecological lens may move the needle for molecular diagnostics, as discussed in the previous chapter. In this chapter I describe the bioinformatics and experimental methods used in this thesis. First, an overview is provided of the pre-processed DNA and RNA datasets accessed. Second, the bioinformatics methods used for analysis are outlined. Lastly, the experimental methods used to isolate and RNA profile microenvironmental cell-types from lung tissue are described.

2.2 Data

2.2.1 TRACERx multi-region NSCLC cohort

Tumour samples and clinical data were collected from 100 patients with NSCLC enrolled in the TRACERx Lung study and subjected to complete surgical resection with curative intent (Jamal-Hanjani et al., 2017). The TRACERx study (accession code: NCT01888601) is sponsored by University College London (UCL/12/0279) and has been approved by an independent research ethics committee (13/LO/1546).

2.2.1.1 Whole exome sequencing

Processing of WES was performed by Gareth A Wilson, Nicholas McGranahan, Nicolai J Birkbak, and Thomas BK Watkins. Exome capture was performed on 1-2μg of DNA isolated from genomic libraries with median insert size of 190bp for each tumour and matched germline sample. A customized Agilent Human All Exome V5 kit was used according to the manufacturer's protocol. Samples were 100bp paired-end multiplex sequenced on the Illumina HiSeq 2500 and HiSeq 4000 at the Advanced Sequencing Facility at The Francis Crick Institute. The median sequencing depth was 431 (range 83-986) for tumour regions and 415 (range 107-765) for matched germline.

Raw paired-end sequencing reads were aligned to hg19, including all contigs, obtained from the GATK bundle (v2.8) using bwa mem (bwa-0.7.8). Files from the same patient region were cleaned, sorted, merged, and duplicate reads removed using Picard tools (v1.107). SAMtools mpileup (0.1.19) was used to find non-reference positions in tumour and germline samples. Bases with low phred score (<20) or reads with low mapping quality scores (<20) were removed. Somatic variants were identified using VarScan2 somatic (v2.3.6) and extracted using VarScan2 processSomatic (Koboldt et al., 2012). All SNV calls were filtered for false positives using VarScan2's fpfilter.pl script. All indel (small insertion/deletion) calls in reads classified by VarScan2 as "high confidence" were kept for downstream filtering. Additionally, MuTect (v1.1.4) was used to identify SNVs (Cibulskis et al., 2013). These variants were filtered according to the filter parameter "PASS". To avoid false positive variant calls, additional filter steps were taken. Variants called by both VarScan2 and MutTect were considered true positives if the variant allele frequency (VAF) was >2%. If the variant was only identified by VarScan2, a VAF of >5% was required. Furthermore, the sequencing depth in each region was required to be >=30 and >=5 sequence reads had to support the call. To ensure the variant was not a germline event, the number of reads containing the variant in the germline data had to be <5 and VAF <=1%. To utilize the multi-region sequencing aspect of the cohort, individual mutations called across each region from the same tumour were compared. The threshold for detection of a somatic variant in one tumour region was reduced to VAF >=1% if the same variant had been detected at the VAF>=5% in another tumour region from the same tumour. Indels were filtered using the same parameters as SNVs, except >=10 reads had to support the variant call and the region had to have a sequencing depth >=50. All variants were annotated using Annovar (Wang et al., 2010) and COSMIC (v75).

Varscan2 copynumber was run to generate copy number data from paired tumour-normal samples, which produced per-region log-ratio (logR) values, that were subsequently GC corrected (Koboldt et al., 2012). Homozygous and heterozygous single nucleotide polymorphisms (SNPs) were identified from the germline sample using Platypus (v0.8.1) (Rimmer et al., 2014). The B-allele frequency (BAF) of each

SNP was calculated as the proportion of the reads at that position that contained the variant base. The logR and BAF values were used with ASCAT (v2.3) (Loo et al., 2010) in order to generate segmented allele-specific copy number data, purity, and ploidy estimates. Gene-level amplifications were called if the log2(mean gene copy number/ploidy) was >1. Gene-level deletions were called if the log2(mean gene copy number/ploidy) was <-1. To determine genome-wide copy-number gain and loss, copy-number data for each sample were divided by the sample mean ploidy, then log2 transformed. Gain and loss were defined as log2[2.5/2] and log2[1.5/2], respectively. Gene-level clonal copy-number gain and loss were defined as all regions from an individual tumour showing either gain or loss, in the same direction. Gene-level subclonal copy-number gain and loss were defined as at least one region (but not all regions) from an individual tumour showing copy-number gain or loss. Only subclonally gained or lost copy-number segments were used to analyze the effect of copy-number alterations on gene expression. To ensure proper copy-number variation, only samples with an absolute copy-number difference of 0.5 on a log2 scale were included. Tumour purity was also quantified using ASCAT (Loo et al., 2010).

To estimate whether mutations were clonal or subclonal, a modified version of PyClone was used (Roth et al., 2014). For each mutation, an observed cancer cell fraction (CCF, obsCCF) and a phylogenetic CCF (phyloCCF), which took into consideration any subclonal copy number events potentially altering the CCF, was calculated. Mutations were clustered using PyClone Dirichlet process clustering

2.2.1.2 RNA sequencing

RNA-Seq processing was performed by Nicolai J Birkbak and Rachel Rosenthal. RNA was extracted from the TRACERx 100 cohort using a modification of the AllPrep kit (Qiagen), as previously described (Jamal-Hanjani et al., 2017), and RNA integrity was assessed by TapeStation (Agilent Technologies). Of the cohort of 100 TRACERx tumours, RNA samples of sufficient quality (RNA integrity score ≥ 5) were obtained for 174 regions from 68 tumours, and were sent to the Oxford Genomics Centre for whole-RNA (RiboZero- depleted) paired-end sequencing. Of

these, at least two regions were available from 48 tumours, yielding the TRACERx RNA M-Seq cohort.

Alignment was performed using the STAR package (Dobin et al., 2013) (version 2.5.2b), to map reads to the human genome (GRCh37/hg19). Transcript expression was quantified using the RSEM package (Li and Dewey, 2011) (version 1.3.0) to generate count and transcript per million (TPM) expression values. An expression filter was applied, keeping genes with an expression value of at least 1 TPM in at least 20% (30/156) of tumour samples in the TRACERx multi-region RNA-Seq dataset. In total, 16,286 genes were filtered out of the 25,343 unique genes outputted by RSEM. Lastly, a variance stabilizing transformation was applied to counts from filtered genes using the DESeq2 package (Love et al., 2014) (version 1.14.1), assuming a negative binomial distribution for count values, to output homoscedastic and library size-normalized count values.

2.2.2 TCGA

2.2.2.1 RNA-Seq data for NSCLC patients

Pre-processed RNA-Seq and clinical data were downloaded for 959 patients with NSCLC (469 lung adenocarcinoma, LUAD; plus 490 lung squamous cell carcinoma, LUSC) enrolled in the TCGA research network lung trials (The Cancer Genome Atlas Research Network, 2014, 2012) using the TCGA2STAT package (Wan et al., 2016) (version 1.2). An expression filter was applied, keeping genes with at least 0.5 counts per million in at least two tumour samples, before normalized count values were obtained for filtered genes using a variance-stabilizing transformation from the DESeq2 package (Love et al., 2014) (version 1.14.1).

2.2.2.2 Whole exome sequencing data for nine cancer-types

Processing of WES was performed by Saioa López. Whole exome-sequencing data was accessed from the TCGA data portal for 3,545 patients from nine major cancer-types. From the TCGA repository, raw.bam files were downloaded and processed through the TRACERx pipeline (Jamal-Hanjani et al., 2017). BWA-MEM

was used to align the reads to the reference genome (hg19). Platypus (Rimmer et al., 2014) was used for SNP calling on the germline, and Varscan2 (Koboldt et al., 2012) and MuTect (Cibulskis et al., 2013) for somatic mutation calling. Functional annotation of genomic variants was performed using ANNOVAR (Wang et al., 2010). Purity, ploidy and copy number profiles of tumour cells were obtained with ASCAT (Loo et al., 2010), using the matching germline data. Mutations in regions of loss-of-heterozygosity (LOH) were timed as early or late based on the mutation and major allele copy number. Following a conservative approach, early mutations were considered as those with a mutation copy number ≥1.75 and a major allele copy number ≥1.75. Mutations were classified as late if they had a mutation copy number of ≤1.25 and major allele copy number of ≥1.75. Clonal mutations that could not be timed were classified as unknown. Mutations were defined as mutations in LOH if the minor allele copy number was <0.25.

2.2.3 Uppsala II NSCLC cohort

Pre-processed Uppsala RNA-Seq and clinical data were downloaded for 170 patients with NSCLC (103 LUAD plus 67 LUSC) enrolled in the Uppsala NSCLC II cohort (Djureinovic et al., 2016) from the Gene Expression Omnibus (accession code: GSE81089). ENSEMBL gene IDs were converted to HUGO Gene Nomenclature Committee IDs using the biomaRt package (Durinck et al., 2009) (version 2.30.0), and maximum values were selected for multi-mapping probes. Genes identified as lowly expressed in the TRACERx RNA-Seq dataset were filtered, then a variance-stabilizing transform was applied using the DESeq2 package (Love et al., 2014) (version 1.14.1) to output normalized count values. Additional clinical information was provided in private communication with the authors; this included adjuvant treatment status, patient age, World Health Organization (WHO) performance status, smoking status, patient gender and Ki67 staining.

2.2.4 Microarray NSCLC cohorts

Microarray data (.RMA files) and clinical data were downloaded from the Gene Expression Omnibus for four patient cohorts: 442 patients with LUAD enrolled by Shedden et al. (Shedden et al., 2008) (GSE68465); 85 patients with LUAD enrolled

by Rousseaux et al. (Rousseaux et al., 2013) (GSE30219); 147 patients with LUAD enrolled by Okayama et al. (Okayama et al., 2012) (GSE31210); and 127 patients with LUAD enrolled by Der et al. (Der et al., 2014) (GSE50081). Affy IDs were mapped to HUGO Gene Nomenclature Committee IDs, and the 'best' probe was selected using the Jetset package (Li and Dewey, 2011) (version 3.4.0).

2.2.5 MET500

Stefan Boeing performed alignment and transcript counting for the MET500 RNA-Seq data. Gene expression data were downloaded via dbGaP (accession number: phs000673.v2.p1.) for metastatic samples from patients in the MET500 cohort (Robinson et al., 2017) with LUAD primary tumours and RNA-Seq data available (n = 8). Alignment was performed using the STAR package (Dobin et al., 2013) (version 2.5.2) to map reads to the human genome (Ensembl GRCh38-release-89). Transcript expression was quantified using the RSEM package (Li and Dewey, 2011) (version 1.3.0) to generate count expression values. Normalized count values were obtained using a variance-stabilizing transformation from the DESeq2 package (Love et al., 2014) (version 1.14.1).

2.2.6 Pan-cancer prognostic score datasets

2.2.6.1 PRECOG

Pan-cancer gene-wise prognostic values were downloaded from the PRECOG resource (http://precog.stanford.edu). Gentles et al. (Gentles et al., 2015) had applied univariate Cox regression to microarray data from ~18,000 tumours across 39 cancer types, quantifying gene-wise survival associations as *z* scores (a $|z|$ score > 1.96 is equivalent to a two-sided $P < 0.05$).

2.2.6.2 Human Pathology Atlas.

As part of the Human Protein Atlas effort (www. proteinatlas.org/pathology), Uhlen et al. (Uhlen et al., 2017) had calculated gene-wise survival associations as log-rank *P* values for RNA-Seq datasets from 17 different cancer types. The pan-cancer gene-wise prognostic values were downloaded as supplementary table 6 from the original publication.

2.2.7 Single-cell RNA-Seq datasets

2.2.7.1 Lambrechts et al

Lambrechts et al. (Lambrechts et al., 2018) performed single-cell RNA-Seq on 52,698 cells sourced from five patients with NSCLC, then defined seven clusters of stromal cell genes and provided a per-cluster expression measure for every gene. Gene-wise relative expression levels were downloaded as supplementary information from the original publication.

2.3 Bioinformatics analyses

2.3.1 Statistical analysis

All statistical tests were performed in R (version 3.3.1). No statistical methods were used to predetermine sample size. All statistical tests were two-sided, unless otherwise stated.

2.3.1.1 Correlation analysis

Tests involving correlations were performed using cor.test with either Spearman's method or Pearson's method, as specified. Tests involving comparisons of distributions were performed using wilcox.test or t.test, as stated.

2.3.1.2 Survival analysis

Hazard ratios and *P* values were calculated using the survival package (https://CRAN.R- project.org/package=survival; version 2.41.3), through univariate or multivariate Cox regression analyses, as stated. Kaplan–Meier plots were generated using the survminer package (https://CRAN.R-project.org/package=survminer; version 0.4.2). Meta-analysis was performed using the rmeta package (https://CRAN.R-project.org/package=rmeta; version 3.0).

2.3.2 Gene expression analysis

2.3.2.1 Clustering

Hierarchical clustering was performed using complete linkage and Euclidean distance, with the ward.D2 setting in the “hclust” function in the R package stats. Principal component analysis (PCA) was performed using the “prcomp” function from the stats R package. Uniform Manifold Approximation and Projection (UMAP) was performed using the umap R package (McInnes et al., 2018).

For pairwise correlation analysis, using the Spearman correlation coefficient, first a correlation matrix of Spearman’s rho was calculated between all samples. Then correlations were converted to a distance metric (1 – ρ). Lastly hierarchical clustering was performed (Lance–Williams dissimilarity update formula, average linkage). The resulting dendrogram tree of clustering similarities was constructed using the neighbor-joining approach in the ape package in R (Paradis et al., 2004), based on pairwise Spearman correlational distances between samples.

2.3.2.2 Differential expression analysis

Differential expression analysis was performed on raw counts from RSEM using the DESeq2 package (Love et al., 2014) (version 1.14.1). Genes were considered to be expressed differentially by any comparison when the DESeq2 analysis resulted in an adjusted P value (Benjamini–Hochberg method) less than 0.05 and an absolute fold change larger than 2.

2.3.2.3 Pathway analysis

Pathway enrichment analysis was performed using the ReactomePA package (Yu and He, 2016) (version 1.24.0). Significance was evaluated based on a Bonferroni-adjusted *P* value < 0.01.

2.3.2.4 Gene set variation analysis

Pathway analyses were performed on the 50 hallmark pathways described in the Broad molecular signature database (Subramanian et al., 2005). To assign

pathway activity estimates to cell-types, I applied the gene set variation analysis (GSVA) package (Hänzelmann et al., 2013) using standard settings.

2.3.2.5 TME cell-type enumeration

The gene-lists for four marker-gene-based TME scoring methods were accessed from the original publications as follows:

- From Rooney et al, Supplementary Table 1c signature genes (Rooney et al., 2015);
- From Davoli et al, Supplementary Table 4d (Davoli et al., 2017);
- From Danaher et al, Supplementary Table 4 selected markers (Danaher et al., 2017);
- From Bindea et al, Supplementary Table 3 qPCR geners (Bindea et al., 2013).

2.3.3 Mutual exclusivity analysis

2.3.3.1 TCGA mutation filtering

From TCGA WES data (see 2.2.2.2), nonsense and missense mutations were selected for use in downstream analysis. Specifically, all mutations with 'Variant_Classification' of 3Flank, 3UTR, 5Flank, 5UTR, Frame_Shift_Del, Frame_Shift_Ins, In_Frame_Del, In_Frame_Ins, Intron, Nonstop_Mutation, RNA, Silent, Splice_Site, and Translation_Start_Site were removed. Mutations were further subsetted to candidate driver genes. For this purpose, a pan-cancer driver list issued by Bailey and colleagues was used (Bailey et al., 2018). From Supplementary Table 1 of the original publication, genes annotated as "PANCAN" were selected, yielding a list of 200 oncogenes and tumour suppressor genes.

2.3.3.2 TiMEx and DISCOVER

Point mutation data were arranged in a binary patient-by-gene format for input to mutual exclusivity detection tools. Pairwise gene-gene mutual exclusivities were tested using DISCOVER (Canisius et al., 2016) and TiMEx (Constantinescu et al., 2016); significance was defined as a P-value < 0.05.

2.4 Experimental methods

2.4.1 *Ex vivo* purification of lung stromal cell-types

A cohort of patients with treatment-naïve lung cancer underwent surgical resection with curative intent in the TRACERx study and at the University of Edinburgh. Following surgical resection, tumour and paired non-malignant tissue materials excess to clinical diagnosis requirements were processed in the research lab to yield single-cell suspensions of stromal cells. TRACERx donors (n=23 NSCLC patients) were 17 LUAD cases, 5 LUSC cases and 1 other histology. University of Edinburgh donors (n=5 NSCLC patients) were 4 LUAD cases, and 1 LUSC case.

2.4.2 Stromal cell isolation

Stromal cells were isolated from lung tissue samples using a standard tissue processing assay, as follows. The sample was placed in a 60mm petri dish, and Collagenase (Gibco cat No. 17018029) and DNAse (Roche/Sigma cat No. 10104159001) were added in plain RPMI. The sample was cut into the smallest possible pieces (2-3 mm) using sterile scalpels. Tissue chunks and remaining media were transferred into a GentleMACS tube (Milteni cat No. 130-096-334), which was loaded onto a GentleMACS cell dissociator machine with heated cuffs. The GentleMACS machine incubated and mixed the sample: rapid mixing for 30 secs, then heating at 37 C for 1 hour with constant slow mixing. Next, the sample was transferred to another tube via a 70um cell strainer, and washed with 5mL complete cRPMI (only 2% FBS) to make a single cell suspension. The single-cell suspension was transferred to a 15ml centrifuge tube, under laid with 3ml Ficoll (Human Ficoll-Paque Plus (GE)/ VWR cat No. 17-1440-03) and centrifuged (at 750 g for 10 minutes, no brake). The buffy coat was collected and transferred to a new 15ml tube, then washed by topping up to 10-15mls with cRPMI. Isolated cells were centrifuged at 400g for 5 minutes, and resuspended in 3 mls cRPMI. The aliquot was transferred into a cryotube with freezing media (90% FBS and 10% DMSO; Sigma, HybriMax cat No D2650-100ML), then frozen at -80 C.

2.4.3 Cell sorting and RNA extraction

Cells were thawed and washed twice in PBS before staining with the Zombie NIR live-dead exclusion kit on ice as per manufacturer instructions (https://www.biolegend.com/en-us/products/zombie-nir-fixable-viability-kit-8657). FACS (fluorescence-activated cell sorting) panel master-mixes were then added directly and cells stained for 20 minutes on ice before 2 washes with ice-cold FACS buffer (PBS + 2% FBS + 2mM EDTA) and sorting directly into cell lysis buffer (0.8% v/v Triton-X/H2O) in the presence of 2U/ul RNase inhibitor.

Three multiparameter panels were used for FACS. The antibodies used in each panel are listed below.

Panel 1: PD1 [BV421], (Biolegend); CD45RA [BV510], (Biolegend); CD45 [BV605], (Biolegend); CD25 [BV650], (Biolegend); CD27 [BV785], (Biolegend); Vδ1 [FITC], (Thermo); CD3 [PerCP-Cy5.5], (Biolegend); Vδ2 [PE], (Biolegend); CD4 [PE-Dazzle-594], (Biolegend);TCRgd [PE-Cy7], (Biolegend);CD103 [APC], (Biolegend);CD8 [AF700], (Biolegend);Zombie NIR Live-Dead [APC-Cy7], (Biolegend).

Panel 2: CD11c [BV421], (Biolegend);CD16 [BV510], (Biolegend);CD45 [BV605], (Biolegend);CD11b [BV650], (Biolegend);CD15 [FITC], (Biolegend);CD3 [PerCP-Cy5.5], (Biolegend);HLA-DR [PE], (Biolegend);CD14 [PE-Cy7], (Biolegend);CD56 [APC], (Biolegend);CD19 [AF700], (Biolegend);Zombie NIR Live-Dead [APC-Cy7], (Biolegend).

Panel 3: CD31 [BV421], (Biolegend);CD33 [BV510], (Biolegend);CD45 [BV605], (Biolegend);CD90 [BV650], (Biolegend);CD15 [FITC], (Biolegend);EpCAM [PerCP-Cy5.5], (Biolegend);PDGFRb [PE], (Thermo);E-Cadherin [PE-Cy7], (Biolegend);FAP [APC], (R&D);CD3 [AF700], (Biolegend);Zombie NIR Live-Dead [APC-Cy7], (Biolegend).

Following FACS, RNA was extracted from the sorted cell-types using RNeasy Plus Micro Kit (Qiagen).

2.4.4 RNA-Sequencing

RNA samples were sent to the Oxford Genomics Centre for Smart-Seq2 library preparation (Picelli et al., 2014) and whole-RNA (RiboZero depleted) paired-end sequencing. Stefan Boeing performed alignment and transcript counting. Alignment was performed using the STAR package (Dobin et al., 2013) version 2.5.2b to map reads to the human genome (GRCh37/hg19). Transcript expression was quantified using the RSEM package (Li and Dewey, 2011) version 1.3.0 to generate TPM expression values.

Chapter 3. RNA intra-tumour heterogeneity: mechanisms and clinical impact

3.1 Introduction

The phenotype of a cancer cell is defined through its transcriptome, which is sculpted by genetic and epigenetic events. Multi-region RNA profiling studies have described widespread transcriptomic intra-tumour heterogeneity (RNA-ITH) across cancer types (Bachtiary et al., 2006; Barranco et al., 1994; Blackhall et al., 2004; Gyanchandani et al., 2016; Lee et al., 2018; Morrissy et al., 2017; Suda et al., 2018). How the cancer transcriptome is shaped by genetic ITH, and the broader implications of RNA-ITH for biomarker discovery, has received little attention to date.

Early microarray studies demonstrated a mechanistic link between aneuploidy and gene expression changes in human cancers (Pollack et al., 2002; Tonon et al., 2005), with karyotype abnormalities giving rise to corresponding alterations in gene dosage. This correspondence has been further substantiated by recent proteogenomic characterization (Sinha et al., 2019; Vasaikar et al., 2019), and a recent pan-cancer analysis of paired RNAseq and WGS data from 1,000 tumours confirmed SCNAs to be the predominant genetic event, driving 17% of RNA variation (Calabrese et al., 2020). While the mechanisms of cancer genome evolution are broadly characterized (see 1.3.3), its relation to transcriptional diversity within individual tumours is less well-studied. Exploring the genomic determinants of RNA-ITH may shed light on “functional heterogeneity” – what proportion of the cancer genome is ancestral, versus encoding transcriptionally active events. In 1984, Heppner speculated that this might be a complex relationship, with a “gulf between genotype and phenotype of a cell”, the latter being an “emergent property” of the direct and pleiotropic actions of many genes (Heppner, 1984). This could also aid prioritization of events “hard-wired” in tumour evolution for therapeutic targeting (Morrissy et al., 2017; Rosenthal et al., 2019).

The transcriptional read-out of a tumour can also serve as a clinically informative molecular portrait (see 1.2.3.1). In breast cancer, for example, prognostic gene expression signatures have received clinical approval for use discriminating ER+ node-negative patients at high versus low-risk of recurrence (Paik et al., 2004; Parker et al., 2009; van ’t Veer et al., 2002). Unfortunately, the success of breast cancer biomarkers is not the general pattern. For example in lung cancer, several published prognostic gene expression signatures have failed to validate when tested in independent patient cohorts, and have been criticized for limited clinical utility beyond current practice standards (Subramanian and Simon, 2010a; Vargas and Harris, 2016).

A spatially heterogeneous transcriptome can give rise to the diagnostic challenge of tumour sampling bias, wherein a molecular biomarker yields different predictions of clinical outcome for the same tumour depending on where the biopsy needle is placed (see 1.4.1). Given that genetic ITH is pervasive in NSCLC, with a third of mutations and up to half of chromosomal copy-number changes occurring subclonally (Jamal-Hanjani et al., 2017), RNA-ITH may be a substantial confounding factor for the discovery of robust molecular biomarkers in lung cancer.

In this chapter I leveraged the largest cohort of lung cancer patients with paired multi-region exome- and RNA-seq data explored to date to investigate the causes, consequences and clinical implications of RNA-ITH. I defined a measure for RNA-ITH, perform a detailed dissection of its genomic determinants, and assessed its clinical impact by quantifying the prevalence of tumour sampling bias in lung cancer.

The results presented in this chapter forms sections of a first-author paper published during this thesis (Biswas et al., 2019).

3.2 A measure of RNA intra-tumour heterogeneity

3.2.1 Multi-region RNA-Sequencing

Tracking Non-Small-Cell Lung Cancer Evolution through Therapy (TRACERx) is a prospective cohort study (ClinicalTrials.gov number, NCT01888601) targeting enrollment of 842 patients with primary NSCLC. Multi-region and longitudinal tumour sampling is performed on treatment-naïve NSCLC tumours, recruited from one of thirteen sites in the UK. A primary study aim is to define the relationship between intra-tumour heterogeneity and clinical outcomes in early-stage NSCLC (Jamal-Hanjani et al., 2014).

Previously, the results from analysis of WES data from the first 100 NSCLC patients enrolled in the TRACERx study had been published (Jamal-Hanjani et al., 2017). From this 100-patient cohort, paired RNA-Seq data was generated where sample quality allowed. After excluding tumour regions with insufficient RNA quality (RNA Integrity Number < 5), and including tumours with at least two regions to analyse, there were 156 tumour regions from 48 TRACERx patients (Figure 3-1). This multi-region RNA-sequencing cohort (median: 3 regions per tumour; range: 2-7) was comprised of a mixture of NSCLC histologies: 28 LUAD patients (stage I = 15, stage II = 6, stage III = 7); 14 LUSC patients (stage I = 7, stage II = 6, stage III = 1); 6 other histology patients (stage I = 2, stage II = 2, stage III = 2).

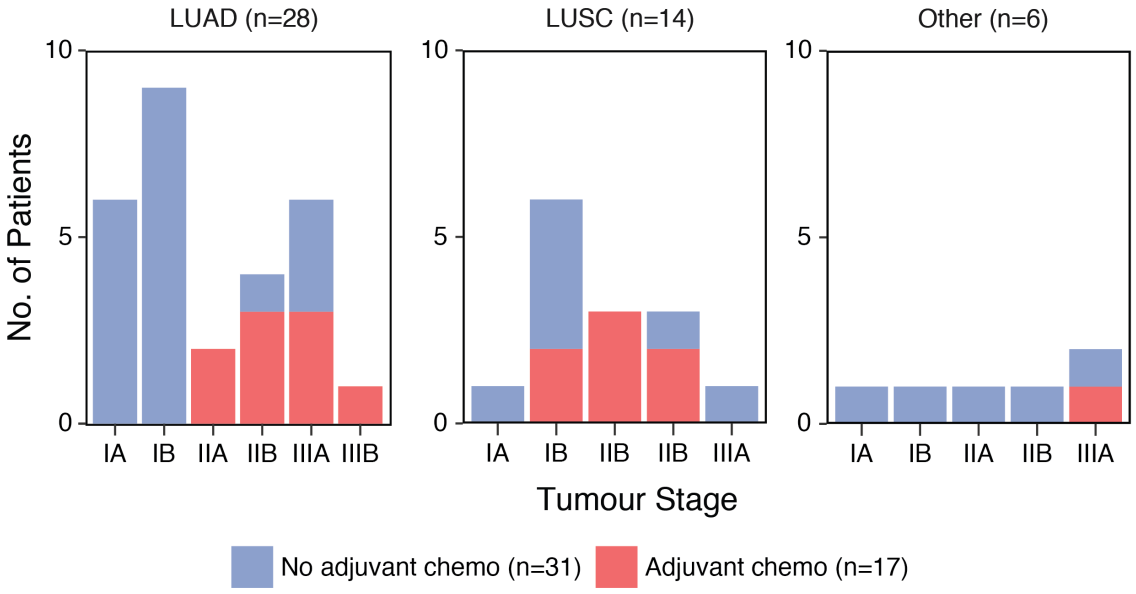

Figure 3-1 TRACERx lung RNA-Seq cohort

Bar plot showing the patient composition of the TRACERx RNA-Seq dataset (n=48 NSCLC patients). TNM tumour stage and adjuvant treatment status (colour) is indicated for LUAD (left panel), LUSC (middle) and other (right) histologies.

3.2.2 Defining RNA-ITH

In order to characterize the mechanisms driving RNA heterogeneity within individual tumours, I developed gene-level and patient-level metrics for RNA-ITH.

RNA-ITH was quantified using the multi-region RNA-Seq dataset from TRACERx (156 regions, 48 NSCLC patients). I defined RNA-ITH as follows (Figure 3-2). For a particular gene (e.g. *EDC4*) the standard deviation in expression values (count data, normalised using a variance stabilizing transform) between tumour regions is calculated for each individual tumour (e.g. patient CRUK003 has 7 regions with RNA-Seq data available). This yielded values of RNA-ITH that were specific to individual patients and genes (e.g. *ECD4* in CRUK003 has $\sigma_{g,p} = 0.075$). These values can then be summarised by taking the median value, either for each gene to calculate a gene-level RNA-ITH score (e.g. *ECD4* has $\sigma_g = 0.096$), or for each patient giving a patient-level RNA-ITH score (e.g. CRUK004 has $\sigma_p = 0.483$). Gene-level RNA-ITH scores can then be compared, for example *ECD4* ($\sigma_g = 0.096$) has a lower value than *PROM1* ($\sigma_g = 1.38$), indicating *ECD4* tends to have a more uniform expression profile between regions sampled from individual TRACERx tumours. This suggests *ECD4* may be less subject to sampling bias than *PROM1*, with potential implications for the design of robust molecular biomarkers. Similarly, patient-level RNA-ITH scores can also be compared, for example CRUK004 ($\sigma_p = 0.483$) has a higher value than CRUK001 ($\sigma_p = 0.135$). It may be of interest to rank tumours according to RNA-ITH status. The clinicopathological or genomic forces driving differing levels of RNA heterogeneity between patients may then be explored.

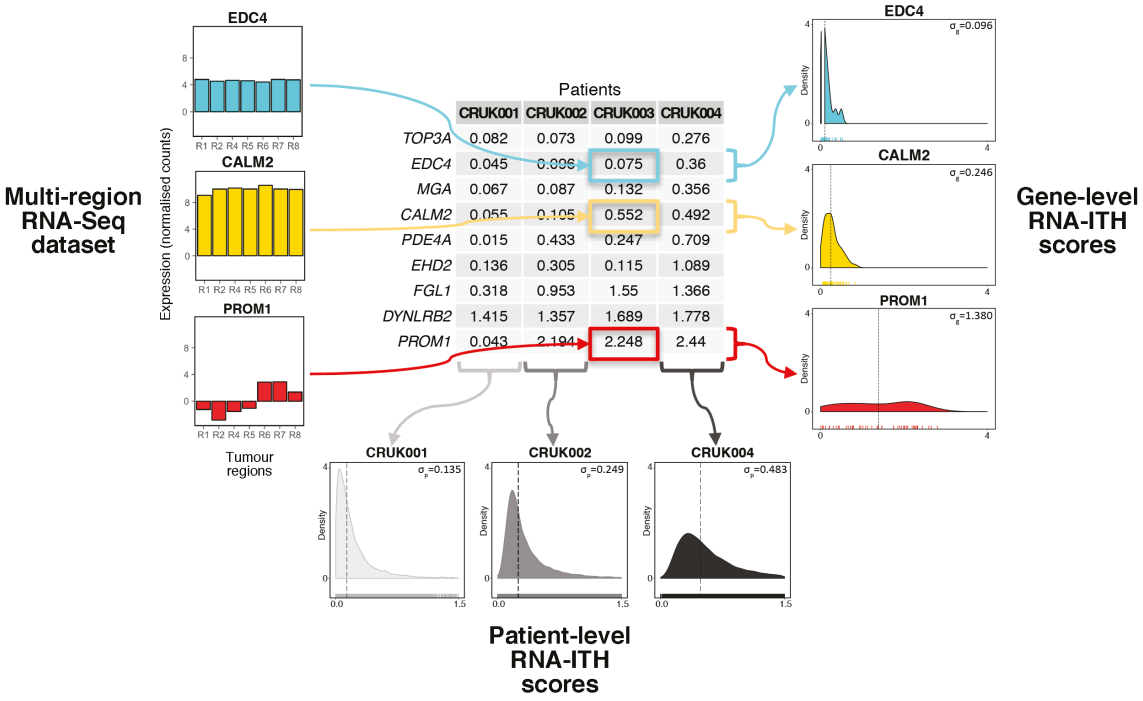

Figure 3-2 Strategy to calculate intra-tumour RNA heterogeneity scores at the patient- and gene-level

Gene- and patient-specific scores of RNA-ITH (middle, table) were calculated using multi-region RNA-Seq data from the TRACERx cohort (left, bar plots). These scores could then be summarised by gene (right, frequency distribution plots) or by patient (bottom, frequency distribution plots).

While standard deviation has been used previously to quantify RNA-ITH (Morrissy et al., 2017), other methods have also been applied (Bachtiary et al., 2006; Blackhall et al., 2004). I considered alternative measures to capture RNA variability within tumours (Figure 3-3) in the cohort of TRACERx LUAD patients (n=28 LUAD patients, 89 tumour regions, stage I-III). I found strong correlation between gene-level RNA-ITH values calculated using standard deviation and either median absolute deviation (R_s=0.965, P<0.001) or the coefficient of variation (R_s=0.956, P<0.001).

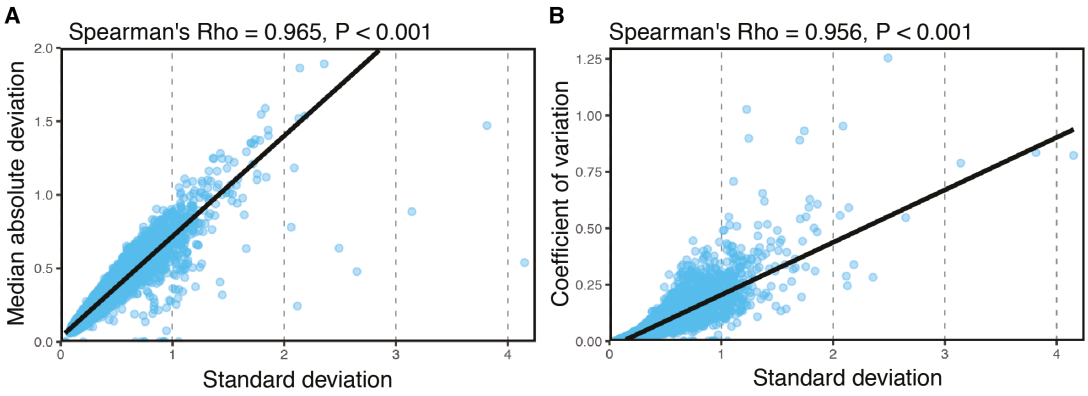

Figure 3-3 Alternative metrics for RNA-ITH
Gene-level RNA-ITH scores, calculated using the standard deviation per tumour then summarised across the cohort, were correlated with alternative RNA-ITH measures: mediation absolute deviation (A) or coefficient of variation (B). Spearman correlation was performed in LUAD patients from the TRACERx cohort (n=28).

I also considered an alternative approach for quantifying RNA-ITH based on unsupervised hierarchical clustering. Using multi-region RNA-Seq data from TRACERx tumours (89 regions, 28 LUAD patients, stage I-III), a clustering method developed by Gyanchandani and colleagues (Gyanchandani et al., 2016) was applied to calculate gene-level metrics for RNA-ITH (Figure 3-4A). For each expressed gene (14,009 genes) hierarchical clustering (Manhattan distance, Ward method) of all tumour regions across the TRACERx cohort was performed. The proportion of patients with tumour regions assigned to the same cluster was extracted and plotted for increasing numbers of clusters, from 2 (the minimum dendrogram cut-point) to 28 (the total number of patients in the cohort). The plotted curves for each gene varied markedly, taking *CKMT2* for example, there was a sharp decrease to zero in the proportion of patients with all regions clustering together. By contrast, for *HOXC11* the decline in clustering concordance was less steep, and plateaued at half the patients with all tumour regions in the same cluster. To capture this variability, gene-level clustering concordance was scored as the integral of the curve, yielding clustering concordance scores for all expressed genes (Figure 3-4B).

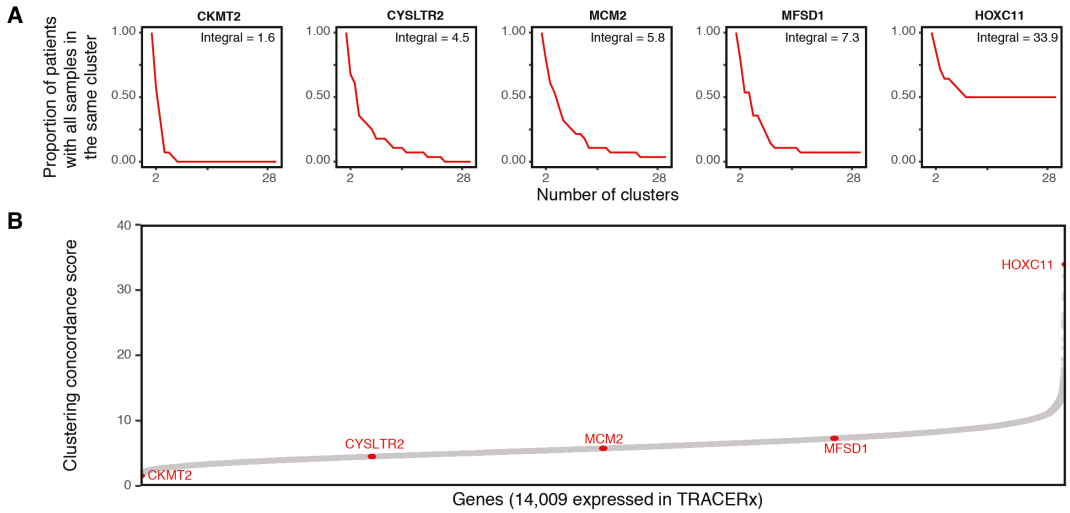

Figure 3-4 RNA clustering concordance scores

Clustering concordance scores calculated in TRACERx. A, For each gene a curve is calculated for the number of patients with all regions in the same cluster against the number of clusters (2-28 clusters). Curves for five genes (minimum=*CKMT2*, lower quartile=*CYSLTR2*, median=*MCM2*, upper quartile=*MFSD1*, maximum=*HOXC11*) are shown. B, The summarised clustering concordance scores for all genes, with the five genes from (a) highlighted in red.

Overall, the RNA-ITH metric calculated using standard deviation correlated well with scores generated using either median absolute deviation or coefficient of variation. Therefore standard-deviation-based scores were used as the primary metric for RNA-ITH in subsequent analyses. The clustering concordance score offered an alternative approach to quantifying RNA-ITH, and was used as a secondary metric on rare occasions as stated.

3.2.3 Dependence on multi-region sampling, clinicopathological and immune correlates

Previous studies of genetic ITH have described a positive association between number of regions sampled for an individual tumour and the level of measured ITH (Gerlinger et al., 2014; Turajlic et al., 2018). This can give rise to the “illusion of clonality”, wherein mutations may falsely appear ubiquitous due to under-sampling. Conversely, it is unclear whether measured ITH saturates at a certain number of sampled regions. The TRACERx cohort of NSCLC patients (156 regions, 48 patients, stage I-III) provided a rich multi-region dataset (median: 3 regions per patient, range: 2-7 regions) to explore how RNA-ITH estimates for an individual tumour tracks with the number of regions sequenced.

Simply plotting measures of RNA-ITH against the number of regions sequenced suggested that the patient-level estimates of RNA-ITH scaled with the number of regions sequenced (Figure 3-5).

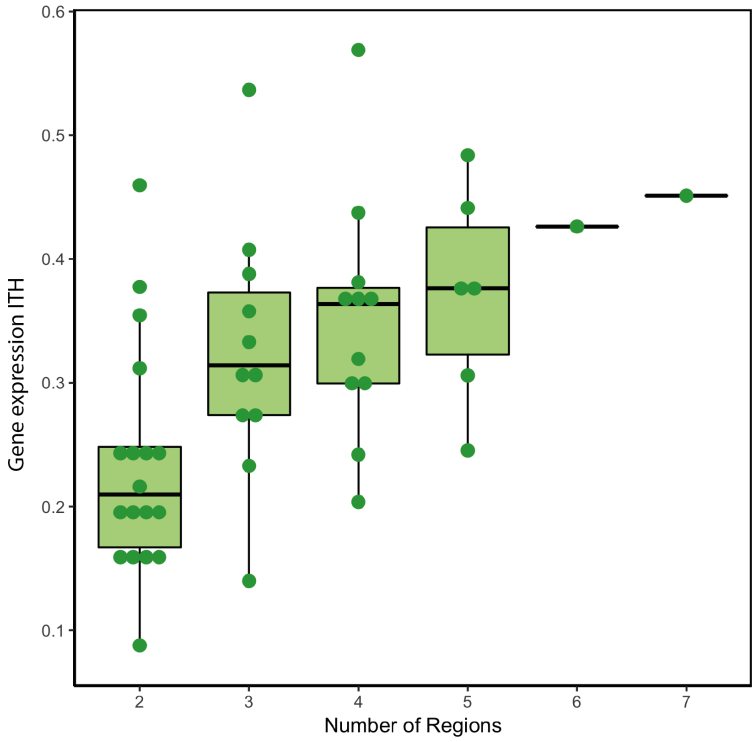

Figure 3-5 Dependence of patient-level RNA-ITH scores on multi-region sampling Correspondence between the number of tumour regions sequenced per tumour and RNA-ITH.

To see how the RNA-ITH estimate for a particular tumour would have impacted by sampling fewer regions, and evaluate whether this leveling-off point held true for individual tumours, I performed a down-sampling analysis (Figure 3-6). For a given tumour (e.g. CRUK0029), one to *N* biopsies was sampled (*N* is the total number of biopsies available for that tumour, e.g. *N* for CRUK0029 = 7 regions). RNA-ITH scores were then calculated for all possible combinations of tumour regions (e.g. for CRUK0029, an RNA-ITH score was calculated for every 2-region combination, every 3-region combination, and so forth, until a single score was calculated using all 7 regions available). This analysis indicated that estimates of RNA-ITH tend to increase with multi-region sampling, plateauing at around four regions sampled per tumour.

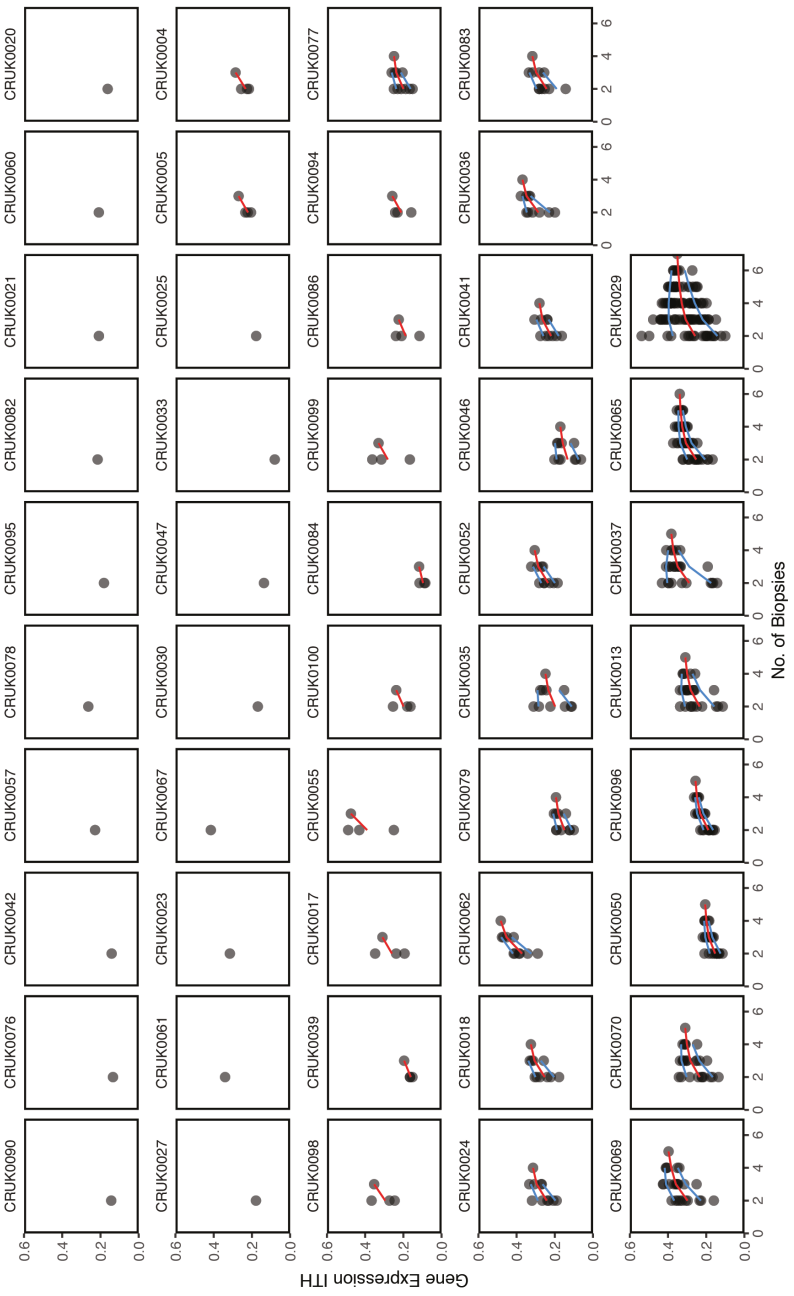

Figure 3-6 Down-sampling analysis of patient-level RNA-ITH scores

Scatter-plots showing for a individual tumours (each panel), the down-sampled RNA-ITH scores (y-axis) plotted against the number of regions sampled (x-axis). The lines depict the mean (red line) and standard deviation (blue lines) values. The analysis was conducted for each patient in the TRACERx cohort (n=48 NSCLC patients): one to *N* regions was sampled and this subset of regions was used to calculate RNA-ITH; this procedure was repeated for all possible subgroups.

Analyses linking RNA-ITH to genetic drivers in the TRACERx cohort (156 regions, 48 NSCLC patients, stage I-III) may be biased if interacting terms, such as tumour stage or purity, go unaccounted. To identify potential confounding factors, I assessed the dependence of patient-level RNA-ITH scores on clinicopathological and immune features. RNA-ITH did not significantly associate with tumour stage or histology (Figure 3-7).

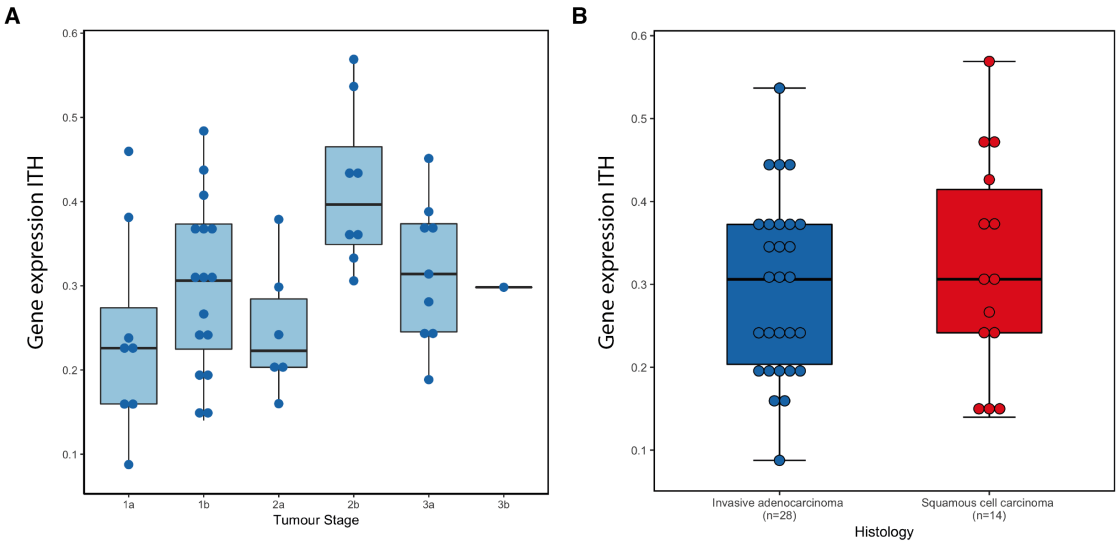

Figure 3-7 RNA-ITH by tumour stage and histology
Examining the dependence of RNA-ITH by tumour stage (A) or histology (V). All group-wise comparisons were did not attain significance (P<0.05). Statistical significance was tested with a two-sided Wilcoxon signed-rank test.

Tumour immune infiltration was scored using an RNA-Seq-based method, described by Danaher and colleagues (Danaher et al., 2017). RNA-ITH did not significantly associate with the level of immune infiltration measured for any of the 22 defined subsets (Figure 3-8A). Tumour purity was also quantified using WES data from TRACERx tumours, using the ASCAT method (Loo et al., 2010), and did not significantly associate with RNA-ITH (Figure 3-8B). Taken together, these data imply clinical features and tumour cellular composition were not substantive confounding factors in my estimation of patient-level RNA-ITH scores. An alternative approach, taking a random-effect model per sample, could have been used to incorporate sample-specific purity effects.

Overall, these results highlight the benefit of multi-region sequencing for uncovering spatial heterogeneity in gene expression, and indicate the estimates of RNA-ITH were not biased by clinical or immune parameters.

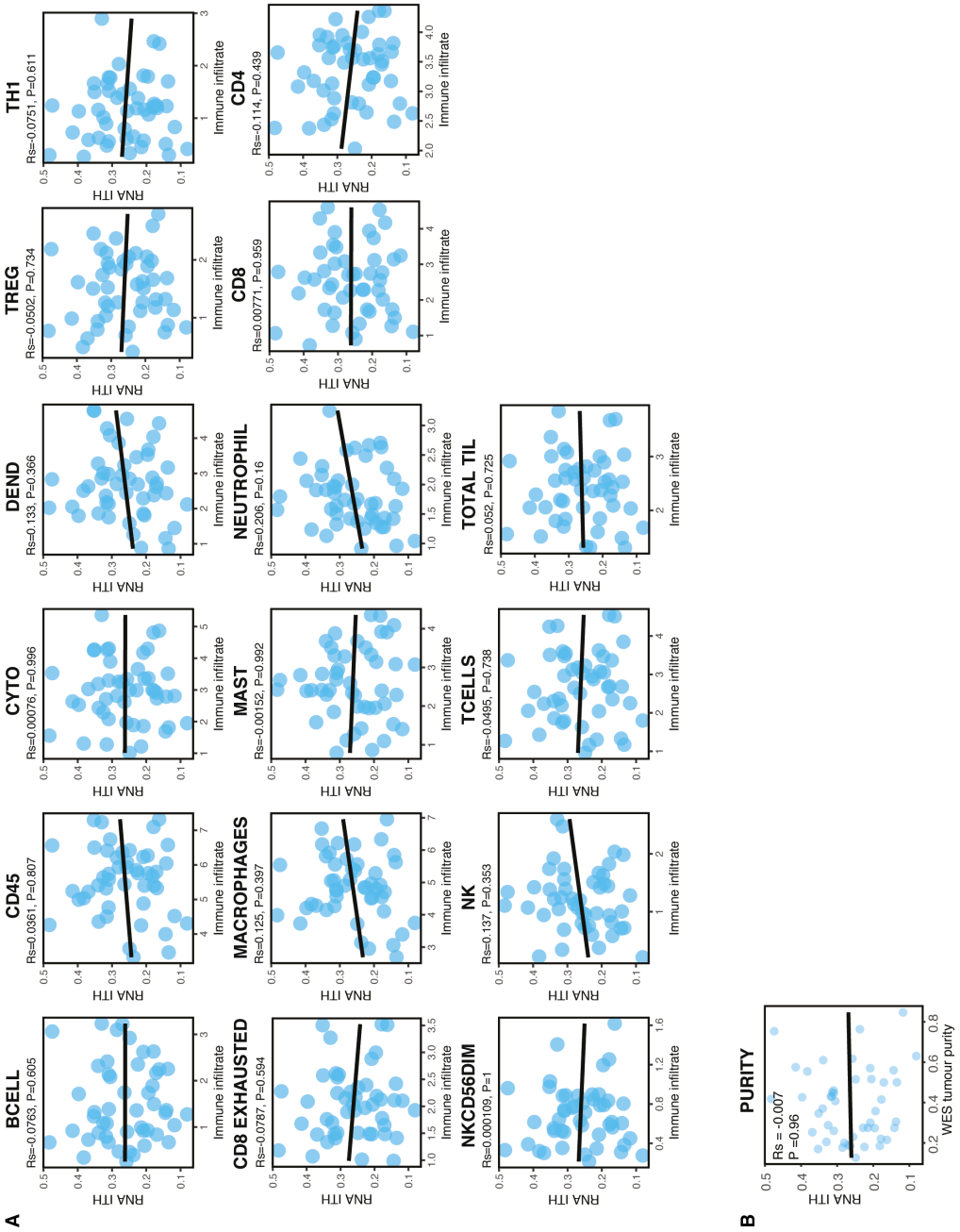

Figure 3-8 RNA-ITH by immune infiltration and tumour purity

RNA-ITH scores correlated with immune infiltration scores for 16 cell-types generated from RNA-Seq data using a method developed by Danaher and colleagues (A), and tumour purity inferred from WES data using ASCAT (B). Spearman correlation was performed in the TRACERx cohort (n=48 NSCLC patients).

3.3 RNA heterogeneity reflects chromosomal instability

3.3.1 Genetic correlates of RNA-ITH

I examined the genetic determinants of RNA-ITH by accessing the published results from WES analyses of the first 100 NSCLC patients enrolled in the TRACERx study (327 regions, 100 NSCLC patients) (Jamal-Hanjani et al., 2017), then exploring dependencies in the subset of TRACERx tumours with multi-region RNA-Seq data available (156 regions, 48 NSCLC patients, stage I-III).

Briefly, SNVs were detected using a consensus of VarScan2 and MuTect calls. The burden of point mutations was calculated per patient as the total number of non-synonymous SNVs across all tumour regions. SNVs were also classified as clonal or subclonal through PyClone clustering, and patient-level summaries of SNV-ITH were calculated (fraction of subclonal SNVs). RNA-ITH was not associated with either point mutation burden (Figure 3-9A, R_s=0.23, P=0.12) or mutational heterogeneity (Figure 3-9B, R_s=0.27, P=0.068).

Segmented allele-specific copy-number states were called using VarScan2 and ASCAT tools. The overall burden of copy number aberrations was defined as the proportion of the genome deviating from the tumour ploidy status, calculated as the average across tumour regions (weighted genome integrity index, wGII). SCNAs were classified as clonal if present across all regions from each tumour, or subclonal if absent in at least one region, permitting generation of patient-level estimates of SCNA-ITH (fraction of subclonal SCNAs). Intriguingly, copy-number ITH, a proxy measure for chromosome instability, was correlated with RNA-ITH (Figure 3-9C, R_s=0.54, P=0.00014). By contrast, a static measure of the copy number aberration burden was not associated with RNA-ITH (Figure 3-9D, Rs=0.26, P=0.077).

Overall, this suggests “functional” ITH of lung cancer transcriptomes positively correlates with dynamic and ongoing chromosomal instability, rather than karyotype complexity per se.

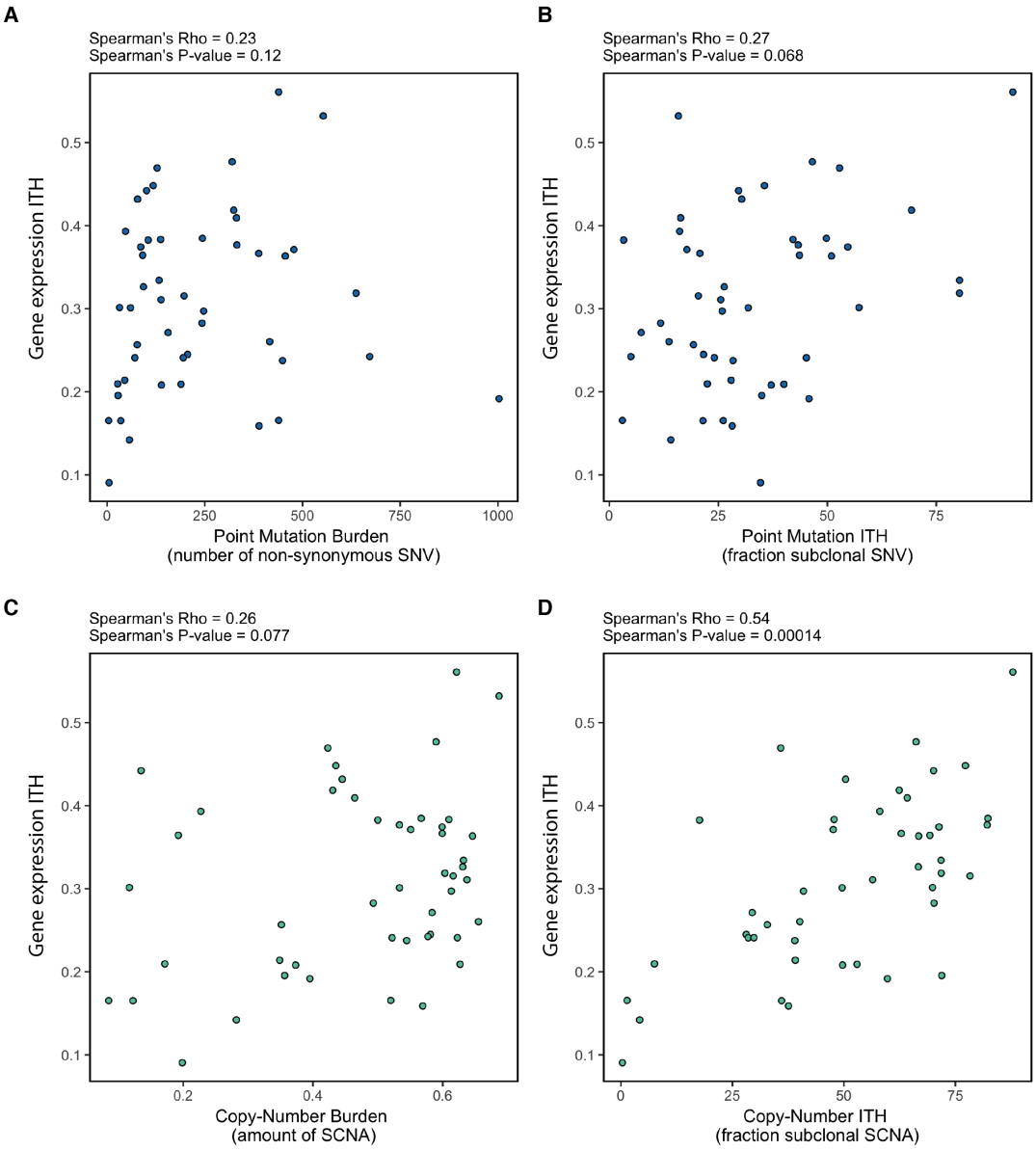

Figure 3-9 Genetic correlates of RNA-ITH

The association of RNA-ITH with genetic measures was investigated: non-synonymous mutation burden (A), mutational ITH (B), whole genome integrity index (C), copy-number ITH (D). Spearman correlation was performed in the TRACERx cohort (n=48 NSCLC patients).

3.3.2 Linking chromosomal instability, gene dosage, and prognosis

To dissect the relationship between copy-number ITH and RNA-ITH in greater detail, I tested whether gene expression tracks subclonal copy-number state at the level of individual SCNAs.

Mining the WES data, genes with a heterogenous SCNA profile between regions of an individual tumour were classified as subclonal copy-number gains or losses. Expression levels for subclonal SCNAs were then compared between copy-number aberrant and non-aberrant tumour regions. Overall 118,943 paired SCNA and RNA values were identified in TRACERx (143 regions from 44 NSCLC tumours with ASCAT data). This analysis revealed SCNA gains or losses distinct to tumour regions were linked with corresponding alterations in gene expression (Figure 3-10A, $P < 2.2 \times 10^{-16}$).

Analyses of WES data from 100 TRACERx patients reported elevated SCNA-ITH associates with increased risk of recurrence or death in NSCLC (Jamal-Hanjani et al., 2017). To explore whether RNA-ITH could mirror and provide a functional read-out for SCNA-ITH, I investigated its prognostic association in the reduced cohort of 48 TRACERx patients with multi-region RNA-Seq data. However, while patients with elevated RNA-ITH tended to have poorer disease-free survival outcomes – with visible splitting of Kaplan-Meier survival curves – this relationship was non-significant (Figure 3-10B, P=0.094).

Altogether, these data support the hypothesis that RNA-ITH may reflect dynamic chromosomal instability, the transcribing of heterogeneous aneuploidy karyotypes into functional ITH, and the selection of subclonal DNA copy-number events.

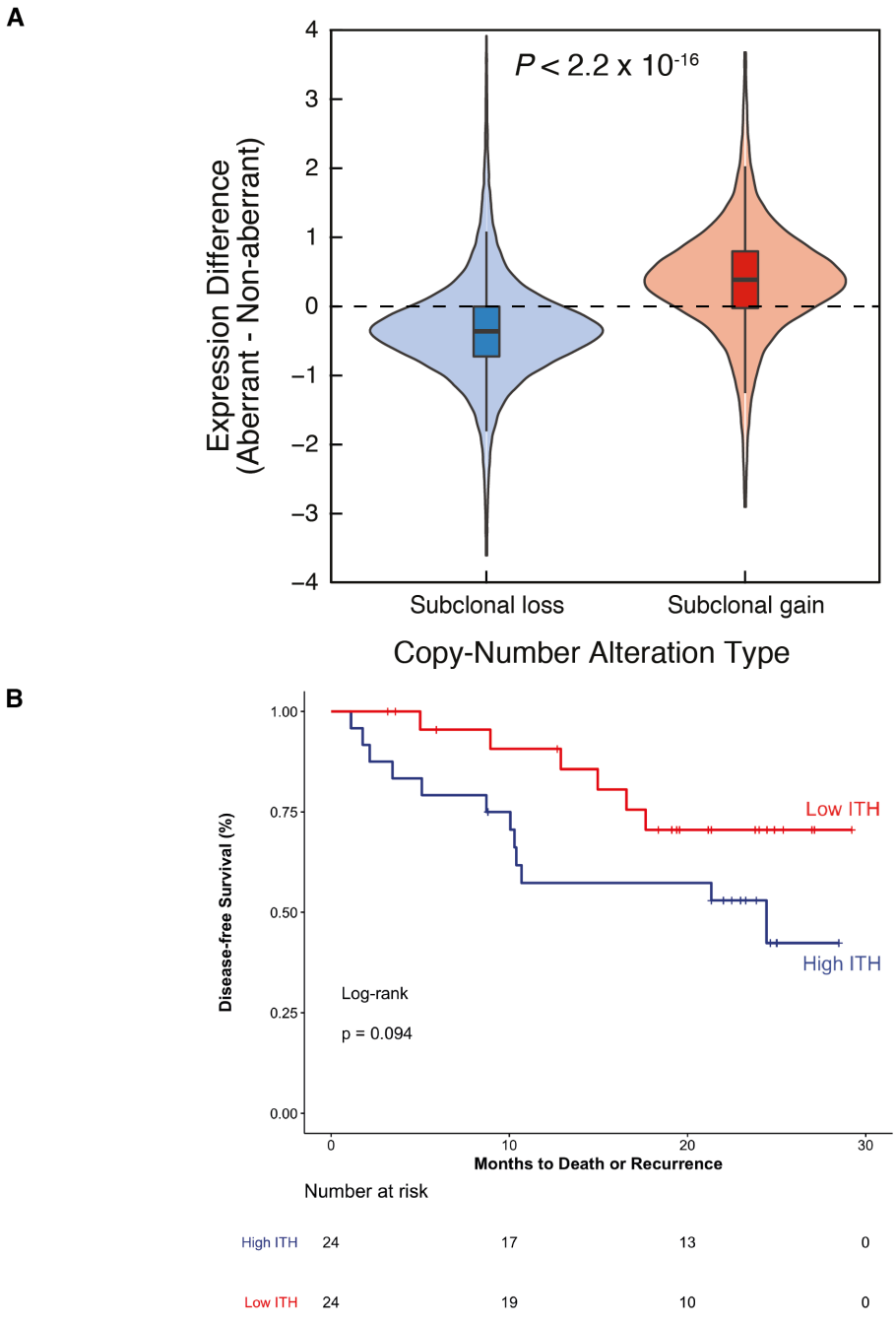

Figure 3-10 RNA-ITH associations with subclonal chromosomal copy-number changes and prognosis

A, Subclonal SCNAs were identified in the TRACERx cohort (n=44 NSCLC tumours with ASCAT calls available) and compared with gene expression. B, Percentages of TRACERx patients who were disease-free according to whether the patients had a high RNA-ITH (above the median) or a low RNA-ITH (below the median) score.

3.4 Tumour sampling bias confounds molecular biomarkers

3.4.1 Literature search for LUAD prognostic signatures

To explore patterns of gene expression associated with patient survival in the light of inter- and intra-tumour RNA heterogeneity, I performed a literature search to identify published lung cancer prognostic signatures. Early attempts to derive a prognostic signature for lung cancer patients treated NSCLC as a homogenous group (Boutros et al., 2009; Chen et al., 2007; Lau et al., 2007; Wigle et al., 2002; Zhu et al., 2010). However, most modern approaches, recognising histology is a potential confounding factor, have focussed on LUAD as the most common NSCLC subtype. Accordingly I restricted the scope of the study to LUAD prognostic signatures.

I searched the PubMed database to find literature reporting LUAD prognostic signatures (Bunn et al., 2014; Subramanian and Simon, 2010a; Zhu et al., 2009). The text and supplementary tables for each article were manually reviewed. Signatures developed from genome-wide RNA profiling studies and correlated with patient survival were considered for inclusion. Critically, if the full gene-list was not completely specified, then it could not be taken forward for subsequent analysis, and many signatures were excluded on this basis. As gene names change over time, several were updated to match the latest HUGO nomenclature to ensure fair comparison and integration with the TRACERx RNA-Seq dataset.

The literature search identified nine signatures from studies published between 2001 and 2017 (Figure 3-11). Each signature was comprised of 31 genes on average, though this varied greatly from a four-gene signature (Shukla et al., 2017) to a 97-gene signature (Beer et al., 2002). A range of RNA technologies had been used for signature derivation, including six microarray signatures (Beer et al., 2002; Bianchi et al., 2007; Garber et al., 2001; Krzystanek et al., 2016; Raz et al., 2008; Wistuba et al., 2013), two RNA-Seq signatures (Bailiang Li et al., 2017; Shukla et al., 2017), and one qPCR signature (Kratz et al., 2012) identified. Two of these signatures are available as commercial assays (Zheng and Bueno, 2015), namely

the “Pervenio Lung RS” (Kratz et al., 2012) and “Myriad MyPlan” signatures (Wistuba et al., 2013).

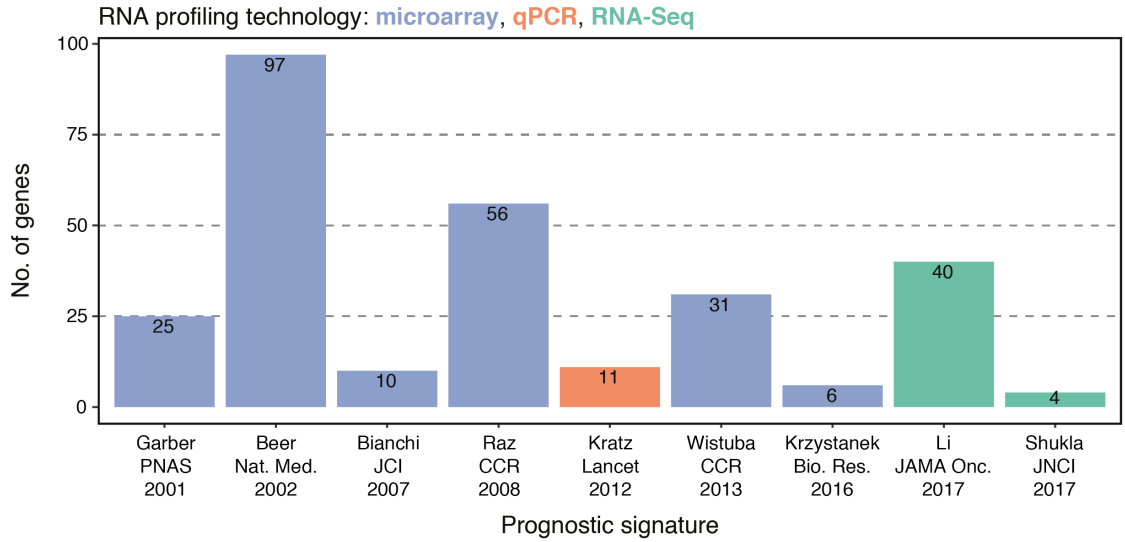

Figure 3-11 Published LUAD prognostic signatures
Bar plot showing the number of genes for each of nine published signatures, plotted in order of publication year. Bars are coloured by the technology used for gene expression profiling in the respective study.

3.4.2 Quantifying the sampling bias of RNA-Seq-based prognostic signatures

I determined the prevalence of sampling bias for RNA-Seq based prognostic signatures using RNA-Seq data from the cohort of TRACERx LUAD patients (89 tumour regions, 28 LUAD patients, stage I-III).

For the four-gene signature described by Shukla et al (Shukla et al., 2017), model coefficients from the original publication were applied to TPM data from the multi-region TRACERx study. A risk-score was calculated for every tumour region, then the risk thresholds defined in the original publication were used to stratify tumour regions as either high- or low-risk. Lastly, stratification of patients into more precise disease subtypes was attempted. If all regions from an individual tumour exhibited concordant risk classification, patients were labelled as concordant low- or high-

risk; alternatively, patients were labelled as “discordant” if different regions from the same tumour were classified as harbouring distinct profiles of molecular risk.

Discordant risk classification was observed in 43% of the TRACERx cohort (12/28 LUAD patients), indicating sampling bias was a substantial unaddressed confounding factor for this signature, potentially limiting its clinical application (Figure 3-12).

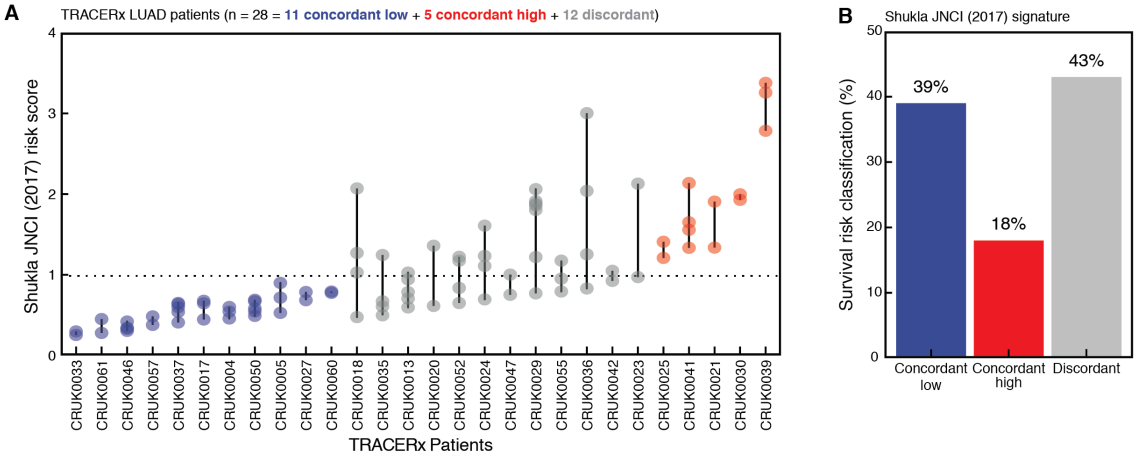

Figure 3-12 Tumour sampling bias for prognostic signature from Shukla et al Molecular risk-scores were calculated in multi-region tumours from the TRACERx cohort (n=28 LUAD patients), using the RNA-Seq signature described by Shukla et al. Risk-scores for all tumour regions is shown for each individual patient (A), and summarised as percentages of patients across the cohort (B). Tumours are classified as concordant low (blue), discordant (gray), or concordant high (red).

Indeed, the high- and low-risk patient stratifications outputted by the signature from Shukla et al were not informative for prognostication in the TRACERx cohort (Figure 3-13), though the small number of patients tempers this result. This result was independent of whether discordant risk tumours were classified based on the minimum, maximum, or median scoring tumour region, or excluded completely.

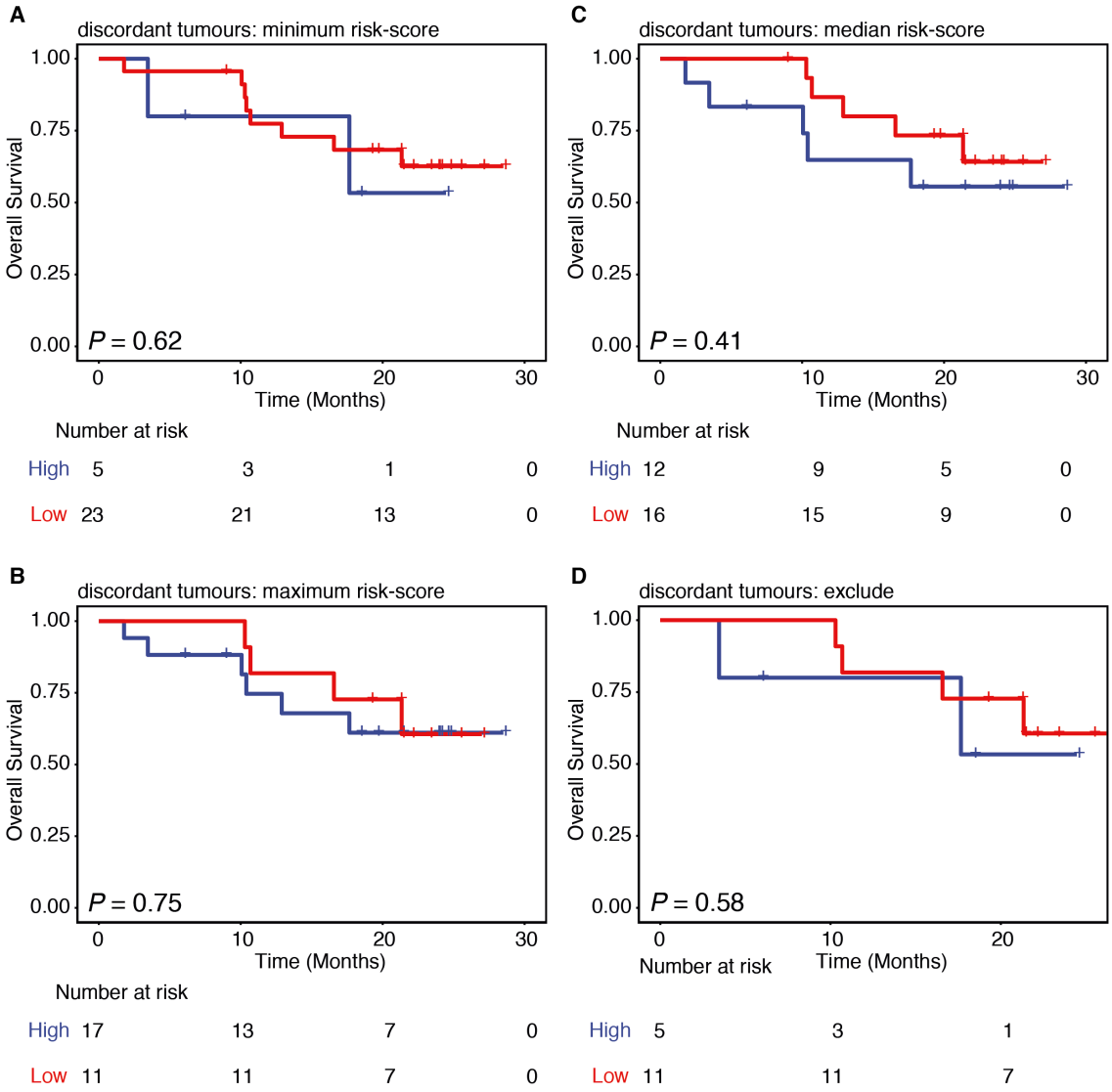

Figure 3-13 Prognostic information for prognostic signature from Shukla et al
Using the RNA-Seq signature described by Shukla and colleagues, TRACERx tumours (n=28 LUAD patients) were classified as concordant low risk (n=11), discordant (n=12), and concordant high risk (n=5). Prognostic ability was assessed for concordant high- and low-risk tumours, with the discordant tumours classified according to their minimum risk score (A), maximum risk score (B), median risk score (C), or excluded (D). Kaplan-Meier survival curves, statistical significance was tested with a two-sided log-rank test.

The same analysis was conducted for the signature described by Li and colleagues (Bailiang Li et al., 2017), an RNA-Seq signature that estimates survival risk based on “immune-related gene pairs”. The 40-gene signature was applied to TRACERx TPM data, using the median risk-score as the threshold to classify tumour regions. This revealed discordant classification in 29% of the TRACERx cohort (8/28 LUAD patients), providing further evidence for the limited clinical utility of existing signatures (Figure 3-14).

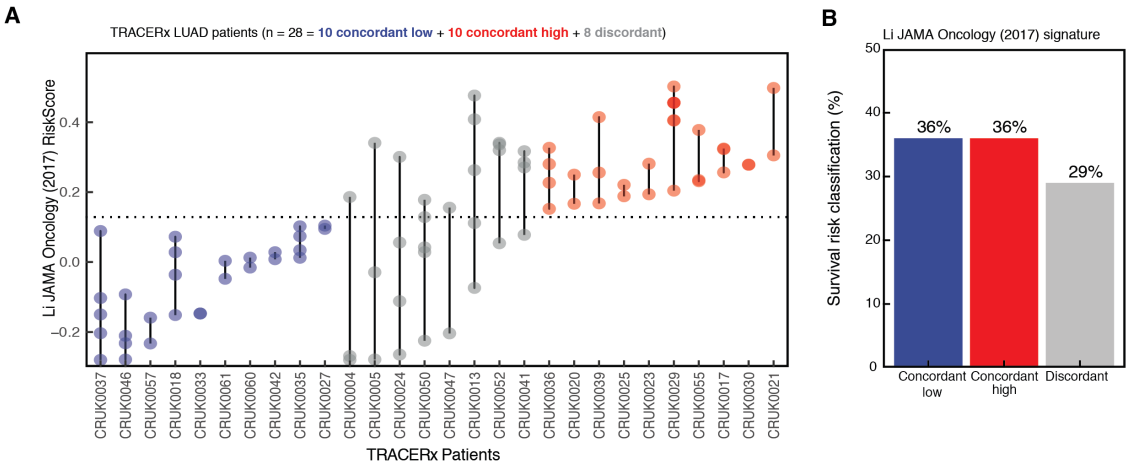

Figure 3-14 Tumour sampling bias for prognostic signature from Li et al
Molecular risk-scores were calculated in multi-region tumours from the TRACERx cohort (n=28 LUAD patients), using the RNA-Seq signature described by Li et al. Risk-scores for all tumour regions is shown for each individual patient (a), and summarised as percentages of patients across the cohort (b). Tumours are classified as concordant low (blue), discordant (gray), or concordant high (red).

3.4.3 Quantifying sampling bias of prognostic signatures invariant of RNA profiling technology

To date, the majority of gene expression based prognostic signatures in LUAD have been defined through expression profiling on microarray technology, rather than RNA-Seq. Therefore, to assess the pervasiveness of tumour sampling bias among LUAD prognostic signatures in RNA-Seq data from the cohort of TRACERx LUAD patients (89 tumour regions, 28 LUAD patients, stage I-III), I performed clustering to quantify the similarity between tumour regions from the same patient. This enabled the evaluation of discordance in a manner invariant of the technology used to derive the signature.

I adopted a method developed by Gyanchandani et al (Gyanchandani et al., 2016) to examine sampling bias in a multi-region breast cancer cohort. This involves hierarchical clustering (Manhattan distance, Ward method) of all tumour regions by the genes comprising each signature. Clustering discordance rate is then defined as the proportion of patients with tumour regions assigned to separate groups.

The clustering approach is shown for the Pervenio Lung RS signature (Kratz et al., 2012) to illustrate how discordance rates are calculated (Figure 3-15A). The clustering discordance metric is influenced by the number of clusters considered (dendrogram height), therefore I performed the analysis iteratively from 2 clusters (splitting the dataset into two groups) to 28 (splitting the dataset into the total number of patients – here, perfect concordance means all tumour regions from each patient cluster together). At 2 clusters, the Pervenio Lung RS signature has a clustering discordance rate of 11% (3/28 patients) at 2 clusters (Figure 3-15B). This metric increases with the number of clusters considered, from 18% (5/28 patients) at 3 clusters, 29% at 14 clusters (8/28 patients), and 50% (14/28 patients) at 28 clusters (Figure 3-15B).

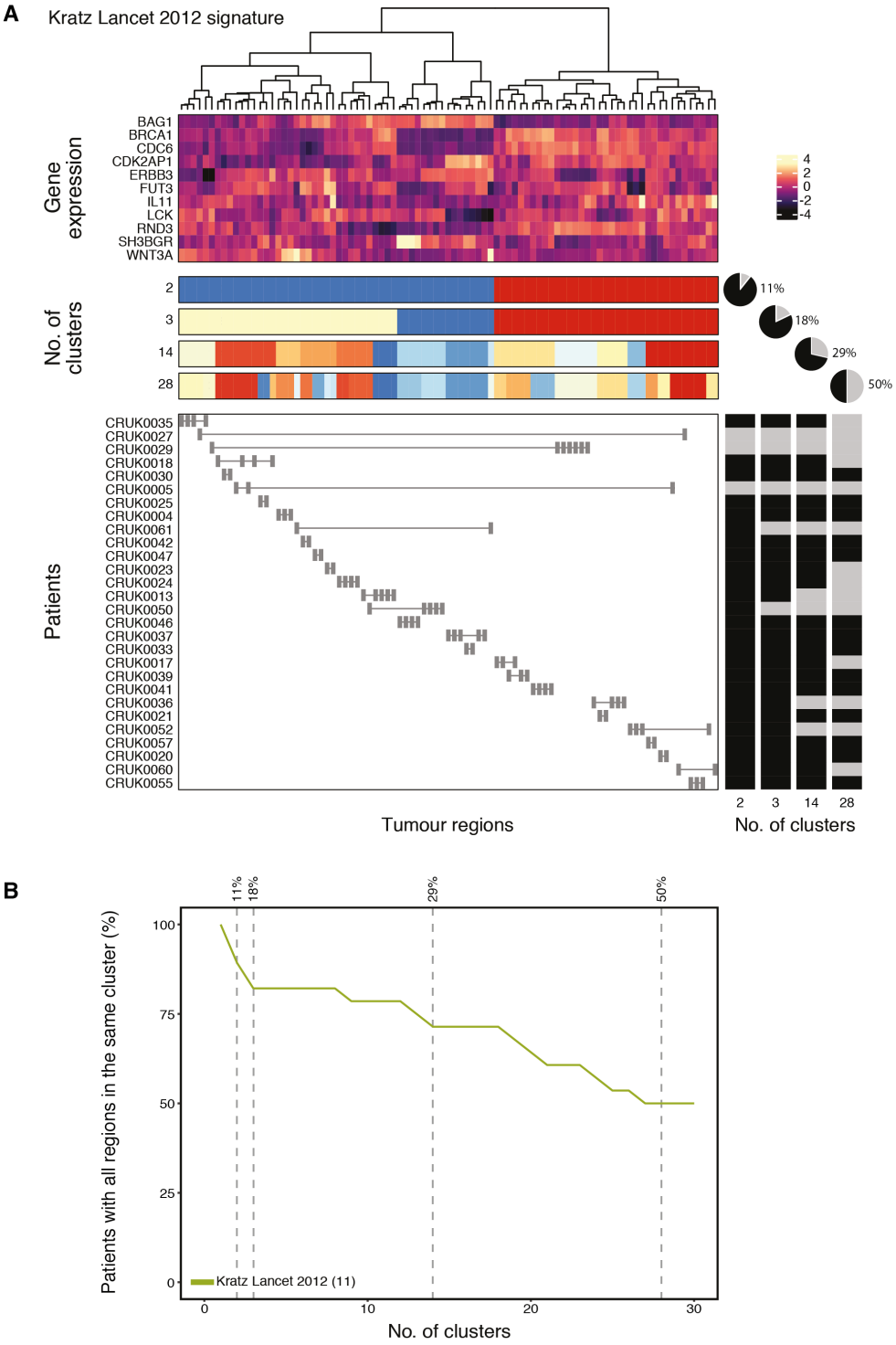

Figure 3-15 Tumour sampling bias for prognostic signature from Kratz et al Discordance rate measured in TRACERx (n=28 LUAD patients) using the qPCR signature described by Kratz et al. A, The dendrogram and heatmap (top) use the expression profiles of the genes-list forming the prognostic signature (middle) to cluster tumour regions (bottom). Patients with tumour regions assigned to

discordant clusters are highlighted (right, bar plots) and calculated as a percentage of all patients from the cohort (middle, pie charts), for a range of clusters (2, 3, 14, 28). B, The fraction of patients with all tumour regions assigned to the same cluster is taken to indicate discordance, and iteratively calculated from 2 to 28 clusters. Dashed vertical lines mark the discordance scores for a range of clusters (2, 3, 14, 28).

I extended the clustering approach to the 9 published LUAD prognostic signatures identified by the literature search. Discordance rates were calculated for each signature from 2 to 28 clusters. At 28 clusters the median clustering discordance rate was 50% (15.5/28 LUAD tumours, range = 18-82%), indicating that half the tumour regions would be vulnerable of incorrect risk stratification due to sampling bias (Figure 3-16).

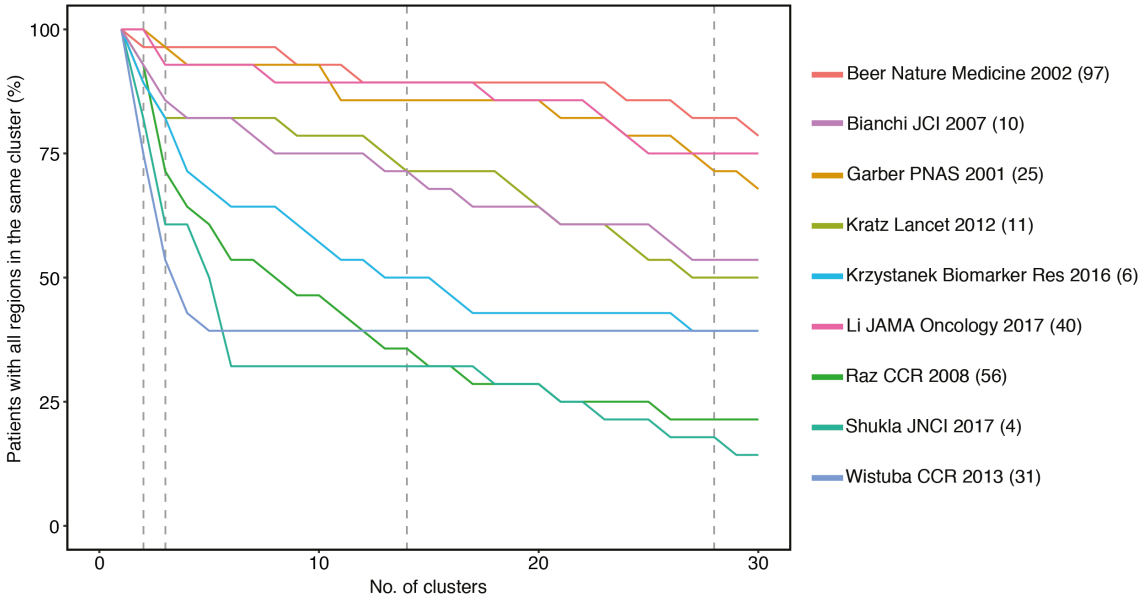

Figure 3-16 Tumour sampling bias for prognostic signatures from nine studies Discordance scores were calculated for nine prognostic signatures in TRACERx (n=28 LUAD patients) using the hierarchical clustering approach. Dashed vertical lines mark the discordance scores for a range of clusters (2, 3, 14, 28).

Taken together, these data suggest sampling bias is a prevalent problem amongst published prognostic signatures, which may contribute to the low validation rate of gene expression signatures.

3.5 Conclusions

3.5.1 Summary of findings

The studies of NSCLC patients from the TRACERx study in this chapter have demonstrated the utility of multi-region sequencing to measure RNA-ITH, uncovered chromosomal instability as a major underlying mechanism, and identified tumour sampling bias as a substantial unaddressed challenge for biomarker discovery in lung cancer (Figure 3-17).

I explored the relationship between aneuploidy and gene dosage heterogeneity at the level of individual chromosomes, observing gene expression has a 50% correlation with copy number at the gene level, consistent with previous observations in human cancer (Pollack et al., 2002; Tonon et al., 2005). Importantly, this relationship held for cases where SCNA is altered subclonally in the multi-region dataset. To the best of my knowledge, the transcription of heterogeneous chromosomal states into functional ITH has not previously been described in the literature.

The in-depth evaluation of nine published LUAD prognostic signatures revealed these are subject to significant sampling bias, exhibiting a 50% discordance rate on average, whereby different regions from the same tumour may be classified as harbouring distinct profiles of molecular risk. This result greatly expands on a recent multi-region microarray study of 10 NSCLC patients, reporting discordance rates of 10-70% for two published NSCLC prognostic signatures (Lee et al., 2018).

In summary, the evidence presented here suggests RNA-ITH correlates with chromosomal instability and may confound single-biopsy driven biomarker approaches if unaddressed. Having established that existing signatures may be limited by sampling bias, I proceed to study the impact of controlling RNA-ITH on biomarker performance in the next chapter.

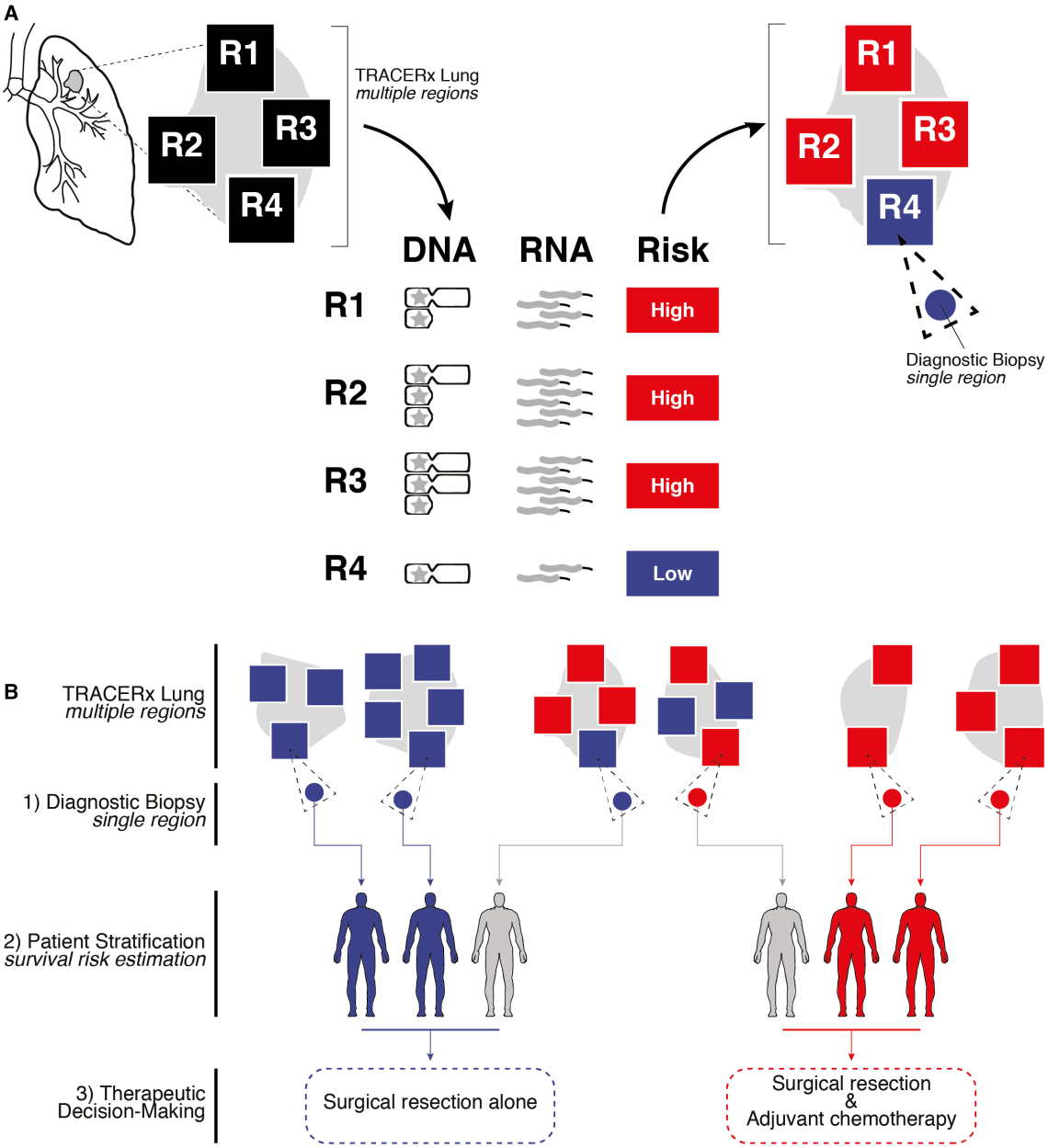

Figure 3-17 Chromosomal instability associates with RNA-ITH, giving rise to tumour sampling bias

A, In TRACERx, multiple regions are sampled from each individual tumour (marked as R1-R4). The genomic profile of the tumour is shown for a single high-risk prognostic gene (gray). The chromosomal state ("DNA", gray star), and the corresponding transcriptional read-out ("RNA", gray transcripts) are indicated. Gene expression signatures score the RNA profile of a tumour biopsy as high-risk (three red regions) or low-risk (one blue region). Only one biopsy is taken for diagnosis in the routine clinical setting (indicated by dashed triangle). This tumour is vulnerable to sampling bias, as the diagnostic biopsy (circle) is taken

from the sole low-risk region. B, A diagnostic tumour biopsy is taken and tested using a prognostic gene expression signature (1), which classifies patients into more precise disease subtypes based on estimated survival risk (2), and helps to inform clinical decision-making (3). While useful in distinguishing high-risk (red) from low-risk (blue) patients, prognostic signatures are confounded by tumour sampling bias (gray), leading to a sub-optimal treatment and follow-up strategy.

3.5.2 Future work

The novel metric developed for RNA-ITH in this chapter was based on the standard deviation in expression values between multiple regions sampled from an individual tumour. Future analyses may further hone this RNA-ITH metric, possibly through explicitly modeling expression levels as a function of spatial coordinates as described by the SpatialDE tool (Svensson et al., 2018). In addition, my analyses of RNA-ITH did not incorporate cis-effects (gene expression scales proportional to copy-number) or trans-effects (gene expression scales disproportionately with copy-number, typically due to targeting by transcription factors). The inclusion of this information may further refine the mechanistic linkage between CIN and RNA-ITH.

While mutation clonality can be inferred from single-sample WES data, using PyClone for example (Roth et al., 2014), it has been speculated that it would be difficult to infer RNA-ITH without multi-region RNA-Seq data (Alizadeh et al., 2015). Yet the extraction of allele-specific expression, using tools such as phASER (Castel et al., 2016) or Texomer (Wang et al., 2019), may provide a means to quantify RNA-ITH using single-samples.

The extent to which tumour stromal and immune components influences the measurement of RNA-ITH from bulk sequencing data is unclear. Accounting for sample-specific purity could partially address this problem (see 3.2.3). In future, a definitive solution may be provided by deconvolving cancer from stromal gene expression in bulk samples (discussed further in section 5.2 of this thesis).

Chapter 4. Designing molecular biomarkers in the light of cancer evolution

4.1 Introduction

Lung cancer is the leading cause of global cancer mortality (Siegel et al., 2019) and represents a high impact area for precision medicine strategies to improve patient outcomes (Vargas and Harris, 2016). For the majority of NSCLC patients, adjuvant chemotherapy remains the first-line therapy of choice (Pignon et al., 2008). As such, decision-making over adjuvant therapy is informed by prognostic biomarkers. NSCLC patients are currently stratified for chemotherapy on the basis of TNM staging (Goldstraw et al., 2016). However, TNM stage is an imperfect predictor, as patients diagnosed with the same disease stage can have markedly different clinical outcomes (see 1.2.1). Integrating diagnostic criteria with molecular correlates of tumour aggressiveness, such as gene expression signatures, may improve risk prediction in NSCLC, meeting an urgent clinical need (Subramanian and Simon, 2010a; Vargas and Harris, 2016).

Studies across cancer types have revealed that ITH, which gives rise to the diagnostic challenge of tumour sampling bias, may preclude the development of robust prognostic assays from single tumour biopsies (Gerlinger et al., 2012; Gulati et al., 2015, 2014; Gyanchandani et al., 2016; Lee et al., 2018; Tofigh et al., 2014). Indeed, in the previous chapter, two RNA-Seq-based prognostic signatures for LUAD displayed a discordant molecular read-out in 29% and 43% of tumours (Figure 3-12, Figure 3-14).

In this chapter I set out to address the confounding effects of RNA-ITH in biomarker derivation, with the aim of providing a pragmatic solution to tumour sampling bias, and stratifying tumours into groups with distinct evolutionary fates and clinical outcomes.

The results presented in this chapter forms sections of a first-author paper published during this thesis (Biswas et al., 2019).

4.2 The status quo for molecular prognostication in lung cancer

4.2.1 The curse of dimensionality for RNA biomarkers

A fundamental challenge for the derivation of prognostic signatures is feature selection: subsetting from ~20,000 expressed genes to a small number of genes (<100 genes) that is compatible with use on a clinical platform (Figure 4-1). Feature selection is fundamentally difficult in such high dimensional space, as noise predictors reduce ability to recover signal predictors (Altman and Krzywinski, 2018). In cancer RNA datasets, over-fitting is easy and it is possible to identify numerous equally significant signatures (Boutros et al., 2009). In NSCLC, previous supervised solutions to this challenge have included data-driven approaches – such as simply correlating with survival (Shukla et al., 2017) – and knowledge-based approaches, selecting immune (Bailiang Li et al., 2017) or cell cycle progression genes (Wistuba et al., 2013) (Figure 4-1).

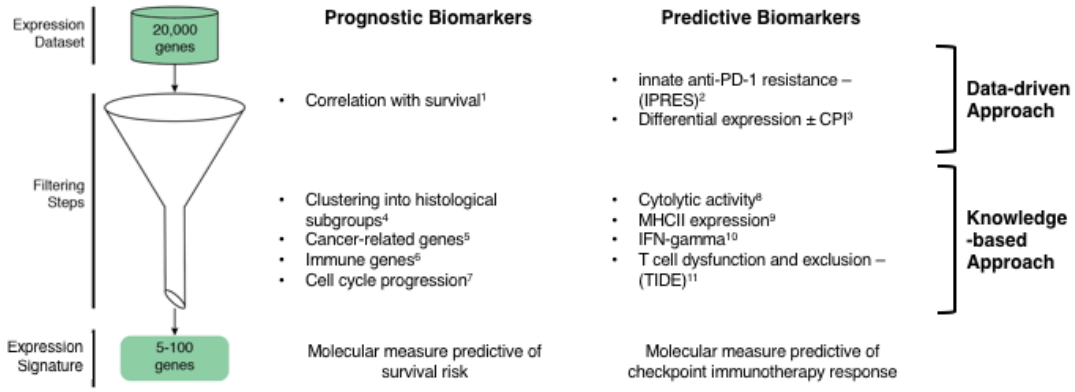

Figure 4-1 Approaches to designing gene-expression biomarkers for lung cancer The design of an expression-based signature typically begins with a genome-wide RNA dataset of thousands of genes (the result of an expensive microarray or RNA-seq experiment). Feature selection ("filtering steps") is then performed to develop a prognostic or predictive biomarker, typically 5 to 100 genes in length. These signatures are compatible with technologies such as qPCR or Nanostring that are cheaper and have a faster turnaround time, so are much better suited for routine clinical use. Previous solution to the challenge of feature selection include data-driven approaches (e.g. simple Cox regression against survival) or knowledge-based approaches (e.g. using cell cycle genes as a surrogate measure for tumour aggressiveness). Superscript numbers indicate published approaches: 1) (Beer et al., 2002; Bianchi et al., 2007; Krzystanek et al., 2016; Shukla et al., 2017). 2) (Hugo et al., 2016). 3) (Chen et al., 2016; Gubin et al., 2014). 4) (Garber et al., 2001). 5) (Kratz et al., 2012; Raz et al., 2008). 6) (Bailiang Li et al., 2017). 7) (Wistuba et al., 2013). 8) (Rooney et al., 2015). 9) (Johnson et al., 2016). 10) (Ayers et al., 2017). 11) (Jiang et al., 2018).

4.2.2 Factors limiting the clinical adoption of prognostic signatures in lung cancer

A number of factors have been suggested for consideration when developing a prognostic signature for patients with LUAD. A primary factor is reproducibility: for clinical use, a biomarker must validation upon testing in independent patient cohorts (Shedden et al., 2008; Sun et al., 2008). Medical utility is another key factor, specifically further classifying LUAD patients with stage I disease into risk-groups has been identified as a high impact area for precision medicine (Subramanian and Simon, 2010b; Vargas and Harris, 2016). Lastly, demonstrating utility on routinely collected clinical samples (typically diagnostic samples are FFPE, rather than fresh-frozen as required by NGS studies) to fast track a molecular diagnostic test for clinical use (Zhu and Tsao, 2014).

At present, the major contender for clinical adoption in LUAD is the 'Razor Genomics' signature. Over the last decade, this signature has been developed from research study (Raz et al., 2008), through assay development (Kratz et al., 2013), to retrospective (Kratz et al., 2012) and prospective (Woodard et al., 2018) validation studies. A recent study suggested a "TNM-B" (B for biology) diagnostic scheme, demonstrating how a molecular risk-score might be usefully integrated with tumour staging in LUAD (Kratz et al., 2019).

There is a prevailing sentiment of disappointment about expression signatures as biomarkers in LUAD. In 2010, Subramanian and colleagues reviewed 16 prognostic signatures for NSCLC (Subramanian and Simon, 2010a). Three criteria were assessed: appropriateness of the study protocol, whether the signature was validated in an independent dataset, and if the signature was clinically useful beyond current practice standards (showing risk separation in stage I, improved predictive value above known risk factors). The authors concluded "none of the studies succeeded in showing improvement in predictive power for gene expression signature over and above known risk factors". In addition, external testing of two signatures (Chen et al., 2007; Lau et al., 2007) revealed both failed to maintain a survival association in the sub-group of stage I patients. In a separate

meta-analysis of 42 published NSCLC prognostic signatures, Tang and colleagues showed that less than half (18/42 signatures) performed significantly better than randomly generated signatures (Tang et al., 2017).

Tumour sampling bias of LUAD signatures is an unaddressed confounding factor. A multi-region microarray study of 35 tumour regions from 10 NSCLC patients, found a previously published 6-gene prognostic signature (Boutros et al., 2009) was discordant in 1/10 tumours, and another tested signature (Zhu et al., 2010) was discordant in 7/10. In the previous chapter of this thesis, the sampling bias of nine prognostic signatures for LUAD was assessed. The average discordance rate was 50% (see 3.4); the 'Razor Genomics' signature (Kratz et al., 2012) was discordant in 50% of tumours (14/28 patients). Conceivably, refining feature selection to mitigate sampling bias might improve signature performance, and could represent a major technical advance for the design of molecular biomarkers.

4.3 Defining clonal transcriptomic signals in lung cancer

4.3.1 Global analysis of RNA heterogeneity

A method to stratify patients by prognosis based on gene expression must exhibit three key criteria:

1) it must exhibit sufficient diversity between patients' tumours (high inter-tumour heterogeneity), enabling clear stratification into distinct informative subgroups;
2) it must be robust to sampling bias, whereby it is not heavily influenced by diversity within tumours (low intra-tumour heterogeneity);
3) it must be reliably prognostic, demonstrated through validation in independent cohorts.

While both the first and third criteria have previously been considered when defining prognostic biomarkers, ensuring the stability of a transcriptomic signature to sampling bias has not been previously been addressed in a systematic fashion, and this may be a root cause of the low validation rate of lung cancer biomarkers (Vargas and Harris, 2016).

To explore intra- and inter-tumour RNA heterogeneity (criteria one and two above), I performed a global unsupervised clustering analysis in the TRACERx dataset (156 tumour regions, 48 NSCLC patients, stage I-III). After subsetting for the 500 genes with highest variance across all patients and tumour regions, hierarchical clustering (Euclidean distance, complete linkage) was performed.

In every case, the regions from each individual tumour clustered together, indicating that the variation of gene expression between regions from the same tumour was less than the variation between tumours from different patients (Figure 4-2A). A variably selected subset of genes can therefore represent each tumour with a unique and identifiable expression profile.

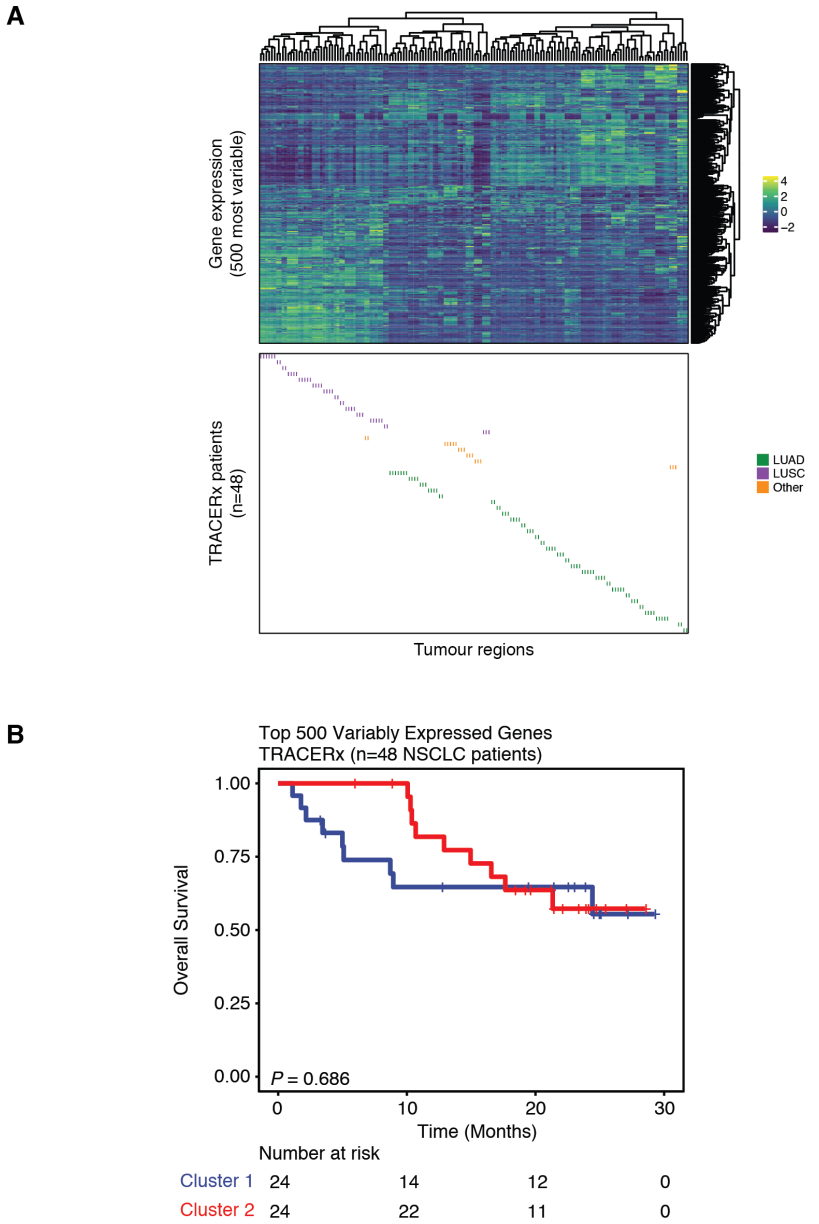

Figure 4-2 Analysis of the most variably expressed genes in TRACERx

A, Hierarchical clustering was performed on samples from the TRACERx multi-region RNA-Seq cohort, using the top 500 variably expressed genes. The upper panel is an expression heatmap, with genes as rows, and columns as tumour samples. The lower panel highlights how tumour regions cluster, with each row as a patient, and histologies coloured differently. B, The dendrogram from (A) was cut into two clusters. Survival analysis of was performed, comparing patients from these two subgroups, shown as a Kaplan-Meier survival curve. Statistical significance was tested with a two-sided log-rank test.

However, while the subset of top variant genes may be robust to sampling bias, they were not prognostic (criteria three above) in the TRACERx dataset. When tumours were stratified into two groups based on the global clustering analysis, there was not a significant difference in survival times between the two patient subgroups (log-rank P = 0.686, Figure 4-2B).

Of interest, the tumour regions from the different NSCLC histologies (LUAD, LUSC, other) largely clustered separately (Figure 4-2A). This is consistent with the distinct clustering patterns reported by early single-sample RNA profiling studies examining the transcriptional differences between LUAD and LUSC histologies (Bhattacharjee et al., 2001; Takeuchi et al., 2006).

4.3.2 Defining RNA heterogeneity quadrants

In the previous chapter, RNA-ITH scores were derived based on the variance in gene expression within individual TRACERx tumours (see 3.2.2). Here, I generated RNA inter-tumour heterogeneity scores to identify variable molecular signals between TRACERx patients. These two axes of RNA heterogeneity were then paired to derive a quadrant-based scheme, with the aim of identifying robust molecular biomarkers.

Estimates of inter-tumour RNA heterogeneity were calculated in the cohort of LUAD patients from TRACERx (89 regions, 28 LUAD patients, stage I-III). One region was randomly sampled per patient from the multi-region dataset, to overcome the confounding effect of considering all regions from a tumour. This yielded a sham single-region cohort (Figure 4-3A). From the resulting sample set, inter-tumour heterogeneity scores were calculated per gene as the standard deviation in expression values between patients. The process of random sampling was repeated ten times, generating stable estimates of RNA inter-tumour heterogeneity scores. The TCGA cohort was leveraged to confirm that repeated random sampling of the TRACERx cohort was representative of a true single-region cohort. A highly significant positive association (Pearson r = 0.947, P<0.001)

was observed between scores generated in each cohort (Figure 4-3B), indicating the reproducibility of the approach taken for TRACERx.

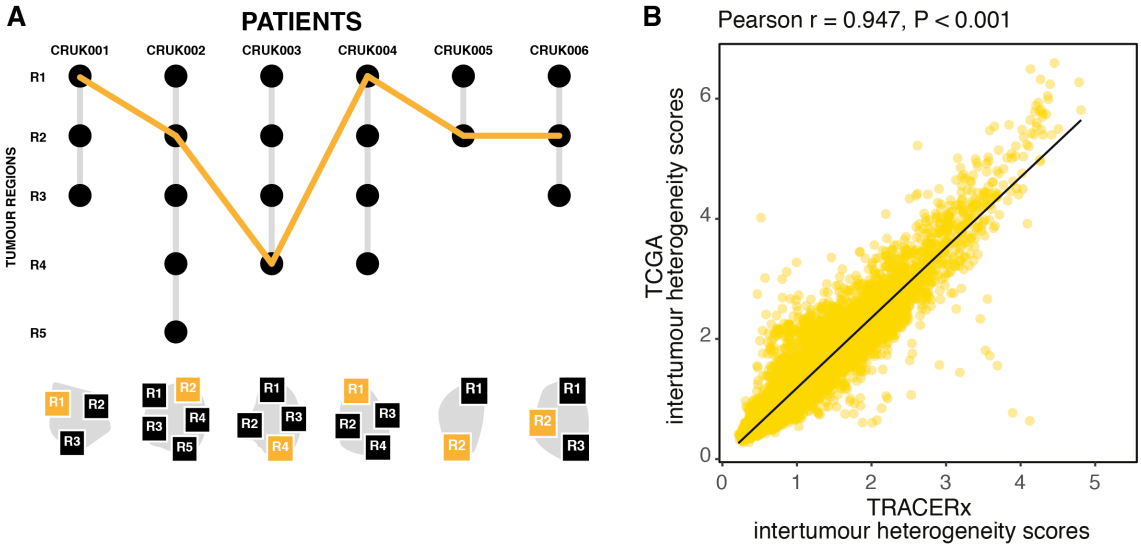

Figure 4-3 Inter-tumour RNA heterogeneity scores

A, Schematic showing how gene-wise inter-tumour RNA heterogeneity scores were generated via the random sampling of tumour regions from the multi-region TRACERx cohort (89 regions, 28 LUAD patients, stage I-III). B, Association between inter-tumour RNA heterogeneity scores calculated in TRACERx (a sham single-biopsy cohort) and TCGA (a true single-biopsy cohort).

The distributions of gene-level RNA inter- and intra-tumour heterogeneity scores were compared (Figure 4-4A). Overall, RNA inter-tumour heterogeneity exceeds intra-tumour heterogeneity in primary NSCLC tumours (Wilcoxon signed P < 2.2e-16). This is in line with the global analysis of RNA heterogeneity in the previous section (Figure 4-2A). Next, a scheme was developed to control for levels of inter- and intra-tumour RNA heterogeneity in biomarker derivation. For each RNA heterogeneity metric, the distribution was plotted as a density curve and bisected by the mean, resulting in four RNA heterogeneity quadrants (Figure 4-4B):

1) low inter- and high intra-tumour heterogeneity (Q1 = 798 genes);
2) low inter- and low intra-tumour heterogeneity (Q2 = 9,642 genes);
3) high inter- and high intra-tumour heterogeneity (Q3 = 4,766 genes);
4) high inter- and low intra-tumour heterogeneity (Q4 = 1,080 genes).

Putatively, the 1,080 genes in Q4 harboured the properties of an ideal biomarker, possessing both low RNA-ITH while remaining informative of differences between patients.

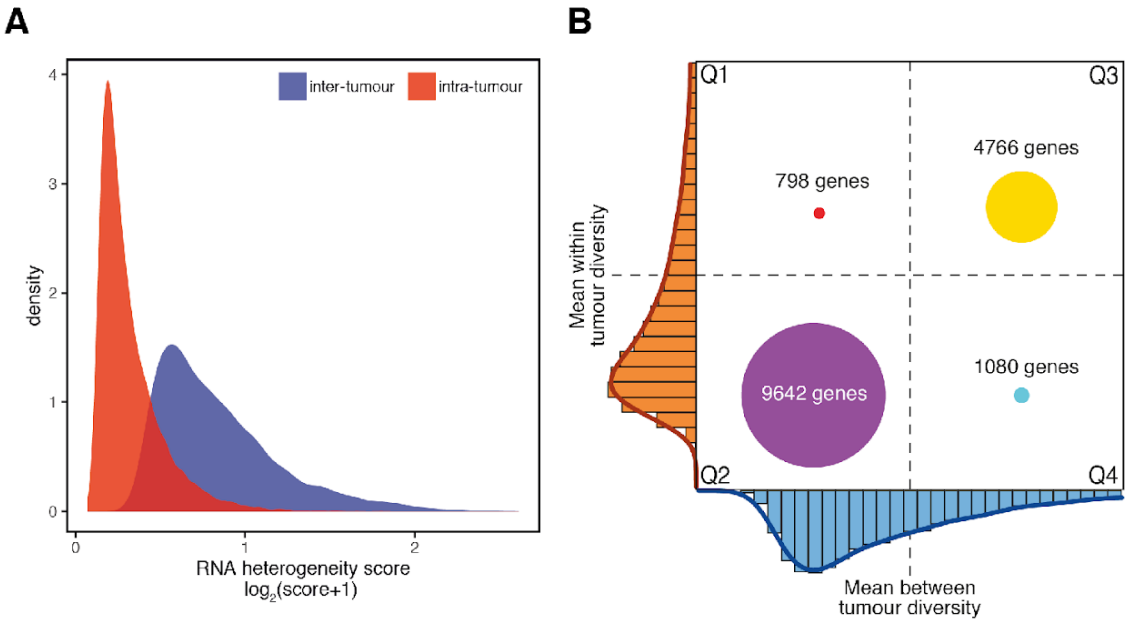

Figure 4-4 RNA heterogeneity quadrants

A, Density curves for RNA inter- and intra-tumour heterogeneity scores are shown on a log-scale. B, RNA inter-tumour (x-axis) and intra-tumour (y-axis) heterogeneity quadrants, calculated in TRACERx, plotted on the axes as density curves. The plot is divided into quadrants by the mean intra-tumour (dashed horizontal line) and mean inter-tumour (dashed vertical line) heterogeneity scores. The quadrants are numbered and coloured (Q1=red, Q2=purple, Q3=yellow, Q4=blue), with the number of genes per quadrant indicated. The RNA heterogeneity scores displayed were calculated from TRACERx LUAD patients (89 regions, 28 LUAD patients, stage I-III). RNA heterogeneity quadrants are indicated by colour: Q1 = red; Q2 = purple; Q3 = yellow; Q4 = blue.

Please note: the procedures described here were applied to TRACERx LUAD patients (89 regions, 28 LUAD patients, stage I-III), enabling a focus on LUAD biomarker discovery; separately all TRACERx NSCLC patients (156 regions, 48 NSCLC patients, stage I-III) were also used to generate RNA heterogeneity quadrants, permitting genomic and biological characterization without biasing to LUAD-specific genes.

4.3.3 An RNA heterogeneity quadrant driven by clonal chromosomal gains early in tumour evolution

Previous work has demonstrated the correspondence between gene expression and aberrations in chromosome copy-number in human tumours (Calabrese et al., 2020; Pollack et al., 2002; Tonon et al., 2005). In the previous chapter I showed this correspondence held true for subclonal SCNA events in NSCLC (see 3.3.2). To define the genetic source for RNA inter- and intra-tumour variability, here I examined differences in copy-number states between RNA heterogeneity quadrants derived in the TRACERx cohort (156 regions, 48 NSCLC patients, stage I-III).

Within each individual tumour, all genes were categorized according to copy-number state as compared to the paired germline sample (gain, loss, or no change). If applicable, the timing of the copy-number aberration (clonal or subclonal) was also taken into consideration. For each gene, the proportion of tumours within the TRACERx cohort subjected to each category of copy-number change was quantified. Lastly, each category of copy-number change was evaluated for relative enrichment or depletion in the genes from each RNA heterogeneity quadrant. A number of significant (Fisher's exact $P < 0.05$) associations were found between RNA heterogeneity quadrants and copy-number status (Figure 4-5). Notably, Q4 was enriched for clonal SCNA gains ($OR=1.64$; $P=1.18\times10-5$).

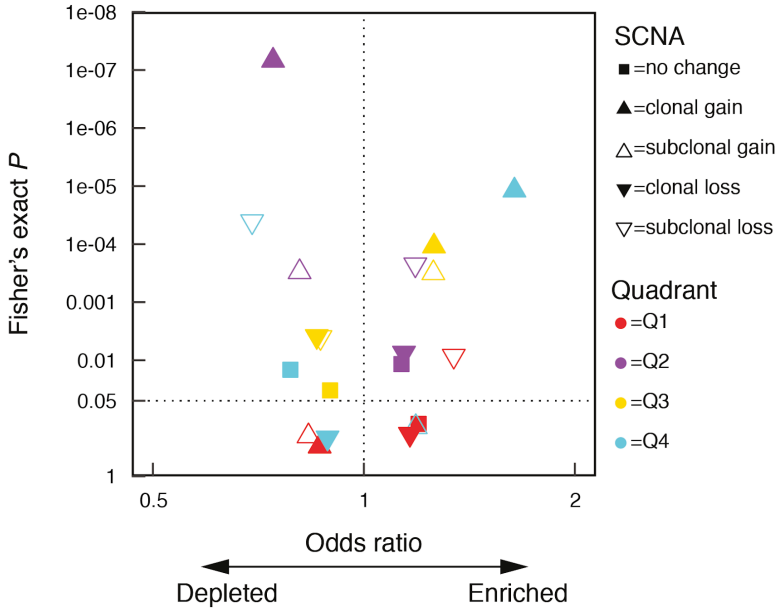

Figure 4-5 Genomic underpinning of RNA heterogeneity quadrants
Enrichment or depletion of specific copy-number states by RNA heterogeneity quadrant. All genes were assigned a copy-number state across all samples (clonal/subclonal gain or loss, or no change). Genes were then tested for enrichment or depletion of a specific category by RNA heterogeneity quadrant. Odds ratios are plotted on a natural log scale. Statistical significance was tested with a Fisher's exact test. RNA heterogeneity quadrants are indicated by colour: Q1 = red; Q2 = purple; Q3 = yellow; Q4 = blue.

These data suggest Q4 genes were related to clonal SCNAs, with expression attributable to chromosomal gains occurring early in tumour evolution. This subset of genes, enriched for ancestrally selected copy number changes, is henceforth referred to as either "Q4" or "homogeneously expressed" genes.

4.4 Characterizing the biological and prognostic properties of clonal transcriptomic signals in lung cancer

4.4.1 Homogeneously expressed genes are enriched for cell proliferation pathways

Assigning biological function to the different RNA heterogeneity quadrants may help shed light on their relevance for an evolving tumour. I performed a pathway analysis on the genes from each quadrant, using the gene-sets from the Reactome database. The top 10 significantly (Bonferroni-adjusted P-value < 0.01) enriched pathways for each quadrant were plotted (Figure 4-6A).

Q1 displayed no significant pathway enrichment. This may reflect the small number of genes in this quadrant (<5% of all expressed genes, 798/16,286), limiting statistical power to detect significantly enriched gene-sets.

Q2 was involved in mRNA splicing, transcription, and rRNA processing. As this quadrant consists of genes with both low intra- and inter-tumour heterogeneity, a plausible biological interpretation is that this represents a core module of “house-keeping” genes required by every tumour and within every cancer cell.

Q3 was enriched for extracellular matrix signaling and G protein-coupled receptor signaling pathways. This subset of genes harbour high intra- and inter-tumour heterogeneity scores. It is possible that genes involved in extracellular matrix signaling are up-regulated at the invasive front of particularly invasive tumours. However, this would require separate validation incorporating spatial information.

Q4 encoded gene-sets involved in cancer cell proliferation (Figure 4-6B). Integrated with the results from the copy-number analysis, this suggested that “homogeneously expressed” Q4 genes reflect the selection of high-risk SCNA gains in proliferation genes early in tumour evolution.

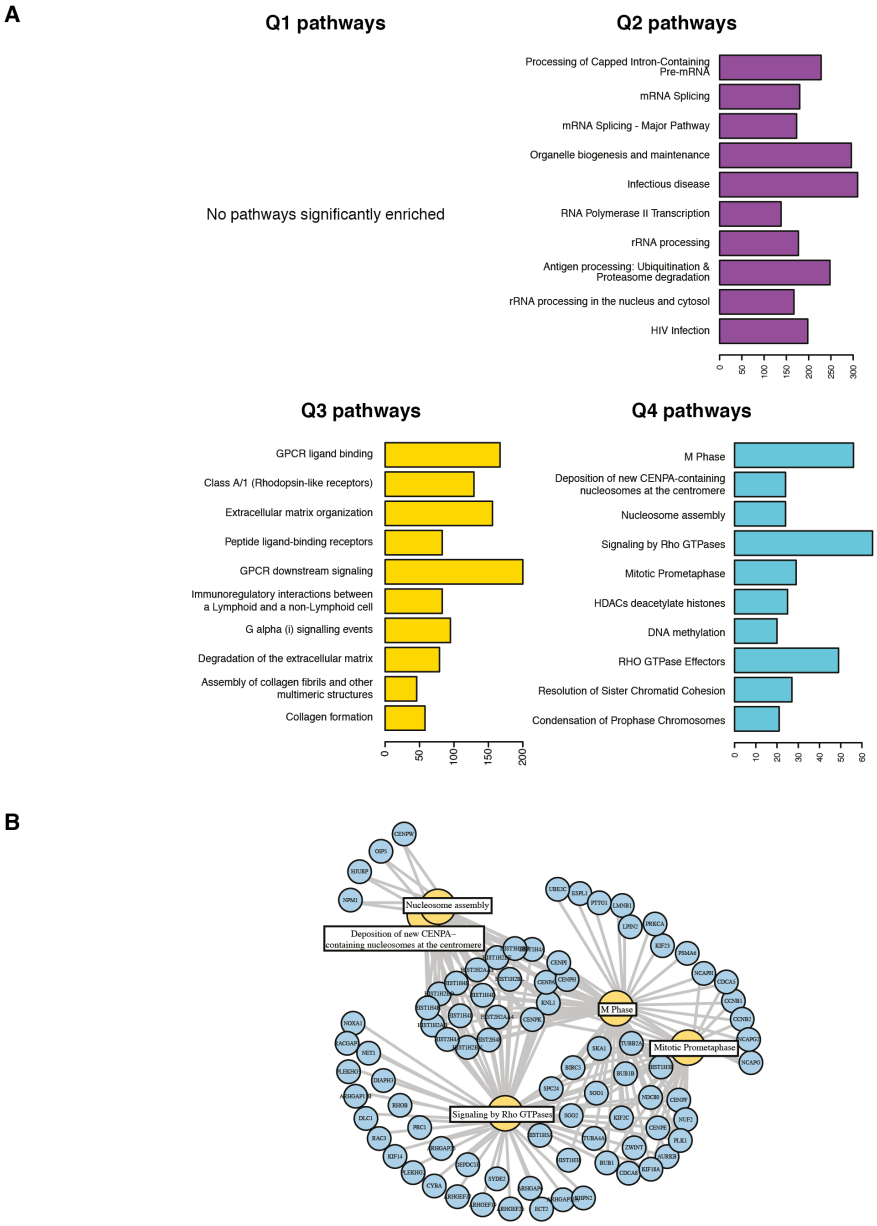

Figure 4-6 Pathway analysis of RNA heterogeneity quadrants

A, Pathway analysis on Q4 genes using Reactome, showing the top five pathways most significantly enriched in Q4 genes (low intra-tumour heterogeneity and high inter-tumour heterogeneity). B, The top ten Reactome pathways for each RNA heterogeneity quadrant. RNA heterogeneity quadrants are indicated by colour: Q1 = red; Q2 = purple; Q3 = yellow; Q4 = blue.

4.4.2 Individual homogeneously expressed genes are enriched for robust survival associations

I reasoned that homogeneously expressed genes from RNA heterogeneity Q4 (low intra- and high inter-tumour heterogeneity) might be more robust to sampling bias, and yield biomarkers with superior reproducibility between patient cohorts. Following this logic, previous biomarker studies may naturally enrich for Q4 genes even without explicitly selecting for homogeneously expressed genes in their derivation. Here, enrichment would be measured relative to the 7% of all expressed genes (1,080/16,286) comprised by Q4 (Figure 4-4B).

To test this hypothesis, I individually evaluated published prognostic signatures by RNA heterogeneity quadrant. In the previous chapter I had collated the gene-lists of 9 published prognostic biomarkers for LUAD (275 genes in total, including 33 overlapping between multiple signatures,,see 3.4.1). Here, I observed that several signatures appeared to be comprised of a relatively high proportion of Q4 genes (Figure 4-7A). In particular, both signatures approved for commercially approved prognostic assays (labelled as ‘Kratz Lancet 2012’ and ‘Wistuba CCR 2013’) were composed of at least 25% Q4 genes. To formally test this observation, I compared the expected distribution from all expressed genes, with the observed distribution from the collated gene-list from the 9 signatures (Figure 4-7A). Overall, 20% of genes from existing biomarkers fell in Q4 (54/275), a three-fold enrichment (P=1.39e-12, Figure 4-7B).

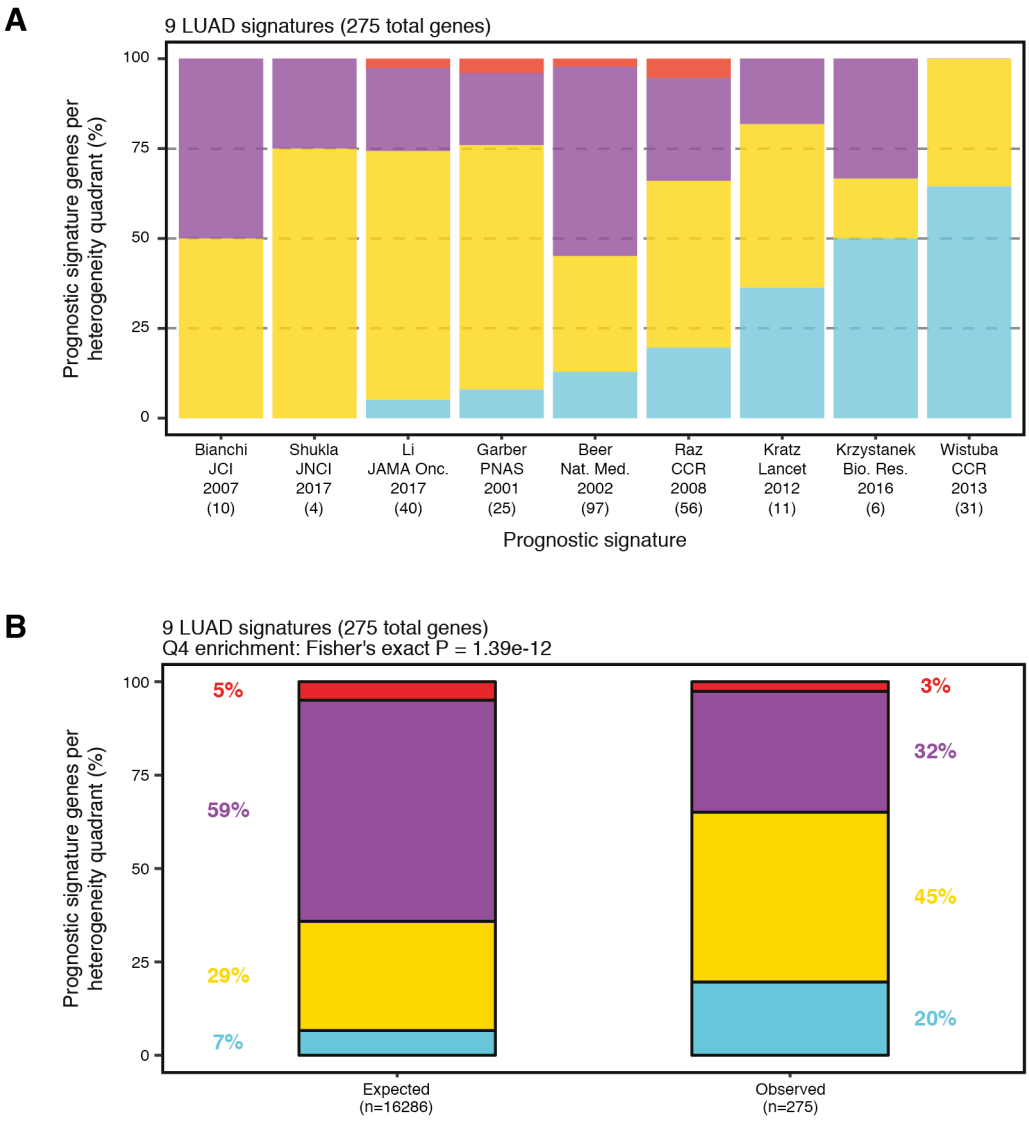

Figure 4-7 Analysis of published prognostic signatures by RNA heterogeneity quadrant

A, Bar plots showing the composition of published prognostic signatures by RNA heterogeneity quadrant, plotted in order of increasing percentage of Q4 genes (low intra- and high inter-tumour heterogeneity). B, Bar plots showing the percentage of genes expected per RNA heterogeneity quadrant (total no. genes, as indicated in Figure 1-3) versus observed (in 9 published prognostic signatures) per RNA heterogeneity quadrant. Statistical significance was tested with a two-sided Fisher's exact test. RNA heterogeneity quadrants are indicated by colour: Q1 = red; Q2 = purple; Q3 = yellow; Q4 = blue.

To further examine the tendency of Q4 genes to provide biomarkers with superior reproducibility, I accessed publicly available data from independent cohorts of lung cancer patients, and analysed the prognostic performance of genes by RNA heterogeneity quadrant. Expression and clinical information was downloaded from five cohorts of LUAD patients with stage I-III disease (see Methods for description of datasets): (1) TCGA (n = 469); (2) Shedden et al (n = 469); (3) Okayama et al (n = 147); (4) Der et al (n = 127); (5) Rousseaux et al (n = 83). The expression profiling technology for cohort 1 was RNA-Seq, and microarray was used for cohorts 2-5.

The prognostic value of a pooled gene-list from nine published prognostic signatures for LUAD (242 unique genes) was evaluated in the RNA-Seq dataset from TCGA. Using Cox univariate analysis, genes from Q4 correlated with survival significantly better than genes from other quadrants (Q2 versus Q4: $P=6.5\times10-8$; Q3 versus Q4: $P=4.0\times10-4$; there were insufficient genes in Q1 for Q1 versus Q4 comparison; Figure 4-8).

Probes for the full set of 242 genes, previously defined as prognostic, could not be recovered in every microarray dataset, hence varying numbers of genes tested in each cohort: 85% (205/242) Shedden et al; 99% (239/242) Okayama et al; 99% (239/242); Der et al; 99% (239/242) Rousseaux et al. In spite of the technology differences with RNA-Seq data, the four cohorts with microarray data yielded similarly robust associations for Q4 genes (Figure 4-8).

Overall, these analyses of the composition and reproducibility of published signatures, in the context of RNA heterogeneity quadrants, supported the hypothesis that Q4 genes may be enriched for robust survival associations, providing a basis for building robust biomarkers.

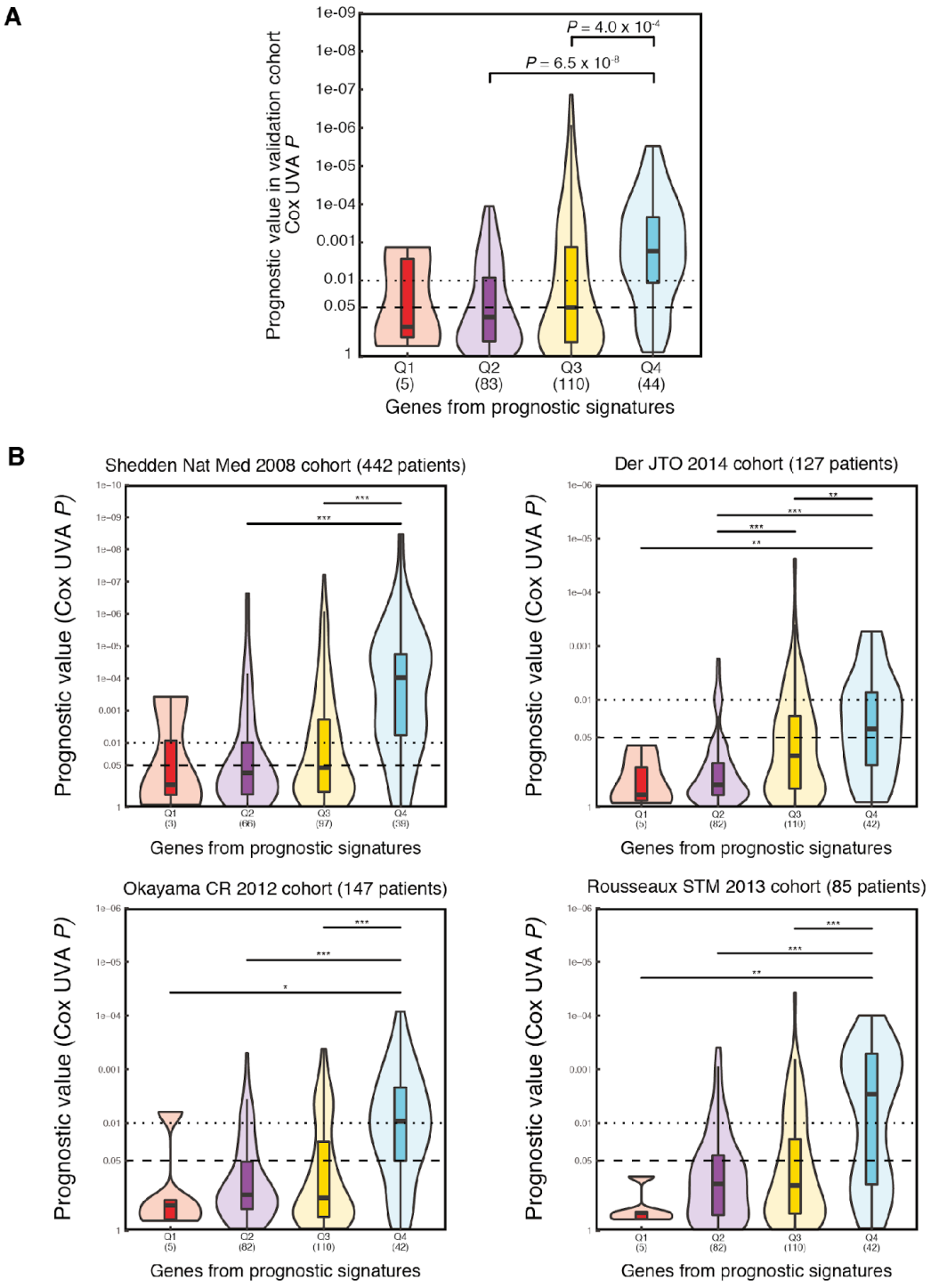

Figure 4-8 Reproducible survival association of published prognostic genes by RNA heterogeneity quadrant

The ability of the genes pooled from 9 published prognostic signatures to maintain prognostic value in independent cohorts of LUAD patients, assessed as the gene-wise Cox univariate P value (y-axis) stratified by RNA heterogeneity

quadrant (x-axis). A, Analysis in one RNA-Seq dataset from TCGA (n=469 LUAD patients). B, Analysis of four microarray datasets, Shedden et al, Okayama et al, Der et al, Rousseaux et al. Statistical significance was tested with a two-sided Wilcoxon signed rank sum test. * indicates a P value < 0.05, ** indicates a P value < 0.01, * indicates a P value < 0.001. RNA heterogeneity quadrants are indicated by colour: Q1 = red; Q2 = purple; Q3 = yellow; Q4 = blue.**

4.4.3 The selection of clonal genes in biomarker design improves performance

The design of prognostic biomarkers in transcriptomic datasets conventionally involves selecting a subset of genes associated with survival, and then using a machine learning algorithm to generate a prognostic model, outputting a gene expression signature. Here I performed a head-to-head test, comparing published methods against clonal gene selection, to evaluate any added benefit on biomarker performance

A range of methods has been employed in the literature to derive prognostic signatures in LUAD. In order to faithfully replicate published methods, a literature search was performed for LUAD prognostic signatures in the previous chapter (see 3.4.1). Here I identified published studies with sufficient information in the Methods of to replicate the approach taken. I opted to focus on 5 methods for conventional biomarker design (Figure 4-9A). These were centred around the following machine learning algorithms (Chen et al., 2007; Kratz et al., 2012; Reka et al., 2014; Shukla et al., 2017): stepwise AIC (akaike information criterion) regression; stepwise BIC (bayesian information criterion) regression; tree classification; random forest regression; elastic-net (lasso) regression. In parallel, I implemented a clonal version of each signature. The published pipeline steps were replicated, with one alteration: selecting only Q4 genes in the prognostic model (Figure 4-9A). Each conventional and clonal biomarker design process is described in detail below.

The TCGA RNA-Seq cohort (n = 469 patients with stage I–III LUAD) was used as the training cohort for signature development. To evaluate the prognostic value of

each signature in an independent patient cohort for validation, the Uppsala RNA-Seq dataset was used (n = 103 patients with stage I–III LUAD).

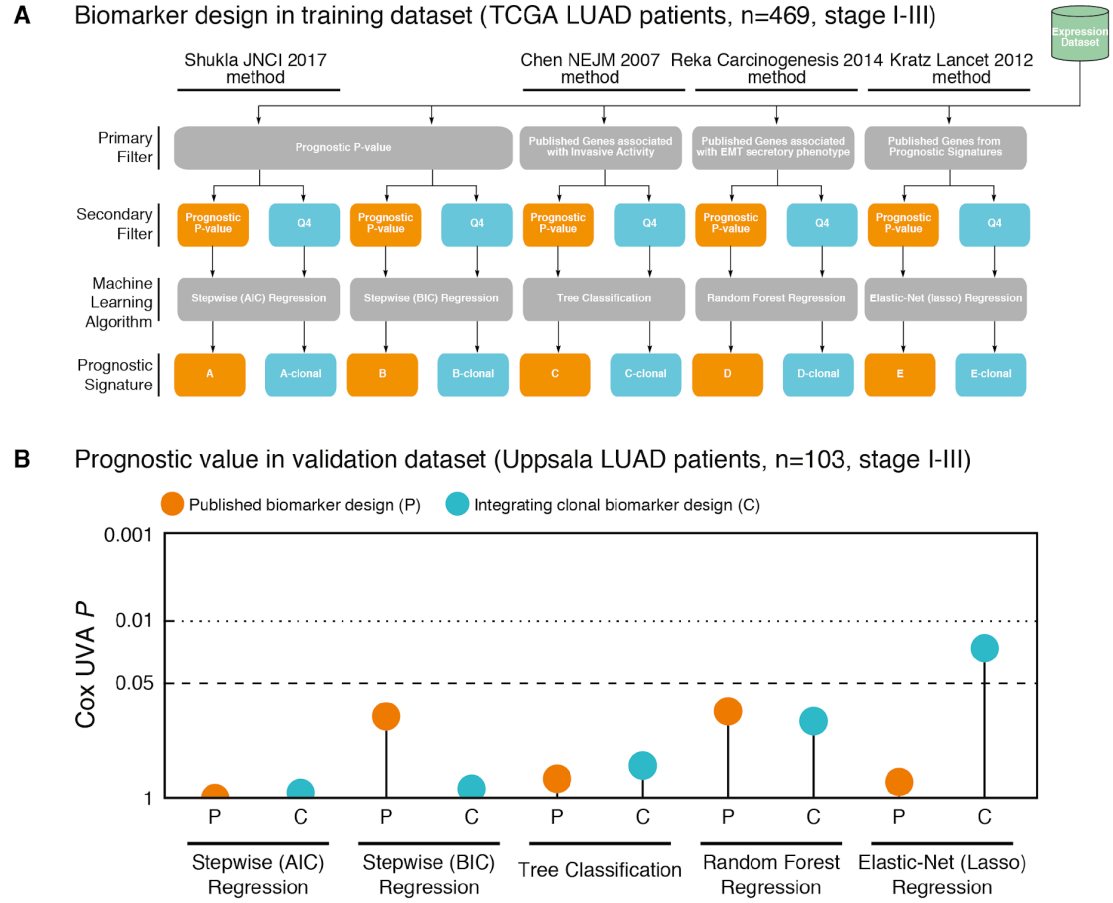

Figure 4-9 Conventional and clonal prognostic signature design and performance

A, Biomarkers are designed using state-of-the-art signature construction methods (marked in orange), replicated from Shukla et al (signature A and B), Chen et al (signature C), Reka et al (Signature D) and Kratz et al (signature E). In parallel, the "prognostic significance" filters present in each signature construction method were substituted with "homogeneous expression" filters, generating corresponding clonal signatures (signatures A-clonal, B-clonal, C-clonal, D-clonal, and E-clonal; marked in blue). Published signature construction methods are indicated in orange; novel methods integrating clonal biomarker design are indicated in blue. All signatures are developed in TCGA LUAD patients (n=469, stage I-III) as the training dataset. B, The prognostic performance of the resulting signatures was assessed in the Uppsala RNA-Seq

dataset (n=103 patients with stage I-III) as the Cox univariate P value (y-axis), correlating the risk-score for each signature (x-axis) against overall survival.

Stepwise regression. A published method to derive a prognostic signature, based around stepwise regression (Shukla et al., 2017), was replicated. Univariate Cox regression analysis was conducted using all expressed genes in the training cohort, to apply a primary filter based on the survival association of individual genes (univariate Cox analysis $P < 0.00025$), identifying 108 genes. This long-list of 108 genes was used to derive a signature purely based on prognostic information, by further subsetting for the genes with the most significant survival association (univariate Cox analysis false discovery rate < 0.02), generating a short-list of 15 genes that were used for forward conditional stepwise (Akaike information criterion) regression, outputting a six-gene prognostic signature (signature A); alternatively, stepwise (Bayesian information criterion) regression outputted a three-gene signature (signature B). In parallel, the long-list of 108 genes was also subsetted using a 'homogeneous expression' filter (selecting Q4 genes using heterogeneity scores calculated in TRACERx; n = 28 patients with stage I–III LUAD), generating a short-list of 15 genes, then outputting a seven-gene signature using stepwise (Akaike information criterion) regression (signature A—clonal). In addition, stepwise (Bayesian information criterion) regression generated a six-gene signature (signature B—clonal).

Tree classification. In two separate studies, Chen et al identified a set of 672 genes associated with invasive activity (Chen et al., 2001), then used tree classification to derive a prognostic signature (Chen et al., 2007). From the first study, 656 of 672 genes could be found using HUGO gene symbols. Then, replicating the method taken in the second study, a prognostic filter was applied, short-listing 8 genes significantly associated with survival (univariate Cox analysis $P < 0.00005$). Inputted to tree classification, this generated an eight-gene prognostic signature (signature C). In parallel, a 'homogeneous expression' selection step (subsetting to Q4 genes using heterogeneity scores calculated in TRACERx; n = 28 patients with stage I–III LUAD) was applied to the list of 656 genes associated with invasive

activity, outputting a nine-gene signature by tree classification (signature C—clonal).

Random forest regression. Reka et al (Reka et al., 2014) used a gene-set of an epithelial-mesenchymal transition secretory phenotype to fit a prognostic model using random forest regression. A purely prognostic model was made by first using the full list of 97 genes to fit a random forest model, then using the variable importance scores to re-fit the model using the top ten highest-scoring genes, outputting a ten-gene prognostic signature (signature D). In parallel, a 'homogeneous expression' selection step (subsetting to Q4 genes using heterogeneity scores calculated in TRACERx; n = 28 patients with stage I–III LUAD) identified nine genes, generating a nine-gene signature by random forest regression regression (signature D—clonal).

Elastic-net (lasso) regression. In two separate studies, Kratz et al derived a prognostic signature by pooling lists of prognostic genes and manually curating this list to generate a shortlist of 65 cancer-related genes (Raz et al., 2008), then applying elastic-net (lasso) regression (Kratz et al., 2012). To replicate this, a gene-list was assembled from published LUAD prognostic signatures (249 genes) (Beer et al., 2002; Bianchi et al., 2007; Garber et al., 2001; Kratz et al., 2012; Krzystanek et al., 2016; Bailiang Li et al., 2017; Raz et al., 2008; Shukla et al., 2017; Wistuba et al., 2013). Next, 56 of the 65 cancer-related genes could be recovered from the first study (Raz et al., 2008) and was used to select genes for lasso regression, outputting a 24-gene prognostic signature (signature E). In parallel, a 'homogeneous expression' selection step (subsetting to Q4 genes using heterogeneity scores calculated in TRACERx; n = 28 patients with stage I–III LUAD) was applied to the list of 249 genes, identifying 44 genes, and outputting a 14-gene signature by lasso regression (signature E—clonal).

For each prognostic signature, risk-scores were calculated in the validation cohort, and correlated with overall survival. The linear models – derived using stepwise AIC regression, stepwise BIC regression and elastic-net (lasso) regression – were used to calculate a risk score for each patient as a linear combination of gene

expression values, weighted by regression coefficients. Similarly, a risk score for each patient in the validation cohort for the tree models derived using tree classification and random forest regression. Signature E-clonal (the clonal signature derived using elastic-net regression) was the only biomarker significantly associated with overall survival in the validation dataset (Cox univariate analysis $P < 0.05$, Figure 4-9B). This underscores the limited reproducibility of conventional prognostic biomarker design.

4.4.4 Random signatures built from homogeneously expressed genes harbour cross-cohort prognostic significance

Recent studies in breast and lung cancer have showed that a surprisingly high percentage of randomly generated signatures maintain prognostic significance upon testing and can even out-perform conventionally crafted biomarker design (Tang et al., 2017; Venet et al., 2011). I examined the cross-cohort performance of randomly derived signatures to further assess the ability of Q4 genes to reproducibly associate with survival.

For each RNA heterogeneity quadrant, 1,000 random signatures were generated. First 20 genes were randomly sampled from a particular RNA heterogeneity quadrant, and then the TCGA RNA-Seq cohort (n = 469 patients with stage I–III LUAD) was used as the training cohort for model fitting by elastic-net (lasso) regression. The prognostic values of the randomly generated signatures were then assessed in four microarray-based cohorts (combined: n = 801 patients with stage I–III LUAD). Patients were classified as high- or low-risk using the median value of the first principle component, as in the method described by Venet and colleagues (Venet et al., 2011). The random signatures from Q4 genes maintained cross-cohort prognostic significance better than signatures derived from other quadrants (Figure 4-10): 56% of Q4 signatures were significant across four cohorts compared to 0%, 0.7% and 7.3% for Q1, Q2 and Q3 genes, respectively.

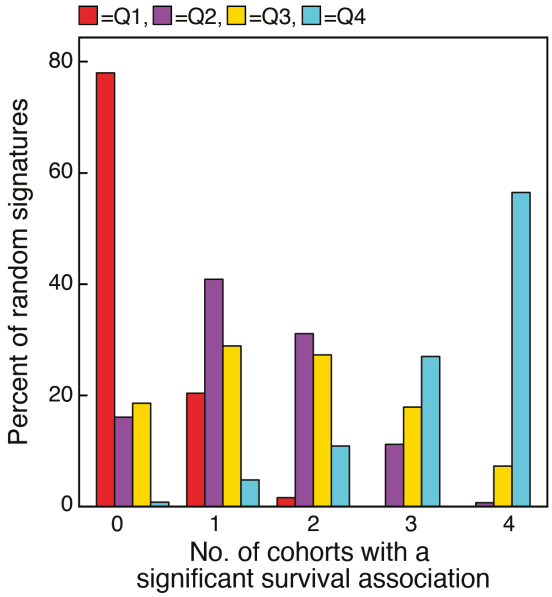

Figure 4-10 Cross-cohort performance of random signatures
A total of 1,000 random signatures were developed in the TCGA RNA-Seq cohort (n = 469 patients with stage I–III LUAD), derived using 20 genes randomly sampled from each RNA heterogeneity quadrant, then tested for prognostic ability across four microarray cohorts comprising patients with stage I–III LUAD (Shedden et al.: n = 442; Okayama et al.: n = 147; Der et al.: n = 127; Rousseaux et al.: n = 85).

This result further indicated that Q4 is highly enriched for genes with robust prognostic value and may provide a superior basis for building molecular biomarkers.

4.5 A biomarker based on cancer evolutionary principles associates with lung cancer mortality

4.5.1 Development of a clonal, prognostic, expression biomarker

Integrating clonal biomarker design with a published signature construction pipeline based on elastic-net regression yielded a prognostic signature that out-performed conventional methods. Moreover, even randomly selected subsets of homogeneously expressed genes displayed a tendency to yield biomarkers with cross-cohort prognostic associations. Based on these observations, here I inputted homogeneously expressed genes to the elastic-net regression algorithm, to explore the potential for novel biomarker discovery. This yielded a novel prognostic biomarker, termed an Outcome Risk Associated Clonal Lung Expression (ORACLE) signature. RNA-Seq data from the TCGA cohort (n = 469 patients with stage I–III LUAD) was used as the training cohort for signature development.

Starting with all expressed genes (19,024 genes) in the TCGA cohort, four criteria were sequentially applied to identify genes that were expressed, prognostic and clonal (Figure 4-11A):

1) An expression cut-off was applied, filtering out genes with below-median expression (9,512/19,024 genes), restricting noise due to the detection limits as a standard pre-processing step (Campbell et al., 2016);
2) Genes associated with survival (Cox univariate $P < 0.05$) were selected (2,023/9,512 genes), an established method in prognostic signature design (Chen et al., 2007; Shukla et al., 2017);
3) RNA heterogeneity scores were used as a primary method of identifying homogeneously expressed genes, selecting Q4 genes (176/2,023 genes);
4) Clustering concordance scores were used as a secondary method of identifying homogeneously expressed genes, determining the optimum number (90/176 genes) using ten-fold cross-validation in the training cohort (Figure 4-11B).

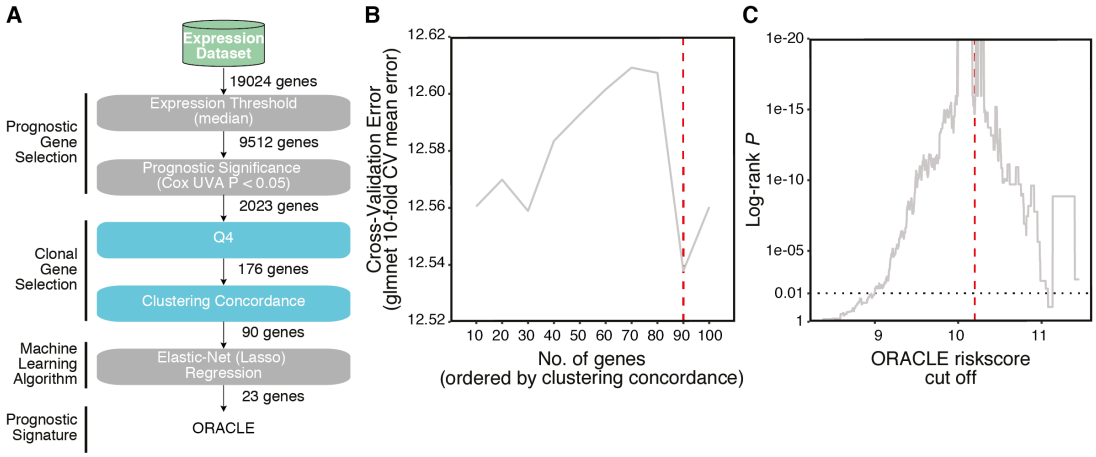

Figure 4-11 ORACLE signature design: gene selection and parameter tuning
A, Flow diagram illustrating the gene selection steps for ORACLE. Criteria to identify prognostic and homogeneously expressed genes, and the number of genes selected at each step are indicated. B, Optimization of the number of genes to select at the clustering concordance step through 10-fold cross-validation in the training cohort (TCGA, n=469 LUAD patients, stage I-III). The optimal number of genes, with the lowest cross-validation error, is shown by the vertical red line. C, The cut-off to dichotomize the ORACLE risk-score into 'high' and 'low' risk groups is optimized in the training cohort (TCGA, n=469 LUAD patients, stage I-III). The horizontal blue line indicates a log-rank P-value = 0.01 and the optimal cut-off is shown by the vertical red line. Statistical significance was tested with a two-sided log-rank test.

The 90 genes outputted by the four criteria were used to fit a prognostic model against overall survival in the training cohort using elastic-net (lasso) regression (Figure 4-11A). As part of the model fitting step, lasso regression performs further feature selection, yielding a 23-gene signature with a model coefficient for each gene. This signature was termed ORACLE (Table 1).

Gene Symbol	Model Coefficient	Gene Name	Description of Gene Function	Published Signature
ANLN	0.058692239	Anillin Actin Binding Protein	Required for cytokinesis (cleavage furrow)	-
ASPM	0.003462241	Abnormal Spindle Microtubule Assembly	Mitotic spindle regulation	Krzystanek Biomarker Res 2016, Wistuba CCR 2013
CDCA4	0.041940166	Cell Division Cycle Associated 4	Regulates cell proliferation via E2F/RB pathway	-
ERRFI1	0.013237564	ERBB Receptor Feedback Inhibitor 1	Up-regulated with cell growth, negatively regulates EGFR signaling	-
FURIN	0.208437458	Furin, Paired Basic Amino Acid Cleaving Enzyme	Pro-protein convertase binding TGFβ NGF, and MMP1 amonst others.	Beer Nat Med 2002
GOLGA8A	-0.028493707	Golgin A8 Family Member A	Maintains structure of golgi apparatus	-
ITGA6	0.058464556	Integrin Subunit Alpha 6	Essential for IGF1 and IGF2 signaling	-
JAG1	0.012599497	Jagged 1	Ligand for Notch signalling	-
LRP12	0.038410107	LDL Receptor Related Protein 12	involved in the internalization of lipophilic molecules and/or signal transduction, may act as a tumour suppressor	-
MAFF	0.075070616	MAF BZIP Transcription Factor F	Involved in transcriptional activation and repression	-
MRPS17	0.146466169	Mitochondrial Ribosomal Protein S17	Mitochondrial protein synthesis	-
PLK1	0.029842311	Polo Like Kinase 1	Ser/Thr kinase involved in cell proliferation and cell survival; M-phase of cell cycle	Wistuba CCR 2013
PNP	0.01177481	Purine Nucleoside Phosphorylase	Involved in (de novo) nucleotide salvage pathway, which is often interrupted by chemotherapy drugs	Beer Nat Med 2002
PPP1R13L	0.062382956	Protein Phosphatase 1 Regulatory Subunit 13 Like	Inhibitor of p53	-
PRKCA	0.038900124	Protein Kinase C Alpha	Ser/Thr kinase involved in cell proliferation (via cell cycle)	Raz CCR 2008
PTTG1	0.082889189	Pituitary Tumour-Transforming 1	Regulatory protein involved in chromosome stability, p53 pathway, and DNA repair	Wistuba CCR 2013
PYGB	0.143943497	Glycogen Phosphorylase B	Regulates glycogen mobilization	-
RPP25	0.019158495	Ribonuclease P And MRP Subunit P25	Component of ribonuclease P, a protein complex that generates mature tRNA molecules by cleaving their 5-ends	-
SCPEP1	-0.00145441	Serine Carboxypeptidase 1	May be involved in vascular wall (and kidney) homeostasis	-
SLC46A3	-0.031597666	Solute Carrier Family 46 Member 3	Lysosomal transmembrane protein; effective transporter of the cancer cytotoxic drug maytansine.	-
SNX7	0.133634555	Sorting Nexin 7	involved in intracellular trafficking	-
TPBG	0.012242067	Trophoblast Glycoprotein	oncofetal antigen that is specific to trophoblast cells, in adults this protein is highly expressed in many tumour cells and is associated with poor clinical outcome in numerous cancers.	Beer Nat Med 2002
XBP1	-0.121354561	X-Box Binding Protein 1	Transcription factor regulating 1) MHCII genes and 2) ER stress during Unfolded Protein Response	-

Table 1 ORACLE signature

Gene list and model coefficients for the Outcome Risk Associated Clonal Lung Expression signature. Descriptions of gene function, and references to usage in published prognostic signatures are also provided.

As a prognostic signature with an underlying linear model, ORACLE risk-scores are calculated as a linear combination of the expression values of the 23 genes comprising the signature, weighted by the model coefficients. To transform this continuous risk-score into binary classifications, in order to stratify patients as high- or low-risk, a risk-score cut-off is required. This was calculated as the median risk-score in the training cohort among significant (log-rank $P < 0.01$) cut-off values (Figure 4-11C).

Thus, a novel homogeneous expression biomarker for lung adenocarcinoma was derived. Many of the genes are involved in cellular division and proliferation (Table 1). To the best of my knowledge, only 30% of the list of genes comprising ORACLE (7/23 genes) has previously been used in LUAD prognostic signatures (*ASPM, FURIN, PLK1, PNP, PRKCA, PTTG1* and *TPBG*).

4.5.2 Validation as a clinically informative biomarker

The validation of a prognostic biomarker should ideally include demonstrating reproducible survival associations in at least one external dataset (preferably several) and demonstration of clinical utility, indicating prognostic value independent of existing clinicopathological risk factors and in patient subgroups where there is an urgent clinical need for improved stratification (Subramanian and Simon, 2010a; Vargas and Harris, 2016).

The reproducibility and clinical utility of ORACLE was assessed. Five independent cohorts of LUAD patients with stage I-III disease were used for signature validation: one RNA-Seq dataset from the Uppsala cohort (n = 103); four microarray datasets from Shedden et al (n = 469), Okayama et al (n = 147), Der et al (n = 127), and Rousseaux et al (n = 83).

Applying the ORACLE biomarker to the RNA-Seq-based validation cohort, the continuous risk-score displayed a highly significant survival association (Cox UVA P=0.00474, Figure 4-12B) that out-performed the signatures derived in the previous section (Figure 4-9B). Using the risk-score cut-off to dichotomize the cohort, the hazard ratio between risk-groups was 3.16 (1.4–7.0, log-rank P = 0.006, Figure 4-12A), and three-year overall survival was 80% (68–94%) in the low-risk group and 57% (46–71%) in the high-risk group.

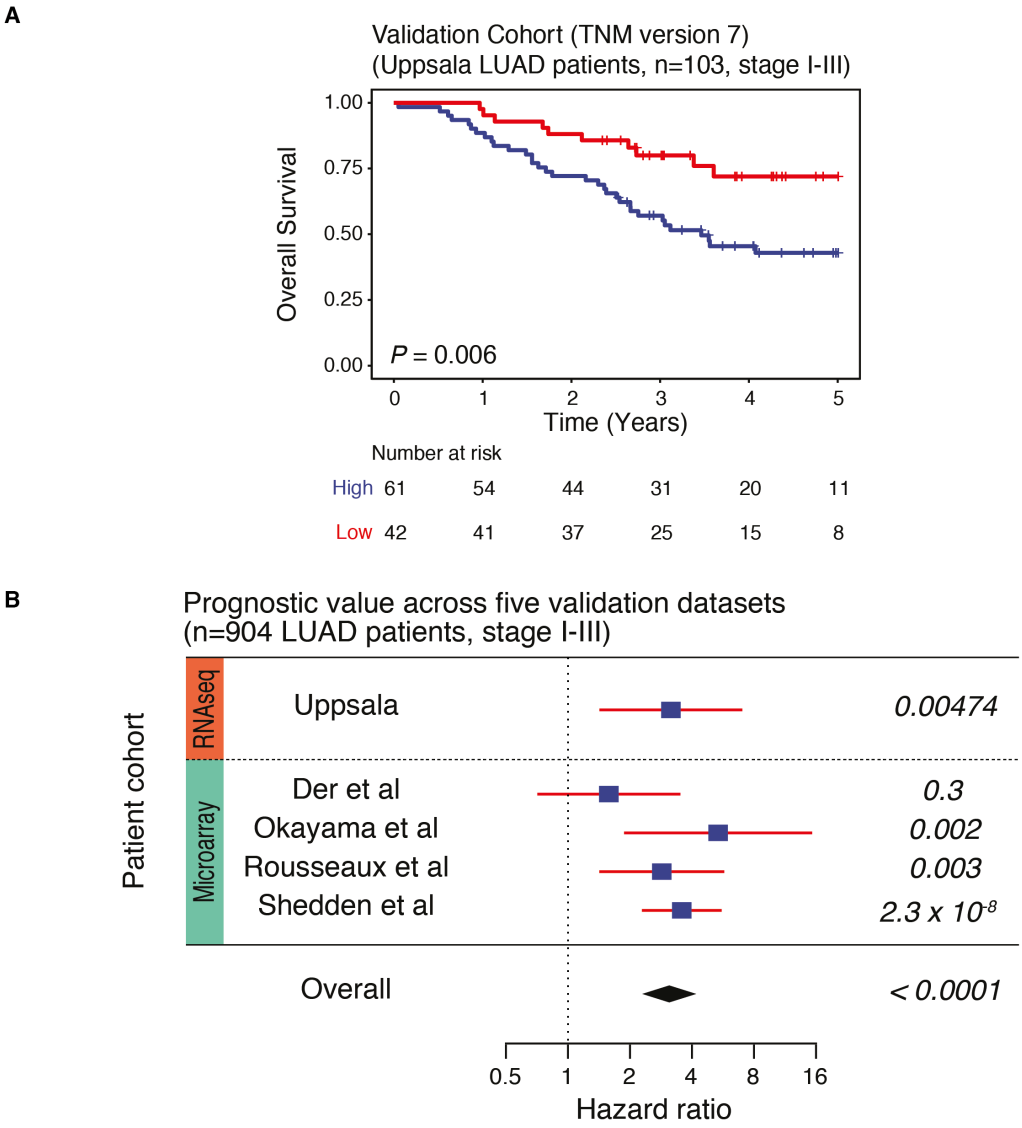

Figure 4-12 Reproducible survival association of ORACLE

A, Kaplan-Meier plot of ORACLE in the RNAseq-based validation cohort (Uppsala, n=103 LUAD patients, stage I-III). Statistical significance was tested with a two-sided log-rank test. B, Prognostic value of ORACLE assessed in a meta-analysis across five validation cohorts of patients with LUAD (n = 904 patients with stage I–III LUAD). Univariate Cox analysis was performed in one RNA-Seq dataset (Uppsala) and four microarray datasets (Shedden et al., Okayama et al., Der et al. and Rousseaux et al.). Hazard ratios with a 95% confidence interval are shown for each cohort and are plotted on a natural log scale. The diamond indicates the hazard ratio for the meta-analysis of the five validation cohorts.

To investigate concordance across multiple cohorts, I conducted a meta-analysis of the prognostic value of ORACLE in the RNA-Seq-based validation cohort and four further microarray datasets. Only 19/23 genes in the ORACLE signature could be recovered from microarray probe sets (*ASPM, CDCA4, FURIN, GOLGA8A, ITGA6, JAG1, LRP12, MAFF, MRPS17, PLK1, PNP, PPP1R13L, PRKCA, PYGB, SCPEP1, SLC46A3, SNX7, TPBG* and *XBP1*). This was expected to impair signature performance in the microarray cohorts, yet ORACLE maintained prognostic value in three out of the four microarray datasets (univariate Cox regression: P=0.002; HR=5.4 (Okayama et al. cohort); P=0.003; HR=2.9 (Rousseaux et al. cohort); P=2.3×10−8; HR=3.6 (Shedden et al. cohort); and P=0.3, HR=1.6 (Der et al. cohort). In the meta-analysis pooling all validation cohorts (combined: n=904 patients with stage I–III LUAD), ORACLE correlated with mortality with a hazard ratio of 3.57 (2.94–3.54, P < 0.0001, Figure 4-12B), indicating a survival association across multiple external datasets, and robust to differences in expression profiling technology.

As the fully specified 23-gene prognostic model for ORACLE could be applied to the RNA-Seq-based validation cohort, I focused on this dataset to examine the clinical utility. Partnering with the curators of this cohort to access detailed clinicopathological annotations, an array of prognostic risk factors were assessed: TNM stage, adjuvant treatment status, age, WHO performance status, smoking history, gender and Ki67 staining percentage. ORACLE maintained prognostic significance in a multivariate analysis adjusted for these risk factors, with an adjusted hazard ratio of 2.64 (1.15–6.05, P = 0.0216, Figure 4-13). This result indicated ORACLE might provide additional predictive utility independent of existing clinicopathological risk factors

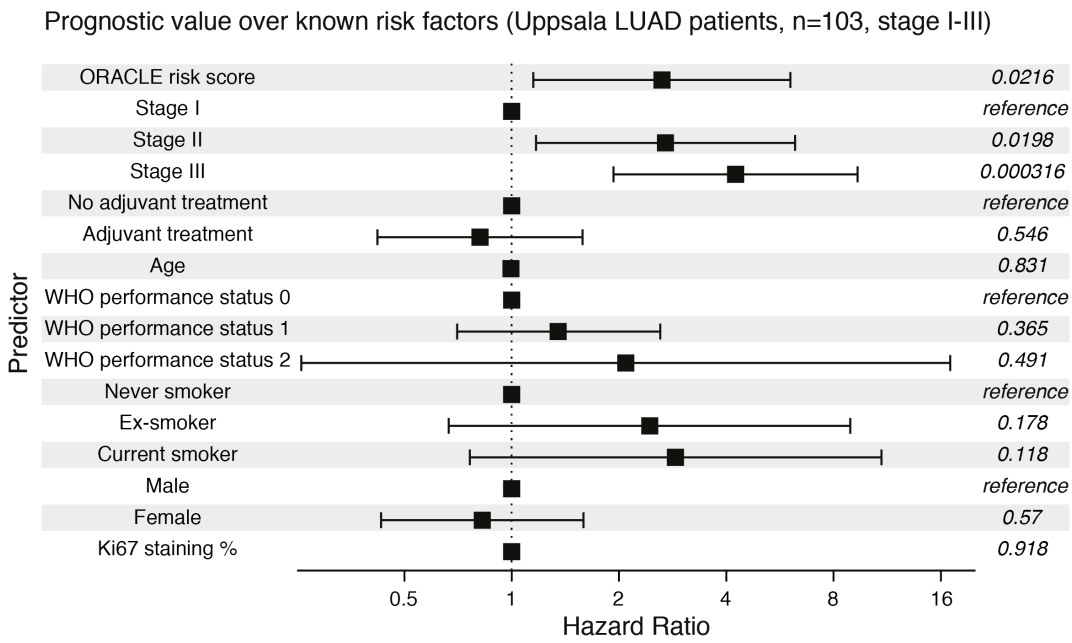

Figure 4-13 Prognostic value of ORACLE beyond existing clinicopathological risk factors

Prognostic value of ORACLE over known risk factors. Multivariate Cox analysis was performed in the Uppsala RNA-Seq dataset (n = 103 patients with stage I–III LUAD), incorporating the ORACLE risk score, tumour stage, adjuvant treatment status, patient age, WHO performance status, smoking status, patient gender and Ki67 staining percentage. Hazard ratios with a 95% confidence interval are shown for each predictor and are plotted on a natural log scale.

Risk stratification of stage I LUAD patients has been highlighted as an urgent clinical need, with implications for therapeutic decision-making (Subramanian and Simon, 2010a; Vargas and Harris, 2016). To evaluate the prognostic ability of ORACLE in this patient subgroup, I selected stage I patients from the RNA-Seq-based validation cohort (n = 60 patients with stage I LUAD). Sub-staging criteria, the existing clinical marker for stage I patients (Goldstraw et al., 2016), stratified patients into stage IA (n=42 patients) and IB groups (n=18 patients) but was not associated with survival in this small cohort of patients (Figure 4-14). By contrast, ORACLE high-risk (n=32 patients) and low-risk (n=28 patients) classifications did separate stage I patients into groups with significantly different mortality outcomes (log-rank P = 0.02, Figure 4-14). Both analyses were repeated using the recently updated TNM version 8 staging criteria (Goldstraw et al., 2016), giving the same result (log-rank P: sub-staging = not significant, ORACLE = 0.018; Figure 4-14). These data suggest that ORACLE is associated with survival outcomes in patients with stage I LUAD.

Taken together, the ORACLE biomarker showed reproducible survival associations in a meta-analysis of more than 900 patients with microarray or RNA-Seq data available, and provided molecular information beyond existing clinicopathological risk factors, specifically in the subgroup of stage I LUAD patients.

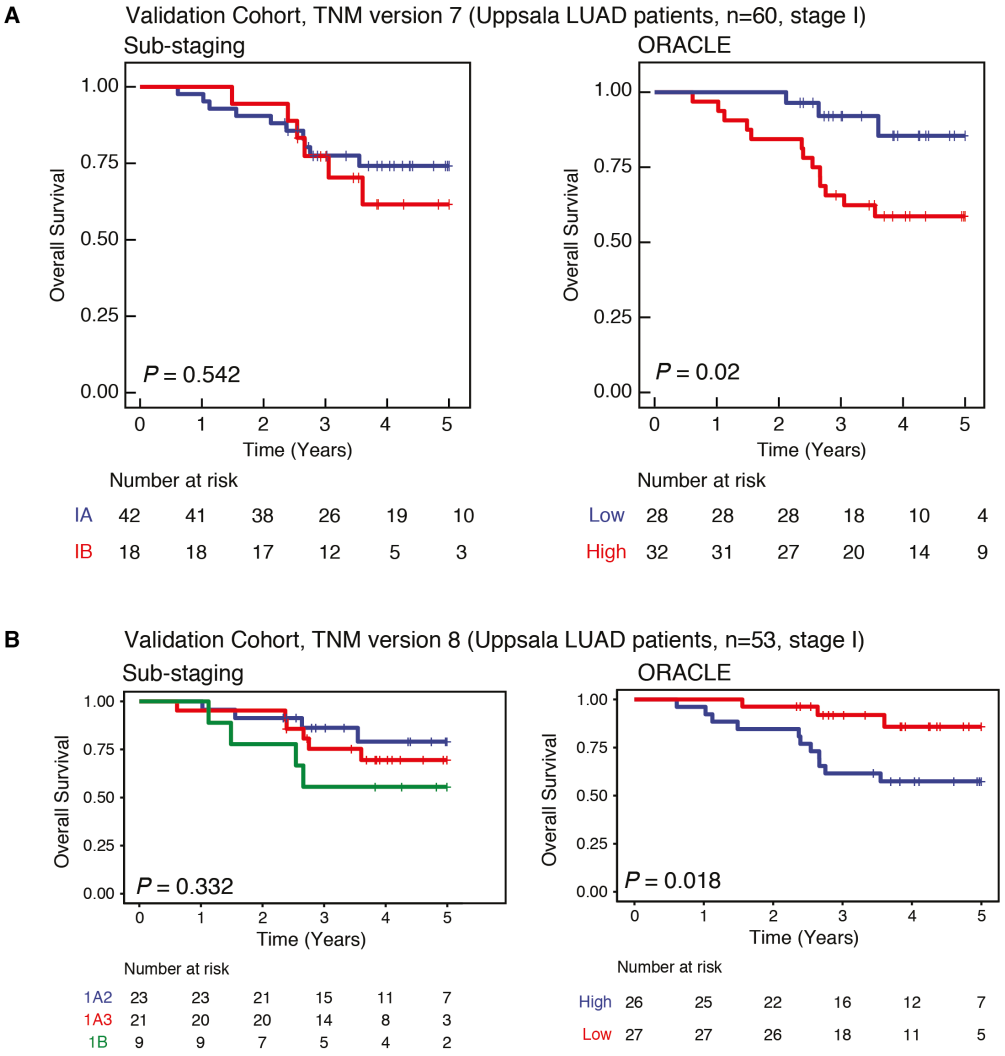

Figure 4-14 Prognostic value of ORACLE in LUAD patients with stage I disease A, The ability of substaging criteria (left) versus ORACLE (right) to split patients into prognostically informative groups was tested in patients with stage I disease. Kaplan–Meier plots with log-rank P values, calculated using data from the Uppsala RNA-Seq dataset (n = 60 patients with stage I LUAD) are shown. B, The ability of substaging criteria (left) and ORACLE (right) to split patients into prognostically informative groups is tested in stage I patients using the updated TNM version 8 criteria, shown as Kaplan-Meier plots for the Uppsala RNAseq dataset (n=53 LUAD patients, stage I, TNMv8). Statistical significance was tested with a two-sided log-rank test.

4.5.3 Benchmark performance against published signatures

The ORACLE signature was checked against a published biomarker – a four-gene RNA-Seq signature (Shukla et al., 2017) mentioned in the previous chapter (see 3.4.1) – to test whether it has better prognostic power. For this analysis the RNA-Seq dataset from the Uppsala cohort (n = 103, stage I-III) was used as an external validation cohort, as described in previous sections (4.4.3 and 4.5.2). Model signature coefficients from the original publication (Shukla et al., 2017) were applied to the validation dataset, calculating a risk-score for each tumour (Figure 15A). Correlating the risk estimates against survival, the continuous risk-score did not exhibit a significant survival association (Cox UVA P=0.156). Moreover, using the median risk-score as a cut-off to dichotomize the cohort, the survival times between risk-groups were not significantly different (log-rank P = 0.1, Figure 15B). In this cohort ORACLE risk estimates were significantly associated with overall survival in both univariate (Figure 4-12A) and multivariate (Figure 4-13) analyses, suggesting it may have greater prognostic power than the published signature in this validation cohort.

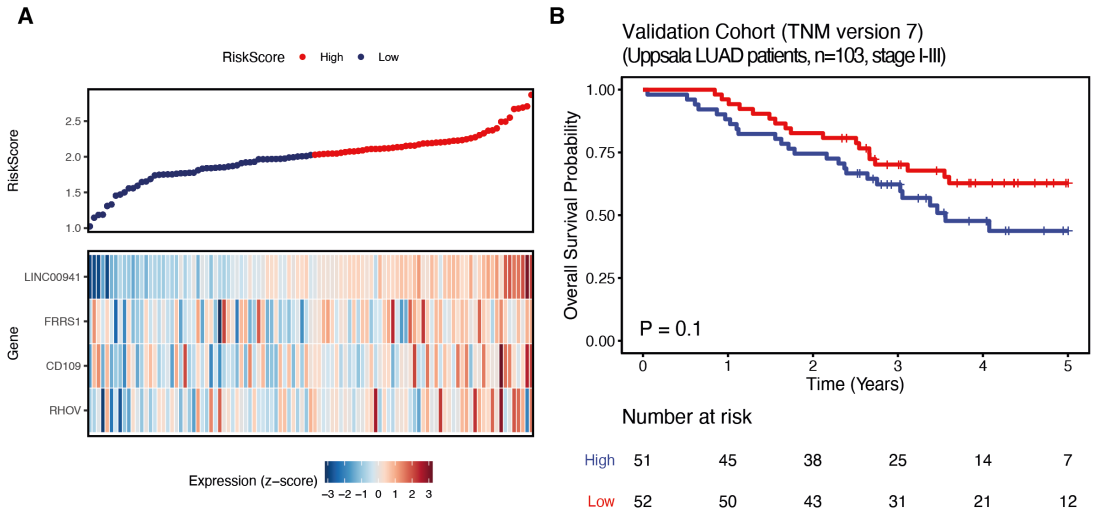

Figure 15 Testing performance of a published RNA-Seq signature

A published RNA-Seq signature (Shukla et al., 2017) **was applied to the RNA-Seq validation dataset from Uppsala University (n=103, stage I-III). A, Expression matrix for the four genes comprising the signature (bottom) and risk-score distribution (top). B, Kaplan-Meier plot of the four-gene signature. Statistical significance was tested with a two-sided log-rank test.**

4.5.4 Biological underpinning

Gene expression signatures can serve as prognostic biomarkers irrespective of their biological meaning, though the limited interpretability of such "black box" classifiers may discourage clinical adoption. By contrast, correlating a prognostic signature with specific biological processes can suggest the underlying mechanism, and help indicate the biomarker may be robustly informative (Topalian et al., 2016). Here, I further developed the biological grounding of ORACLE, querying whether the proposed signature is predominantly expressed on cancer cells or stromal cells, and exploring the axes of correlation between the molecular risk-score and clinicopathological features.

To clarify that the signature is predominantly expressed on cancer cells, correlative analyses was performed in tumour samples from the TRACERx cohort (89 tumour regions from 28 patients with stage I–III LUAD). Firstly, the expression of individual ORACLE genes tracked the copy-number state at the corresponding gene locus, with 91% (21/23) of genes exhibiting a significant ($P<0.05$) positive correlation (Figure 4-16A). Next, I investigated the correlation between ORACLE risk-scores and metrics of immune infiltration derived from bulk sequencing data in TRACERx. There was a significant negative correlation between ORACLE risk scores and most (11/16) immune cell subsets defined using an RNA-Seq- based metric of immune infiltration (Danaher et al., 2017) (Figure 4-16B). A non-significant but trending negative correlation was observed with a WES-based measure of tumour purity (Loo et al., 2010) (Figure 4-16C). Lastly, I accessed a published single-cell RNA-Seq dataset comprised of 52,698 stromal cells sourced from 5 NSCLC patients (Lambrechts et al., 2018). In this scRNAseq study, Lambrechts et al had defined clusters for seven stromal cell-types (alveolar, B cell, epithelial, fibroblast, myeloid, T cell, and vascular). Examining the ORACLE signature in the context of these stromal clusters, most (20/23) of the individual genes in ORACLE displayed negligible expression levels relative to marker genes for stromal cell-types (Figure 4-16D).

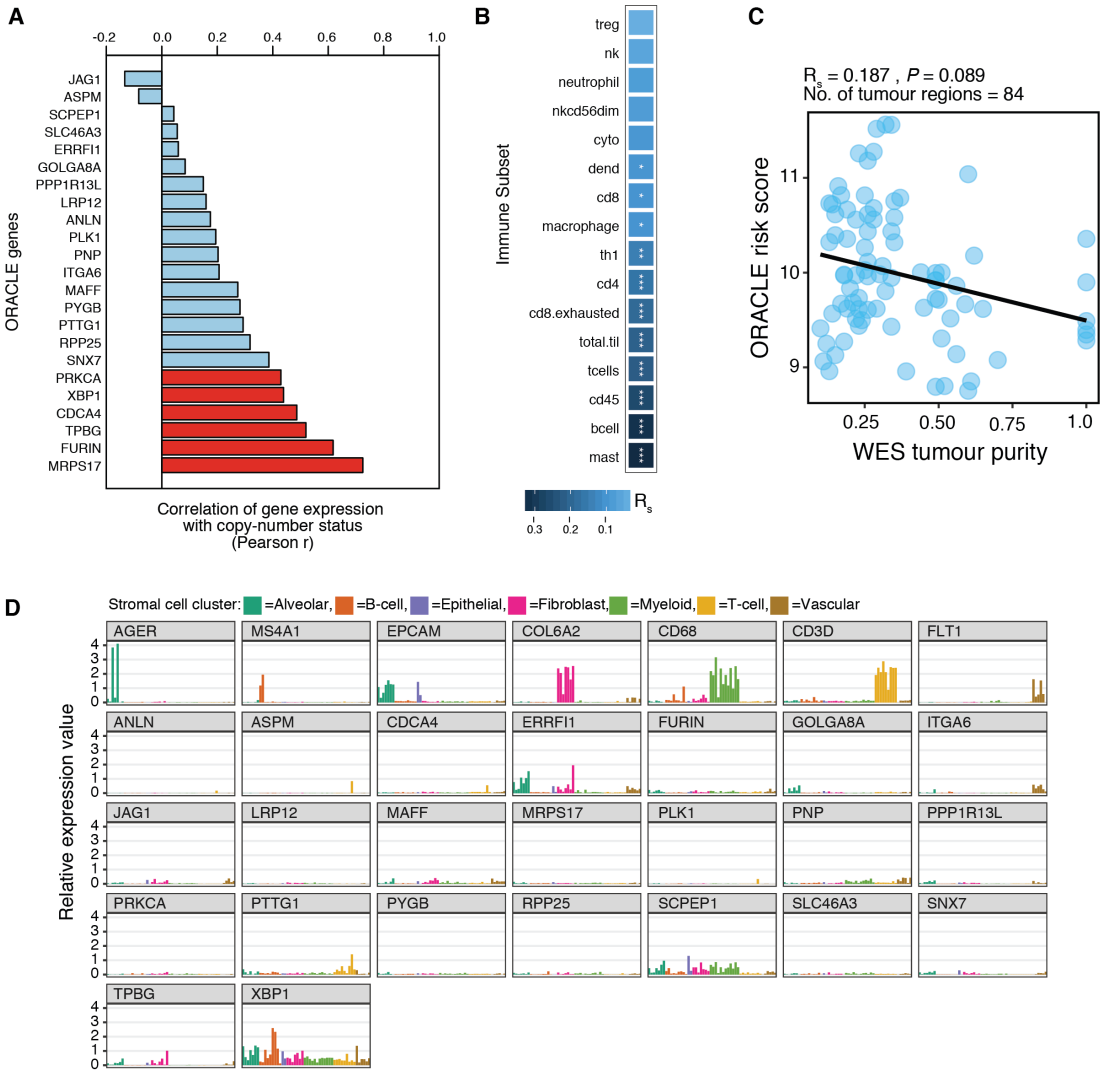

Figure 4-16 ORACLE as a cancer cell expression signature

A, Pearson correlations between the expression of individual ORACLE genes and copy-number state at the corresponding gene locus in the TRACERx cohort (n=28 LUAD patients, 89 tumour regions, stage I-III). Significant correlations (P<0.05, without a multiple-testing correction) are marked in red, non-significant correlations are marked in blue. B, Spearman correlations between the infiltration of immune cell subsets, calculated from RNAseq data using the method described by Danaher et al, and ORACLE risk-scores in the TCGA dataset (n=469 patients, stage I-III). C, The scatter plot shows the Spearman correlation between ORACLE risk score and tumour purity assessed from whole-exome sequencing data using ASCAT, as described by Van Loo et al, in TRACERx (n=28 LUAD patients, 84 tumour regions, stage I-III). D, Lambrechts et al performed single-cell RNAseq on 52,698 cells sourced from 5 NSCLC patients,

then defined 7 clusters of stromal cell genes and provided a per-cluster expression measure for every gene. The relative expression levels (y-axis) for each stromal cluster (coloured by cell-type, see figure legend) is plotted for all 23 genes comprising the ORACLE signature (bottom 3 rows). To aid interpretation, a marker gene for each of the 7 stromal cell clusters is also plotted (top row) for comparison: alveolar (*AGER*), B cell (*MS4A1*), epithelial (*EPCAM*), fibroblast (*COL6A2*), myeloid (*CD68*), T cell (*CD3D*), and vascular (*FLT1*) cell-types.

The correlation between ORACLE risk and established features of tumour aggressiveness was assessed. In the RNA-Seq-based validation cohort, the ORACLE risk scores tracked TNM tumour stage (Figure 4-17A). In addition, I accessed RNA-Seq data for a set of metastatic samples seeded by primary LUAD tumours (n=8 metastatic samples from the MET500 cohort (Robinson et al., 2017)), finding ORACLE expression to be significantly higher relative to primary tumour samples (Figure 4-17A). Immunohistochemical staining for Ki67, a histological marker for cancer cell proliferation, had previously been performed in the TRACERx cohort (Jamal-Hanjani et al., 2017), and was found to be positively correlated with ORACLE risk-scores (Spearman's rho = 0.44; P = 0.0000205, Figure 4-17B).

Taken together, these data suggest that the genes comprising ORACLE are expressed in cancer cells, may serve as a molecular read-out for tumour aggressiveness and metastatic potential, and is more robust to the challenge of tumour sampling bias than existing prognostic signatures.

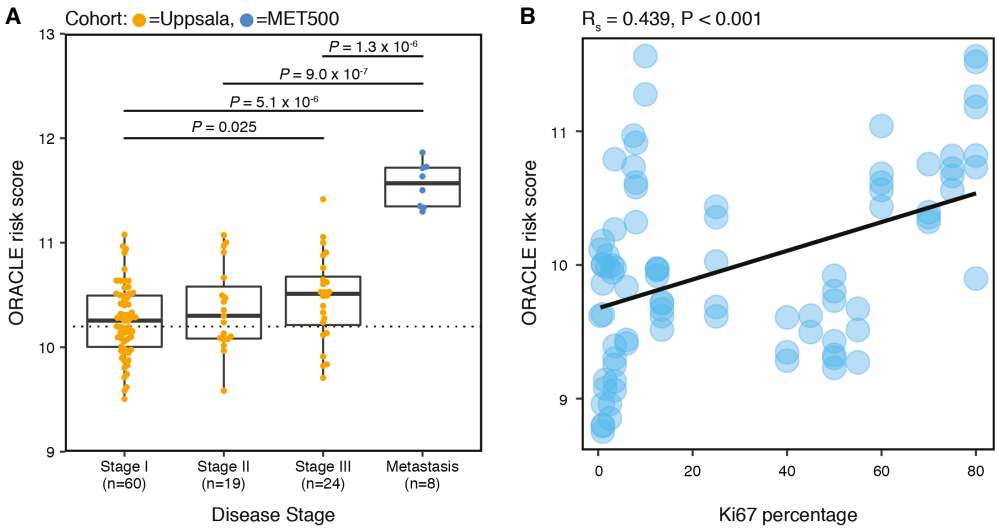

Figure 4-17 ORACLE as a molecular correlate for tumour aggressiveness

A, Boxplots showing the distribution of ORACLE risk scores by disease stage, for the Uppsala cohort (n=103 LUAD patients, stage I-III) and the MET500 cohort (n=8 metastatic samples from patients with LUAD primary tumours). Statistical significance was tested with a Wilcoxon signed rank sum test. No corrections were made for multiple comparisons. B, The scatter plot shows the Spearman correlation between Ki67 staining % and ORACLE risk-scores in the TRACERx cohort (n=28 LUAD patients, 89 tumour regions, stage I-III).

4.5.5 Tumour sampling bias

In the previous chapter, the sampling bias of published prognostic signatures for LUAD was assessed in the multi-region RNA-Seq dataset of TRACERx LUAD patients. The discordance rates of two RNA-Seq-based prognostic signatures was directly quantified as 29% and 43%. Separately, a clustering metric was used to assess the discordance of 9 published signatures (including microarray and qPCR signatures) invariant of the expression profiling technology, revealing an average discordance rate was 50%.

The sampling bias of ORACLE was assessed in the multi-region RNA-Seq dataset of TRACERx LUAD patients. Only 11% of the cohort (3/28 patients) exhibited discordant classification (Figure 4-18). This indicates ORACLE may be more robust to the problem of sampling bias then previous approaches agnostic to RNA-ITH, though would need to be confirmed in an external multi-region RNA-Seq validation dataset.

It is worth considering why the clonal approach taken here did not completely eliminate the problem of sampling bias in lung cancer. In their analysis of expression data from >5000 breast tumours, Tofigh and colleagues suggested that a subset of patients were “inherently difficult” due to high levels of ITH, and should be separately classified (Tofigh et al., 2014). Along these lines, it is notable that the three patients displaying discordant risk classification for ORACLE did not consist of border-line samples on either side of the risk-score cut-off (Figure 4-18). Rather, these three tumours were amongst the highest for variance in risk-score between tumour regions, possibly indicating a higher global state of RNA-ITH.

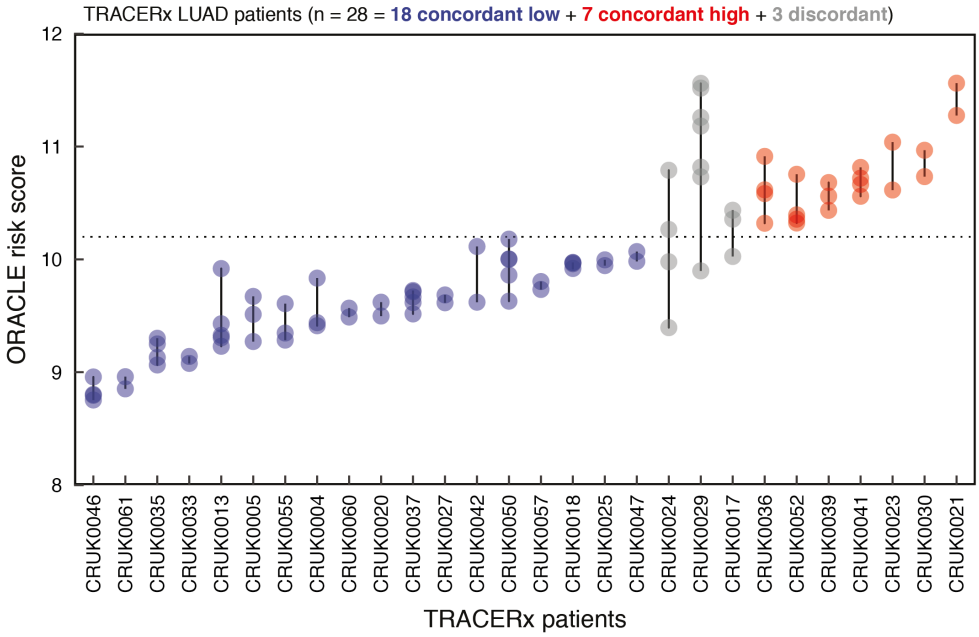

Figure 4-18 Tumour sampling bias of ORACLE

Tumour sampling bias of the ORACLE signature assessed using multi-region RNAseq data from TRACERx (n=28 LUAD patients, 89 tumour regions, stage I-III). Each point represents a single tumour region, vertical lines display the range for each patient, and patients are ordered by predicted survival risk score. Points are coloured according to the risk classification of tumour regions within a patient: concordant low-risk (blue), concordant high-risk (red), or discordant (gray).

4.6 Prognostic relevance of homogeneously expressed genes across cancer types

4.6.1 Pan-cancer analysis

The sampling bias problem for molecular biomarkers has been described in histologies other than lung cancer, including renal, breast and prostate cancer (Boutros et al., 2015; Gerlinger et al., 2012; Gyanchandani et al., 2016).

To explore whether clonal biomarker design may hold prognostic relevance across other cancer types, I downloaded gene-wise prognostic values from two pan-cancer resources:

1) Prediction of Clinical Outcomes from Genomic Profiles (PRECOG) dataset, survival associations (z scores) calculated from 166 microarray datasets covering 39 cancer types (Gentles et al., 2015);
2) Human Pathology Atlas, survival associations (log-rank P values) calculated from RNA-Seq data of 17 cancer types (Uhlen et al., 2017).

RNA heterogeneity quadrants were calculated using the full TRACERx cohort with multi-region RNA-Seq data available (156 regions, 48 NSCLC patients, stage I-III). The proportion of genes within each quadrant that were found to give a significant prognostic value was assessed, both pan-cancer and for individual histologies.

Assessing pan-cancer survival associations in the PRECOG dataset, Q4 genes were significantly enriched in prognostic genes compared with all other quadrants (Q1 versus Q4: P = 8.9 × 10−27; Q2 versus Q4: P = 9.3 × 10−8; Q3 versus Q4: P = 1.9 × 10−18, Figure 4-19). In a finer-grained analysis, assessing each of the 39 histologies individually, 49% (19/39) of cancer types were significantly enriched for prognostic genes in Q4; only one cancer type, head and neck cancer, was significantly depleted (3% of cancer types (1/39)). Conversely, Q1 (high intra-tumour variability and low inter-tumour variability) was significantly depleted in 56% (22/39) of cancer types, and enriched in 0% (0/39). Both Q2 (low intra- and inter-tumour variability) and Q3 (high intra- and inter- tumour variability) showed similar numbers of depleted and enriched cancer types. The subset of genes in Q4 was also prognostically relevant across several cancer-types from the Human

Pathology Atlas dataset: 35% of cancer-types (6/17) were significantly enriched for prognostic genes, and none (0/17) were depleted.

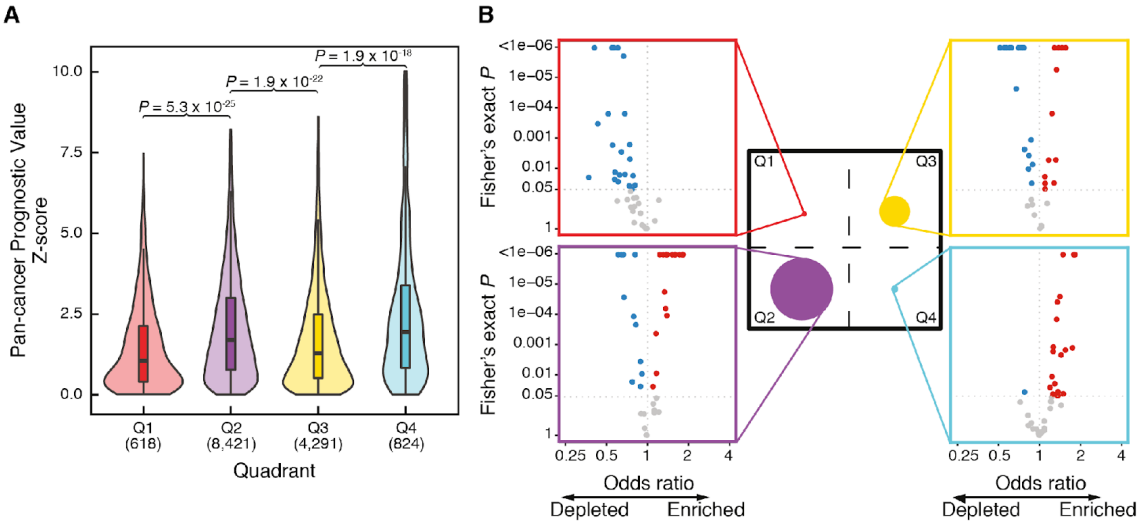

Figure 4-19 Survival association of RNA heterogeneity quadrants across cancer types

Pan-cancer prognostic scores sourced from the PRECOG database (n = 17,808 tumours from 39 malignant histologies) and evaluated in the context of RNA heterogeneity quadrants. A, Box plots showing gene-wise pan-cancer survival associations are evaluated by NSCLC RNA heterogeneity quadrant. Z scores were sourced from the PRECOG database (n = 17,808 tumours from 39 malignant histologies). A |z| score > 1.96 is equivalent to a two-sided P < 0.05. Statistical significance was tested with a two-sided t-test. B, Survival association of RNA heterogeneity quadrants for individual cancer types. Each point corresponds to 1 out of 33 cancer types. The number of prognostically significant genes (|z| score > 1.96, equivalent to a P value < 0.05) per NSCLC RNA heterogeneity quadrant is indicated for each cancer type as non-significant (gray), significantly enriched (red; odds ratio > 1) or significantly depleted (blue; odd ratio < 1). Odds ratios are plotted on a natural log scale. Statistical significance was tested with a two-sided Fisher's exact test. No corrections were made for multiple comparisons.

These analyses indicated that homogeneously expressed biomarkers, derived as such in a multi-region lung cancer dataset, displayed a significant enrichment for prognostic genes in 35-49% of cancer types from two pan-cancer datasets

4.7 Conclusions

4.7.1 Summary of findings

The results of this chapter provide a means to address the diagnostic challenge of tumour sampling bias in lung cancer, and possibly other histologies.

The global analysis of RNA heterogeneity revealed greater inter- than intra-tumour RNA heterogeneity. This result is in line with results from other multi-region studies of cancer transcriptomes. Gyanchandani et al profiled 181 samples from 71 ER+ breast tumours, finding samples clustered by patient in 86% of cases (Gyanchandani et al., 2016). Similarly, in a small cohort of medulloblastoma patients, Morrissy et al described that multi-region samples from 8 patients tightly clustered together (Morrissy et al., 2017). Extending to metastatic disease, Suda et al performed RNA profiling of 30 samples from five NSCLC patients (Suda et al., 2018) – including primary tumours, and intra/extra-thoracic metastatic lesions – finding all primary and metastatic samples clustered by NSCLC patient. Overall, these analyses suggest that the subset of most variably expressed genes could represent a molecular fingerprint unique to individual NSCLC tumours. However, these global analyses do not incorporate prognostic information, so may not provide a clinically informative signature.

To perform feature selection in a manner that overcame sampling bias, a core set of genes were defined with low intra- yet high inter-tumour RNA heterogeneity that were expressed uniformly within individual tumours, so robust to sampling bias, but are also highly variable between tumours, so they remained informative for patient stratification. These genes were enriched for chromosome copy-number gains early in tumour evolution, hence were termed “homogeneously expressed”, and was significantly enriched for genes that reproducibly maintained prognostic value in validation datasets of lung cancer patients (five separate cohorts) and in a pan-cancer analysis (39 cancer-types). Taken together, these data strongly suggest that homogeneously expressed genes may be optimal candidates for the development of biomarker assays, both in lung cancer and possibly as a general strategy for refining biomarkers across cancer types.

In addition to defining homogeneously expressed genes, further selection of genes associated with survival yielded a novel Outcome Risk Associated Clonal Lung Expression (ORACLE) signature. ORACLE was discordant in 11% of LUAD patients from the multi-region RNA-Seq cohort, which compares favorably with the discordance rates of two RNA-Seq-based prognostic signatures of 29% and 43%. In addition, 100% (23/23) of the ORACLE genes are homogeneously expressed, compared with 36% (11/14) of genes from the clinically approved Razor Genomics signature (Kratz et al., 2019). This indicates ORACLE may be more robust to the problem of sampling bias then previous approaches agnostic to RNA-ITH.

Failure to validate in independent patient cohorts, possibly due to differences in patient factors such as ethnicity or diet, has been highlighted as a major weakness of previous prognostic signatures in lung cancer (Subramanian and Simon, 2010a). ORACLE associated with survival in a meta-analysis involving 904 patients from five independent cohorts, indicating the signature may be driven robust tumour intrinsic features. Biomarker based classification of patients with stage I disease has been identified as a high impact area for thoracic oncology (Subramanian and Simon, 2010a; Vargas and Harris, 2016). ORACLE stratified stage I patients into high- and low-risk subgroups with significantly different survival times, providing prognostic value that substaging criteria (IA/IB) (Goldstraw et al., 2016) could not achieve in the small cohort of patients available for this analysis (n=60).

Overall, these results describe a technical advance in the field of expression-based prognostic prediction and provide a promising molecular biomarker with the potential to improve diagnostic precision in lung cancer beyond the TNM staging system if further validated as a clinical assay.

4.7.2 Future work

Whether ORACLE is exclusively expressed by cancer cells remains an outstanding question (see section 4.5.4). Spatially resolved RNA analysis of the genes comprising ORACLE from intact tissue – leveraging emerging technologies such as spatial transcriptomics (Ståhl et al., 2016), STARmap (Wang et al., 2018), or Digital Spatial Profiling (Merritt et al., 2020) – could provide an answer.

Given the rapid developments in targeted therapy and immunotherapy, in both the metastatic disease setting and the surgical adjuvant setting, the prediction of response to adjuvant therapy is a key question. Two expression-based predictive biomarkers for CPI, the IPRES (Hugo et al., 2016) and TIDE (Jiang et al., 2018) signatures, were evaluated in the TRACERx cohort revealing discordance rates of 33% and 44% respectively (Rosenthal et al., 2019). This indicates the design of homogeneously expressed biomarkers may have wider applications outside of global prognostication. Indeed, the published results of this chapter have been independently cited to support the need for a clonal biomarker of CPI sensitivity (Suda and Mitsudomi, 2020).

Chapter 5. *In silico* dissection of the tumour microenvironment

5.1 Introduction

The tumour microenvironment consists of the non-malignant cells present in the tumour bulk (including fibroblasts, endothelial, and immune cells), as well as extracellular matrix and signaling molecules. In treatment-naive lung cancer, the cellular components of the TME have been shown to influence cancer initiation (Mascaux et al., 2019; Pennycuick et al., 2020) and the outgrowth of immune-evasive clones (AbdulJabbar et al., 2020; Rosenthal et al., 2019). Moreover, signals from the lung stromal niche govern the propensity of primary tumours in other organs to initiate pulmonary metastases (Malanchi et al., 2012). Immune infiltration has a prognostic impact in both early- and late-stage NSCLC (Dieu-Nosjean et al., 2008; Goc et al., 2014; Hirayama et al., 2012; O'Callaghan et al., 2015; Ohri et al., 2009). The clinical relevance of the lung TME is further highlighted under treatment, providing a safe haven from genome-targeted therapies (Katayama et al., 2012; W. Wang et al., 2009), and playing a role in determining responses to checkpoint blockade immunotherapy (Ganesan et al., 2017; Thommen et al., 2018).

In silico dissection of the TME from bulk expression data provides an attractive approach for quantifying the cellular composition of the stromal components of tumours. A highly accurate computational tool could help expedite the delivery of genomics-driven precision oncology (Dijkstra et al., 2016). In this chapter, I first provide an overview of existing RNA-based methods for TME cell-type enumeration. Next, I describe how global transcriptional profiles were generated for stromal cell-types that were purified *ex vivo* from lung tissue. Lastly, I present interim results from two sets of analyses. The first aims to demonstrate how purified stromal transcriptomes might yield biological insights into phenotype molding within the lung TME. The second suggests this dataset could provide a foundation for deriving higher-fidelity stromal signatures, addressing some of the shortcomings of existing computational methods.

5.2 RNA deconvolution of the tumour microenvironment

5.2.1 Anatomy of an RNA-based TME enumeration tool

There is a growing ambition to incorporate quantitative measures of TME composition into clinical practice, using more fine-tuned descriptions than “immune-hot” or “immune-cold”, as prognostic or predictive biomarkers (Chen and Mellman, 2017; Hirata and Sahai, 2017; Sharma et al., 2017). A major obstacle is the difficulty in applying traditional immunophenotyping techniques like flow cytometry, CyTOF or multiplexed IHC to clinical samples. These techniques are limited by sample throughput, complex tissue preparation requirements and cell extraction bias (Newman and Alizadeh, 2016). The computational deconvolution of RNA data from bulk tumours offers a means to overcome these limitations (Newman and Alizadeh, 2016).

Gene expression data from bulk tumours contains multiple levels of biological heterogeneity, including variation in cell-type proportions and the differing activation states of individual cell-types, both of which can be markedly influenced by tissue pathology (Shen-Orr and Gaujoux, 2013). The anatomy of a typical RNA-based cell-type enumeration tool is illustrated (Figure 5-1A). A bulk RNA admixture (Figure 5-1B) and a reference matrix of cell-type signatures (Figure 5-1C) are both taken as input. There are two major classes of enumeration method: enrichment and deconvolution (Figure 5-1D). Both classes select genes from the signature matrix to calculate cell-type-specific enumeration scores. Some tools also output additional information, such as cell-type-specific activation states (Newman et al., 2019) or a measure of confidence in the estimation (Newman et al., 2015).

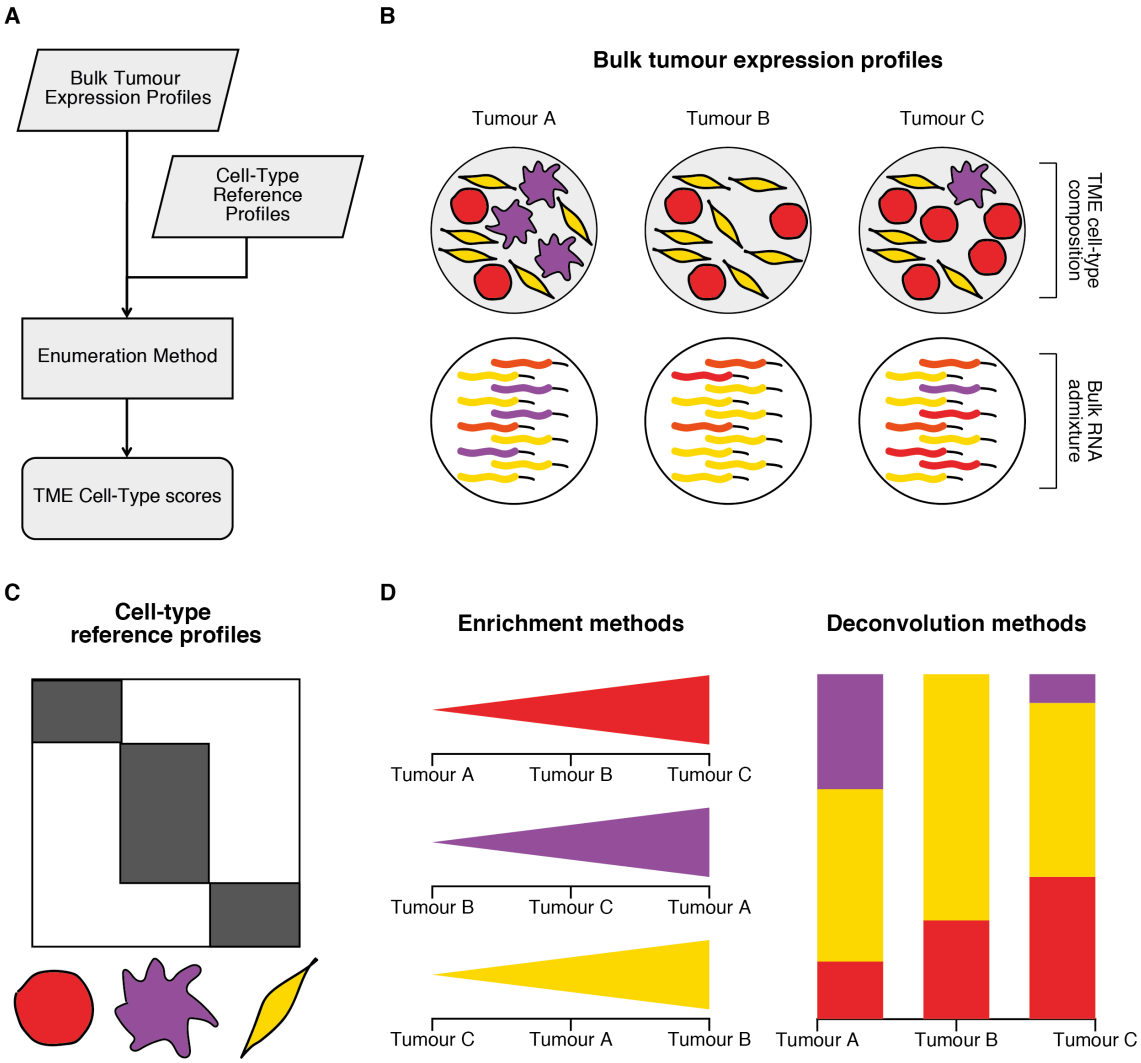

Figure 5-1 Anatomy of an RNA-based TME enumeration tool.
(A) Schematic diagram to display the computational pipeline for a typical RNA deconvolution tool: bulk tumour transcriptomes and a reference matrix of cell-type signatures are inputted to an enumeration method, outputting scores estimating the abundance of TME-cell-types. (B) Illustration of three tumours, showing how variation in stromal cellular compositions drives the transcriptional patterns observed in bulk RNA data. (C) Cartoon illustration of the gene expression heatmap for a set of TME signatures. The heatmap rows correspond to genes from cell-type signatures, and the heatmap columns are expression experiments from purified cells for each cell-type. (D) The differing outputs for two types of TME cell-type enumeration methods: "low-resolution" rankings for enrichment methods (left); "high-resolution" proportions for deconvolution methods (right).

Here I highlight a few published tools to discuss the benefits and limitations of existing methods.

ESTIMATE. The ESTIMATE method, developed by Yoshihara and colleagues (Yoshihara et al., 2013), uses “stromal” and “immune” gene-sets (each containing 141 genes) to quantify the abundance of broad TME cell classes. An enrichment type method is used for enumeration, specifically single-sample GSEA. The method works with both RNA-Seq and microarray data,

Cytolytic activity score. The cytolytic score method, developed by Rooney and colleagues (Rooney et al., 2015), aims to capture the cytolytic activity of tumour infiltrating immune cells from tumour RNAseq data by taking the geometric mean of two cytolytic effectors, granzyme A (*GZMA*) and perforin 1 (*PRF1*). This is another enrichment type method that can be applied to tumour RNA-Seq data.

CIBERSORT. The CIBERSORT tool was an early adopter of the deconvolution class of enumeration method (Newman et al., 2015). This provided a blueprint to translate ideas about RNA-based deconvolution from immunology into the cancer field in 2015, and the CIBERSORT tool has since been widely used for research applications. The cell-type reference matrix contains signatures for 22 immune cell subsets, and was derived from public datasets of cell-types extracted from healthy human blood. Deconvolution is performed using linear support vector regression. The signature coefficients were derived using microarray data, which may limit applicability to RNA-Seq datasets.

TIMER. Li and colleagues designed an alternative enumeration method relying on deconvolution (Li et al., 2016). Here, gene-sets were derived for 6 immune subsets, based on negative correlations with tumour purity. Constrained least-squares fitting was the approach used for deconvolution.

5.2.2 Limitations of existing tools

Accuracy is the major limitation of existing RNA-based TME enumeration tools. Current tools exhibit systematic error compared to “ground-truth” assays like flow cytometry and IHC, even under ideal conditions. In an analysis of peripheral blood mononuclear cells, comparison of CIBERSORT estimated cell-type fractions to FACS-purified cell populations revealed poor accuracy in the identification of key subsets such as activated memory CD4 T cells (~70%), plasma cells (~60%), and γδ T cells (~40% accuracy) (Gentles et al., 2015; Newman et al., 2015). Error introduced by the systematic over- or under-estimation of the infiltration of certain cell-types might contribute to the limited clinical translation of existing tools. A recent PD1-inhibitor trial in patients with metastatic melanoma found that CIBERSORT did not predict CPI response (Liu et al., 2019), despite previous studies demonstrating a clear association of intra-tumoural CD8+ T-cells with response to CPI therapy (Edwards et al., 2018).

A minor criticism is a failure to include key cell-types or quantify cell-types at fine granularity. For the majority of TME enumeration tools, the cell-type reference matrix is comprised solely of immune cell-type signatures, neglecting the fibroblast compartment for example. The fitting of an incomplete reference matrix to a bulk RNA admixture, that contains additional cell-types, both introduces noise (Racle et al., 2017) and restricts biological interpretation (Becht et al., 2016).

In the past, tools have also been limited by platform restrictions. For example, the original CIBERSORT tool was developed for use with microarray data (Newman et al., 2015), so cannot easily be applied to RNA-Seq data due to probe bias and differences in dynamic range (Ali et al., 2016; Charoentong et al., 2017). However, this critique has become out-dated as most recent tools are platform agnostic (Newman et al., 2019).

5.2.3 Cell-type reference profiles

The set of cell-type reference profiles inputted to a TME enumeration tool (Figure 5-1C) is typically a matrix of genes and cell-types, which should reflect cell-type-specific expression in the human tumour microenvironment. However, the majority of reference profiles for existing tools were not derived using data from human cancers. For example, CIBERSORT was developed using RNA data from immune cells isolated from the peripheral blood and bone marrow of healthy volunteers (Newman et al., 2015). Another method, derived by Davoli et al, trained a reference matrix using murine immune subsets (Davoli et al., 2017). The EPIC tool is a notable exception, which has reference profiles derived using published scRNAseq data from human cancers (Racle et al., 2017). The CIBERSORT authors suggested that "the most significant current limitation of CIBERSORT is the fidelity of reference profiles ... sampling a larger expression space, for example tumour-infiltrating immune cells, may mitigate this issue" (Newman et al., 2015).

Indeed, there is growing evidence that the molecular profile of stromal cells in primary tumours differs from healthy tissue. Through in-depth profiling of CD8+ T-cells from a cohort of NSCLC patients, Ganesan and colleagues established that TILs displayed signals of increased cycling and TCR-activation relative to cells isolated from adjacent non-malignant lung tissue, concluding that transcriptional profiling of purified TILs might help inform clinical decision-making over the use of CPI therapy (Ganesan et al., 2017). Similarly, Thommen and colleagues found that TIL populations from lung tumours harboured a distinct transcriptional profile from cells isolated from healthy blood, exhibiting up-regulated cell cycle and cell division modules (Thommen et al., 2018).

In a meta-analysis of existing tools, Sturm and colleagues tested analytical sensitivity to determine the limits of detection (Sturm et al., 2019). Using "pseudo-bulk" tumours, generated by mixing known cellular proportions from single-cell datasets, the ability of each tool to reliably detect the abundance of a particular TME cell subset as significantly different from the background was assessed. The best performing tool in this benchmark analysis, Xcell (Aran et al., 2017), could

detect most cell-types at >5% infiltration. This performance was attributed to the fidelity of the Xcell reference matrix (Sturm et al., 2019).

Overall, this highlights the need to understand the difference between blood-, healthy tissue- and TME-derived signatures. Functional changes for each cell-type between environmental contexts may undermine the performance of existing cell-type signatures. Moreover, multiple lines of evidence suggest that the derivation of tumour-specific cell-type signatures will improve the fidelity of reference profiles, potentially increasing prediction accuracy.

5.2.4 Enumeration methods

Approaches for quantifying the presence of cell subsets in heterogeneous samples fall into two categories (Figure 5-1D): enrichment methods and deconvolution methods (Newman and Alizadeh, 2016; Shen-Orr and Gaujoux, 2013).

Enrichment methods define marker genes, as clusters of genes enriched in specific TME cell-types, and output low-resolution estimates of cell presence that can be ranked. Rooney and colleagues justified the use of *GZMA* and *PRF1* expression levels as marker genes for immune cytotoxic activity as these genes were tightly co-expressed in patient samples and exclusively expressed by NK (natural killer) and T-cell subsets (Rooney et al., 2015). Davoli and colleagues developed a set of signatures through pairwise differential expression of RNA data from the from the ImmGen database, selecting the top 20 over-expressed genes per cell-type, then further manually subsetting to genes specific to individual immune cell-types (Davoli et al., 2017). Instead of geometric mean, this method is applied using Gene-Set Enrichment Analysis (GSEA). Enrichment methods are robust to platform-specific noise. For example, an IFN-γ signature predicting response to PD1 blockade was originally derived using RNA-Seq data (Ayers et al., 2017), and recently successfully validated on the NanoString nCounter platform (Cristescu et al., 2018). However, the low-resolution enumeration outputs of marker gene methods are of limited clinical utility. Furthermore, if marker gene expression is not

cell-type-specific, these methods can be confounded by collinear expression between closely related cell-types.

Deconvolution methods yield high-resolution numeric estimates of cell-type proportions. This is akin to performing *in silico* flow cytometry on admixed RNA data from bulk tumours. The CIBERSORT method performs deconvolution of RNA admixtures using support vector regression, a non-linear machine learning algorithm that fits a regression hyperplane to as many data points as possible, with hyperplane orientations outputted as equal to estimated cell-type proportions (Newman et al., 2015). Machine learning algorithms could unpick subtle transcriptomic differences, overcoming the need for exclusive cell-type-specific expression for all genes in the reference matrix. Moreover, the CIBERSORT deconvolution approach was able to accurately enumerate artificially generated RNA admixtures of increasingly correlated cell-types. However, there is an ongoing debate over the choice of deconvolution method. Li and colleagues developed TIMER, which used linear regression-based deconvolution (Li et al., 2016), and have argued strongly that linear methods are sufficient for the problem of TME deconvolution (Bo Li et al., 2017; Newman et al., 2017).

Both enrichment and deconvolution approaches have been widely used in the literature for discovery reasons, but a consensus approach and reproducibility would be necessary for the next step towards clinical translation.

5.3 RNA profiling of stromal cells from lung cancer patients

5.3.1 *Ex vivo* purification of 15 TME cell subsets

A cohort of patients with treatment-naïve lung cancer underwent surgical resection with curative intent in the TRACERx study and also at the University of Edinburgh. Following surgical resection, tumour and paired non-malignant tissue materials excess to clinical diagnosis requirements were processed in the research lab to yield single-cell suspensions of stroma cells. Briefly, tumour and tissue chunks were finely minced with sterile scalpels before digestion with DNase and collagenase, followed by removal of dead cells by Ficoll gradient isolation. Single cell suspensions were isolated from the Ficoll interface and frozen.

Three multiparameter panels were used for FACS to isolate 15 stromal cell-types. The recovered cell-types can be broadly grouped into three categories, comprised of lymphoid immune cells, myeloid immune cells, and non-immune stromal cells. Lymphoid immune cell-types included CD8+ T-cells, CD8+PD1-high T-exhausted cells, CD8+PD1-low T-effector cells, CD4+ T-cells, CD4+CD25+ T-regulatory cells, two γδ T-cell subsets, B-cells and NK cells. Myeloid immune cell-types included neutrophils, dendritic cells (DC), monocytes, and macrophages. Lastly, non-immune stromal cells were fibroblasts, and endothelial cells.

Two multiparameter panels were used to isolate T-cell subsets and other leucocyte subsets from TRACERx samples (Figure 5-2, Figure 5-3). The third multiparameter panel was used to isolate fibroblasts and endothelial cells from University of Edinburgh samples **(**Figure 5-4). Overall, 194 samples of stromal cell subsets were isolated from 28 patients with NSCLC.

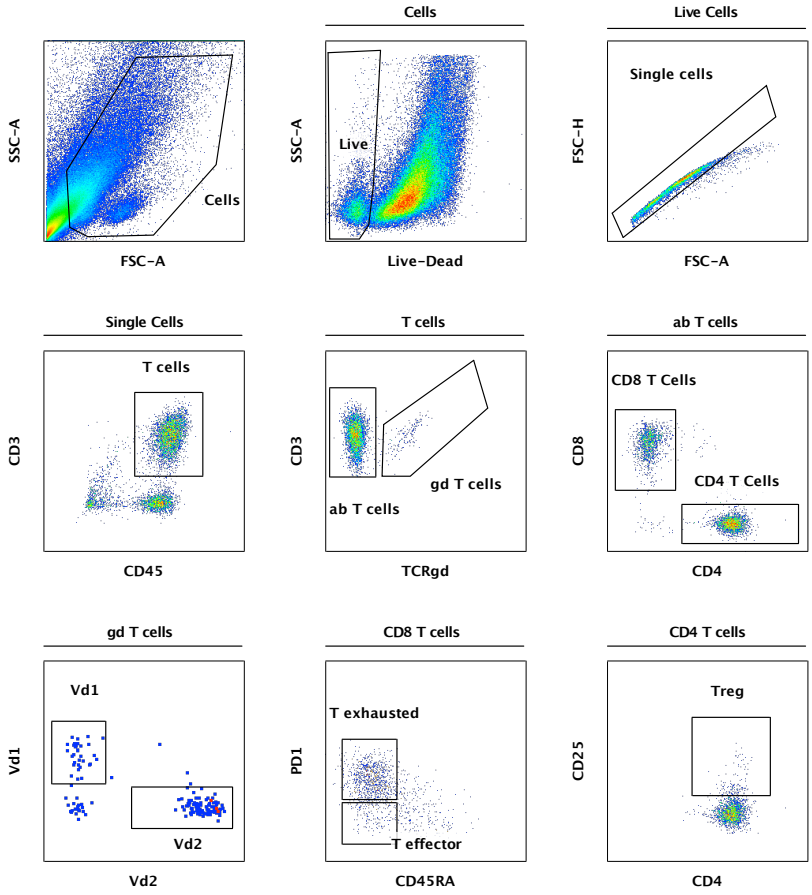

Figure 5-2 FACS gating strategy for T-cell subsets

Representative samples demonstrating gating strategies of T-cell subsets. Purified cell-types included CD8+ T-cells, CD4+ T-cells, two γδ T-cell subsets, CD8+PD1-high T-exhausted cells, CD8+PD1-low T-effector cells, and CD4+CD25+ T-regulatory cells.

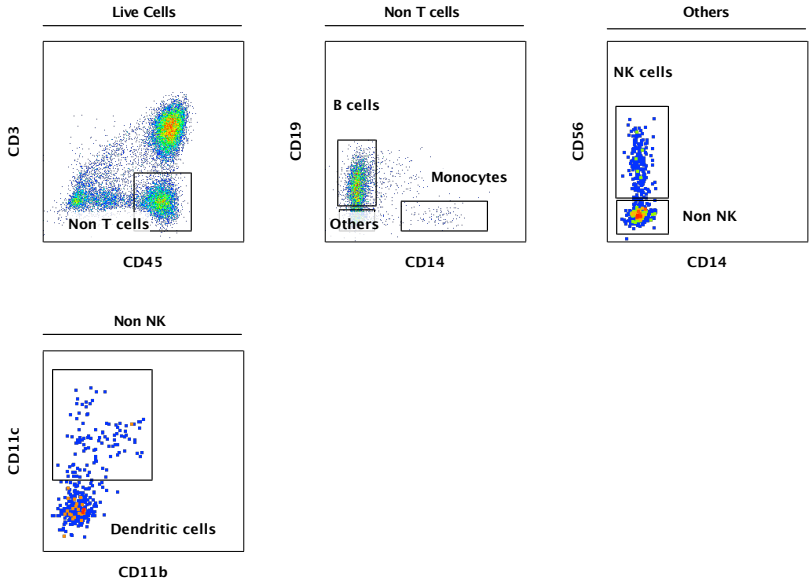

Figure 5-3 FACS gating strategy for other leucocyte subsets

Representative samples demonstrating gating strategies of other leucocyte subsets. Purified cell-types included B-cells, monocytes, NK cells and DCs.

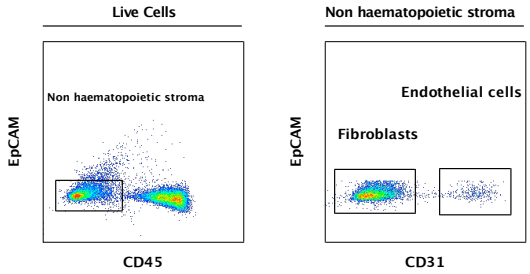

Figure 5-4 FACS gating strategy for non-immune stromal cell subsets

Representative samples demonstrating gating strategies of non-immune stromal cell subsets. The purified cell-types were fibroblasts, and endothelial cells.

5.3.2 Genome-wide RNA profiling of isolated cell-types

Following FACS, the sorted cell-types were processed using RNA extraction and a protocol for low input amounts of RNA (Smart-Seq2 (Picelli et al., 2014)) was used for library preparation. Genome-wide RNA expression levels were quantified through RNA-Seq, to a depth of ~20 million reads per sample, across the 15 stromal cell subsets. For quality control prior to downstream analysis, samples were filtered according to two quality metrics: flow cytometry (antibody staining) and RNA-Seq (number of genes uniquely aligned). In the flow cytometry quality control step, 16 samples were excluded (15 γδ T-cell samples, and 1 T-reg sample) due to poor CD8+ staining. The cutoff for the number of genes uniquely aligned was set to >3,500. In this quality control step 19 additional samples were excluded. After quality filtering, genome-wide expression values were obtained for 159 samples from 24 patients. Of these, 87 samples originated from lung tumours and 72 from matched non-malignant lung tissue.

The expression profiles of canonical cell-type marker genes were examined to assess the purity of cell populations isolated by FACS, and also RNA-Seq efficacy (Figure 5-5). This was broadly reassuring, for example the cell surface glycoprotein *CD8B* was exclusively expressed by the three subsets of CD8+ T-cells as would be expected. Similarly, the genes coding for the B-cell lineage marker (*CD19*), and endothelial cell lineage marker (*CD31*) were exclusively expressed by their respective cell-types. The expression profiles also verified subtler FACS gating. For example the PD1 gene (*PDCD1*) was expressed by both T-effector and T-exhausted cell subsets, but at different levels reflecting the use of FACS gating threshold. Of note, PD1 expression was also observed in neutrophils and macrophages. A biological role for PD1 expression in tumour-associated macrophages is becoming established, increasing with disease stage in human cancers and impairing phagocytosis of cancer cells in a mouse model (Gordon et al., 2017). However, while characterized in other disease settings such as infection with tuberculosis bacteria or human immunodeficiency virus), the role of PD1-high neutrophils in cancer is less clear. This simple analysis also revealed the potential

of unbiased transcriptomic characterization to uncover novel biology around the *in situ* phenotype of stromal subsets.

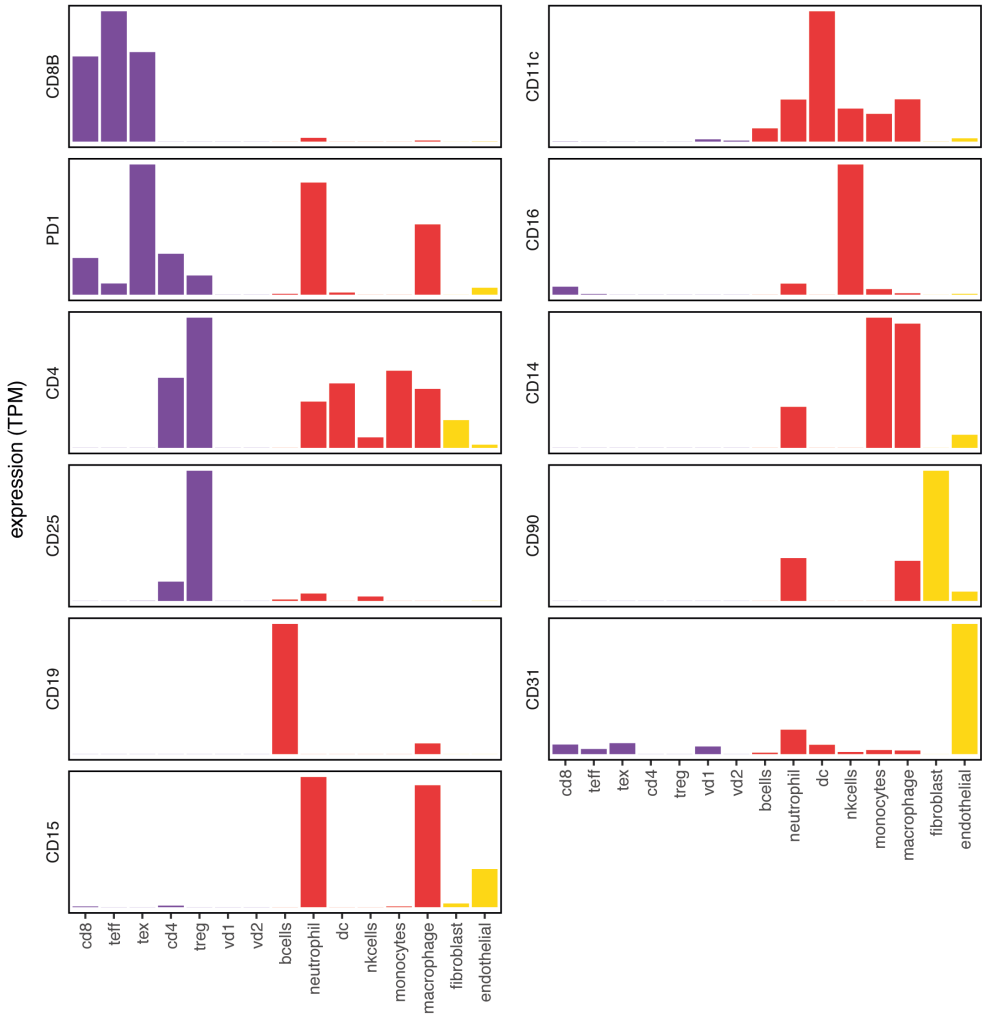

Figure 5-5 Expression of cell surface marker genes used for FACS
The expression of individual marker genes are plotted for lymphoid immune (purple), myeloid immune (red), and non-immune (yellow) stromal populations. Lymphoid immune subsets: CD8 T-cells (*CD8B*), Tex (*PD1*-high), Teff (*PD1*-low), CD4 T-cells (*CD4*), Treg (*CD25*), B cells (*CD19*), and natural killer cells (*CD16*). Myeloid immune subsets: neutrophils (*CD15*), dendritic cells (*CD11c*), monocytes and macrophages (both *CD14*-high). Non-immune stromal subsets: fibroblasts (*CD90*), endothelial cells (*CD31*).

5.3.3 Global expression profiles reflect cell-type of origin

To decipher transcriptional patterns between all the stromal lung samples, unsupervised clustering algorithms were applied to their global expression profiles (Figure 5-6). The UMAP analysis revealed cell-type of origin was a major discriminating factor between samples, with samples from several cell-types clustering together. This included αβ T-cells, NK cells, B-cells, neutrophils, endothelial cells, and fibroblasts as indicated on the UMAP (Figure 5-6A-B). Lineage restrictions for individual cell-types might be expected to have a large bearing on global expression profiles. For example, transcriptional diversity (measured as the total number of genes expressed by a cell) has recently been shown to decrease during normal differentiation (Gulati et al., 2020).

By contrast, the tissue of origin had a varying influence between cell-types, as can be seen from the PCA. Examining the means of PC1 and PC2, for each individual cell-type, the γδ T-cell samples exhibited the clearest distinction between normal and cancerous lung tissue (Figure 5-6C-D). To decipher subtler effects of cell-extrinsic factors, such as hypoxia in the TME, in the next section I moved to exploring the pathways and genes involved in tissue-specific expression profiles.

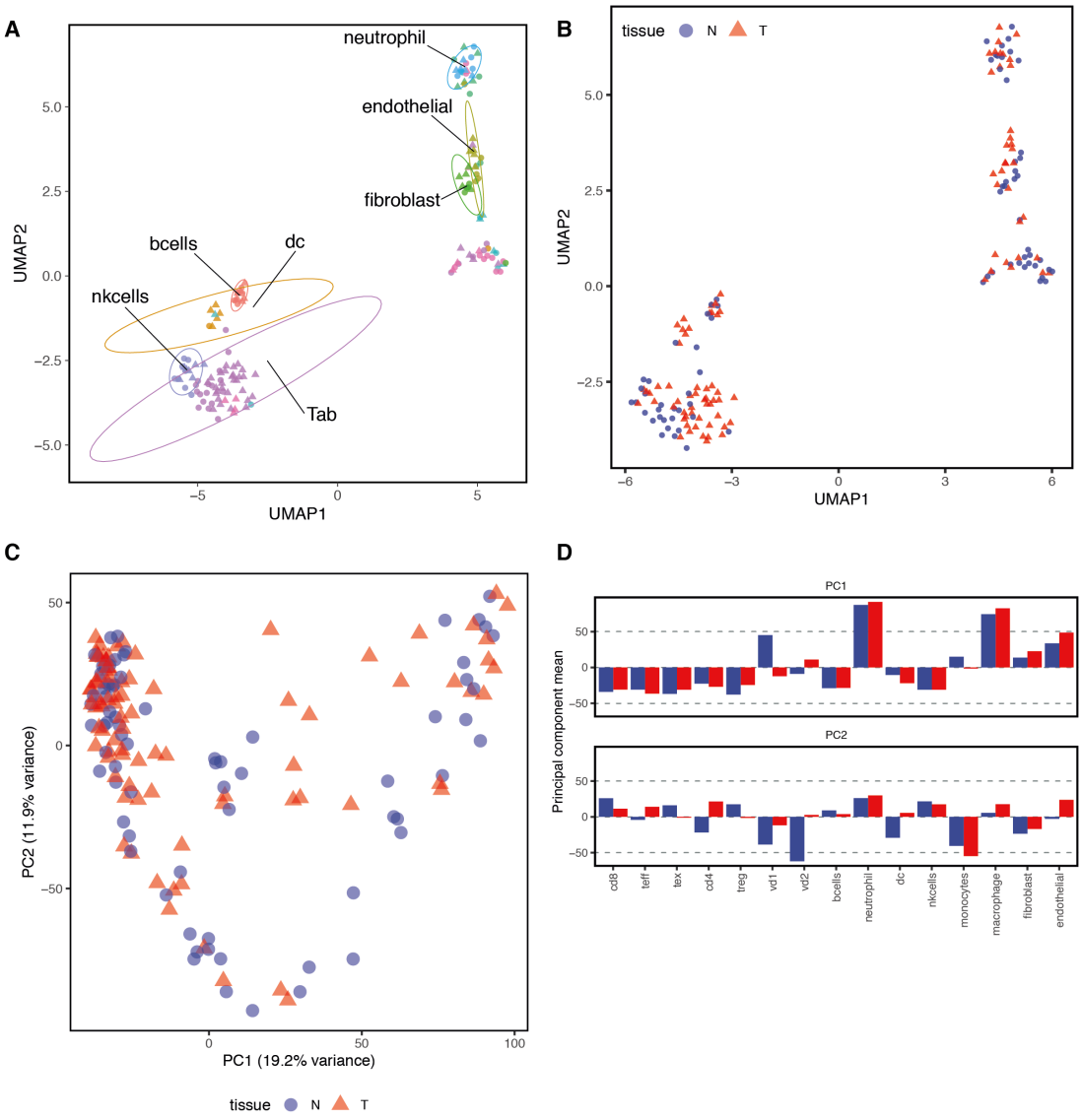

Figure 5-6 Global transcriptomic analysis

Unsupervised clustering analyses of the relationship between global expression profiles for all the lung stromal cell-types assessed. UMAP shown with the colour scheme highlighting cell-type (A) or tissue (B) of origin. PCA (C) and bar plots for the means of the PC1 and PC2 values per cell-type(D).

5.4 Tissue-specific signals of stromal cells in the lung tumour microenvironment

5.4.1 Global tissue differences

To identify cell-type-specific molecular signals related to tumour infiltration, here I analysed the transcriptomes from the 15 stromal cell-types purified from tumour tissue and – the best control tissue available – adjacent non-cancerous lung.

For a broad insight into normal-tumour transcriptomic differences within individual stromal cell-types, I performed a pathway analysis of the 50 hallmark gene-sets from the Broad Molecular Signatures database (Subramanian et al., 2005). This analysis revealed most (12/15) cell-types displayed differences in hallmark pathway activities (Figure 5-7); no pathways were significantly altered in Vδ2 cells, fibroblasts or endothelial cells. Interestingly, the Vδ1 subset was the cell-type with differential activation in the greatest number of hallmark pathways, which may reflect mounting evidence that these cells may be tissue-resident immunological rheostats for epithelial transformation. Indeed, they are present and enriched in the epithelium of myriad organs and can mount rapid and potent responses to conserved molecular signals of malignant transformation (Cruz et al., 2018; Mikulak et al., 2019; Wu et al., 2019).

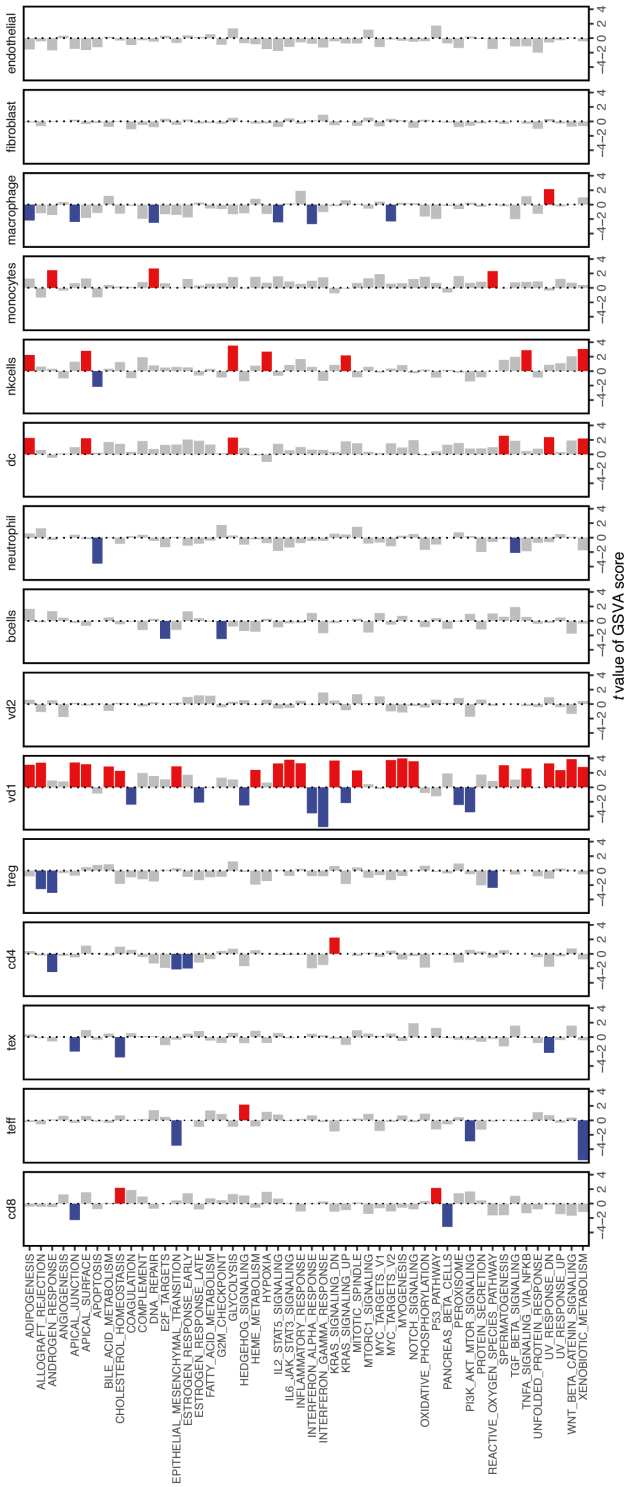

Figure 5-7 Pathway differences between normal and cancerous lung

Differences in pathway activities between normal or cancerous lung tissue for each stromal cell subset. The 50 hallmark gene-sets from the Broad Molecular

Signatures database were used. Significant t-values indicated for gene-sets enriched in tumour (red) or normal (blue) lung tissue.

5.4.2 Tissue differences specific to individual T-cell subsets

For an unbiased exploration of tumour-normal differences, differential expression analysis was performed for cell-types of the T-cell compartment (Figure 5-8). This analysis identified a number of differentially expressed genes (DEGs) by tumour infiltrating T-cells relative to expression in normal lung: 89 DEGs in CD8+ T-cells, 116 DEGs in T-exhausted cells, 270 DEGs in T-effector cells, 87 DEGs in CD4+ T-cells, 501 DEGs in T-regulatory cells, 208 DEGs in γδ Vδ1 T-cells, and 84 DEGs in γδ Vδ2 T-cells.

The expression of some immune checkpoint molecules were up-regulated in the TME, including the ligand for CTLA4 (*CD80*) in CD8+ T-cells, and the gene encoding the TIM3 inhibitory receptor (*HAVCR2*) in T-exhausted cells (Figure 5-8A). Ganesan and colleagues have recently shown that CD8+ TILs expressed higher levels the T-cell co-stimulatory molecule 41BB (*TNFSF9*), reflecting TCR-engagement (Ganesan et al., 2017). In my analysis, I observed a similar signal restricted to the T-effector subset of CD8+ T-cells. Tumour infiltrating T-cells also displayed enhanced cytotoxic potential, with the upregulation of granzyme molecules in T-exhausted (*GZMM*) and γδ Vδ1 (*GZMA, GZMB*) T-cell subsets (Figure 5-8A & D). The over-expression of genes involved in DNA synthesis (*CDC45* in CD8+ T-cells), DNA repair (*POLE2* and *RAD51* in CD8+ T-cells; *POLA2* in CD4+ T-cells and T-regs), and cell cycle progression (*CDK1* in T-effector cells; *CDK3* in T-exhausted cells and T-regs) suggested the increased division and activation of T-cells in the TME (Figure 5-8A-B). This unbiased analysis indicated major changes in the gene expression landscape of CD8+ T-cells in lung tumour tissue, broadly in line with previous findings.

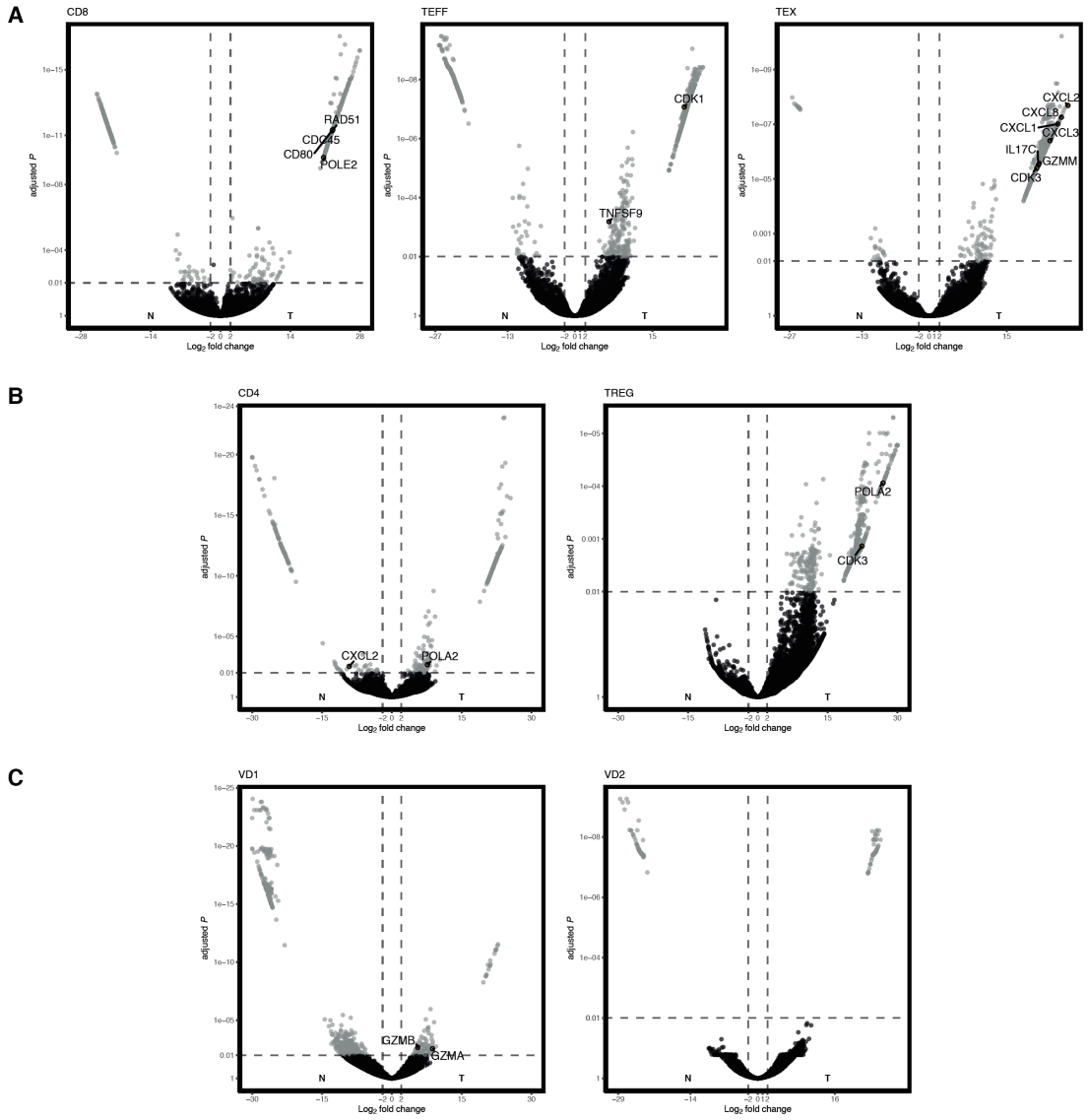

Figure 5-8 Transcriptomic profiles of tumour infiltrating T-cells
Volcano plots of differentially expressed genes in T-cells sourced from tumour versus normal lung tissue. Subsets of CD8+ T-cells (A), CD4+ T-cells (B), and γδ T-cells (C) are shown. Significantly differentially expressed genes are highlighted (gray): Log_2 Fold Change >2, BH adjusted P-value < 0.01. T = tumour over-expression, N = normal over-expression.

T-exhausted cells are known to show impaired anti-tumour function, with cell-intrinsic restrictions to cancer cell killing (Philip et al., 2017; Thommen et al., 2018). Intriguingly, in my dataset, a number of neutrophil chemoattractant genes were up-regulated in T-exhausted cells within the TME (Figure 5-8A right panel), including members of the CXC (*CXCL2*, *CXCL8*, *CXCL1*, *CXCL3*) and interleukin (*IL17C*)

families of pro-inflammatory chemokines. In a previous analysis of TME cellular composition, neutrophils were found to be the immune cell-type most adversely associated with survival outcomes across >18,000 tumours (Gentles et al., 2015). Therefore, this preliminary finding could indicate that “bad” T-exhausted cells might serve a pro-tumour function in recruiting neutrophils to the TME.

An important caveat to the differential expression results presented here are the extremely large fold-change values (Figure 5-8), particularly as a pronounced signal differentiating normal from tumour samples was not observed in unsupervised clustering analysis (see 5.4.1). Similar fold-change values have been reported for sorted cell-types (Uhlen et al., 2019). However, technical artifacts could be present. For example, there are a substantial number of zero-expressed genes in RNA-Seq data generated from low-input RNA samples, which may exaggerate fold-change values.

5.4.3 Tissue context may influence the expression of canonical cell-type markers

The phenotype of stromal cells might be substantially altered by cell-extrinsic stresses operating in the TME, such as tissue hypoxia (Lambrechts et al., 2018), increased glycolysis (Bohn et al., 2018; Rice et al., 2018), or altered ionic gradients (Eil et al., 2016). Recent work has shown “drifts” in gene expression between stromal cells in non-malignant and cancerous lung (Ganesan et al., 2017; Lambrechts et al., 2018). The impact of such “drifts” on the performance of RNA-based TME enumeration methods is currently unknown (Newman and Alizadeh, 2016).

Here I assessed four marker-gene-based TME scoring methods, developed by Rooney et al, Davoli et al, Danaher et al, and Bindea et al (Bindea et al., 2013; Danaher et al., 2017; Davoli et al., 2017; Rooney et al., 2015). The expression levels of these published signatures were evaluated in my RNA-Seq dataset of *ex vivo* purified lung stromal cell-types. This analysis focussed on cell-types with at least 5 samples for both normal and tumour tissue available, to enable

comparisons. A summary metric was generated for the expression levels of each signature, taking the geometric mean across genes specified in the gene-list. The sample-specific scores were calculated for each cell-type, and were plotted separately for normal and tumour samples (Figure 5-9).

In the analysis of six CD8+ T-cell signatures, scores resulting from the method developed by Bindea et al (Bindea et al., 2013) differed significantly between stromal cells isolated from normal versus tumour (Figure 5-9A). The Bindea CD8+ T-cell signature was based on the expression of *CD8A* and *PRF1* genes. *CD8A* might be expected to be core transcriptional features of this cell-type, whereas *PRF1* might be more subject to phenotype molding by tissue environment. The examination of two CD4+ T-cell signatures and four NK cell signatures did not indicate strong tissue-specificity (Figure 5-9B-C). However, evaluating six macrophage signatures revealed the gene-list determined by Danaher et al (Danaher et al., 2017) was relatively over-expressed in macrophages isolated from non-malignant lung tissue relative to macrophages purified from tumour samples (Figure 5-9D). The Danaher macrophage signature also relied on genes generally regarded as canonical marker-genes (*CD163*, *CD68*, *CD84*, *MS4A4A*). Overall, this analysis suggested that, in some cases, it might be useful to discriminate molecular features invariantly linked to cell-type, regardless of tissue environment.

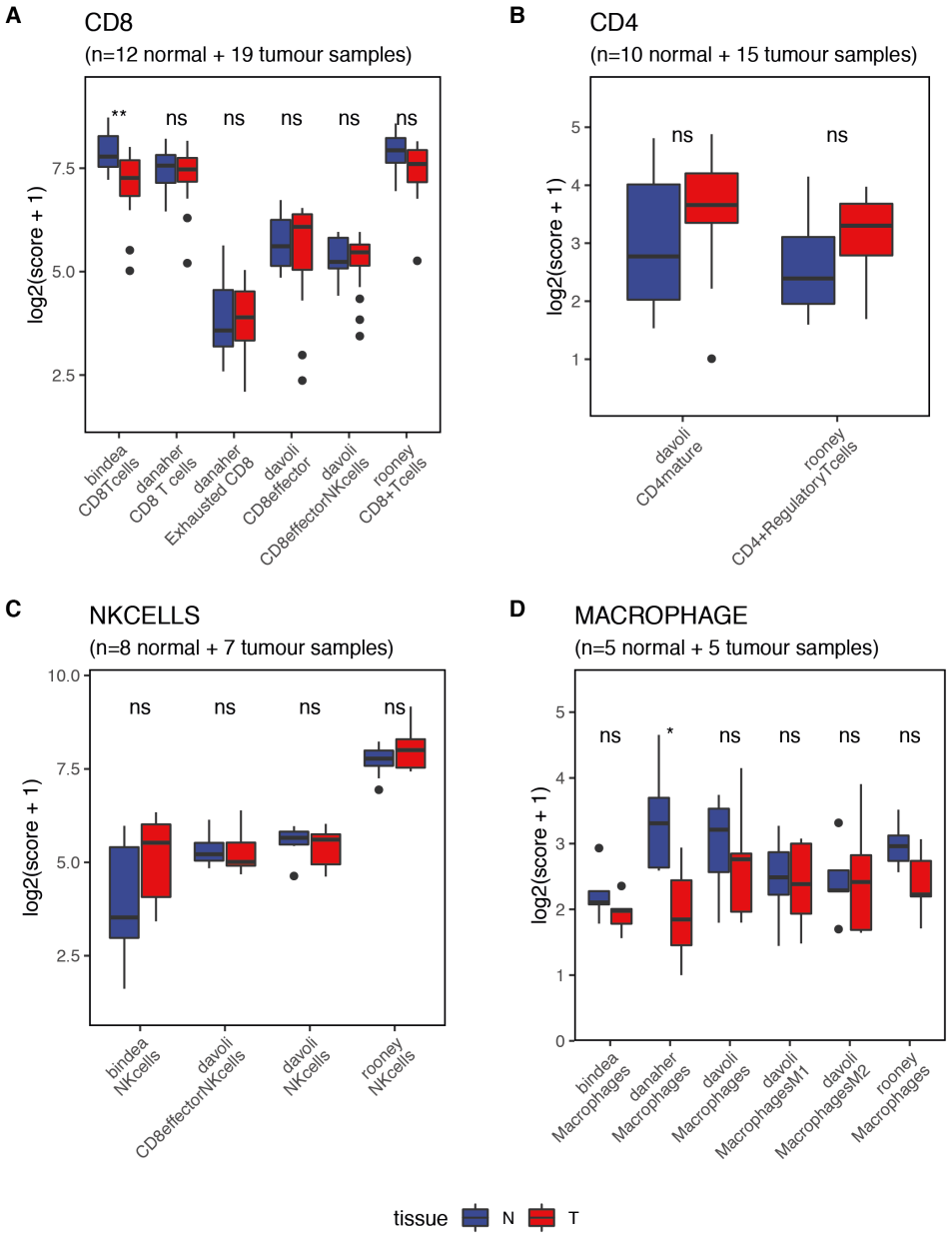

Figure 5-9 Impact of tissue source on performance of TME marker genes
Box plots of the scores (y-axis) of published TME signatures (x-axis) in isolated TME cell-type populations, stratified by whether the cells were sourced from normal (blue) or cancerous lung tissue (red). The performance of signatures for CD8+ T-cells (A), CD4+ T-cells (B), Natural Killer cells (C), and macrophages (D) are shown. Statistical significance was tested with a two-sided Wilcoxon signed rank sum test. "*" indicates a P-value < 0.05, "" indicates a P-value < 0.01, "ns" indicates a non-significant P-value.**

5.5 Cell-type-specific expression profiles for lung stroma

5.5.1 Genome-wide similarity analysis of cell-type expression profiles

To further decipher the phenotypic relationships between purified lung stromal cell-types, I calculated pairwise correlations of the transcriptomic landscape for the 15 TME cell-types, and then performed unsupervised hierarchical clustering on the similarity measures (Figure 5-10). The correlation coefficients indicated that most of the lymphoid immune cell-types formed a cluster of highly correlated ($R_s > 0.75$) cell-types. The γδ Vδ1 and Vδ2 T-cells subsets formed the exception, clustering instead with non-immune stromal cells (endothelial cells, fibroblasts) and monocytes. Neutrophils and macrophages formed a separate cluster.

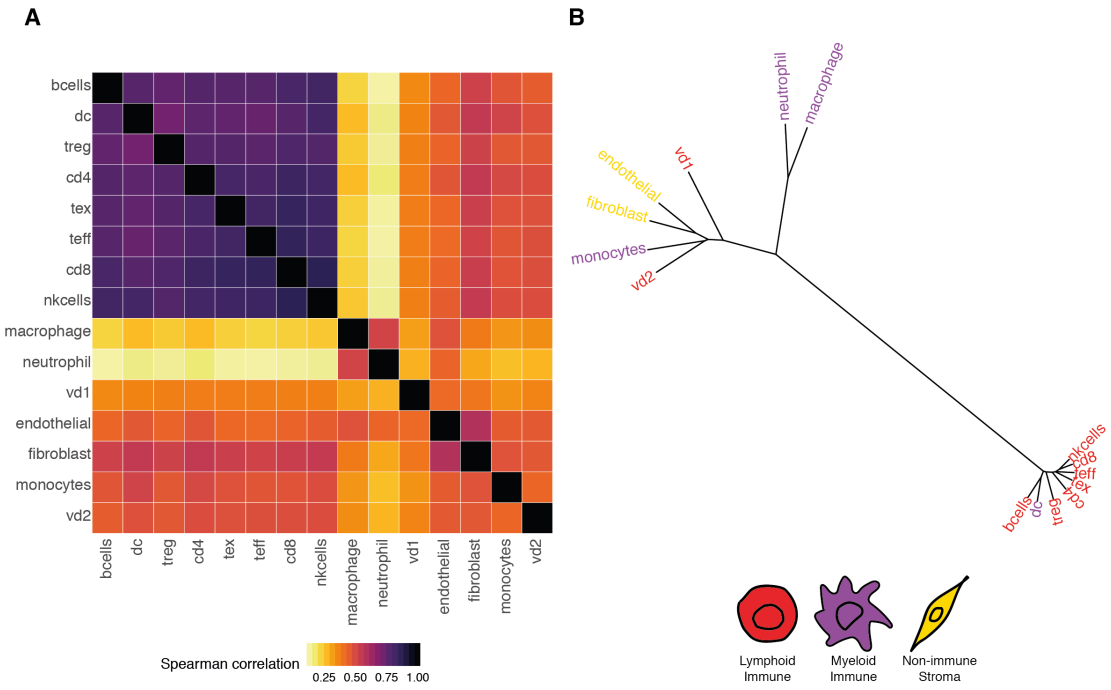

Figure 5-10 Pairwise correlation analysis of the transcriptomic landscape for stromal cell-types

A, Heatmap showing the pairwise Spearman correlation between the transcriptomic landscape for the 15 analysed lung stromal cell subsets. B, Dendrogram showing the clustering similarities in transcriptomic landscapes between different stromal cell subsets.

5.5.2 Derivation of marker genes specific to individual stromal cell-types

To investigate the potential to derive cell-type-specific marker genes from my dataset, the cell-type expression specificity was evaluated for each individual gene. I adopted the method described by Uhlen et al (Uhlen et al., 2019) in their recent Human Blood Atlas paper, which was used to derive cell-type specificity categories for gene expression in cell-types isolated from human blood.

All genes were classified into five expression specificity categories according to the following criteria:

1) Cell-type enriched: expression level (TPM) in a cell-type at least four times any other cell-type
2) Group enriched: expression level (TPM) in a group of cell-types (2-10) at least four times any other cell-type
3) Cell-type enhanced: expression level (TPM) in a group of cell-types (2-10) at least four times the average (mean) of other cell-types
4) Low cell-type specificity: detectable expression level (TPM ≥1) in at least one cell-type, but not elevated in any cell-type
5) Not detected: low expression level TPM (< 1) in all cell-types

The proportion of genes in each of the five specificity categories was calculated (Figure 5-11A-B). Of all 24,372 aligned genes, more than half (59.6%, 14,535/24,372) displayed detectable but non-specific expression across the 15 stromal cell-types (group enriched). Only 10.1% (2,452/24,372) of genes were classified as showing enriched expression unique to one of the cell-types (cell-type enriched). Neutrophils (700), Vδ1 subset (485), and macrophages (446) had the largest number of cell-type enriched genes. Whereas most lymphoid immune cell subsets harboured substantially fewer cell-type enriched genes: CD8+ T-cells (3), T-exhausted cells (20), T-effector cells (5), CD4+ T-cells (24), T-regulatory cells (66), B-cells (38) and NK cells (9). These data were consistent with the similarity analysis from the previous section (Figure 5-10), and highlight the challenge of identifying robust marker genes in cell-types with a largely shared differentiation hierarchy and close phenotypic alignment.

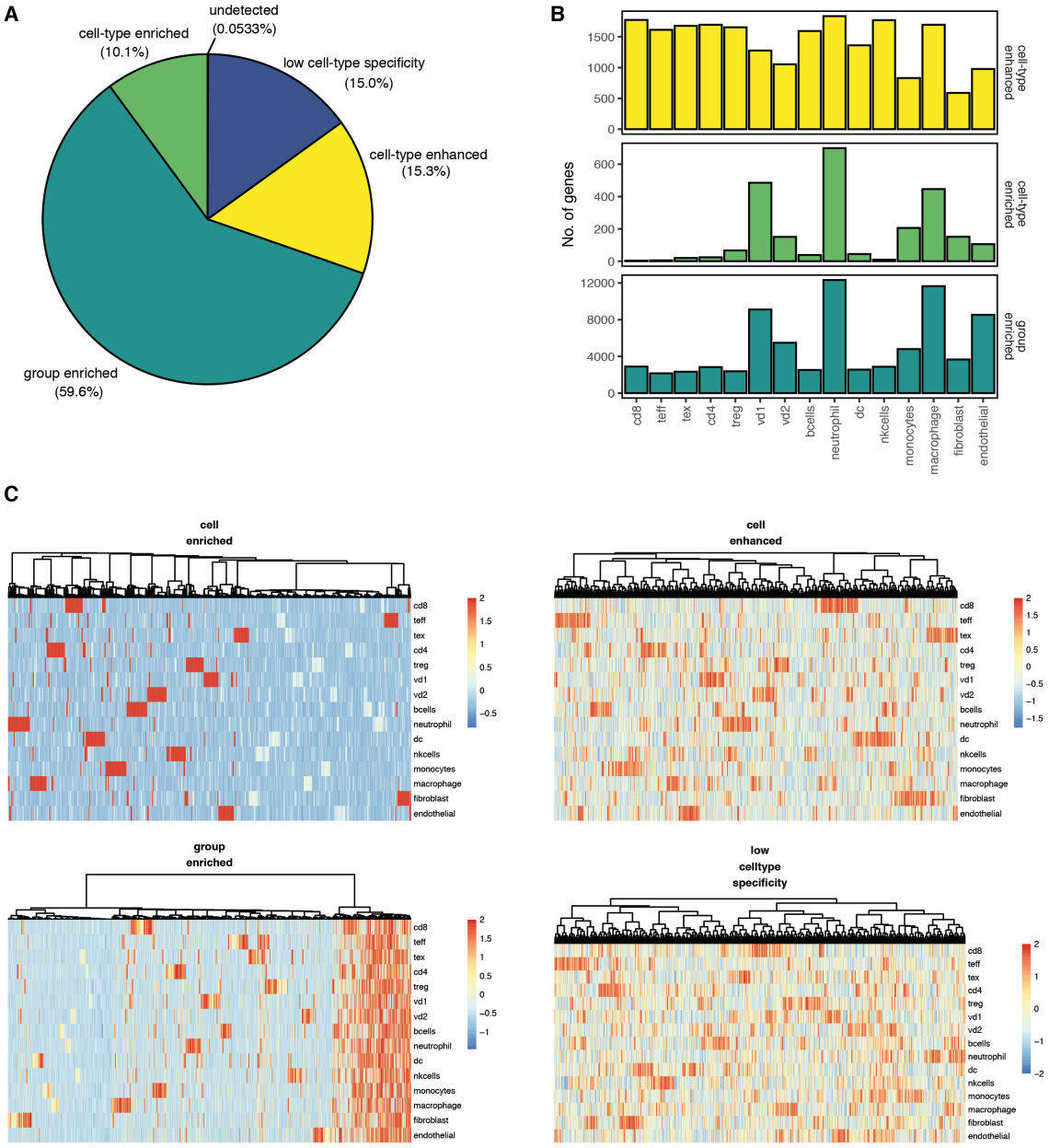

Figure 5-11 Candidate cell-type-specific marker genes

The number of genes categorized by specificity of expression, shown as summary percentages across all 15 TME cell-types (A), and the breakdown for individual cell-types (B). Heatmaps plotting gene expression for genes (x-axis) across by cell-type (y-axis) the 15 stromal subsets (C), separated by specificity category: cell-type enriched (top left), cell enhanced (top right), group enriched (bottom left), and low cell-type specific (bottom right) genes.

Lastly, I examined whether cell-type specific genes could discriminate between stromal subsets. Hierarchical clustering was performed on genes from four of the expression specificity categories (Figure 5-11C). The genes from the cell-type enriched specificity category (10.1%, 2,452/24,372) clustered together within –and were mostly expressed uniquely by – individual stromal cell-types. This pattern of tightly clustered modules was recapitulated, to some extent, by genes from the group-enriched specificity category (59.6%, 14,535/24,372), with more promiscuous expression across stromal cell subsets. By contrast, genes from the cell-type enhanced (15.3%, 3,722/24,372) and low cell-type specificity categories (15.0%, 3,650/24,372) were both homogeneously expressed between cell-types, with little apparent clustering of genes. This analysis indicated that the subset of cell-enriched genes (and possibly also the group-enriched specificity categories) might represent core transcriptional features of individual cell-types. Such genes could provide a foundation for the derivation of robust marker genes.

5.6 Conclusions

5.6.1 Summary of findings

In this chapter I have developed an atlas of genome-wide expression profiles for lung stromal cell-types (Figure 5-12). The 15 cell-types profiled comprised seven subsets of T-cells, B-cells, five subsets of the innate immune system, as well as fibroblast and vascular cells. Overall, bulk RNA-Seq data was generated for 159 samples from 24 patients; 87 samples from lung tumours and 72 from adjacent non-malignant lung tissue).

Preliminary analyses of tissue differences revealed the phenotypic adaptation of stromal cells to the lung TME. For example, tumour infiltrating T-cell subsets displayed signals of increased cell cycling and TCR-activation, consistent with recent analyses (Ganesan et al., 2017; Lambrechts et al., 2018). In addition, the subset of CD8+PD1-high T-exhausted cells was observed to over-express neutrophil chemoattractants in the tumour milieu. If further validated, this could suggest a novel pro-tumour function of the CD8+PD1-high T-exhausted cell subset, beyond the well-characterized cell-intrinsic restrictions to cancer cell killing (Philip et al., 2017; Thommen et al., 2018). I also assessed whether published marker genes methods displayed “drifts” in gene expression according to tissue environment. A CD8+ T-cell and a macrophage signature significantly differed between stromal cells in non-malignant and cancerous lung tissue in my dataset. This indicates, in some cases, paired tumour-normal analyses of purified stromal cell subsets might be useful to further discriminate molecular features invariantly linked to cell-type.

Analyses of cell-type similarities revealed the global expression profiles of several lymphoid immune cell-types were highly correlated, underlining the challenge of deriving marker genes robust to confounding by collinear expression between closely related cell-types. Overall, 10% of genes were classified as showing cell-type-specific expression unique to an individual cell-type, which could provide a foundation for the derivation of robust marker genes.

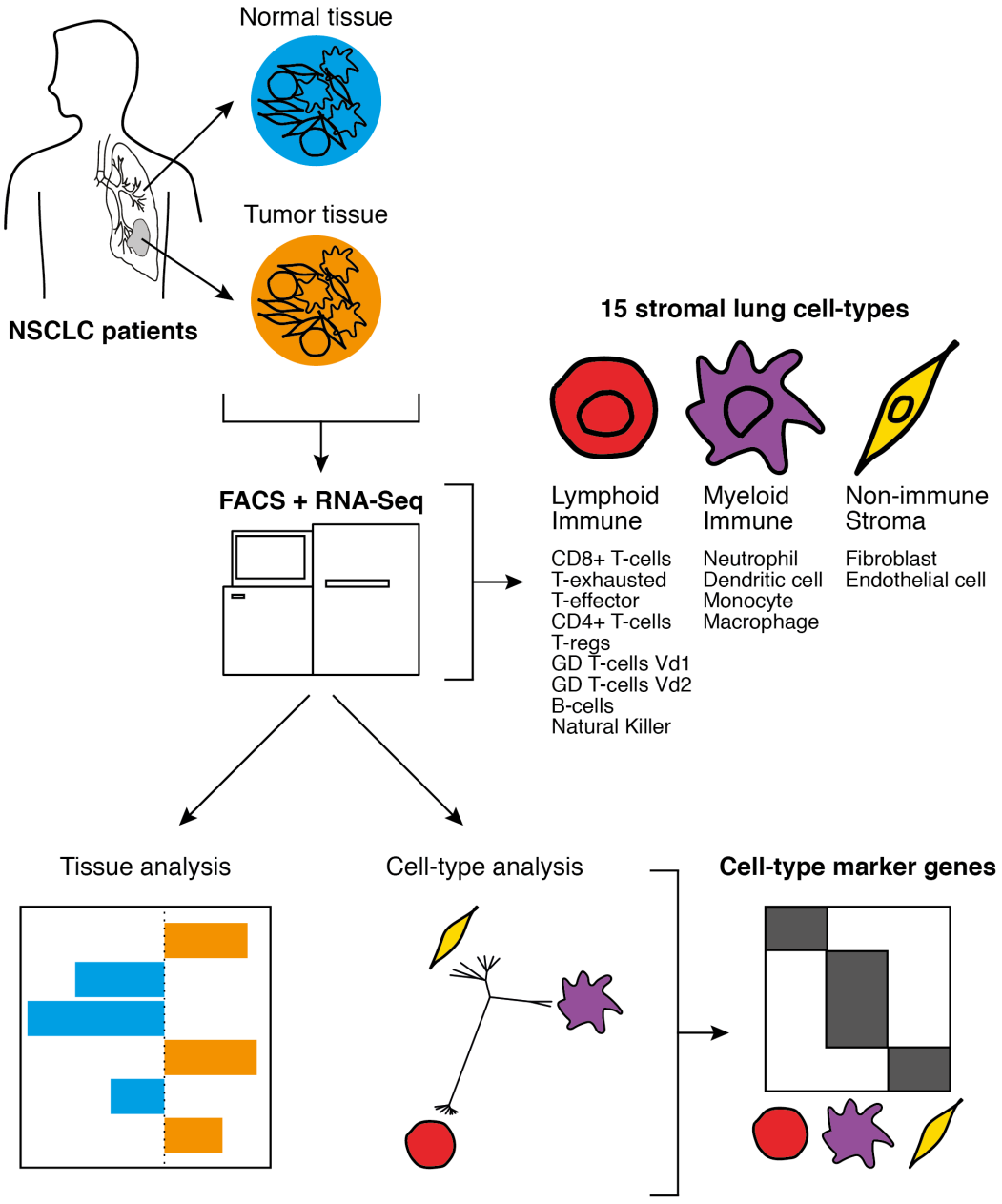

Figure 5-12 Outline of the analysis of stromal cell-types from lung tissue
A diagram illustrating the experimental and informatics workflow to analyse RNA profiles in lung stromal cell-types, sourced from tumour and adjacent non-malignant lung tissue, and to derive marker genes. The 15 cell-types listed include seven subsets of T-cells, B-cells, five subsets of the innate immune system, as well as fibroblast and vascular cells.

5.6.2 Future work

In future work, I will aim to develop a computational tool to accurately deconvolute immune and stromal TME cell-types from bulk tumour RNAseq data. As described in the background, a litany of tools for RNA-based TME enumeration is currently available. The approach taken in this chapter has two major novelties over existing methods. Firstly, the *ex vivo* purification of TME cell subsets in a granular and comprehensive manner. The 15 stromal cell-types profiled here encompass major adaptive and innate immune classes, and also rarer subsets of emerging clinical interest such as CD8+PD1-high T-exhausted cells (Thommen et al., 2018). Moreover, the inclusion of primary fibroblasts (both normal and cancer-associated fibroblasts) and endothelial cells contribute towards a comprehensive molecular map of the cells constituting the lung TME (Becht et al., 2016). Secondly, the purification of stromal populations present in both tumour samples and adjacent non-malignant lung tissue (the best available control) enables the discrimination of features linked to lung-tissue residence from those related to tumour infiltration (Ganesan et al., 2017; Lambrechts et al., 2018). The purification of cell-types directly post digest will also help characterize the *in situ* phenotype of stromal cells.

To identify the optimal algorithm for TME deconvolution in the setting of high-fidelity reference profiles, I will perform a head-to-head comparison of a number of supervised machine learning methods, including linear least- squares regression (Li et al., 2016), quadratic programming (Gong and Szustakowski, 2013) and support vector regression (Newman et al., 2015). The algorithms will be trained on pseudo-bulk tumour generated from publically available scRNAseq datasets (Sturm et al., 2019). Orthogonal validation will be conducted leveraging a large cohort of patients (n≥200) with tumour RNAseq data from TRACERx, and using paired H&E counting TIL estimates and flow phenotyping to provide a ground-truth measure of TME cell-types.

The availability of high-fidelity cell-reference profiles and an optimised enumeration method could pave the way for accurate digital dissection of the TME, helping to expedite the delivery of precision immune-oncology (Dijkstra et al., 2016). As

discussed in section 1.5 of this thesis, potential clinical applications include evaluating immune contexture as a diagnostic framework and resolving the milieu for environment-mediated drug resistance.

A particularly exciting avenue of future work would be to test the contribution of the TME signatures to RNA-ITH, linking the results of this chapter to Chapter 3 and Chapter 4. Recent work suggests it is likely that intra-tumoural immune variation may influence the patient-level estimates of RNA-ITH derived in this thesis (section 3.2). Analysing multi-region RNA-Seq data from a cohort of patients with NSCLC, Rosenthal et al discovered that 28% of patients exhibited immunologic heterogeneity, and that these tumours tended to exhibit higher levels of genetic ITH than tumours with uniformly low levels of immune infiltration (Rosenthal et al., 2019). Immune ITH has also been observed within individual ovarian tumours (Zhang et al., 2018) and between metastatic sites in patients with colorectal cancer (Mlecnik et al., 2018, p. 201).

In addition, ascribing the contribution of different tumoural cell populations to the expression levels of individual genes could enable further dissection of gene-level RNA-ITH (see section 4.3). Potentially the bulk TME cell populations identified in this chapter would be sufficient for a low-resolution analysis, for example Puchalski et al examined “anatomic” ITH of glioblastomas by defining gene-sets corresponding to immune-infiltrated, cellular or microvascular tumour regions (Puchalski et al., 2018). Distinct RNA profiles for immune, stromal and cancerous cells can also be discovered from unsupervised analysis of bulk spatial transcriptomics data, as demonstrated in prostate tumours (Berglund et al., 2018). Tracking gene expression down to the level of individual cancer clones is likely to be a nuanced challenge however, which may require single-cell resolution (discussed further in section 7.2.1). Moreover, inter-cellular RNA heterogeneity has been reported even within TME cell populations: in breast cancer, Costa et al identified four fibroblast subtypes, which could be distinguished based on surface marker expression, and exhibited distinct phenotypic properties (Costa et al., 2018).

Chapter 6. Evolutionary dependencies

6.1 Introduction

In most cancer types it is not currently possible to chart and forecast the progression of an evolving tumour in a predictable manner. Yet several lines of evidence hint at the existence of evolutionary constraints, including reports of parallel evolution or conserved mutational orderings (Greaves, 2015; McGranahan and Swanton, 2017), as discussed in the overview of literature (1.3.4).

Several computational tools have been developed to systematically detect combinatorial patterns of mutations in cancer NGS datasets (Deng et al., 2019). However, the design of these tools overlooks the branching clonal architecture that characterizes most cancer genomes. This might restrict the tools' ability to detect epistatic interactions involving subclonal mutations, and partially explain their limited utility in discovering core evolutionary dependencies across cancer-types (Vandin et al., 2012).

In this chapter an overview of existing computational tools to detect epistatic interactions in cancer genomes is provided. Their limitations are also mentioned, including evidence from the literature that mutation clonality might represent an unaddressed confounding factor for their use. Lastly, I analysed mutation clonality and mutual exclusivity in driver genes across nine cancer-types, to examine whether the clonal status of driver genes influenced the detection of epistatic interactions.

6.2 Deciphering epistatic interactions in cancer genomes

6.2.1 Combinatorial patterns of mutations in cancer

Large-scale cancer genomics projects have helped to define a set of driver mutations, which are causally implicated in tumourigenesis (Bailey et al., 2018; Kandoth et al., 2013) and, in some cases, can serve as predictive biomarkers for genome-targeted therapies (Hyman et al., 2017). Studying the combinatorial patterns of gene mutations in cancer might further reveal functional relationships between driver genes, and ultimately help inform clinical decision-making over treatment (Yeang et al., 2008).

Mutations in cancer driver pathways tend to exhibit one of two mutually exclusive (ME) patterns. “Soft” mutual exclusivity patterns, with partially overlapping mutational events, are consistent with Darwinian evolution as cancer cells with multiple mutations in the same cellular pathway are rarely conferred with an added selective advantage (Yeang et al., 2008). For example, Sparks and colleagues conducted targeted sequencing for mutations in the B-catenin pathway in a cohort of *APC*-wildtype colorectal tumours, discovering that 48% of patients harboured mutations in *CTNNB1* (Sparks et al., 1998). This mutually exclusive relationship indicated *CTNNB1* mutations might have a similar phenotypic effect to *APC* inactivation, and that B-catenin signalling is a core pathway in colorectal tumourigenesis.

Alternatively, “hard” patterns of ME display little to no overlap between mutational events, occurring when alterations to a second pathway member decreases cellular fitness (Babur et al., 2015; Ciriello et al., 2012). Such synthetic lethal relationships can occur within a core linear signal transduction pathway or between subunits of an essential protein complex (Kaelin, 2005). For example, A ME interaction between *CCNE1* gene amplification and *BRCA1/2* mutation was observed in the TCGA dataset of high-grade serous ovarian cancers (Ciriello et al., 2012), and later verified as a synthetic lethal relationship through an *in vitro* short-hairpin RNA screen (Etemadmoghadam et al., 2013).

By contrast, mutations of genes from different pathways might yield additive or even synergistic effects, so might be expected to co-occur (CO) (Yeang et al., 2008). For example, loss of *Pbrm1* cooperated with *Kras* in driving tumour development in a mouse model of pancreatic cancer (Varela et al., 2011). Co-occurring mutational patterns are also relevant for predicting response to treatment. Pre-treatment profiling of patients with *EGFR*-mutant lung cancer receiving EGFRi revealed limited responses in tumours with co-occurring alterations in cell cycle genes (median PFS = 0.7 months in *CDK4/6*-altered versus 11.2 months in *CDK4/6*-wildtype) (Blakely et al., 2017), and co-occurring alterations in *TP53* or *RB1* was associated with acquired resistance through transformation to small-cell carcinoma (Lee et al., 2017).

6.2.2 Computational tools for the systematic identification of epistatic interactions in cancer NGS datasets

Over the last decade the availability of large NGS datasets has allowed development of several tools to systematically detect combinatorial patterns of mutations. These tools can identify driver mutations, including novel genes overlooked by frequency-based methods (Babur et al., 2015), and assign the identified drivers to biological pathways, permitting discovery of novel tumourigenic roles (Ciriello et al., 2012; Hua et al., 2016; Miller et al., 2011).

The MEMo (Mutual Exclusivity Modules in cancer) tool, developed by Ciriello and colleagues, was an early success of such approaches (Ciriello et al., 2012). In glioblastoma (GBM) samples from the TCGA pilot project, MEMo identified ME interactions between the Rb, TP53, and RTK pathways, suggesting the deregulation of one component in each of these core pathways relieved the selective pressure for additional alterations. This relationship had a high “coverage” (the number of patient samples in which at least one alteration occurred), with 74% of the GBM patient cohort harbouring aberrations in all three pathways (Cancer Genome Atlas Research Network, 2008). This suggested that aberrant signalling of all three pathways might represent a core evolutionary dependency for GBM pathogenesis

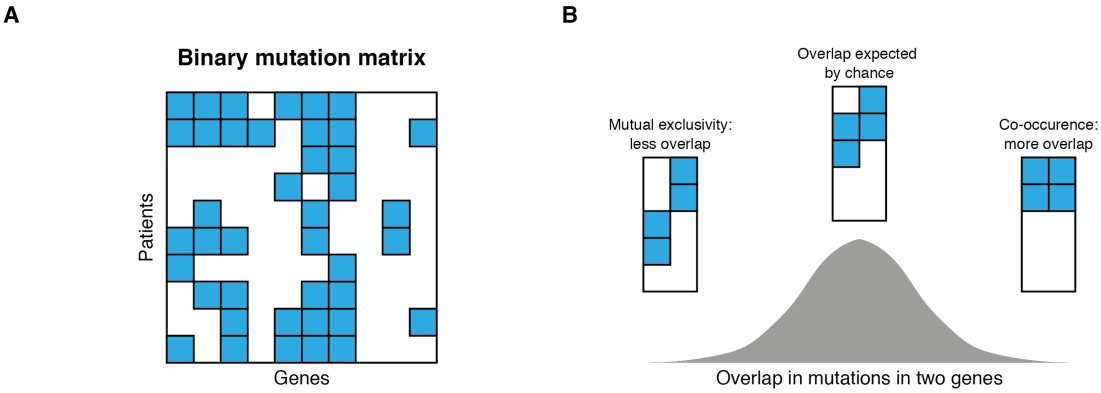

Figure 6-1 The detection of combinatorial patterns in cancer genomics datasets A, ME/CO detection tools take as input a binary mutation matrix, classifying mutations in genes (columns) as present (blue) or absent (white) for each patient (rows). B, The identification of ME/CO interactions involves the assessment of whether the overlap between genes is greater than expected by chance (indicating CO), or less (ME).

Existing tools for ME/CO detection take binary mutation matrices as input (Figure 6-1A). Using the mutation matrix, genes with more or less overlap than would be expected by chance are detected as significant CO or ME respectively (Figure 6-1B). Tools can be classified as *de novo*, or requiring prior pathway information, such as protein-protein interaction networks (Ciriello et al., 2012), pathways from the KEGG database (Hua et al., 2016), or the results of synthetic lethal screens (Jerby-Arnon et al., 2014). Discovering ME/CO interactions at the pathway or gene-set level is an NP-hard problem. For example, in cancer datasets there are 10^8-10^{11} possible combinations of four genes (Vandin et al., 2012). The search methods used to circumvent this problem, and discover significant ME/CO interactions, differ between tools. Some tools use heuristic algorithms, such as the Markov Chain Monte Carlo method (Leiserson et al., 2015; Vandin et al., 2012), others use a generative probabilistic model (Constantinescu et al., 2016; Szczurek and Beerenwinkel, 2014). Initially limited to point mutation data, recent ME/CO detection tools can take a range of inputs, including SCNA (Mina et al., 2017) and expression changes (Zhao et al., 2012).

Here, I used two approaches to assess ME relationships.

TiMEx. A generative probabilistic model that detects pairwise or gene-set level ME relationships (Constantinescu et al., 2016). Viewing tumourigenesis as a dynamic process, TiMEx models the alteration process for each gene as a Poisson process. This enables functional relations to be inferred based on a temporal representation of underlying mutational processes.

DISCOVER. The assumption that gene alterations across tumours are independent and identically distributed (i.i.d) is commonly made by tests for ME/CO, including TiMEx. Yet this assumption may be unrealistic for cancer genomics data, and might invalidate estimates of significance. The DISCOVER (Discrete Independent Statistic Controlling for Observation with Varying Event Rates) tool aims to address this (Canisius et al., 2016). A Poisson-binomial model is used to estimate gene alteration probabilities for each tumour individually, permitting different tumours to have different mutation rates for the same gene. The DISCOVER authors concluded that statistical tests assuming i.i.d. might over-detect CO relationships, and under-detect ME relationships.

6.2.3 Hypothesis: mutation clonality may be an unaddressed confounding factor for ME detection

The utility of existing tools for ME detection is limited by a number of challenges, including the low coverage of detected ME interactions. Most reported ME gene-sets typically have far less than 100% coverage, casting doubt on their importance for oncogenic progression. In the latest lung cancer paper from the TCGA consortium, the RTK–Ras–Raf pathway was not altered in 15–25% of LUAD tumours (Campbell et al., 2016). Most authors suggest technical challenges, including measurement noise or false mutation calls, are to blame (Szczurek and Beerenwinkel, 2014). However, Vandin and colleagues have previously speculated that ITH between subpopulations of tumour cells could be an important source of "false negatives" (Vandin et al., 2012). Enabling detection of subclonal ME interactions may help increase driver pathway coverage. Indeed, existing ME detection tools take tumour-level information (a binary mutation matrix of patients by genes) as input, ignoring the clonal architecture of individual tumours.

I hypothesised that mutation clonality may be an unrecognised confounding factor for ME detection (Figure 6-2). This hypothesis suggests that the presence of subclonal mutations in separate lineages of a tumour's phylogenetic tree, that are mutually exclusive within the individual tumour, would wrongly be classified as co-occurring.

There is direct evidence for such an effect. In a cohort of melanoma patients, mutations in *NRAS* and *BRAF* exhibited a co-occurring relationship. However, when examined at the single-cell level, the two mutated oncogenes were never present within the same cancer cell, indicating a "hard" mutual exclusivity (Sensi et al., 2006). Similarly, in a multi-region cohort of renal tumours *BAP1* and S*ETD2*/*PBRM1* mutations were found to co-occur at the tumour-level, yet a clone-level analysis revealed a true ME relationship, with events in the same tumour often occurring in spatially separated subclones (Turajlic et al., 2018).

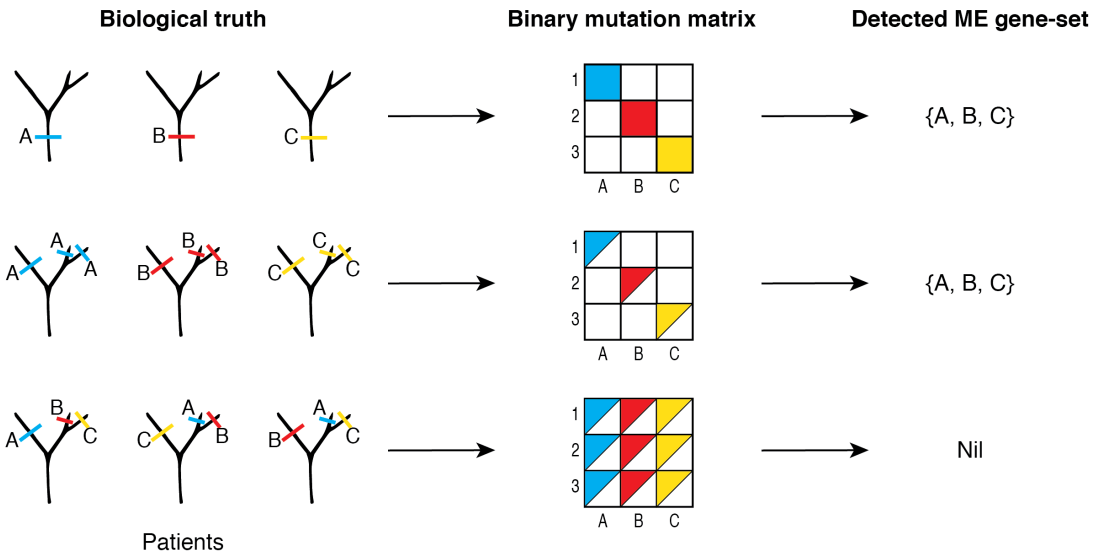

Figure 6-2 Hypothesis: existing ME detection tools may be biased to detect interactions between clonally mutated genes

Schematic diagram showing how tools for ME detection may fail to detect ME interactions between subclonal mutations. Under "biological truth" (left) the phylogenetic trees are shown for three patients (1,2,3). In the first row, each patient harbours a clonal mutation in one of three different genes (A, B, C) that, hypothetically, could be involved in the same signalling pathway. In the second row, each patient harbours subclonal mutations with the same gene altered in every branch of the tumour's phylogenetic tree; this phenomenon is referred to as parallel evolution. Lastly, in the third row, all three genes are subclonally mutated in the branches of each individual tumour. The "binary mutation matrix" plots (middle) show how the tumour's evolutionary history would be simplified for input to a ME detection tool, with mutations in each gene (columns) classified as present or absent at the patient-level (rows). The "detected ME gene-set" (right) reveals the impact of this simplification: true ME interactions between clonally mutated genes can be detected (top); similarly, in the rare case of parallel evolution within the same gene, ME interactions between subclonally mutated genes can also be recovered; however, if distinct genes from the same pathway are subclonally mutated within individual tumours, the ME interaction will not be detected, even though mutations may never co-occur in the same cancer cell.

My hypothesis also suggests that existing ME/CO detection tools are biased to detect clonal mutations in driver pathways. The Dendrix algorithm has previously identified two mutually exclusive gene sets in LUAD tumours from TCGA (Vandin et al., 2012): the first ME gene-set consisted of *EGFR*, *KRAS*, and *STK11*; the second contained *TP53* and *ATM*. Indeed, these five genes were all classified as “early” clonal drivers (pre-genome doubling initiating mutations or post-genome doubling clonal mutations) in an analysis of multi-region WES data the first 100 patients from the TRACERx lung study (Jamal-Hanjani et al., 2017).

Therefore, in this chapter I examine the influence of mutation clonality on ME detection in a pan-cancer analysis.

6.3 The clonal status of driver genes associates with the proportion of significant findings in mutual exclusivity analyses

6.3.1 Classifying mutation clonality and mutual exclusivity in driver genes

To explore whether mutation clonality confounds ME detection, I analysed somatic mutation data from the pan-cancer TCGA study. A focussed analysis was performed on the nine cancer-types recently examined by Haar and colleagues in their analysis of the mutation load artifact on the performance of ME detection tools (Haar et al., 2019).

Saioa López ran data pre-processing steps, including variant calling and estimation of mutation clonality. This was fully described in her recent publication (López et al., 2020), and briefly summarised here. Whole exome-sequencing data was accessed from the TCGA data portal for 3,545 patients from nine major cancer-types (Figure 6-3A): bladder urothelial carcinoma (BLCA, n=384 patients), breast invasive carcinoma (BRCA, n=643), colon adenocarcinoma (COAD, n=276), LUAD (n=463), LUSC (n=447), rectal adenocarcinoma (READ, n=85), skin cutaneous melanoma (SKCM, n=443), stomach adenocarcinoma (STAD, n=380), uterine corpus endometrial carcinoma (UCEC, n=424). This data was processed through the TRACERx bioinformatics pipeline, to which several members of the Swanton and McGranahan labs have contributed (Jamal-Hanjani et al., 2017); see Methods for more detail.

To test my hypothesis, I performed further filtering of somatic mutation calls. Nonsense and missense mutations were selected for use in downstream analysis. Mutations were further subsetted to candidate driver genes, using a pan-cancer gene-list published by Bailey and colleagues, which consists of 200 oncogenes and tumour suppressor genes (Bailey et al., 2018). Across the nine cancer-types, filtering for driver genes yielded a workable number of genes for use with ME detection tools (median=182 genes, range=139-187 genes, Figure 6-3A).

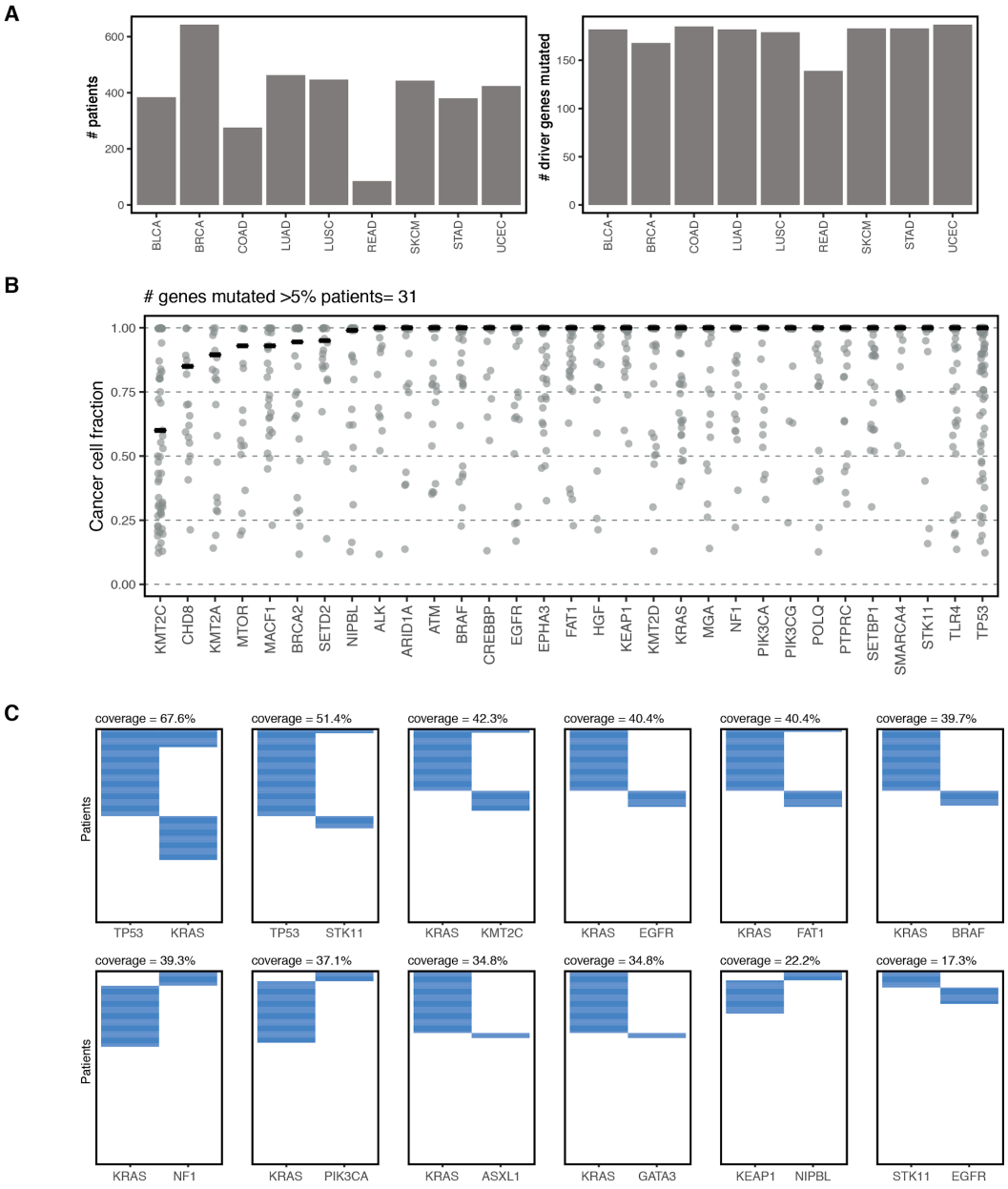

Figure 6-3 Classifying mutation clonality and mutual exclusivity in driver genes A, Overview of mutation data from nine TCGA cancer-types. The number of patients (left) and the total number of driver genes mutated (right) for each cancer-type are shown. B, The distribution of cancer cell fractions scores for commonly-mutated driver mutations in LUAD is shown for individual samples (gray points) and summarised per gene (black line). Driver genes are selected from the pan-cancer gene-list provided by Bailey et al (Bailey et al., 2018). Only commonly mutated genes (mutation present in >5% of patients) are shown here. C, Using the DISCOVER tool, the top-scoring results of pairwise mutual

exclusivity analysis in LUAD are shown (threshold for significance = qvalue < 0.05).

I first analyzed results for the LUAD cohort. Examining the CCF distributions per gene, the median value across the cohort provided a summary metric of mutation clonality (Figure 6-3B). The majority (58%, 106/182 genes) of the driver genes assessed in LUAD tended to be clonally mutated, with an average CCF = 1. This included several canonical LUAD driver genes, such as *TP53*, *KRAS*, *EGFR* and *STK11*. Of the genes previously reported as LUAD-specific drivers in a histology-specific analysis of the TCGA study (The Cancer Genome Atlas Research Network, 2014), only one gene (*SETD2)* had a median CCF < 1.

Next a binary mutation matrix was created, classifying mutations in the set of driver genes as present (1) or absent (0) in each LUAD patient, and inputted to the DISCOVER tool for ME detection. Twelve gene-pairs were discovered with highly significant ME interactions (Figure 6-3C, adjusted P-value < 0.05). The gene-set with the highest coverage (*TP53, KRAS*) was present in 67.6% of patients; overall, the median coverage across the nine ME gene-pairs was 39.5% (range=17.3-67.6%). Of the 182 genes inputted for ME analysis, ME relationships were detected between 13 unique genes (*ASXL1, BRAF, EGFR, FAT1, GATA3, KEAP1, KMT2C, KRAS, NF1, NIPBL, PIK3CA, STK11, TP53*). Notably, *KRAS* was involved as one of the partners in nine of the detected ME pairs, and three genes (*EGFR*, *STK11*, *TP53*) were involved in two ME pairs. Next I adopted the method described by Haar and colleagues (Haar et al., 2019), to calculate the percentage of the full set of pairwise interactions of a gene that had a significant (P<0.05) ME relationship. The *KRAS* gene had the highest percentage of significant findings, with a significant ME relationship detected in 14.9% (27/181) of the potential pairwise comparisons of driver genes. High proportions of statistically significant ME interactions were also observed for the canonical LUAD driver genes *EGFR* (3.3%, 6/181) and *STK11* (6.1%, 11/181). Overall, these data highlight how a handful of driver genes can account for the majority of the ME relationships detected within a particular histology.

6.3.2 The tendency of a gene to be clonally mutated correlates with the proportion of significant findings in mutual exclusivity analyses

The relationship between mutation clonality and the number of statistically significant ME interactions was assessed for each gene. There was a highly significant positive correlation between the clonality of mutations in a gene and the proportion of significant ME interactions in LUAD (Rs=0.2, P=0.00685, Figure 6-4A top panel). Applying the DISCOVER tool to other cancer-types, significant positive associations were also observed in BLCA (Rs=0.224, P=0.0024, Figure 6-4A middle panel) and UCEC (Rs=0.187, P=0.0107, Figure 6-4A bottom panel). This correlation suggests that genes which tend to be clonally mutated are more likely to be detected as exhibiting a ME relationship with other genes.

To test the generalizability of this finding, the same analysis was conducted using the TiMEx tool, which uses a different underlying model and set of assumptions to detect pairwise ME interactions (Constantinescu et al., 2016). TiMEx also identified significant positive associations in LUAD (Rs=0.166, P=0.0251, Figure 6-4B top panel) and BLCA (Rs=0.196, P=0.00814, Figure 6-4B middle panel), but not in UCEC (Rs=0.0361, P=0.624, Figure 6-4B bottom panel). This demonstrates that the influence of mutation clonality on ME detection is not specific to a particular tool.

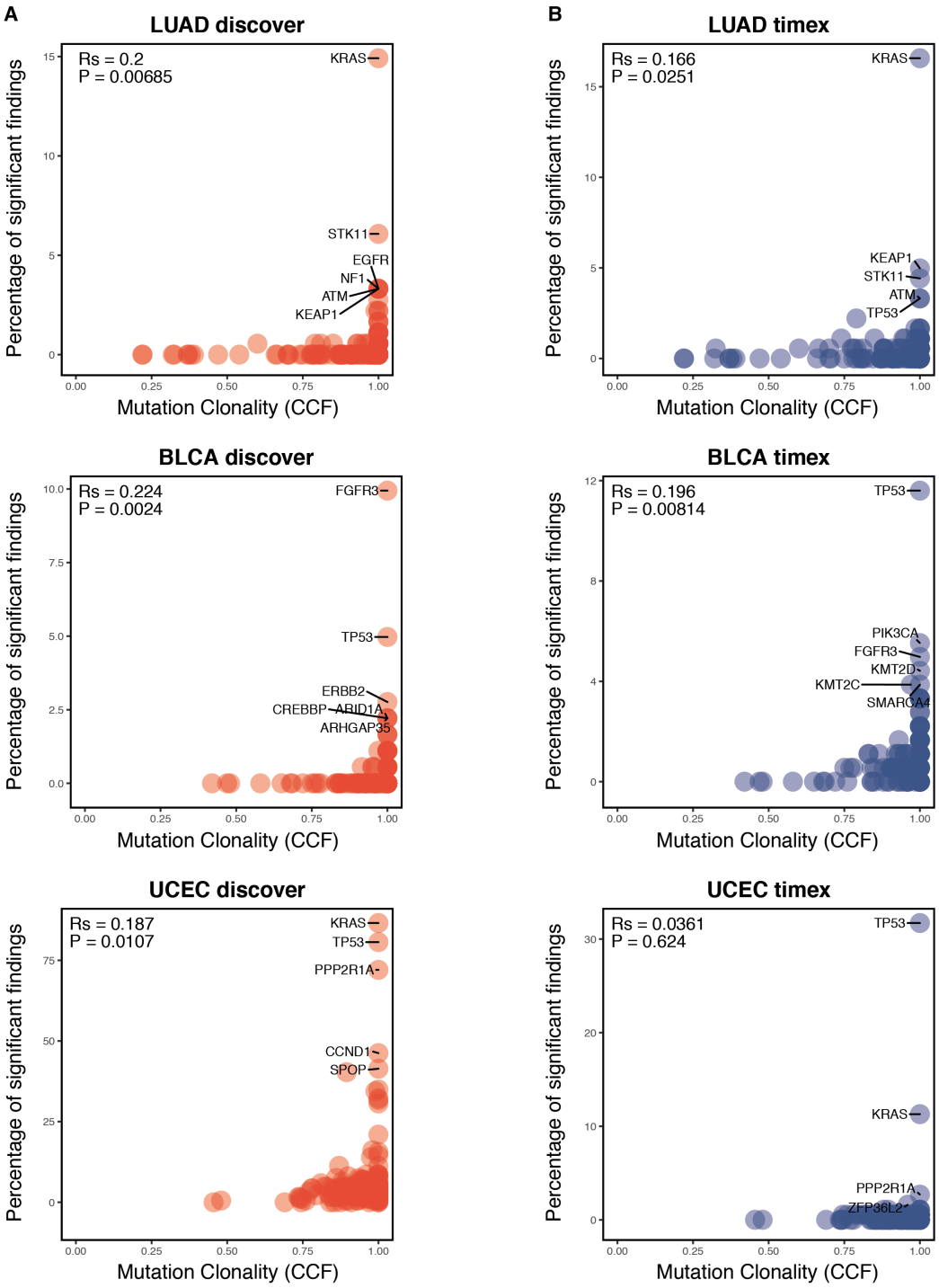

Figure 6-4 Correlating the tendency of a gene to be clonally mutated with the proportion of significant findings in mutual exclusivity analyses

A, The proportion of statistically significant ME interactions correlated with mutation clonality. The DISCOVER tool was used to determine significant (P<0.05) ME interactions in LUAD (left), BLCA (middle) and UCEC (right), plotted

against the gene's tendency to be clonally mutated. B, The same layout as A for the TiMEx tool.

Somatic mutation data from nine TCGA cancer-types was analysed to determine the extent of the mutation clonality artifact. Significant positive correlations between mutation clonality and the number of statistically significant ME interactions were found for 78% (7/9) of cancer-types using DISCOVER, and 44% (4/9) using TiMEx (Figure 6-5A). Overall, both ME detection tools exhibited a tendency for positive correlations overall (DISCOVER median Rs = 0.174, range = 0.097-0.224; TiMEx median Rs = 0.058, range = -0.123-0.200; Figure 6-5B). Taken together, this result suggests mutation clonality might represent an unaddressed confounding factor for the detection of significant ME interactions across cancer-types.

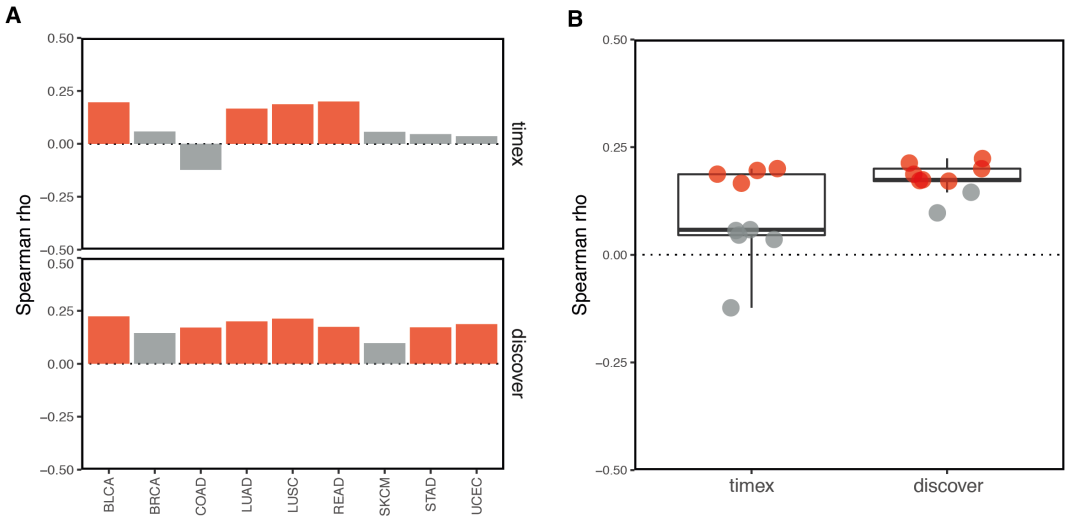

Figure 6-5 Analysis of nine cancer-types indicates the significant findings of ME detection tools tend to clonally mutated drivers
Association between mutation clonality and the number of statistically significant ME interactions across nine TCGA cancer-types using DISCOVER and TiMEx tools for ME detection. A bar-plot highlighting individual cancer-types (A), and a box-plot showing the distribution per tool (B) show the Spearman correlation coefficient (y-axis). The colour-scheme indicates a significant (red) or non-significant (gray) correlation.

6.3.3 The effect of recurrent mutation

Mutational frequency may bias the detection of ME interactions, as recurrently mutated genes have more power to detect mutual exclusivity (Deng et al., 2019; Yeang et al., 2008). Subclonal mutations typically occur at much lower frequencies than clonal mutations (Dentro et al., 2020; McGranahan et al., 2015). Here, I conduct a simple analysis to examine whether recurrent mutation influences the relationship between mutation clonality and ME interactions.

The distribution of mutation frequencies in driver genes were evaluated by cancer-type (Figure 6A). As previously reported (Lawrence et al., 2013), there was wide heterogeneity in overall mutation rates between cancer-types, and the mutation frequency for individual driver genes varied by cancer-type as well. Therefore, to stratify driver genes by recurrence in a histology-specific manner, mutation frequencies were split into quartiles by cancer-type (Figure 6A). In LUAD, for example, the top quartile ("Q4") comprised canonical driver genes including *TP53*, *KRAS*, *STK11*, and *EGFR*.

Next, the correlation coefficients between clonality and ME detection were re-calculated piecewise for each mutation frequency quartile (Figure 6B). Dissecting significant positive correlations by mutation frequency did not reveal a clear pattern for TiMEx (BLCA Q4 significant, LUAD all quartiles non-significant, LUSC Q2 significant, READ all quartiles non-significant; Figure 6B, top row). Indeed, none of the mutation frequency quartiles were significantly enriched for significant correlations across all 9 cancer-types (Figure 6C, left). By contrast, using DISCOVER, there was a trend for recurrently mutated ("Q4") driver genes to harbour more positive correlations between clonality and ME interactions (Q4 significant for LUAD, COAD and UCEC; all quartiles non-significant for BLCA, LUSC, READ and STAD; Figure 6B, bottom row), and this was reflected across all cancer-types (Q3 versus Q4: P= 0.0464; Figure 6C, right). Overall, mutation frequency did not account for the positive correlations observed between mutation clonality and the number of statistically significant ME interactions.

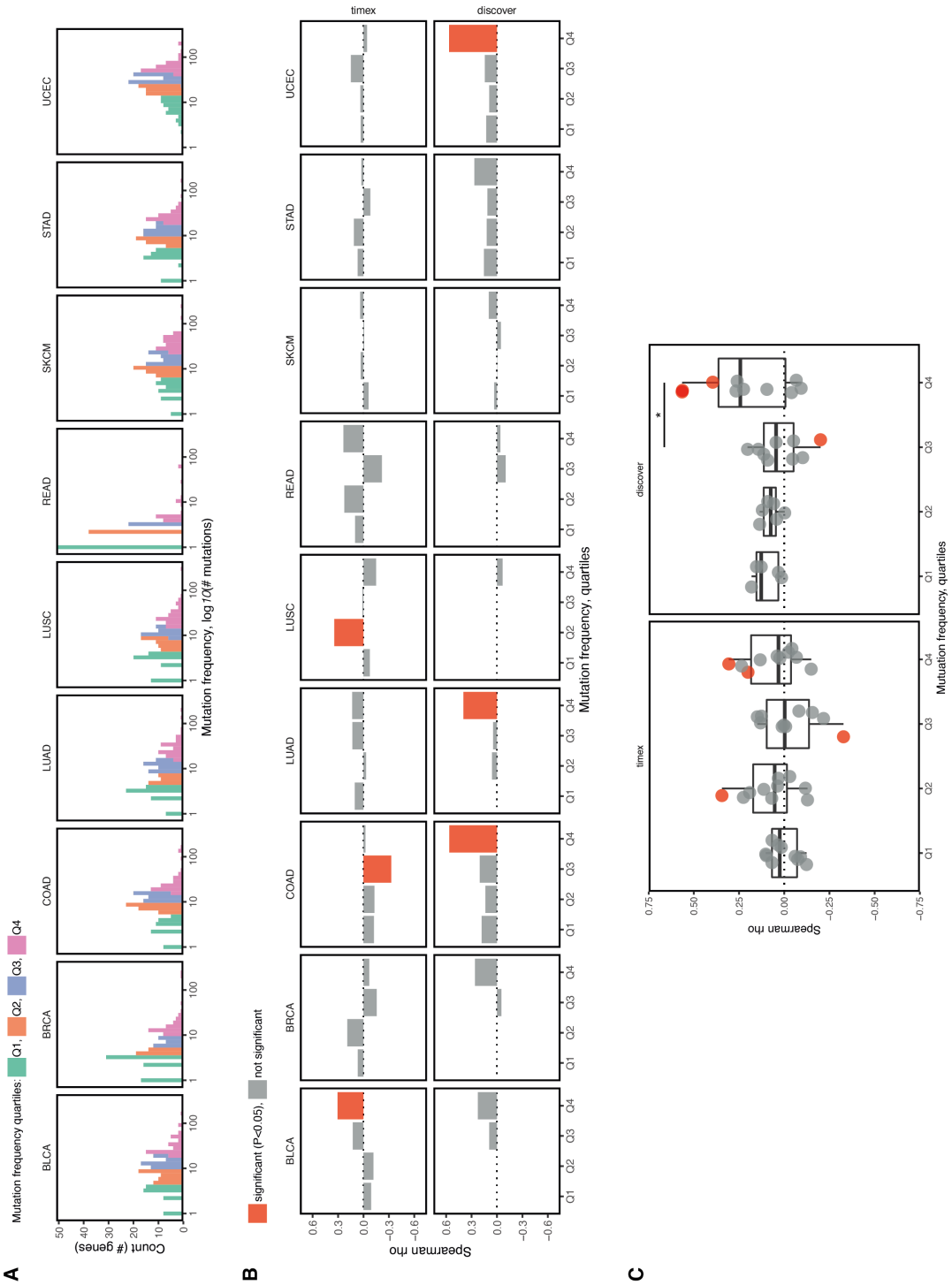

Figure 6 The effect of recurrent mutation

Distribution of mutation frequencies in driver genes by cancer-type (A). Spearman correlation coefficients between mutation clonality and the number of statistically significant ME interactions, calculated piecewise for each mutation frequency quartile, are shown by cancer-type (B) and by tool (C). Statistical significance was tested with a two-sided Wilcoxon signed-rank test.

6.4 Conclusions

6.4.1 Summary of findings

In this chapter, a pan-cancer analysis was conducted to assess whether existing ME detection tools are biased to detect interactions between clonally mutated genes (Figure 6-7). Specifically, I evaluated the relationship between the clonal status of driver genes and the proportion of significant ME interactions detected using existing DISCOVER and TiMEx across nine cancer-types. Overall a tendency for positive correlations was observed (DISCOVER median Rs = 0.174, TiMEx median Rs = 0.058). In 44-78% of the cancer-types assessed, driver genes that tend to be clonally mutated were more likely to be detected as exhibiting a ME relationship with other genes.

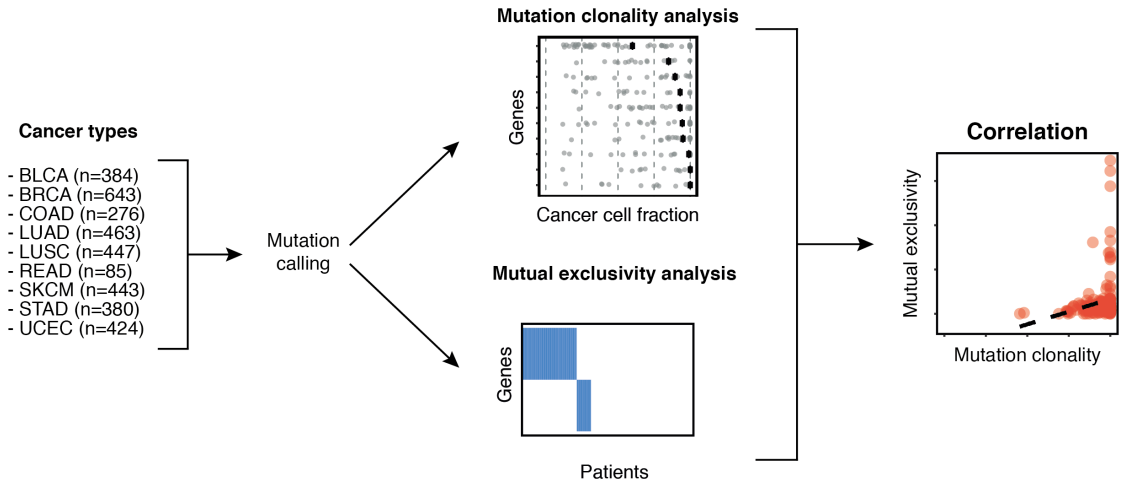

Figure 6-7 Schematic overview of the processes used to examine the correlation between mutation clonality and ME detection
Nine cancer-types from the TCGA study were included in this analysis. Mutation calls were assessed for their clonality (using cancer cell fraction) and for the presence of significant ME interactions (P < 0.05 using DISCOVER or TiMEx tools). Both axes of information were then correlated to examine the influence of mutation clonality on percentage of significant ME interactions.

6.4.2 Future work

Confounding factors – other than ITH – for the detection of ME interactions, include cancer subtypes, gene-set imbalances and mutation frequency (Deng et al., 2019). Resolving the effects of each factor, individually and in combination, will be essential for robust detection of ME gene-sets. In section 6.3.3, a simple analysis separating genes into mutation frequency categories indicated this did not account for the positive correlations observed between mutation clonality and the number of statistically significant ME interactions. However, the DISCOVER tool seemed more dependent on mutation frequency than TiMEx. Broadening the set of tools evaluated, in future analyses, could better quantify the effect of recurrent mutation and associated power to detect ME interactions.

In my analysis of existing tools for ME detection, I classified individual driver genes as tending to be mutated clonally or subclonally within a cancer-type, then correlated these data with gene-wise results from ME analysis. Park and colleagues used a different approach to investigate whether ITH might bias the detection of ME/CO interactions (Park and Lehner, 2015). The authors hypothesized that a cancer-type with a high level of ITH might be expected to display a higher rate of false-positive CO interactions and false-negative ME interactions. However, after classifying cancer-types as heterogeneous or non-heterogeneous, Park and colleagues found that both classes had similar odd ratios between CO and ME. The authors highlighted GBM as an illustrative example of a highly heterogeneous cancer-type with both ME and CO interactions that were stronger than others. The discrepancy between these results and my findings in this thesis can be explained as follows. By performing the analysis at gene-level resolution, my approach avoided the simplifying assumption of treating all tumours and genes within a particular cancer-type as homogenous or heterogeneous.

Future work could address the mutation clonality artifact by inputting clone-level information, rather than tumour-level, to ME/CO detection tools. For example, in an analysis of multi-region mutational data from the TRACERx renal trial, Turajlic and colleagues divided the phylogenetic trees from individual tumours into a “truncal”

lineage (containing all the clonal mutations) or “terminal” lineages (containing clonal and subclonal mutations unique to a specific branch) (Turajlic et al., 2018). Directly inputting truncal and terminal lineages to an existing ME/CO detection tool yielded strikingly different results. For example, *BAP1* and S*ETD2*/*PBRM1* mutations were found to co-occur at the tumour-level, yet were ME in an analysis of terminal lineages. An alternative solution is the direct analysis of ME/CO at the clone-level. For example, Moore and colleagues recently developed GeneAccord as a tool to detect pairs of mutated genes that are mutually exclusive within the clones of tumours (Moore et al., 2018).

Assembling a set of epistatic interactions implicated in a high proportion of patients, and involving both clonal and subclonal mutations, might help define a core set of evolutionary dependencies. Integration of this list with mutational timing information may further understanding of the role of driver pathways at different stages of tumour evolution, and help identify conserved trajectories of tumour evolution.

Chapter 7. Discussion

7.1 Novel findings in this thesis

These studies were undertaken to evaluate the hypothesis that refining molecular portraits of cancer in the light of their evolutionary and ecological features could improve diagnostic prevision. Here, I briefly highlight the major original findings in this thesis.

My analyses of multi-region RNA-Seq data from NSCLC patients from the TRACERx study have shed light on the mechanisms and clinical impact of RNA-ITH. A metric for RNA-ITH was proposed and compared with other possible approaches. A paired analysis with multi-region WES data revealed the transcription of heterogeneous chromosomal states into functional ITH, indicating that RNA-ITH is driven by chromosomal instability. The evaluation of published prognostic biomarkers revealed these are vulnerable to tumour sampling bias, typically displaying a 50% discordance rate, which suggested existing single-biopsy driven biomarker approaches may be confounded by RNA-ITH.

To address the diagnostic challenge of tumour sampling bias in lung cancer, I explore the potential to design molecular biomarkers in the light of cancer evolution. Homogeneously expressed genes were defined as a subset of genes with low intra- yet high inter-tumour RNA heterogeneity, which were enriched for chromosome copy-number gains early in tumour evolution. These genes were enriched for signals maintaining prognostic value between independent cohorts of patients. Therefore, a novel Outcome Risk Associated Clonal Lung Expression (ORACLE) signature was developed from homogeneously expressed genes, which was more robust to the problem of sampling bias than existing approaches. Indeed, validation of ORACLE showed a reproducible survival association in a meta-analysis of >900 patients from five independent cohorts. Moreover, ORACLE could identify high-risk stage I patients, that were otherwise missed by known risk factors, suggesting its medical utility. This diagnostic based on cancer evolutionary principles is now in the next phase of clinical translation.

Existing methods for the *in silico* dissection of the tumour microenvironment hold the promise of quantifying the immune contexture of tumours to guide clinical decision-making, yet fall short of clinical-grade accuracy. To characterize molecular profiles of cell-types comprising the tumour microenvironment, I performed *ex vivo* purification and RNA-Seq of 15 stromal cell-types from lung tumours and adjacent non-malignant lung tissue. The cell-types included seven subsets of T-cells, B-cells, five subsets of the innate immune system, fibroblast and endothelial cells, providing a holistic view of the cellular components of cancer ecology. Analysis of tumour-normal differences revealed the phenotypic adaptation of stromal cells, which could undermine the performance of existing computational tools for digital tumour dissection. Furthermore, I identified a subset of genes showing cell-type-specific expression unique to individual stromal subsets. In combination with tissue-specific analyses, this dataset could be leveraged to identify marker genes robustly associated with a specific cell-type, regardless of tissue context. This could pave the way for the accurate and granular deconvolution of the cellular composition of tumours using clinical samples, helping to expedite the delivery of precision immune-oncology.

Using knowledge of evolutionary constraints to predict a tumour's next evolutionary move has implications for pro-active approaches to personalised medicine. However, existing computational methods to systematically detect combinatorial patterns of mutations in cancer genomics datasets overlooks the branching clonal architecture that characterizes most cancer genomes. A pan-cancer analysis established that existing detection tools were biased to detect epistatic interactions between clonally mutated genes in 44-78% of the cancer-types assessed. Overcoming this mutation clonality artifact in future analyses could help reveal evolutionary dependencies.

7.2 Alternative approaches and future directions

Throughout this thesis, specific limitations and immediate next steps are discussed in the Results on a chapter-by-chapter basis. Here, I provide a synthesis on alternative approaches and future research avenues opened up by this thesis.

7.2.1 Is single-cell resolution required?

The analyses of RNA-Seq data conducted in this thesis were limited to quantifying the bulk average of transcripts pooled from millions of cells. By contrast, scRNAseq approaches enable the resolution of transcripts specific to individual cancer or stromal cells (Kolodziejczyk et al., 2015).

In this thesis, ORACLE has been designed as a pragmatic solution to the sampling bias problem (see 4.5.1), which can be applied to single-region biopsies in routine pathological evaluation. However, the RNA-ITH of molecular biomarkers has been observed at the single-cell level, potentially contributing to tumour sampling bias. For example, through scRNAseq in a cohort of metastatic melanoma patients, Tirosh and colleagues discovered the presence of a gene expression program conferring RAFi/MEKi drug resistance in a minority of cancer cells, which was absent in matched bulk RNA-Seq samples (Tirosh et al., 2016). Similarly, Patel and colleagues observed that established GBM subtype classifiers were variably expressed at the single-cell level across individual tumours, possibly undermining their prognostic utility (Patel et al., 2014). It is likely that ORACLE, as a “bulk” cancer cell proliferation signature, will be sufficient for application to “bulk” tissue samples from diagnostic biopsy in the clinical setting. Yet an examination of inter-cellular heterogeneity of the homogeneously expressed genes defined in this thesis may be of interest.

For digital tumour dissection, some existing tools, such as EPIC (Racle et al., 2017), have leveraged scRNAseq data for the development of cell-type reference profiles. The use of scRNAseq datasets does provide high-resolution of cell-type counts, at the cost of low cell-type granularity. In published analyses, marker-gene

annotation was used for unsorted scRNAseq datasets, which could identify T-cells but not more granular subsets, such as distinguishing betweeen CD4+ and CD8+ T-cells (Lambrechts et al., 2018; Lee et al., 2020). By contrast, the FACS and bulk RNA-seq strategy taken in this thesis (see 5.3) enabled the identification of granular cell-types, such as subsets of T-effector (CD8+PD1-low) and T-exhausted (CD8+PD1-high) cells. Moreover, my approach permitted the recovery of rare cell populations that may be missed in unsorted scRNAseq studies. For example, the CIBERSORT signature for γδ T-cells was the most vulnerable to noise (Newman et al., 2015). In future, this could potentially be addressed using the high-fidelity RNA profiles I have generated in this thesis.

7.2.2 Overcoming the curse of dimensionality for RNA biomarkers

The derivation of RNA biomarkers requires feature selection: subsetting from ~20,000 expressed genes to a small number of genes (<100 genes) that is compatible with use on a clinical platform (see 4.2.1).

Prognostic signature derivation typically involves a gene selection step, then a model fitting step using a machine learning algorithm. I have taken a simplistic approach to both steps in this thesis, focusing instead on dissecting the impact of clonal versus conventional gene selection on biomarker performance (see 4.4.3). Gene selection may be further refined, for example through further sub-setting for specific pathways, such as immune (Bailiang Li et al., 2017) or cell cycle progression (Wistuba et al., 2013) genes. Alternatively, the balanced representation of several pathways, to reduce information redundancy among genes, may be achieved using systems biology (Tang et al., 2013) or blind compression (Cleary et al., 2017) approaches.

Similarly, in identifying candidate cell-type-specific marker genes for *in silico* dissection of the TME, I opted to take an approach that classified genes as cell-type-enriched, cell enhanced, group enriched, or of low cell-type specificity (see 5.5.2). Alternative approaches adopted in the literature include pairwise differential expression analysis, for example Davoli and collagues identified genes over-

expressed in a particular immune cell-type as marker genes (Davoli et al., 2017), or deriving co-expression modules (Jiang et al., 2018).

7.2.3 Reaching the limits of precision oncology: individualised and hierarchical risk prediction

While evidence-based practice aims to improve the health of the average patient within a disease population, precision oncology ultimately seeks to provide a tailored approach for each individual on the basis of patient-specific biomarkers. In deriving a homogeneous expression biomarker, several prognostic classifiers were considered in this thesis (see 4.4.3), including linear (Kratz et al., 2012; Shukla et al., 2017) and tree-based (Chen et al., 2007; Reka et al., 2014) machine learning algorithms. Yet these all output population-level risk estimates and only predict a single clinical end-point. Multi-state modeling has recently been proposed as a more refined prognostic classification scheme to bridge the gap to individualised risk predictions. Recent work has shown multi-state modelling can be used to predict personalised outcomes for individual AML patients (Gerstung et al., 2017), at the limit of precision oncology. This approach has also been used for the discrete prediction of multiple clinical end-points in early-stage breast cancer patients, including the risk of locoregional versus distant relapse (Rueda et al., 2019).

Since 2002, most prognostic gene expression signatures developed for NSCLC patients are histology-specific, in recognition of the biological differences between LUAD and LUSC histologies. In accordance with this, ORACLE has been developed as a LUAD-specific prognostic biomarker (see 4.5). Yet there is growing evidence that further subtypes within LUAD may impact the significance of candidate prognostic markers. For example, Suda and colleagues recently described that a marker of poor prognosis in EGFR-mutant NSCLC tumours might not be informative in NSCLC tumours with *ALK* fusion (Suda, 2020). The impact of ignoring masked patient sub-groups was well described in breast cancer by Tofigh and colleagues, who demonstrated that ER+ status confounded the prognostic ability of published RNA markers (Tofigh et al., 2014). To overcome this, the

authors suggested the use of a “hybrid subtyping” scheme, which would sequentially classify breast cancer patients based on ER mutational status, then intrinsic subtype, and lastly a prognostic gene expression signature would be applied. A similar scheme may be of utility to combine histological subtyping with molecular prognostication in lung cancer.

7.2.4 Multi-omic classifiers

Commercially available prognostic biomarkers for breast (Paik et al., 2004; Parker et al., 2009; van ’t Veer et al., 2002) or lung cancer (Zheng and Bueno, 2015) are currently based on expression alone. However there is growing evidence supporting the use of multi-omic biomarker schemes for prognostication. For example, Neou and colleagues recently proposed a “pan-genomic” scheme for the risk stratification of pituitary neuroendocrine tumours, integrating somatic mutations, chromosomal alterations, DNA methylation, and gene expression changes (Neou et al., 2020). Such multi-omic classifiers have also been found to improve biomarker performance in other cancer-types, including protaste (Sinha et al., 2019) and bladder (Lindskrog et al., 2020) cancer. Multi-omic biomarkers may also be useful in predicting sensitivity to CPI. For example, predictive power may be improved by combining a mutation-panel-based measure of TMB with an expression-based measure of tumour inflammation (Cristescu et al., 2018) or TGFβ pathway activity (Mariathasan et al., 2018).

It is possible that future analyses may identify clonal multi-omic features that could be usefully integrated with the clonal RNA biomarkers derived in this thesis (see 4.3.2). In breast cancer, a paired analysis of genetic and transcriptomic data revealed that certain clonal genetic events were associated with extreme changes in transcription of interacting genes (Shah et al., 2012). Recent single-cell epigenetic and transcriptomic studies revealed evolutionary trajectories in a mouse model of LUAD, identifying core regulatory programs that may serve as useful biomarkers (LaFave et al., 2020; Marjanovic et al., 2020). Therefore, it is conceivable that future multi-omics analysis of clonal features could further improve biomarker performance.

7.2.5 Pan-cancer applicability

The majority of the work in this thesis was conducted in lung cancer, which is a high-impact area for precision medicine strategies to improve patient outcomes (Vargas and Harris, 2016). Though it worth considering whether the results of these analyses could be translated to other cancer-types in future work.

In this thesis, homogeneous expression biomarkers were derived in a multi-region lung cancer cohort (see 4.3.2). A pan-cancer analysis indicated that these lung-derived biomarkers might have prognostic value in other cancer-types (see 4.6.1). The pan-cancer applicability of homogeneous expression biomarkers might be biologically plausible. In my analysis, homogeneously expressed genes in lung cancer were driven by clonal SCNA gains (see 4.3.3), and encoded modules of cancer cell proliferation (see 4.4.1). Similarly, the early selection of modules of cancer cell proliferation was previously established in ER+ breast cancer (Endesfelder et al., 2014). Moreover, in an analysis of 12 TCGA cancer-types, focal SCNAs were positively correlated with the expression of cell proliferation modules (Davoli et al., 2017). Aneuploidy is tissue-specific and drives tissue-specific expression (Hoadley et al., 2018; Sack et al., 2018), so it may be unlikely that the exact 23 genes of the LUAD-specific ORACLE signature will validate across cancer-types. However, the wider pool of 1080 homogeneously expressed genes could drive a new wave of gene expression signatures that offer superior reproducibility and clinical utility if validated in other cancer types.

Using stromal cells isolated from patients with NSCLC, a set of transcriptomic profiles were derived for 15 cell subsets from the TME (see 5.3). Any cell-type marker genes developed using this dataset might be expected to perform better in other cancer-types than existing cell-type reference profiles derived using mouse or human blood (Davoli et al., 2017; Newman et al., 2015). In future work, the series of TME gene signatures would ideally be refined for individual tumour types.

7.2.6 Charting lethal, metastatic trajectories

NGS analyses of metastatic samples have broadened the genomic understanding of cancer outside of the primary tumour setting (Priestley et al., 2019; Robinson et al., 2017).

The timing of metastatic seeding adds an extra dimension to the sampling bias problem. Recent work by Hu and colleagues in colorectal cancer has shown that metastases can be seeded early in tumour evolution, indicating that only a subset of the apparently “clonal” alterations in the primary tumour are shared with metastatic sites (Z. Hu et al., 2019). In this thesis, an unpaired analysis of primary and metastatic samples from separate cohorts suggested that ORACLE might act as a molecular signature of metastatic potential (see 4.5.3). In future, analysis of paired primary-metastasis samples, obtained from the same patient, could validate this hypothesis. In addition, the definition of clonal alterations could be further developed as occurring uniformly between primary tumour regions, and timed prior to metastatic seeding.

Improved understanding of clonal exclusivity (see 6.2.3) could also help decipher the trajectories of lethal, metastatic disease. In a paired analysis of primary and metastatic tumour samples from a small cohort of colorectal cancer patients, Hu and colleagues used CO analysis to define a module of canonical driver genes in the primary tumour, and a novel set of gatekeeping mutations for metastatic dissemination (Z. Hu et al., 2019). While the genomic alterations involved in the development of primary colorectal cancers are well-defined (Vogelstein et al., 1988), the integration of clonality information into ME/CO analyses of paired primary-metastasis samples may be meaningful in other cancer-types.

7.2.7 Moving from diagnostics to therapeutics

Analyses of RNA-ITH in this thesis were focussed around the implications for prognostic biomarker development. Yet RNA-ITH may be equally relevant for the development of novel therapies. For example, in a multi-region RNA-Seq dataset of

brain tumours, Morrissy and colleagues established that the cell-surface targets of immunotherapies (such as *CD276, L1CAM, CD74*) were heterogeneously expressed within individual cancers (Morrissy et al., 2017). Similarly, Schafer and colleagues used immunofluorescence staining to show that *MYCN* displayed RNA-ITH in more than 40% of triple-negative breast cancers, contributing to the failure of effective therapy for these patients (Schafer et al., 2020).

In future work, it may be worth assessing if there are any actionable targets among the homogeneously expressed genes, specifically the SCNA alterations in ORACLE genes (see 4.5.3). A similar analysis was recently performed by Rueda and colleagues for the IntClust subtypes of breast cancer, finding that four tumour subgroups were enriched for SCNA driver alterations that could be therapeutically targeted (Rueda et al., 2019).

7.3 Conclusion

The development of robust molecular biomarkers has the potential to improve diagnostic precision in cancer. The limited clinical translation of previous biomarkers has been linked to their poor reproducibility and restricted medical utility. This research has highlighted a number of ways to refine molecular portraits of cancer in the light of their evolutionary and ecological features. These include a novel diagnostic for lung cancer, based on cancer evolutionary principles, which meets the criteria for further clinical development. Such an approach could harness technologies for tumour biology-based stratification towards the delivery of precision oncology.

Chapter 8. Appendix

8.1 Peer-reviewed publications authored during the PhD

8.1.1 First author publications

8.1.1.1 Articles

1) ‘A Clonal Expression Biomarker Associates with Lung Cancer Mortality’.
Biswas, Dhruva, Nicolai J. Birkbak, Rachel Rosenthal, Crispin T. Hiley, Emilia L. Lim, Krisztian Papp, Stefan Boeing, et al.
Nature Medicine, 7 October 2019, 1–9.

8.1.1.2 Conference abstracts

2) ‘Abstract LB258: Branching Cancer Evolution Biases the Detection of Epistatic Interactions between Driver Mutations’.
Biswas, Dhruva, Nicolai J. Birkbak, Javier Herrero, and Charles Swanton.
Cancer Research 81, no. 13 Supplement (1 July 2021): LB258–LB258.

3) ‘5O - Using Single Cell Data to Validate the Cellular Origins of a Clonal Expression Biomarker in Lung Cancer’
Biswas, D., N. J. Birkbak, N. McGranahan, and C. Swanton.
Annals of Oncology, Abstract Book of Molecular Analysis for Personalised Therapy (MAP) London, UK, 7–9 November 2019, 30 (1 November 2019): vii2.

4) ‘Abstract 2678: A Clonal Expression Biomarker Improves Prognostic Accuracy: TRACERx Lung’.
Biswas, Dhruva, Nicolai J. Birkbak, Rachel Rosenthal, Crispin T. Hiley, Emilia L. Lim, Krisztian Papp, Marcin Krzystanek, et al.
Cancer Research 79, no. 13 Supplement (1 July 2019): 2678–2678.

8.1.1.3 Correspondences

5) ‘The Future of Liquid Biopsy’.
Biswas, Dhruva, Jane Ganeshalingam, and Jonathan C. M. Wan.
The Lancet Oncology 21, no. 12 (1 December 2020): e550.

8.1.2 Co-author publications

8.1.2.1 Reviews

6) ‘Impact of Cancer Evolution on Immune Surveillance and Checkpoint Inhibitor Response’.
Wu, Yin, **Dhruva Biswas**, and Charles Swanton.
Seminars in Cancer Biology, 22 February 2021.

8.1.2.2 Articles

7) Meta-Analysis of Tumor- and T Cell-Intrinsic Mechanisms of Sensitization to Checkpoint Inhibition’.
Litchfield, Kevin, James L. Reading, Clare Puttick, Krupa Thakkar, Chris Abbosh, Robert Bentham, … **Dhruva Biswas**, et al.
Cell 0, no. 0 (27 January 2021).

8) ‘Oncogenic RAS Activity Predicts Response to Chemotherapy and Outcome in Lung Adenocarcinoma’.
East, Philip, Gavin P. Kelly, **Dhruva Biswas**, Michaela Marani, David C. Hancock, Todd Creasy, Kris Sachsenmeier, et al.
BioRxiv, 4 April 2021, 2021.04.02.437896.

9) ‘Pervasive chromosomal instability and karyotype order in tumour evolution’.
Watkins, Thomas B.K., Emilia L. Lim, Marina Petkovic, Sergi Elizalde, Nicolai J. Birkbak, Gareth A. Wilson, … **Dhruva Biswas** et al.
Nature, in press.

10) ‘Scalable and Robust SARS-CoV-2 Testing in an Academic Center’.
Aitken, Jim, Karen Ambrose, Sam Barrell, Rupert Beale, Ganka Bineva-Todd, **Dhruva Biswas**, Richard Byrne, et al.
Nature Biotechnology, 18 June 2020, 1–4.

11) ‘The T Cell Differentiation Landscape Is Shaped by Tumour Mutations in Lung Cancer’.
Ghorani, Ehsan, James L. Reading, Jake Y. Henry, Marc Robert de Massy, Rachel Rosenthal, Virginia Turati, … **Dhruva Biswas** et al.
Nature Cancer 1, no. 5 (May 2020): 546–61.

12) ‘An Innate-like Vδ1+ γδ T Cell Compartment in the Human Breast Is Associated with Remission in Triple-Negative Breast Cancer’.
Wu, Yin, Fernanda Kyle-Cezar, Richard T. Woolf, Cristina Naceur-Lombardelli, Julie Owen, **Dhruva Biswas**, Anna Lorenc, et al.
Science Translational Medicine 11, no. 513 (9 October 2019).

13) ‘Pulmonary Venous Circulating Tumor Cell Dissemination before Tumor Resection and Disease Relapse’.
Chemi, Francesca, Dominic G. Rothwell, Nicholas McGranahan, Sakshi Gulati, Chris Abbosh, Simon P. Pearce, … **Dhruva Biswas** et al.
Nature Medicine, 7 October 2019, 1–6.

8.1.3 Consortium author publications

14) ‘Clinical Outcomes of COVID-19 in Long-Term Care Facilities for People with Epilepsy’.
Balestrini, Simona, Matthias J. Koepp, Sonia Gandhi, Hannah M. Rickman, Gee Yen Shin, Catherine F. Houlihan, Jonny Anders-Cannon, et al.
Epilepsy & Behavior 115 (1 February 2021): 107602.

15) ‘Pandemic Peak SARS-CoV-2 Infection and Seroconversion Rates in London Frontline Health-Care Workers’.
Houlihan, Catherine F., Nina Vora, Thomas Byrne, Dan Lewer, Gavin Kelly, Judith Heaney, Sonia Gandhi, et al.
The Lancet 0, no. 0 (9 July 2020)

16) ‘Geospatial Immune Variability Illuminates Differential Evolution of Lung Adenocarcinoma’.
AbdulJabbar, Khalid, Shan E. Ahmed Raza, Rachel Rosenthal, Mariam Jamal-Hanjani, Selvaraju Veeriah, Ayse Akarca, Tom Lund, et al.
Nature Medicine, 27 May 2020, 1–9.

17) ‘Interplay between Whole-Genome Doubling and the Accumulation of Deleterious Alterations in Cancer Evolution’
López, Saioa, Emilia L. Lim, Stuart Horswell, Kerstin Haase, Ariana Huebner, Michelle Dietzen, Thanos P. Mourikis, et al.
Nature Genetics 52, no. 3 (March 2020): 283–93.

18) ‘Spatial Heterogeneity of the T Cell Receptor Repertoire Reflects the Mutational Landscape in Lung Cancer’.
Joshi, Kroopa, Marc Robert de Massy, Mazlina Ismail, James L. Reading, Imran Uddin, Annemarie Woolston, Emine Hatipoglu, et al.
Nature Medicine 25, no. 10 (October 2019): 1549–59.

19) ‘Neoantigen-Directed Immune Escape in Lung Cancer Evolution’.
Rosenthal, Rachel, Elizabeth Larose Cadieux, Roberto Salgado, Maise Al Bakir, David A. Moore, Crispin T. Hiley, Tom Lund, et al.
Nature, 20 March 2019, 1.

Reference List

AbdulJabbar, K., Raza, S.E.A., Rosenthal, R., Jamal-Hanjani, M., Veeriah, S., Akarca, A., Lund, T., Moore, D.A., Salgado, R., Al Bakir, M., Zapata, L., Hiley, C.T., Officer, L., Sereno, M., Smith, C.R., Loi, S., Hackshaw, A., Marafioti, T., Quezada, S.A., McGranahan, N., Le Quesne, J., Swanton, C., Yuan, Y., 2020. Geospatial immune variability illuminates differential evolution of lung adenocarcinoma. Nature Medicine 1–9. https://doi.org/10.1038/s41591-020-0900-x

Abécassis, J., Hamy, A.-S., Laurent, C., Sadacca, B., Bonsang-Kitzis, H., Reyal, F., Vert, J.-P., 2019. Assessing reliability of intra-tumor heterogeneity estimates from single sample whole exome sequencing data. PLOS ONE 14, e0224143. https://doi.org/10.1371/journal.pone.0224143

Alexandrov, L.B., Kim, J., Haradhvala, N.J., Huang, M.N., Tian Ng, A.W., Wu, Y., Boot, A., Covington, K.R., Gordenin, D.A., Bergstrom, E.N., Islam, S.M.A., Lopez-Bigas, N., Klimczak, L.J., McPherson, J.R., Morganella, S., Sabarinathan, R., Wheeler, D.A., Mustonen, V., Getz, G., Rozen, S.G., Stratton, M.R., 2020. The repertoire of mutational signatures in human cancer. Nature 578, 94–101. https://doi.org/10.1038/s41586-020-1943-3

Ali, H.R., Chlon, L., Pharoah, P.D.P., Markowetz, F., Caldas, C., 2016. Patterns of Immune Infiltration in Breast Cancer and Their Clinical Implications: A Gene-Expression-Based Retrospective Study. PLOS Medicine 13, e1002194. https://doi.org/10.1371/journal.pmed.1002194

Alizadeh, A.A., Aranda, V., Bardelli, A., Blanpain, C., Bock, C., Borowski, C., Caldas, C., Califano, A., Doherty, M., Elsner, M., Esteller, M., Fitzgerald, R., Korbel, J.O., Lichter, P., Mason, C.E., Navin, N., Pe'er, D., Polyak, K., Roberts, C.W.M., Siu, L., Snyder, A., Stower, H., Swanton, C., Verhaak, R.G.W., Zenklusen, J.C., Zuber, J., Zucman-Rossi, J., 2015. Toward understanding and exploiting tumor heterogeneity. Nat Med 21, 846–853. https://doi.org/10.1038/nm.3915

Alizadeh, A.A., Eisen, M.B., Davis, R.E., Ma, C., Lossos, I.S., Rosenwald, A., Boldrick, J.C., Sabet, H., Tran, T., Yu, X., Powell, J.I., Yang, L., Marti, G.E., Moore, T., Hudson, J., Lu, L., Lewis, D.B., Tibshirani, R., Sherlock, G., Chan, W.C., Greiner, T.C., Weisenburger, D.D., Armitage, J.O., Warnke, R., Levy, R., Wilson, W., Grever, M.R., Byrd, J.C., Botstein, D., Brown, P.O., Staudt, L.M., 2000. Distinct types of diffuse large B-cell lymphoma identified by gene expression profiling. Nature 403, 503–511. https://doi.org/10.1038/35000501

Altman, N., Krzywinski, M., 2018. The curse(s) of dimensionality. Nature Methods. https://doi.org/10.1038/s41592-018-0019-x

Anagnostou, V., Smith, K.N., Forde, P.M., Niknafs, N., Bhattacharya, R., White, J., Zhang, T., Adleff, V., Phallen, J., Wali, N., Hruban, C., Guthrie, V.B., Rodgers, K., Naidoo, J., Kang, H., Sharfman, W., Georgiades, C., Verde, F., Illei, P., Li, Q.K., Gabrielson, E., Brock, M.V., Zahnow, C.A., Baylin, S.B., Scharpf, R.B., Brahmer, J.R., Karchin, R., Pardoll, D.M., Velculescu, V.E., 2017. Evolution of Neoantigen Landscape during Immune Checkpoint Blockade in Non–Small Cell Lung Cancer. Cancer Discov 7, 264–276. https://doi.org/10.1158/2159-8290.CD-16-0828

Andor, N., Graham, T.A., Jansen, M., Xia, L.C., Aktipis, C.A., Petritsch, C., Ji, H.P., Maley, C.C., 2016. Pan-cancer analysis of the extent and consequences of intratumor heterogeneity. Nat. Med. 22, 105–113. https://doi.org/10.1038/nm.3984

Angelova, M., Mlecnik, B., Vasaturo, A., Bindea, G., Fredriksen, T., Lafontaine, L., Buttard, B., Morgand, E., Bruni, D., Jouret-Mourin, A., Hubert, C., Kartheuser, A., Humblet, Y., Ceccarelli, M., Syed, N., Marincola, F.M., Bedognetti, D., Van den Eynde, M., Galon, J., 2018. Evolution of Metastases in Space and Time under Immune Selection. Cell 175, 751-765.e16. https://doi.org/10.1016/j.cell.2018.09.018

Aran, D., Hu, Z., Butte, A.J., 2017. xCell: digitally portraying the tissue cellular heterogeneity landscape. Genome Biol 18. https://doi.org/10.1186/s13059-017-1349-1

Aslan, K., Turco, V., Blobner, J., Sonner, J.K., Liuzzi, A.R., Núñez, N.G., Feo, D.D., Kickingereder, P., Fischer, M., Green, E., Sadik, A., Friedrich, M., Sanghvi, K., Kilian, M., Cichon, F., Wolf, L., Jähne, K., Landenberg, A. von, Bunse, L., Sahm, F., Schrimpf, D., Meyer, J., Alexander, A., Brugnara, G., Röth, R., Pfleiderer, K., Niesler, B., Deimling, A. von, Opitz, C., Breckwoldt, M.O., Heiland, S., Bendszus, M., Wick, W., Becher, B., Platten, M., 2020. Heterogeneity of response to immune checkpoint blockade in hypermutated experimental gliomas. Nat Commun 11, 1–14. https://doi.org/10.1038/s41467-020-14642-0

Audeh, M.W., Carmichael, J., Penson, R.T., Friedlander, M., Powell, B., Bell-McGuinn, K.M., Scott, C., Weitzel, J.N., Oaknin, A., Loman, N., Lu, K., Schmutzler, R.K., Matulonis, U., Wickens, M., Tutt, A., 2010. Oral poly(ADP-ribose) polymerase inhibitor olaparib in patients with BRCA1 or BRCA2 mutations and recurrent ovarian cancer: a proof-of-concept trial. Lancet 376, 245–251. https://doi.org/10.1016/S0140-6736(10)60893-8

Ayers, M., Lunceford, J., Nebozhyn, M., Murphy, E., Loboda, A., Kaufman, D.R., Albright, A., Cheng, J.D., Kang, S.P., Shankaran, V., Piha-Paul, S.A., Yearley, J., Seiwert, T.Y., Ribas, A., McClanahan, T.K., 2017. IFN-**γ**–related mRNA profile predicts clinical response to PD-1 blockade. J Clin Invest 127, 2930–2940. https://doi.org/10.1172/JCI91190

Babur, Ö., Gönen, M., Aksoy, B.A., Schultz, N., Ciriello, G., Sander, C., Demir, E., 2015. Systematic identification of cancer driving signaling pathways based on mutual exclusivity of genomic alterations. Genome Biology 16, 45. https://doi.org/10.1186/s13059-015-0612-6

Bachtiary, B., Boutros, P.C., Pintilie, M., Shi, W., Bastianutto, C., Li, J.-H., Schwock, J., Zhang, W., Penn, L.Z., Jurisica, I., Fyles, A., Liu, F.-F., 2006. Gene Expression Profiling in Cervical Cancer: An Exploration of Intratumor Heterogeneity. Clin Cancer Res 12, 5632–5640. https://doi.org/10.1158/1078-0432.CCR-06-0357

Bailey, M.H., Tokheim, C., Porta-Pardo, E., Sengupta, S., Bertrand, D., Weerasinghe, A., Colaprico, A., Wendl, M.C., Kim, J., Reardon, B., Ng, P.K.-S., Jeong, K.J., Cao, S., Wang, Zixing, Gao, J., Gao, Q., Wang, F., Liu, E.M., Mularoni, L., Rubio-Perez, C., Nagarajan, N., Cortés-Ciriano, I., Zhou, D.C., Liang, W.-W., Hess, J.M., Yellapantula, V.D., Tamborero, D., Gonzalez-Perez, A., Suphavilai, C., Ko, J.Y., Khurana, E., Park, P.J., Allen, E.M.V., Liang, H., Caesar-Johnson, S.J., Demchok, J.A., Felau, I., Kasapi, M., Ferguson, M.L., Hutter, C.M., Sofia, H.J., Tarnuzzer, R., Wang, Zhining,

Yang, L., Zenklusen, J.C., Zhang, J. (Julia), Chudamani, S., Liu, J., Lolla, L., Naresh, R., Pihl, T., Sun, Q., Wan, Y., Wu, Y., Cho, J., DeFreitas, T., Frazer, S., Gehlenborg, N., Getz, G., Heiman, D.I., Kim, J., Lawrence, M.S., Lin, P., Meier, S., Noble, M.S., Saksena, G., Voet, D., Zhang, Hailei, Bernard, B., Chambwe, N., Dhankani, V., Knijnenburg, T., Kramer, R., Leinonen, K., Liu, Y., Miller, M., Reynolds, S., Shmulevich, I., Thorsson, V., Zhang, W., Akbani, R., Broom, B.M., Hegde, A.M., Ju, Z., Kanchi, R.S., Korkut, A., Li, J., Liang, H., Ling, S., Liu, W., Lu, Y., Mills, G.B., Ng, K.-S., Rao, A., Ryan, M., Wang, Jing, Weinstein, J.N., Zhang, J., Abeshouse, A., Armenia, J., Chakravarty, D., Chatila, W.K., Bruijn, I. de, Gao, J., Gross, B.E., Heins, Z.J., Kundra, R., La, K., Ladanyi, M., Luna, A., Nissan, M.G., Ochoa, A., Phillips, S.M., Reznik, E., Sanchez-Vega, F., Sander, C., Schultz, N., Sheridan, R., Sumer, S.O., Sun, Y., Taylor, B.S., Wang, Jioajiao, Zhang, Hongxin, Anur, P., Peto, M., Spellman, P., Benz, C., Stuart, J.M., Wong, C.K., Yau, C., Hayes, D.N., Parker, J.S., Wilkerson, M.D., Ally, A., Balasundaram, M., Bowlby, R., Brooks, D., Carlsen, R., Chuah, E., Dhalla, N., Holt, R., Jones, S.J.M., Kasaian, K., Lee, D., Ma, Y., Marra, M.A., Mayo, M., Moore, R.A., Mungall, A.J., Mungall, K., Robertson, A.G., Sadeghi, S., Schein, J.E., Sipahimalani, P., Tam, A., Thiessen, N., Tse, K., Wong, T., Berger, A.C., Beroukhim, R., Cherniack, A.D., Cibulskis, C., Gabriel, S.B., Gao, G.F., Ha, G., Meyerson, M., Schumacher, S.E., Shih, J., Kucherlapati, M.H., Kucherlapati, R.S., Baylin, S., Cope, L., Danilova, L., Bootwalla, M.S., Lai, P.H., Maglinte, D.T., Berg, D.J.V.D., Weisenberger, D.J., Auman, J.T., Balu, S., Bodenheimer, T., Fan, C., Hoadley, K.A., Hoyle, A.P., Jefferys, S.R., Jones, C.D., Meng, S., Mieczkowski, P.A., Mose, L.E., Perou, A.H., Perou, C.M., Roach, J., Shi, Y., Simons, J.V., Skelly, T., Soloway, M.G., Tan, D., Veluvolu, U., Fan, H., Hinoue, T., Laird, P.W., Shen, H., Zhou, W., Bellair, M., Chang, K., Covington, K., Creighton, C.J., Dinh, H., Doddapaneni, H., Donehower, L.A., Drummond, J., Gibbs, R.A., Glenn, R., Hale, W., Han, Y., Hu, J., Korchina, V., Lee, S., Lewis, L., Li, W., Liu, X., Morgan, M., Morton, D., Muzny, D., Santibanez, J., Sheth, M., Shinbrot, E., Wang, L., Wang, M., Wheeler, D.A., Xi, L., Zhao, F., Hess, J., Appelbaum, E.L., Bailey, M., Cordes, M.G., Ding, L., Fronick, C.C., Fulton, L.A., Fulton, R.S., Kandoth, C., Mardis, E.R., McLellan, M.D., Miller, C.A., Schmidt, H.K., Wilson, R.K., Crain, D., Curley, E., Gardner, J., Lau, K., Mallery, D., Morris, S., Paulauskis, J., Penny, R., Shelton, C., Shelton, T., Sherman, M., Thompson, E., Yena, P., Bowen, J., Gastier-Foster, J.M., Gerken, M., Leraas, K.M., Lichtenberg, T.M., Ramirez, N.C., Wise, L., Zmuda, E., Corcoran, N., Costello, T., Hovens, C., Carvalho, A.L., Carvalho, A.C. de, Fregnani, J.H., Longatto-Filho, A., Reis, R.M., Scapulatempo-Neto, C., Silveira, H.C.S., Vidal, D.O., Burnette, A., Eschbacher, J., Hermes, B., Noss, A., Singh, R., Anderson, M.L., Castro, P.D., Ittmann, M., Huntsman, D., Kohl, B., Le, X., Thorp, R., Andry, C., Duffy, E.R., Lyadov, V., Paklina, O., Setdikova, G., Shabunin, A., Tavobilov, M., McPherson, C., Warnick, R., Berkowitz, R., Cramer, D., Feltmate, C., Horowitz, N., Kibel, A., Muto, M., Raut, C.P., Malykh, A., Barnholtz-Sloan, J.S., Barrett, W., Devine, K., Fulop, J., Ostrom, Q.T., Shimmel, K., Wolinsky, Y., Sloan, A.E., Rose, A.D., Giuliante, F., Goodman, M., Karlan, B.Y., Hagedorn, C.H., Eckman, J., Harr, J., Myers, J., Tucker, K., Zach, L.A., Deyarmin, B., Hu, H., Kvecher, L., Larson, C., Mural, R.J., Somiari, S., Vicha, A., Zelinka, T., Bennett, J.,

Iacocca, M., Rabeno, B., Swanson, P., Latour, M., Lacombe, L., Têtu, B., Bergeron, A., McGraw, M., Staugaitis, S.M., Chabot, J., Hibshoosh, H., Sepulveda, A., Su, T., Wang, T., Potapova, O., Voronina, O., Desjardins, L., Mariani, O., Roman-Roman, S., Sastre, X., Stern, M.-H., Cheng, F., Signoretti, S., Berchuck, A., Bigner, D., Lipp, E., Marks, J., McCall, S., McLendon, R., Secord, A., Sharp, A., Behera, M., Brat, D.J., Chen, A., Delman, K., Force, S., Khuri, F., Magliocca, K., Maithel, S., Olson, J.J., Owonikoko, T., Pickens, A., Ramalingam, S., Shin, D.M., Sica, G., Meir, E.G.V., Zhang, Hongzheng, Eijckenboom, W., Gillis, A., Korpershoek, E., Looijenga, L., Oosterhuis, W., Stoop, H., Kessel, K.E. van, Zwarthoff, E.C., Calatozzolo, C., Cuppini, L., Cuzzubbo, S., DiMeco, F., Finocchiaro, G., Mattei, L., Perin, A., Pollo, B., Chen, C., Houck, J., Lohavanichbutr, P., Hartmann, A., Stoehr, C., Stoehr, R., Taubert, H., Wach, S., Wullich, B., Kycler, W., Murawa, D., Wiznerowicz, M., Chung, K., Edenfield, W.J., Martin, J., Baudin, E., Bubley, G., Bueno, R., Rienzo, A.D., Richards, W.G., Kalkanis, S., Mikkelsen, T., Noushmehr, H., Scarpace, L., Girard, N., Aymerich, M., Campo, E., Giné, E., Guillermo, A.L., Bang, N.V., Hanh, P.T., Phu, B.D., Tang, Y., Colman, H., Evason, K., Dottino, P.R., Martignetti, J.A., Gabra, H., Juhl, H., Akeredolu, T., Stepa, S., Hoon, D., Ahn, K., Kang, K.J., Beuschlein, F., Breggia, A., Birrer, M., Bell, D., Borad, M., Bryce, A.H., Castle, E., Chandan, V., Cheville, J., Copland, J.A., Farnell, M., Flotte, T., Giama, N., Ho, T., Kendrick, M., Kocher, J.-P., Kopp, K., Moser, C., Nagorney, D., O'Brien, D., O'Neill, B.P., Patel, T., Petersen, G., Que, F., Rivera, M., Roberts, L., Smallridge, R., Smyrk, T., Stanton, M., Thompson, R.H., Torbenson, M., Yang, J.D., Zhang, L., Brimo, F., Ajani, J.A., Gonzalez, A.M.A., Behrens, C., Bondaruk, J., Broaddus, R., Czerniak, B., Esmaeli, B., Fujimoto, J., Gershenwald, J., Guo, C., Lazar, A.J., Logothetis, C., Meric-Bernstam, F., Moran, C., Ramondetta, L., Rice, D., Sood, A., Tamboli, P., Thompson, T., Troncoso, P., Tsao, A., Wistuba, I., Carter, C., Haydu, L., Hersey, P., Jakrot, V., Kakavand, H., Kefford, R., Lee, K., Long, G., Mann, G., Quinn, M., Saw, R., Scolyer, R., Shannon, K., Spillane, A., Stretch, J., Synott, M., Thompson, J., Wilmott, J., Al-Ahmadie, H., Chan, T.A., Ghossein, R., Gopalan, A., Levine, D.A., Reuter, V., Singer, S., Singh, B., Tien, N.V., Broudy, T., Mirsaidi, C., Nair, P., Drwiega, P., Miller, J., Smith, J., Zaren, H., Park, J.-W., Hung, N.P., Kebebew, E., Linehan, W.M., Metwalli, A.R., Pacak, K., Pinto, P.A., Schiffman, M., Schmidt, L.S., Vocke, C.D., Wentzensen, N., Worrell, R., Yang, H., Moncrieff, M., Goparaju, C., Melamed, J., Pass, H., Botnariuc, N., Caraman, I., Cernat, M., Chemencedji, I., Clipca, A., Doruc, S., Gorincioi, G., Mura, S., Pirtac, M., Stancul, I., Tcaciuc, D., Albert, M., Alexopoulou, I., Arnaout, A., Bartlett, J., Engel, J., Gilbert, S., Parfitt, J., Sekhon, H., Thomas, G., Rassl, D.M., Rintoul, R.C., Bifulco, C., Tamakawa, R., Urba, W., Hayward, N., Timmers, H., Antenucci, A., Facciolo, F., Grazi, G., Marino, M., Merola, R., Krijger, R. de, Gimenez-Roqueplo, A.-P., Piché, A., Chevalier, S., McKercher, G., Birsoy, K., Barnett, G., Brewer, C., Farver, C., Naska, T., Pennell, N.A., Raymond, D., Schilero, C., Smolenski, K., Williams, F., Morrison, C., Borgia, J.A., Liptay, M.J., Pool, M., Seder, C.W., Junker, K., Omberg, L., Dinkin, M., Manikhas, G., Alvaro, D., Bragazzi, M.C., Cardinale, V., Carpino, G., Gaudio, E., Chesla, D., Cottingham, S., Dubina, M., Moiseenko, F., Dhanasekaran, R., Becker, K.-F., Janssen, K.-P., Slotta-Huspenina, J., Abdel-Rahman, M.H., Aziz, D.,

Bell, S., Cebulla, C.M., Davis, A., Duell, R., Elder, J.B., Hilty, J., Kumar, B., Lang, J., Lehman, N.L., Mandt, R., Nguyen, P., Pilarski, R., Rai, K., Schoenfield, L., Senecal, K., Wakely, P., Hansen, P., Lechan, R., Powers, J., Tischler, A., Grizzle, W.E., Sexton, K.C., Kastl, A., Henderson, J., Porten, S., Waldmann, J., Fassnacht, M., Asa, S.L., Schadendorf, D., Couce, M., Graefen, M., Huland, H., Sauter, G., Schlomm, T., Simon, R., Tennstedt, P., Olabode, O., Nelson, M., Bathe, O., Carroll, P.R., Chan, J.M., Disaia, P., Glenn, P., Kelley, R.K., Landen, C.N., Phillips, J., Prados, M., Simko, J., Smith-McCune, K., VandenBerg, S., Roggin, K., Fehrenbach, A., Kendler, A., Sifri, S., Steele, R., Jimeno, A., Carey, F., Forgie, I., Mannelli, M., Carney, M., Hernandez, B., Campos, B., Herold-Mende, C., Jungk, C., Unterberg, A., Deimling, A. von, Bossler, A., Galbraith, J., Jacobus, L., Knudson, M., Knutson, T., Ma, D., Milhem, M., Sigmund, R., Godwin, A.K., Madan, R., Rosenthal, H.G., Adebamowo, C., Adebamowo, S.N., Boussioutas, A., Beer, D., Giordano, T., Mes-Masson, A.-M., Saad, F., Bocklage, T., Landrum, L., Mannel, R., Moore, K., Moxley, K., Postier, R., Walker, J., Zuna, R., Feldman, M., Valdivieso, F., Dhir, R., Luketich, J., Pinero, E.M.M., Quintero-Aguilo, M., Carlotti, C.G., Santos, J.S.D., Kemp, R., Sankarankuty, A., Tirapelli, D., Catto, J., Agnew, K., Swisher, E., Creaney, J., Robinson, B., Shelley, C.S., Godwin, E.M., Kendall, S., Shipman, C., Bradford, C., Carey, T., Haddad, A., Moyer, J., Peterson, L., Prince, M., Rozek, L., Wolf, G., Bowman, R., Fong, K.M., Yang, I., Korst, R., Rathmell, W.K., Fantacone-Campbell, J.L., Hooke, J.A., Kovatich, A.J., Shriver, C.D., DiPersio, J., Drake, B., Govindan, R., Heath, S., Ley, T., Tine, B.V., Westervelt, P., Rubin, M.A., Lee, J.I., Aredes, N.D., Mariamidze, A., Lawrence, M.S., Godzik, A., Lopez-Bigas, N., Stuart, J., Wheeler, D., Getz, G., Chen, K., Lazar, A.J., Mills, G.B., Karchin, R., Ding, L., 2018. Comprehensive Characterization of Cancer Driver Genes and Mutations. Cell 173, 371-385.e18. https://doi.org/10.1016/j.cell.2018.02.060

Bakhoum, S.F., Landau, D.A., 2017. Chromosomal Instability as a Driver of Tumor Heterogeneity and Evolution. Cold Spring Harb Perspect Med 7, a029611. https://doi.org/10.1101/cshperspect.a029611

Balachandran, V.P., Cavnar, M.J., Zeng, S., Bamboat, Z.M., Ocuin, L.M., Obaid, H., Sorenson, E.C., Popow, R., Ariyan, C., Rossi, F., Besmer, P., Guo, T., Antonescu, C.R., Taguchi, T., Yuan, J., Wolchok, J.D., Allison, J.P., DeMatteo, R.P., 2011. Imatinib potentiates antitumor T cell responses in gastrointestinal stromal tumor through the inhibition of Ido. Nat Med 17, 1094–1100. https://doi.org/10.1038/nm.2438

Ballman, K.V., 2015. Biomarker: Predictive or Prognostic? JCO 33, 3968–3971. https://doi.org/10.1200/JCO.2015.63.3651

Barranco, S.C., Perry, R.R., Durm, M.E., Werner, A.L., Gregorcyk, S.G., Bolton, W.E., Kolm, P., Townsend, C.M., 1994. Intratumor Variability in Prognostic Indicators May Be the Case of Conflicting Estimates of Patient Survival and Response to Therapy. Cancer Res 54, 5351–5356.

Becht, E., Giraldo, N.A., Lacroix, L., Buttard, B., Elarouci, N., Petitprez, F., Selves, J., Laurent-Puig, P., Sautès-Fridman, C., Fridman, W.H., de Reyniès, A., 2016. Estimating the population abundance of tissue-infiltrating immune and stromal cell populations using gene expression. Genome Biology 17, 218. https://doi.org/10.1186/s13059-016-1070-5

Beer, D.G., Kardia, S.L.R., Huang, C.-C., Giordano, T.J., Levin, A.M., Misek, D.E., Lin, L., Chen, G., Gharib, T.G., Thomas, D.G., Lizyness, M.L., Kuick, R., Hayasaka, S., Taylor, J.M.G., Iannettoni, M.D., Orringer, M.B., Hanash, S., 2002. Gene-expression profiles predict survival of patients with lung adenocarcinoma. Nat Med 8, 816–824. https://doi.org/10.1038/nm733

Beerman, H., Smit, V.T.H.B.M., Kluin, P.M., Bonsing, B.A., Hermans, J., Cornelisse, C.J., 1991. Flow cytometric analysis of DNA stemline heterogeneity in primary and metastatic breast cancer. Cytometry 12, 147–154. https://doi.org/10.1002/cyto.990120208

Bentley, D.R., Balasubramanian, S., Swerdlow, H.P., Smith, G.P., Milton, J., Brown, C.G., Hall, K.P., Evers, D.J., Barnes, C.L., Bignell, H.R., Boutell, J.M., Bryant, J., Carter, R.J., Keira Cheetham, R., Cox, A.J., Ellis, D.J., Flatbush, M.R., Gormley, N.A., Humphray, S.J., Irving, L.J., Karbelashvili, M.S., Kirk, S.M., Li, H., Liu, X., Maisinger, K.S., Murray, L.J., Obradovic, B., Ost, T., Parkinson, M.L., Pratt, M.R., Rasolonjatovo, I.M.J., Reed, M.T., Rigatti, R., Rodighiero, C., Ross, M.T., Sabot, A., Sankar, S.V., Scally, A., Schroth, G.P., Smith, M.E., Smith, V.P., Spiridou, A., Torrance, P.E., Tzonev, S.S., Vermaas, E.H., Walter, K., Wu, X., Zhang, L., Alam, M.D., Anastasi, C., Aniebo, I.C., Bailey, D.M.D., Bancarz, I.R., Banerjee, S., Barbour, S.G., Baybayan, P.A., Benoit, V.A., Benson, K.F., Bevis, C., Black, P.J., Boodhun, A., Brennan, J.S., Bridgham, J.A., Brown, R.C., Brown, A.A., Buermann, D.H., Bundu, A.A., Burrows, J.C., Carter, N.P., Castillo, N., Chiara E. Catenazzi, M., Chang, S., Neil Cooley, R., Crake, N.R., Dada, O.O., Diakoumakos, K.D., Dominguez-Fernandez, B., Earnshaw, D.J., Egbujor, U.C., Elmore, D.W., Etchin, S.S., Ewan, M.R., Fedurco, M., Fraser, L.J., Fuentes Fajardo, K.V., Scott Furey, W., George, D., Gietzen, K.J., Goddard, C.P., Golda, G.S., Granieri, P.A., Green, D.E., Gustafson, D.L., Hansen, N.F., Harnish, K., Haudenschild, C.D., Heyer, N.I., Hims, M.M., Ho, J.T., Horgan, A.M., Hoschler, K., Hurwitz, S., Ivanov, D.V., Johnson, M.Q., James, T., Huw Jones, T.A., Kang, G.-D., Kerelska, T.H., Kersey, A.D., Khrebtukova, I., Kindwall, A.P., Kingsbury, Z., Kokko-Gonzales, P.I., Kumar, A., Laurent, M.A., Lawley, C.T., Lee, S.E., Lee, X., Liao, A.K., Loch, J.A., Lok, M., Luo, S., Mammen, R.M., Martin, J.W., McCauley, P.G., McNitt, P., Mehta, P., Moon, K.W., Mullens, J.W., Newington, T., Ning, Z., Ling Ng, B., Novo, S.M., O'Neill, M.J., Osborne, M.A., Osnowski, A., Ostadan, O., Paraschos, L.L., Pickering, L., Pike, Andrew C., Pike, Alger C., Chris Pinkard, D., Pliskin, D.P., Podhasky, J., Quijano, V.J., Raczy, C., Rae, V.H., Rawlings, S.R., Chiva Rodriguez, A., Roe, P.M., Rogers, John, Rogert Bacigalupo, M.C., Romanov, N., Romieu, A., Roth, R.K., Rourke, N.J., Ruediger, S.T., Rusman, E., Sanches-Kuiper, R.M., Schenker, M.R., Seoane, J.M., Shaw, R.J., Shiver, M.K., Short, S.W., Sizto, N.L., Sluis, J.P., Smith, M.A., Ernest Sohna Sohna, J., Spence, E.J., Stevens, K., Sutton, N., Szajkowski, L., Tregidgo, C.L., Turcatti, G., vandeVondele, S., Verhovsky, Y., Virk, S.M., Wakelin, S., Walcott, G.C., Wang, J., Worsley, G.J., Yan, J., Yau, L., Zuerlein, M., Rogers, Jane, Mullikin, J.C., Hurles, M.E., McCooke, N.J., West, J.S., Oaks, F.L., Lundberg, P.L., Klenerman, D., Durbin, R., Smith, A.J., 2008. Accurate whole human genome sequencing using reversible terminator chemistry. Nature 456, 53–59. https://doi.org/10.1038/nature07517

Berglund, E., Maaskola, J., Schultz, N., Friedrich, S., Marklund, M., Bergenstråhle, J., Tarish, F., Tanoglidi, A., Vickovic, S., Larsson, L., Salmén, F., Ogris, C., Wallenborg, K., Lagergren, J., Ståhl, P., Sonnhammer, E., Helleday, T., Lundeberg, J., 2018. Spatial maps of prostate cancer transcriptomes reveal an unexplored landscape of heterogeneity. Nature Communications 9, 2419. https://doi.org/10.1038/s41467-018-04724-5

Beroukhim, R., Mermel, C.H., Porter, D., Wei, G., Raychaudhuri, S., Donovan, J., Barretina, J., Boehm, J.S., Dobson, J., Urashima, M., Mc Henry, K.T., Pinchback, R.M., Ligon, A.H., Cho, Y.-J., Haery, L., Greulich, H., Reich, M., Winckler, W., Lawrence, M.S., Weir, B.A., Tanaka, K.E., Chiang, D.Y., Bass, A.J., Loo, A., Hoffman, C., Prensner, J., Liefeld, T., Gao, Q., Yecies, D., Signoretti, S., Maher, E., Kaye, F.J., Sasaki, H., Tepper, J.E., Fletcher, J.A., Tabernero, J., Baselga, J., Tsao, M.-S., Demichelis, F., Rubin, M.A., Janne, P.A., Daly, M.J., Nucera, C., Levine, R.L., Ebert, B.L., Gabriel, S., Rustgi, A.K., Antonescu, C.R., Ladanyi, M., Letai, A., Garraway, L.A., Loda, M., Beer, D.G., True, L.D., Okamoto, A., Pomeroy, S.L., Singer, S., Golub, T.R., Lander, E.S., Getz, G., Sellers, W.R., Meyerson, M., 2010. The landscape of somatic copy-number alteration across human cancers. Nature 463, 899–905. https://doi.org/10.1038/nature08822

Bhandari, V., Liu, L.Y., Salcedo, A., Espiritu, S.M.G., Morris, Q.D., Boutros, P.C., 2018. The Inter and Intra-Tumoural Heterogeneity of Subclonal Reconstruction. bioRxiv 418780. https://doi.org/10.1101/418780

Bhattacharjee, A., Richards, W.G., Staunton, J., Li, C., Monti, S., Vasa, P., Ladd, C., Beheshti, J., Bueno, R., Gillette, M., Loda, M., Weber, G., Mark, E.J., Lander, E.S., Wong, W., Johnson, B.E., Golub, T.R., Sugarbaker, D.J., Meyerson, M., 2001. Classification of human lung carcinomas by mRNA expression profiling reveals distinct adenocarcinoma subclasses. PNAS 98, 13790–13795. https://doi.org/10.1073/pnas.191502998

Bianchi, F., Nuciforo, P., Vecchi, M., Bernard, L., Tizzoni, L., Marchetti, A., Buttitta, F., Felicioni, L., Nicassio, F., Fiore, P.P.D., 2007. Survival prediction of stage I lung adenocarcinomas by expression of 10 genes. J Clin Invest 117, 3436–3444. https://doi.org/10.1172/JCI32007

Bindea, G., Mlecnik, B., Tosolini, M., Kirilovsky, A., Waldner, M., Obenauf, A.C., Angell, H., Fredriksen, T., Lafontaine, L., Berger, A., Bruneval, P., Fridman, W.H., Becker, C., Pagès, F., Speicher, M.R., Trajanoski, Z., Galon, J., 2013. Spatiotemporal Dynamics of Intratumoral Immune Cells Reveal the Immune Landscape in Human Cancer. Immunity 39, 782–795. https://doi.org/10.1016/j.immuni.2013.10.003

Birkbak, N.J., Eklund, A.C., Li, Q., McClelland, S.E., Endesfelder, D., Tan, P., Tan, I.B., Richardson, A.L., Szallasi, Z., Swanton, C., 2011. Paradoxical Relationship between Chromosomal Instability and Survival Outcome in Cancer. Cancer Res 71, 3447–3452. https://doi.org/10.1158/0008-5472.CAN-10-3667

Biswas, D., Birkbak, N.J., Rosenthal, R., Hiley, C.T., Lim, E.L., Papp, K., Boeing, S., Krzystanek, M., Djureinovic, D., Fleur, L.L., Greco, M., Döme, B., Fillinger, J., Brunnström, H., Wu, Y., Moore, D.A., Skrzypski, M., Abbosh, C., Litchfield, K., Bakir, M.A., Watkins, T.B.K., Veeriah, S., Wilson, G.A., Jamal-Hanjani, M., Moldvay, J., Botling, J., Chinnaiyan, A.M., Micke, P., Hackshaw, A., Bartek, J., Csabai, I., Szallasi, Z., Herrero, J., McGranahan,

N., Swanton, C., 2019. A clonal expression biomarker associates with lung cancer mortality. Nat Med 1–9. https://doi.org/10.1038/s41591-019-0595-z

Blackhall, F.H., Pintilie, M., Wigle, D.A., Jurisica, I., Liu, N., Radulovich, N., Johnston, M.R., Keshavjee, S., Tsao, M.-S., 2004. Stability and Heterogeneity of Expression Profiles in Lung Cancer Specimens Harvested Following Surgical Resection. Neoplasia 6, 761–767.

Blakely, C.M., Watkins, T.B.K., Wu, W., Gini, B., Chabon, J.J., McCoach, C.E., McGranahan, N., Wilson, G.A., Birkbak, N.J., Olivas, V.R., Rotow, J., Maynard, A., Wang, V., Gubens, M.A., Banks, K.C., Lanman, R.B., Caulin, A.F., John, J.S., Cordero, A.R., Giannikopoulos, P., Simmons, A.D., Mack, P.C., Gandara, D.R., Husain, H., Doebele, R.C., Riess, J.W., Diehn, M., Swanton, C., Bivona, T.G., 2017. Evolution and clinical impact of co-occurring genetic alterations in advanced-stage *EGFR*-mutant lung cancers. Nature Genetics ng.3990. https://doi.org/10.1038/ng.3990

Blum, A., Wang, P., Zenklusen, J.C., 2018. SnapShot: TCGA-Analyzed Tumors. Cell 173, 530. https://doi.org/10.1016/j.cell.2018.03.059

Bohn, T., Rapp, S., Luther, N., Klein, M., Bruehl, T.-J., Kojima, N., Lopez, P.A., Hahlbrock, J., Muth, S., Endo, S., Pektor, S., Brand, A., Renner, K., Popp, V., Gerlach, K., Vogel, D., Lueckel, C., Arnold-Schild, D., Pouyssegur, J., Kreutz, M., Huber, M., Koenig, J., Weigmann, B., Probst, H.-C., Stebut, E. von, Becker, C., Schild, H., Schmitt, E., Bopp, T., 2018. Tumor immunoevasion via acidosis-dependent induction of regulatory tumor-associated macrophages. Nature Immunology 19, 1319. https://doi.org/10.1038/s41590-018-0226-8

Boon, T., 1983. Antigenic Tumor Cell Variants Obtained with Mutagens, in: Klein, G., Weinhouse, S. (Eds.), Advances in Cancer Research. Academic Press, pp. 121–151. https://doi.org/10.1016/S0065-230X(08)61034-9

Boutros, P.C., 2015. The path to routine use of genomic biomarkers in the cancer clinic. Genome Res. 25, 1508–1513. https://doi.org/10.1101/gr.191114.115

Boutros, P.C., Fraser, M., Harding, N.J., Borja, R. de, Trudel, D., Lalonde, E., Meng, A., Hennings-Yeomans, P.H., McPherson, A., Sabelnykova, V.Y., Zia, A., Fox, N.S., Livingstone, J., Shiah, Y.-J., Wang, J., Beck, T.A., Have, C.L., Chong, T., Sam, M., Johns, J., Timms, L., Buchner, N., Wong, A., Watson, J.D., Simmons, T.T., P'ng, C., Zafarana, G., Nguyen, F., Luo, X., Chu, K.C., Prokopec, S.D., Sykes, J., Pra, A.D., Berlin, A., Brown, A., Chan-Seng-Yue, M.A., Yousif, F., Denroche, R.E., Chong, L.C., Chen, G.M., Jung, E., Fung, C., Starmans, M.H.W., Chen, H., Govind, S.K., Hawley, J., D'Costa, A., Pintilie, M., Waggott, D., Hach, F., Lambin, P., Muthuswamy, L.B., Cooper, C., Eeles, R., Neal, D., Tetu, B., Sahinalp, C., Stein, L.D., Fleshner, N., Shah, S.P., Collins, C.C., Hudson, T.J., McPherson, J.D., Kwast, T. van der, Bristow, R.G., 2015. Spatial genomic heterogeneity within localized, multifocal prostate cancer. Nature Genetics 47, 736. https://doi.org/10.1038/ng.3315

Boutros, P.C., Lau, S.K., Pintilie, M., Liu, N., Shepherd, F.A., Der, S.D., Tsao, M.-S., Penn, L.Z., Jurisica, I., 2009. Prognostic gene signatures for non-small-cell lung cancer. PNAS 106, 2824–2828. https://doi.org/10.1073/pnas.0809444106

Boveri, T., 1914. Zur frage der entstehung maligner tumoren. Fischer.

Brahmer, J.R., Tykodi, S.S., Chow, L.Q.M., Hwu, W.-J., Topalian, S.L., Hwu, P., Drake, C.G., Camacho, L.H., Kauh, J., Odunsi, K., Pitot, H.C., Hamid, O.,

Bhatia, S., Martins, R., Eaton, K., Chen, S., Salay, T.M., Alaparthy, S., Grosso, J.F., Korman, A.J., Parker, S.M., Agrawal, S., Goldberg, S.M., Pardoll, D.M., Gupta, A., Wigginton, J.M., 2012. Safety and activity of anti-PD-L1 antibody in patients with advanced cancer. N. Engl. J. Med. 366, 2455–2465. https://doi.org/10.1056/NEJMoa1200694

Breslow, A., 1970. Thickness, Cross-sectional Areas and Depth of Invasion in the Prognosis of Cutaneous Melanoma. Annals of Surgery 172, 902–908.

Bunn, P.A., Hirsch, F.R., Aisner, D.L., 2014. Is There Clinical Value to Prognostic Signatures in Early-Stage NSCLC? Clin Cancer Res 20, 1727–1729. https://doi.org/10.1158/1078-0432.CCR-13-3387

Burnet, M., 1957. Cancer: a biological approach. III. Viruses associated with neoplastic conditions. IV. Practical applications. Br Med J 1, 841–847. https://doi.org/10.1136/bmj.1.5023.841

Calabrese, C., Davidson, N.R., Demircioğlu, D., Fonseca, N.A., He, Y., Kahles, A., Lehmann, K.-V., Liu, F., Shiraishi, Y., Soulette, C.M., Urban, L., Greger, L., Li, S., Liu, D., Perry, M.D., Xiang, Q., Zhang, F., Zhang, J., Bailey, P., Erkek, S., Hoadley, K.A., Hou, Y., Huska, M.R., Kilpinen, H., Korbel, J.O., Marin, M.G., Markowski, J., Nandi, T., Pan-Hammarström, Q., Pedamallu, C.S., Siebert, R., Stark, S.G., Su, H., Tan, P., Waszak, S.M., Yung, C., Zhu, S., Awadalla, P., Creighton, C.J., Meyerson, M., Ouellette, B.F.F., Wu, K., Yang, H., Brazma, A., Brooks, A.N., Göke, J., Rätsch, G., Schwarz, R.F., Stegle, O., Zhang, Z., 2020. Genomic basis for RNA alterations in cancer. Nature 578, 129–136. https://doi.org/10.1038/s41586-020-1970-0

Campbell, J.D., Alexandrov, A., Kim, J., Wala, J., Berger, A.H., Pedamallu, C.S., Shukla, S.A., Guo, G., Brooks, A.N., Murray, B.A., Imielinski, M., Hu, X., Ling, S., Akbani, R., Rosenberg, M., Cibulskis, C., Ramachandran, A., Collisson, E.A., Kwiatkowski, D.J., Lawrence, M.S., Weinstein, J.N., Verhaak, R.G.W., Wu, C.J., Hammerman, P.S., Cherniack, A.D., Getz, G., Network, C.G.A.R., Zenklusen, J.C., Zhang, J., Felau, I., Demchok, J.A., Yang, L., Wang, Z., Ferguson, M.L., Tarnuzzer, R., Hutter, C.M., Sofia, H.J., Pihl, T., Wan, Y., Chudamani, S., Liu, J., Sun, C., Naresh, R., Lolla, L., Wu, Y., Creighton, C.J., Rathmell, W.K., Auman, J.T., Balu, S., Bodenheimer, T., Hayes, D.N., Hoadley, K.A., Hoyle, A.P., Jones, C.D., Jefferys, S.R., Meng, S., Mieczkowski, P.A., Mose, L.E., Perou, C.M., Roach, J., Shi, Y., Simons, J.V., Skelly, T., Soloway, M.G., Tan, D., Wu, J., Veluvolu, U., Parker, J.S., Wilkerson, M.D., Boice, L., Huang, M., Thorne, L.B., Getz, G., Noble, M.S., Zhang, H., Heiman, D.I., Cho, J., Gehlenborg, N., Saksena, G., Voet, D., Lin, P., Frazer, S., Kim, J., Lawrence, M.S., Chin, L., Tsao, M.-S., Allison, F., Chadwick, D., Muley, T., Meister, M., Dienemann, H., Kucherlapati, R., Park, P., Bowen, J., Gastier-Foster, J.M., Gerken, M., Leraas, K.M., Lichtenberg, T.M., Ramirez, N.C., Wise, L., Zmuda, E., Stuart, J., Collisson, E., Peifer, M., Kwiatkowski, D., Campbell, J.D., Murray, B.A., Cherniack, A.D., Berger, A.H., Sougnez, C., Schumacher, S.E., Shih, J., Beroukhim, R., Zack, T.I., Gabriel, S.B., Meyerson, M., Byers, L.A., Davidsen, T., Laird, P.W., Weisenberger, D.J., Berg, D.J.V.D., Bootwalla, M.S., Lai, P.H., Maglinte, D.T., Baylin, S.B., Herman, J.G., Danilova, L., Cope, L., Crain, D.J., Curley, E., Gardner, J., Lau, K., Mallery, D., Morris, S., Paulauskis, J., Penny, R., Shelton, C., Shelton, T., Sherman, M., Yena, P., Mills, G.B., Artyomov, M.N., Schreiber, R., Govindan, R., Meyerson, M., 2016. Distinct patterns of somatic genome alterations in lung adenocarcinomas and

squamous cell carcinomas. Nature Genetics 48, ng.3564. https://doi.org/10.1038/ng.3564

Campbell, P.J., Pleasance, E.D., Stephens, P.J., Dicks, E., Rance, R., Goodhead, I., Follows, G.A., Green, A.R., Futreal, P.A., Stratton, M.R., 2008a. Subclonal phylogenetic structures in cancer revealed by ultra-deep sequencing. PNAS 105, 13081–13086. https://doi.org/10.1073/pnas.0801523105

Campbell, P.J., Stephens, P.J., Pleasance, E.D., O'Meara, S., Li, H., Santarius, T., Stebbings, L.A., Leroy, C., Edkins, S., Hardy, C., Teague, J.W., Menzies, A., Goodhead, I., Turner, D.J., Clee, C.M., Quail, M.A., Cox, A., Brown, C., Durbin, R., Hurles, M.E., Edwards, P.A.W., Bignell, G.R., Stratton, M.R., Futreal, P.A., 2008b. Identification of somatically acquired rearrangements in cancer using genome-wide massively parallel paired-end sequencing. Nature Genetics 40, 722–729. https://doi.org/10.1038/ng.128

Cancer Genome Atlas Network, 2012. Comprehensive molecular portraits of human breast tumours. Nature 490, 61–70. https://doi.org/10.1038/nature11412

Cancer Genome Atlas Research Network, 2008. Comprehensive genomic characterization defines human glioblastoma genes and core pathways. Nature 455, 1061–1068. https://doi.org/10.1038/nature07385

Canisius, S., Martens, J.W.M., Wessels, L.F.A., 2016. A novel independence test for somatic alterations in cancer shows that biology drives mutual exclusivity but chance explains most co-occurrence. Genome Biol 17. https://doi.org/10.1186/s13059-016-1114-x

Caravagna, G., Giarratano, Y., Ramazzotti, D., Tomlinson, I., Graham, T.A., Sanguinetti, G., Sottoriva, A., 2018. Detecting repeated cancer evolution from multi-region tumor sequencing data. Nature Methods 15, 707–714. https://doi.org/10.1038/s41592-018-0108-x

Carter, S.L., Eklund, A.C., Kohane, I.S., Harris, L.N., Szallasi, Z., 2006. A signature of chromosomal instability inferred from gene expression profiles predicts clinical outcome in multiple human cancers. Nat Genet 38, 1043–1048. https://doi.org/10.1038/ng1861

Castel, S.E., Mohammadi, P., Chung, W.K., Shen, Y., Lappalainen, T., 2016. Rare variant phasing and haplotypic expression from RNA sequencing with phASER. Nature Communications 7, 12817. https://doi.org/10.1038/ncomms12817

Charoentong, P., Finotello, F., Angelova, M., Mayer, C., Efremova, M., Rieder, D., Hackl, H., Trajanoski, Z., 2017. Pan-cancer Immunogenomic Analyses Reveal Genotype-Immunophenotype Relationships and Predictors of Response to Checkpoint Blockade. Cell Rep 18, 248–262. https://doi.org/10.1016/j.celrep.2016.12.019

Chen, D.S., Mellman, I., 2017. Elements of cancer immunity and the cancer-immune set point. Nature 541, 321–330. https://doi.org/10.1038/nature21349

Chen, H.-Y., Yu, S.-L., Chen, C.-H., Chang, G.-C., Chen, C.-Y., Yuan, A., Cheng, C.-L., Wang, C.-H., Terng, H.-J., Kao, S.-F., Chan, W.-K., Li, H.-N., Liu, C.-C., Singh, S., Chen, W.J., Chen, J.J.W., Yang, P.-C., 2007. A Five-Gene Signature and Clinical Outcome in Non–Small-Cell Lung Cancer. NEJM 356, 11–20. https://doi.org/10.1056/NEJMoa060096

Chen, J.J.W., Peck, K., Hong, T.-M., Yang, S.-C., Sher, Y.-P., Shih, J.-Y., Wu, R., Cheng, J.-L., Roffler, S.R., Wu, C.-W., Yang, P.-C., 2001. Global Analysis of Gene Expression in Invasion by a Lung Cancer Model. Cancer Res 61, 5223–5230.

Chen, P.-L., Roh, W., Reuben, A., Cooper, Z.A., Spencer, C.N., Prieto, P.A., Miller, J.P., Bassett, R.L., Gopalakrishnan, V., Wani, K., Macedo, M.P.D., Austin-Breneman, J.L., Jiang, H., Chang, Q., Reddy, S.M., Chen, W.-S., Tetzlaff, M.T., Broaddus, R.J., Davies, M.A., Gershenwald, J.E., Haydu, L., Lazar, A.J., Patel, S.P., Hwu, P., Hwu, W.-J., Diab, A., Glitza, I.C., Woodman, S.E., Vence, L.M., Wistuba, I.I., Amaria, R.N., Kwong, L.N., Prieto, V., Davis, R.E., Ma, W., Overwijk, W.W., Sharpe, A.H., Hu, J., Futreal, P.A., Blando, J., Sharma, P., Allison, J.P., Chin, L., Wargo, J.A., 2016. Analysis of Immune Signatures in Longitudinal Tumor Samples Yields Insight into Biomarkers of Response and Mechanisms of Resistance to Immune Checkpoint Blockade. Cancer Discov 6, 827–837. https://doi.org/10.1158/2159-8290.CD-15-1545

Cibulskis, K., Lawrence, M.S., Carter, S.L., Sivachenko, A., Jaffe, D., Sougnez, C., Gabriel, S., Meyerson, M., Lander, E.S., Getz, G., 2013. Sensitive detection of somatic point mutations in impure and heterogeneous cancer samples. Nature Biotechnology 31, 213. https://doi.org/10.1038/nbt.2514

Cieślik, M., Chinnaiyan, A.M., 2018. Cancer transcriptome profiling at the juncture of clinical translation. Nature Reviews Genetics 19, 93–109. https://doi.org/10.1038/nrg.2017.96

Ciriello, G., Cerami, E., Sander, C., Schultz, N., 2012. Mutual exclusivity analysis identifies oncogenic network modules. Genome Res. 22, 398–406. https://doi.org/10.1101/gr.125567.111

Cleary, B., Cong, L., Cheung, A., Lander, E.S., Regev, A., 2017. Efficient Generation of Transcriptomic Profiles by Random Composite Measurements. Cell. https://doi.org/10.1016/j.cell.2017.10.023

Clemente, C.G., Mihm, M.C., Bufalino, R., Zurrida, S., Collini, P., Cascinelli, N., 1996. Prognostic value of tumor infiltrating lymphocytes in the vertical growth phase of primary cutaneous melanoma. Cancer 77, 1303–1310. https://doi.org/10.1002/(SICI)1097-0142(19960401)77:7<1303::AID-CNCR12>3.0.CO;2-5

Collins, F.S., Varmus, H., 2015. A New Initiative on Precision Medicine. New England Journal of Medicine 372, 793–795. https://doi.org/10.1056/NEJMp1500523

Constantinescu, S., Szczurek, E., Mohammadi, P., Rahnenführer, J., Beerenwinkel, N., 2016. TiMEx: a waiting time model for mutually exclusive cancer alterations. Bioinformatics 32, 968–975. https://doi.org/10.1093/bioinformatics/btv400

Costa, A., Kieffer, Y., Scholer-Dahirel, A., Pelon, F., Bourachot, B., Cardon, M., Sirven, P., Magagna, I., Fuhrmann, L., Bernard, C., Bonneau, C., Kondratova, M., Kuperstein, I., Zinovyev, A., Givel, A.-M., Parrini, M.-C., Soumelis, V., Vincent-Salomon, A., Mechta-Grigoriou, F., 2018. Fibroblast Heterogeneity and Immunosuppressive Environment in Human Breast Cancer. Cancer Cell 0. https://doi.org/10.1016/j.ccell.2018.01.011

Cristescu, R., Mogg, R., Ayers, M., Albright, A., Murphy, E., Yearley, J., Sher, X., Liu, X.Q., Lu, H., Nebozhyn, M., Zhang, C., Lunceford, J.K., Joe, A., Cheng, J., Webber, A.L., Ibrahim, N., Plimack, E.R., Ott, P.A., Seiwert, T.Y., Ribas,

A., McClanahan, T.K., Tomassini, J.E., Loboda, A., Kaufman, D., 2018. Pan-tumor genomic biomarkers for PD-1 checkpoint blockade–based immunotherapy. Science 362, eaar3593. https://doi.org/10.1126/science.aar3593

Cross, W., Kovac, M., Mustonen, V., Temko, D., Davis, H., Baker, A.-M., Biswas, S., Arnold, R., Chegwidden, L., Gatenbee, C., Anderson, A.R., Koelzer, V.H., Martinez, P., Jiang, X., Domingo, E., Woodcock, D.J., Feng, Y., Kovacova, M., Maughan, T., Jansen, M., Rodriguez-Justo, M., Ashraf, S., Guy, R., Cunningham, C., East, J.E., Wedge, D.C., Wang, L.M., Palles, C., Heinimann, K., Sottoriva, A., Leedham, S.J., Graham, T.A., Tomlinson, I.P.M., 2018. The evolutionary landscape of colorectal tumorigenesis. Nat Ecol Evol 2, 1661–1672. https://doi.org/10.1038/s41559-018-0642-z

Cruz, M.S., Diamond, A., Russell, A., Jameson, J.M., 2018. Human αβ and γδ T Cells in Skin Immunity and Disease. Front Immunol 9. https://doi.org/10.3389/fimmu.2018.01304

Danaher, P., Warren, S., Dennis, L., D'Amico, L., White, A., Disis, M.L., Geller, M.A., Odunsi, K., Beechem, J., Fling, S.P., 2017. Gene expression markers of Tumor Infiltrating Leukocytes. Journal for ImmunoTherapy of Cancer 5, 18. https://doi.org/10.1186/s40425-017-0215-8

Darwin, C., 1859. The origin of species, ed. JW Burrow.

Darwin, C., 1845. Voyage of the Beagle round the world. Tess Pres, New York.

Davies, H., Bignell, G.R., Cox, C., Stephens, P., Edkins, S., Clegg, S., Teague, J., Woffendin, H., Garnett, M.J., Bottomley, W., Davis, N., Dicks, E., Ewing, R., Floyd, Y., Gray, K., Hall, S., Hawes, R., Hughes, J., Kosmidou, V., Menzies, A., Mould, C., Parker, A., Stevens, C., Watt, S., Hooper, S., Wilson, R., Jayatilake, H., Gusterson, B.A., Cooper, C., Shipley, J., Hargrave, D., Pritchard-Jones, K., Maitland, N., Chenevix-Trench, G., Riggins, G.J., Bigner, D.D., Palmieri, G., Cossu, A., Flanagan, A., Nicholson, A., Ho, J.W.C., Leung, S.Y., Yuen, S.T., Weber, B.L., Seigler, H.F., Darrow, T.L., Paterson, H., Marais, R., Marshall, C.J., Wooster, R., Stratton, M.R., Futreal, P.A., 2002. Mutations of the BRAF gene in human cancer. Nature 417, 949–954. https://doi.org/10.1038/nature00766

Davoli, T., Uno, H., Wooten, E.C., Elledge, S.J., 2017. Tumor aneuploidy correlates with markers of immune evasion and with reduced response to immunotherapy. Science 355, eaaf8399. https://doi.org/10.1126/science.aaf8399

de Bruin, McGranahan, N., Mitter, R., Salm, M., Wedge, D.C., Yates, L., Jamal-Hanjani, M., Shafi, S., Murugaesu, N., Rowan, A.J., Grönroos, E., Muhammad, M.A., Horswell, S., Gerlinger, M., Varela, I., Jones, D., Marshall, J., Voet, T., Loo, P.V., Rassl, D.M., Rintoul, R.C., Janes, S.M., Lee, S.-M., Forster, M., Ahmad, T., Lawrence, D., Falzon, M., Capitanio, A., Harkins, T.T., Lee, C.C., Tom, W., Teefe, E., Chen, S.-C., Begum, S., Rabinowitz, A., Phillimore, B., Spencer-Dene, B., Stamp, G., Szallasi, Z., Matthews, N., Stewart, A., Campbell, P., Swanton, C., 2014. Spatial and temporal diversity in genomic instability processes defines lung cancer evolution. Science 346, 251–256. https://doi.org/10.1126/science.1253462

Deng, Y., Luo, S., Deng, C., Luo, T., Yin, W., Zhang, H., Zhang, Y., Zhang, X., Lan, Y., Ping, Y., Xiao, Y., Li, X., 2019. Identifying mutual exclusivity across cancer genomes: computational approaches to discover genetic interaction

and reveal tumor vulnerability. Brief Bioinform 20, 254–266. https://doi.org/10.1093/bib/bbx109

Denoix, P., 1946. Enquête permanente dans les centres anticancéreux. Bull Inst Natl Hyg 1, 12–17.

Dentro, S.C., Leshchiner, I., Haase, K., Tarabichi, M., Wintersinger, J., Deshwar, A.G., Yu, K., Rubanova, Y., Macintyre, G., Demeulemeester, J., Vázquez-García, I., Kleinheinz, K., Livitz, D.G., Malikic, S., Donmez, N., Sengupta, S., Anur, P., Jolly, C., Cmero, M., Rosebrock, D., Schumacher, S., Fan, Y., Fittall, M., Drews, R.M., Yao, X., Lee, J., Schlesner, M., Zhu, H., Adams, D.J., Getz, G., Boutros, P.C., Imielinski, M., Beroukhim, R., Sahinalp, S.C., Ji, Y., Peifer, M., Martincorena, I., Markowetz, F., Mustonen, V., Yuan, K., Gerstung, M., Spellman, P.T., Wang, W., Morris, Q.D., Wedge, D.C., Loo, P.V., Consortium, on behalf of the P.E. and H.W.G.P., Consortium, the P., 2020. Characterizing genetic intra-tumor heterogeneity across 2,658 human cancer genomes. bioRxiv 312041. https://doi.org/10.1101/312041

Der, S.D., Sykes, J., Pintilie, M., Zhu, C.-Q., Strumpf, D., Liu, N., Jurisica, I., Shepherd, F.A., Tsao, M.-S., 2014. Validation of a Histology-Independent Prognostic Gene Signature for Early-Stage, Non–Small-Cell Lung Cancer Including Stage IA Patients. Journal of Thoracic Oncology 9, 59–64. https://doi.org/10.1097/JTO.0000000000000042

Dexter, D.L., Kowalski, H.M., Blazar, B.A., Fligiel, Z., Vogel, R., Heppner, G.H., 1978. Heterogeneity of tumor cells from a single mouse mammary tumor. Cancer Res. 38, 3174–3181.

Diaz Jr, L.A., Williams, R.T., Wu, J., Kinde, I., Hecht, J.R., Berlin, J., Allen, B., Bozic, I., Reiter, J.G., Nowak, M.A., Kinzler, K.W., Oliner, K.S., Vogelstein, B., 2012. The molecular evolution of acquired resistance to targeted EGFR blockade in colorectal cancers. Nature 486, 537–540. https://doi.org/10.1038/nature11219

Dieu-Nosjean, M.-C., Antoine, M., Danel, C., Heudes, D., Wislez, M., Poulot, V., Rabbe, N., Laurans, L., Tartour, E., de Chaisemartin, L., Lebecque, S., Fridman, W.-H., Cadranel, J., 2008. Long-Term Survival for Patients With Non–Small-Cell Lung Cancer With Intratumoral Lymphoid Structures. JCO 26, 4410–4417. https://doi.org/10.1200/JCO.2007.15.0284

Dijkstra, K.K., Voabil, P., Schumacher, T.N., Voest, E.E., 2016. Genomics- and Transcriptomics-Based Patient Selection for Cancer Treatment With Immune Checkpoint Inhibitors: A Review. JAMA Oncol 2, 1490–1495. https://doi.org/10.1001/jamaoncol.2016.2214

Ding, L., Ley, T.J., Larson, D.E., Miller, C.A., Koboldt, D.C., Welch, J.S., Ritchey, J.K., Young, M.A., Lamprecht, T., McLellan, M.D., McMichael, J.F., Wallis, J.W., Lu, C., Shen, D., Harris, C.C., Dooling, D.J., Fulton, R.S., Fulton, L.L., Chen, K., Schmidt, H., Kalicki-Veizer, J., Magrini, V.J., Cook, L., McGrath, S.D., Vickery, T.L., Wendl, M.C., Heath, S., Watson, M.A., Link, D.C., Tomasson, M.H., Shannon, W.D., Payton, J.E., Kulkarni, S., Westervelt, P., Walter, M.J., Graubert, T.A., Mardis, E.R., Wilson, R.K., DiPersio, J.F., 2012. Clonal evolution in relapsed acute myeloid leukaemia revealed by whole-genome sequencing. Nature 481, 506–510. https://doi.org/10.1038/nature10738

Ding, L., Wendl, M.C., McMichael, J.F., Raphael, B.J., 2014. Expanding the computational toolbox for mining cancer genomes. Nat Rev Genet 15, 556–570. https://doi.org/10.1038/nrg3767

Djureinovic, D., Hallström, B.M., Horie, M., Mattsson, J.S.M., Fleur, L.L., Fagerberg, L., Brunnström, H., Lindskog, C., Madjar, K., Rahnenführer, J., Ekman, S., Ståhle, E., Koyi, H., Brandén, E., Edlund, K., Hengstler, J.G., Lambe, M., Saito, A., Botling, J., Pontén, F., Uhlén, M., Micke, P., 2016. Profiling cancer testis antigens in non–small-cell lung cancer. JCI Insight 1. https://doi.org/10.1172/jci.insight.86837

Dobin, A., Davis, C.A., Schlesinger, F., Drenkow, J., Zaleski, C., Jha, S., Batut, P., Chaisson, M., Gingeras, T.R., 2013. STAR: ultrafast universal RNA-seq aligner. Bioinformatics 29, 15–21. https://doi.org/10.1093/bioinformatics/bts635

Druker, B.J., Talpaz, M., Resta, D.J., Peng, B., Buchdunger, E., Ford, J.M., Lydon, N.B., Kantarjian, H., Capdeville, R., Ohno-Jones, S., Sawyers, C.L., 2001. Efficacy and safety of a specific inhibitor of the BCR-ABL tyrosine kinase in chronic myeloid leukemia. N. Engl. J. Med. 344, 1031–1037. https://doi.org/10.1056/NEJM200104053441401

Duhen, T., Duhen, R., Montler, R., Moses, J., Moudgil, T., Miranda, N.F. de, Goodall, C.P., Blair, T.C., Fox, B.A., McDermott, J.E., Chang, S.-C., Grunkemeier, G., Leidner, R., Bell, R.B., Weinberg, A.D., 2018. Co-expression of CD39 and CD103 identifies tumor-reactive CD8 T cells in human solid tumors. Nature Communications 9, 2724. https://doi.org/10.1038/s41467-018-05072-0

Dulbecco, R., 1986. A turning point in cancer research: sequencing the human genome. Science 231, 1055–1056. https://doi.org/10.1126/science.3945817

Durinck, S., Spellman, P.T., Birney, E., Huber, W., 2009. Mapping Identifiers for the Integration of Genomic Datasets with the R/Bioconductor package biomaRt. Nat Protoc 4, 1184–1191. https://doi.org/10.1038/nprot.2009.97

Dvorak, H.F., 1986. Tumors: Wounds That Do Not Heal. New England Journal of Medicine. https://doi.org/10.1056/NEJM198612253152606

Early Breast Cancer Trialists' Collaborative Group, 2005. Effects of chemotherapy and hormonal therapy for early breast cancer on recurrence and 15-year survival: an overview of the randomised trials. The Lancet 365, 1687–1717. https://doi.org/10.1016/S0140-6736(05)66544-0

Edwards, J., Wilmott, J.S., Madore, J., Gide, T.N., Quek, C., Tasker, A., Ferguson, A., Chen, J., Hewavisenti, R., Hersey, P., Gebhardt, T., Weninger, W., Britton, W.J., Saw, R.P.M., Thompson, J.F., Menzies, A.M., Long, G.V., Scolyer, R.A., Palendira, U., 2018. CD103+ Tumor-Resident CD8+ T Cells Are Associated with Improved Survival in Immunotherapy-Naïve Melanoma Patients and Expand Significantly During Anti–PD-1 Treatment. Clin Cancer Res 24, 3036–3045. https://doi.org/10.1158/1078-0432.CCR-17-2257

Eil, R., Vodnala, S.K., Clever, D., Klebanoff, C.A., Sukumar, M., Pan, J.H., Palmer, D.C., Gros, A., Yamamoto, T.N., Patel, S.J., Guittard, G.C., Yu, Z., Carbonaro, V., Okkenhaug, K., Schrump, D.S., Linehan, W.M., Roychoudhuri, R., Restifo, N.P., 2016. Ionic immune suppression within the tumour microenvironment limits T cell effector function. Nature 537, 539–543. https://doi.org/10.1038/nature19364

Endesfelder, D., Burrell, R.A., Kanu, N., McGranahan, N., Howell, M., Parker, P.J., Downward, J., Swanton, C., Kschischo, M., 2014. Chromosomal Instability Selects Gene Copy-Number Variants Encoding Core Regulators of Proliferation in ER+ Breast Cancer. Cancer Res 74, 4853–4863. https://doi.org/10.1158/0008-5472.CAN-13-2664

Etemadmoghadam, D., Weir, B.A., Au-Yeung, G., Alsop, K., Mitchell, G., George, J., Group, A.O.C.S., Davis, S., D'Andrea, A.D., Simpson, K., Hahn, W.C., Bowtell, D.D.L., 2013. Synthetic lethality between CCNE1 amplification and loss of BRCA1. PNAS 110, 19489–19494. https://doi.org/10.1073/pnas.1314302110

Farmer, H., McCabe, N., Lord, C.J., Tutt, A.N.J., Johnson, D.A., Richardson, T.B., Santarosa, M., Dillon, K.J., Hickson, I., Knights, C., Martin, N.M.B., Jackson, S.P., Smith, G.C.M., Ashworth, A., 2005. Targeting the DNA repair defect in BRCA mutant cells as a therapeutic strategy. Nature 434, 917–921. https://doi.org/10.1038/nature03445

Fidler, I.J., Kripke, M.L., 1977. Metastasis results from preexisting variant cells within a malignant tumor. Science 197, 893–895. https://doi.org/10.1126/science.887927

Fong, P.C., Boss, D.S., Yap, T.A., Tutt, A., Wu, P., Mergui-Roelvink, M., Mortimer, P., Swaisland, H., Lau, A., O'Connor, M.J., Ashworth, A., Carmichael, J., Kaye, S.B., Schellens, J.H.M., de Bono, J.S., 2009. Inhibition of poly(ADP-ribose) polymerase in tumors from BRCA mutation carriers. N. Engl. J. Med. 361, 123–134. https://doi.org/10.1056/NEJMoa0900212

Frampton, G.M., Fabrizio, D., Chalmers, Z.R., Ross, J.S., Johnson, D.B., Lovly, C.M., Sosman, J.A., Miller, V.A., Stephens, P., 2016. Assessment of tumor mutation burden from >60,000 clinical cancer patients using comprehensive genomic profiling. JCO 34, 11558–11558. https://doi.org/10.1200/JCO.2016.34.15_suppl.11558

Francis, J.M., Zhang, C.-Z., Maire, C.L., Jung, J., Manzo, V.E., Adalsteinsson, V.A., Homer, H., Haidar, S., Blumenstiel, B., Pedamallu, C.S., Ligon, A.H., Love, J.C., Meyerson, M., Ligon, K.L., 2014. EGFR Variant Heterogeneity in Glioblastoma Resolved through Single-Nucleus Sequencing. Cancer Discov 4, 956–971. https://doi.org/10.1158/2159-8290.CD-13-0879

Fridman, W.H., Zitvogel, L., Sautès–Fridman, C., Kroemer, G., 2017. The immune contexture in cancer prognosis and treatment. Nature Reviews Clinical Oncology 14, 717. https://doi.org/10.1038/nrclinonc.2017.101

Fuhr, J.E., Frye, A., Kattine, A.A., Van Meter, S., 1991. Flow cytometric determination of breast tumor heterogeneity. Cancer 67, 1401–1405. https://doi.org/10.1002/1097-0142(19910301)67:5<1401::aid-cncr2820670521>3.0.co;2-4

Futreal, P.A., Coin, L., Marshall, M., Down, T., Hubbard, T., Wooster, R., Rahman, N., Stratton, M.R., 2004. A census of human cancer genes. Nat Rev Cancer 4, 177–183. https://doi.org/10.1038/nrc1299

Galon, J., Angell, H.K., Bedognetti, D., Marincola, F.M., 2013. The Continuum of Cancer Immunosurveillance: Prognostic, Predictive, and Mechanistic Signatures. Immunity 39, 11–26. https://doi.org/10.1016/j.immuni.2013.07.008

Galon, J., Costes, A., Sanchez-Cabo, F., Kirilovsky, A., Mlecnik, B., Lagorce-Pagès, C., Tosolini, M., Camus, M., Berger, A., Wind, P., Zinzindohoué, F., Bruneval, P., Cugnenc, P.-H., Trajanoski, Z., Fridman, W.-H., Pagès, F., 2006. Type, density, and location of immune cells within human colorectal tumors predict clinical outcome. Science 313, 1960–1964. https://doi.org/10.1126/science.1129139

Galon, J., Mlecnik, B., Bindea, G., Angell, H.K., Berger, A., Lagorce, C., Lugli, A., Zlobec, I., Hartmann, A., Bifulco, C., Nagtegaal, I.D., Palmqvist, R.,

Masucci, G.V., Botti, G., Tatangelo, F., Delrio, P., Maio, M., Laghi, L., Grizzi, F., Asslaber, M., D'Arrigo, C., Vidal-Vanaclocha, F., Zavadova, E., Chouchane, L., Ohashi, P.S., Hafezi-Bakhtiari, S., Wouters, B.G., Roehrl, M., Nguyen, L., Kawakami, Y., Hazama, S., Okuno, K., Ogino, S., Gibbs, P., Waring, P., Sato, N., Torigoe, T., Itoh, K., Patel, P.S., Shukla, S.N., Wang, Y., Kopetz, S., Sinicrope, F.A., Scripcariu, V., Ascierto, P.A., Marincola, F.M., Fox, B.A., Pagès, F., 2014. Towards the introduction of the 'Immunoscore' in the classification of malignant tumours. J. Pathol. 232, 199–209. https://doi.org/10.1002/path.4287

Ganesan, A.-P., Clarke, J., Wood, O., Garrido-Martin, E.M., Chee, S.J., Mellows, T., Samaniego-Castruita, D., Singh, D., Seumois, G., Alzetani, A., Woo, E., Friedmann, P.S., King, E.V., Thomas, G.J., Sanchez-Elsner, T., Vijayanand, P., Ottensmeier, C.H., 2017. Tissue-resident memory features are linked to the magnitude of cytotoxic T cell responses in human lung cancer. Nat Immunol 18, 940–950. https://doi.org/10.1038/ni.3775

Gao, Q., Liang, W.-W., Foltz, S.M., Mutharasu, G., Jayasinghe, R.G., Cao, S., Liao, W.-W., Reynolds, S.M., Wyczalkowski, M.A., Yao, L., Yu, L., Sun, S.Q., Caesar-Johnson, S.J., Demchok, J.A., Felau, I., Kasapi, M., Ferguson, M.L., Hutter, C.M., Sofia, H.J., Tarnuzzer, R., Wang, Z., Yang, L., Zenklusen, J.C., Zhang, J. (Julia), Chudamani, S., Liu, J., Lolla, L., Naresh, R., Pihl, T., Sun, Q., Wan, Y., Wu, Y., Cho, J., DeFreitas, T., Frazer, S., Gehlenborg, N., Getz, G., Heiman, D.I., Kim, J., Lawrence, M.S., Lin, P., Meier, S., Noble, M.S., Saksena, G., Voet, D., Zhang, Hailei, Bernard, B., Chambwe, N., Dhankani, V., Knijnenburg, T., Kramer, R., Leinonen, K., Liu, Y., Miller, M., Reynolds, S., Shmulevich, I., Thorsson, V., Zhang, W., Akbani, R., Broom, B.M., Hegde, A.M., Ju, Z., Kanchi, R.S., Korkut, A., Li, J., Liang, H., Ling, S., Liu, W., Lu, Y., Mills, G.B., Ng, K.-S., Rao, A., Ryan, M., Wang, Jing, Weinstein, J.N., Zhang, J., Abeshouse, A., Armenia, J., Chakravarty, D., Chatila, W.K., Bruijn, I. de, Gao, J., Gross, B.E., Heins, Z.J., Kundra, R., La, K., Ladanyi, M., Luna, A., Nissan, M.G., Ochoa, A., Phillips, S.M., Reznik, E., Sanchez-Vega, F., Sander, C., Schultz, N., Sheridan, R., Sumer, S.O., Sun, Y., Taylor, B.S., Wang, Jioajiao, Zhang, Hongxin, Anur, P., Peto, M., Spellman, P., Benz, C., Stuart, J.M., Wong, C.K., Yau, C., Hayes, D.N., Parker, J.S., Wilkerson, M.D., Ally, A., Balasundaram, M., Bowlby, R., Brooks, D., Carlsen, R., Chuah, E., Dhalla, N., Holt, R., Jones, S.J.M., Kasaian, K., Lee, D., Ma, Y., Marra, M.A., Mayo, M., Moore, R.A., Mungall, A.J., Mungall, K., Robertson, A.G., Sadeghi, S., Schein, J.E., Sipahimalani, P., Tam, A., Thiessen, N., Tse, K., Wong, T., Berger, A.C., Beroukhim, R., Cherniack, A.D., Cibulskis, C., Gabriel, S.B., Gao, G.F., Ha, G., Meyerson, M., Schumacher, S.E., Shih, J., Kucherlapati, M.H., Kucherlapati, R.S., Baylin, S., Cope, L., Danilova, L., Bootwalla, M.S., Lai, P.H., Maglinte, D.T., Berg, D.J.V.D., Weisenberger, D.J., Auman, J.T., Balu, S., Bodenheimer, T., Fan, C., Hoadley, K.A., Hoyle, A.P., Jefferys, S.R., Jones, C.D., Meng, S., Mieczkowski, P.A., Mose, L.E., Perou, A.H., Perou, C.M., Roach, J., Shi, Y., Simons, J.V., Skelly, T., Soloway, M.G., Tan, D., Veluvolu, U., Fan, H., Hinoue, T., Laird, P.W., Shen, H., Zhou, W., Bellair, M., Chang, K., Covington, K., Creighton, C.J., Dinh, H., Doddapaneni, H., Donehower, L.A., Drummond, J., Gibbs, R.A., Glenn, R., Hale, W., Han, Y., Hu, J., Korchina, V., Lee, S., Lewis, L., Li, W., Liu, X., Morgan, M., Morton, D., Muzny, D., Santibanez, J., Sheth, M., Shinbrot, E., Wang, L., Wang, M., Wheeler, D.A.,

Xi, L., Zhao, F., Hess, J., Appelbaum, E.L., Bailey, M., Cordes, M.G., Ding, L., Fronick, C.C., Fulton, L.A., Fulton, R.S., Kandoth, C., Mardis, E.R., McLellan, M.D., Miller, C.A., Schmidt, H.K., Wilson, R.K., Crain, D., Curley, E., Gardner, J., Lau, K., Mallery, D., Morris, S., Paulauskis, J., Penny, R., Shelton, C., Shelton, T., Sherman, M., Thompson, E., Yena, P., Bowen, J., Gastier-Foster, J.M., Gerken, M., Leraas, K.M., Lichtenberg, T.M., Ramirez, N.C., Wise, L., Zmuda, E., Corcoran, N., Costello, T., Hovens, C., Carvalho, A.L., Carvalho, A.C. de, Fregnani, J.H., Longatto-Filho, A., Reis, R.M., Scapulatempo-Neto, C., Silveira, H.C.S., Vidal, D.O., Burnette, A., Eschbacher, J., Hermes, B., Noss, A., Singh, R., Anderson, M.L., Castro, P.D., Ittmann, M., Huntsman, D., Kohl, B., Le, X., Thorp, R., Andry, C., Duffy, E.R., Lyadov, V., Paklina, O., Setdikova, G., Shabunin, A., Tavobilov, M., McPherson, C., Warnick, R., Berkowitz, R., Cramer, D., Feltmate, C., Horowitz, N., Kibel, A., Muto, M., Raut, C.P., Malykh, A., Barnholtz-Sloan, J.S., Barrett, W., Devine, K., Fulop, J., Ostrom, Q.T., Shimmel, K., Wolinsky, Y., Sloan, A.E., Rose, A.D., Giuliante, F., Goodman, M., Karlan, B.Y., Hagedorn, C.H., Eckman, J., Harr, J., Myers, J., Tucker, K., Zach, L.A., Deyarmin, B., Hu, H., Kvecher, L., Larson, C., Mural, R.J., Somiari, S., Vicha, A., Zelinka, T., Bennett, J., Iacocca, M., Rabeno, B., Swanson, P., Latour, M., Lacombe, L., Têtu, B., Bergeron, A., McGraw, M., Staugaitis, S.M., Chabot, J., Hibshoosh, H., Sepulveda, A., Su, T., Wang, T., Potapova, O., Voronina, O., Desjardins, L., Mariani, O., Roman-Roman, S., Sastre, X., Stern, M.-H., Cheng, F., Signoretti, S., Berchuck, A., Bigner, D., Lipp, E., Marks, J., McCall, S., McLendon, R., Secord, A., Sharp, A., Behera, M., Brat, D.J., Chen, A., Delman, K., Force, S., Khuri, F., Magliocca, K., Maithel, S., Olson, J.J., Owonikoko, T., Pickens, A., Ramalingam, S., Shin, D.M., Sica, G., Meir, E.G.V., Zhang, Hongzheng, Eijckenboom, W., Gillis, A., Korpershoek, E., Looijenga, L., Oosterhuis, W., Stoop, H., Kessel, K.E. van, Zwarthoff, E.C., Calatozzolo, C., Cuppini, L., Cuzzubbo, S., DiMeco, F., Finocchiaro, G., Mattei, L., Perin, A., Pollo, B., Chen, C., Houck, J., Lohavanichbutr, P., Hartmann, A., Stoehr, C., Stoehr, R., Taubert, H., Wach, S., Wullich, B., Kycler, W., Murawa, D., Wiznerowicz, M., Chung, K., Edenfield, W.J., Martin, J., Baudin, E., Bubley, G., Bueno, R., Rienzo, A.D., Richards, W.G., Kalkanis, S., Mikkelsen, T., Noushmehr, H., Scarpace, L., Girard, N., Aymerich, M., Campo, E., Giné, E., Guillermo, A.L., Bang, N.V., Hanh, P.T., Phu, B.D., Tang, Y., Colman, H., Evason, K., Dottino, P.R., Martignetti, J.A., Gabra, H., Juhl, H., Akeredolu, T., Stepa, S., Hoon, D., Ahn, K., Kang, K.J., Beuschlein, F., Breggia, A., Birrer, M., Bell, D., Borad, M., Bryce, A.H., Castle, E., Chandan, V., Cheville, J., Copland, J.A., Farnell, M., Flotte, T., Giama, N., Ho, T., Kendrick, M., Kocher, J.-P., Kopp, K., Moser, C., Nagorney, D., O'Brien, D., O'Neill, B.P., Patel, T., Petersen, G., Que, F., Rivera, M., Roberts, L., Smallridge, R., Smyrk, T., Stanton, M., Thompson, R.H., Torbenson, M., Yang, J.D., Zhang, L., Brimo, F., Ajani, J.A., Gonzalez, A.M.A., Behrens, C., Bondaruk, J., Broaddus, R., Czerniak, B., Esmaeli, B., Fujimoto, J., Gershenwald, J., Guo, C., Lazar, A.J., Logothetis, C., Meric-Bernstam, F., Moran, C., Ramondetta, L., Rice, D., Sood, A., Tamboli, P., Thompson, T., Troncoso, P., Tsao, A., Wistuba, I., Carter, C., Haydu, L., Hersey, P., Jakrot, V., Kakavand, H., Kefford, R., Lee, K., Long, G., Mann, G., Quinn, M., Saw, R., Scolyer, R., Shannon, K., Spillane, A., Stretch, J., Synott, M., Thompson, J., Wilmott, J., Al-Ahmadie,

H., Chan, T.A., Ghossein, R., Gopalan, A., Levine, D.A., Reuter, V., Singer, S., Singh, B., Tien, N.V., Broudy, T., Mirsaidi, C., Nair, P., Drwiega, P., Miller, J., Smith, J., Zaren, H., Park, J.-W., Hung, N.P., Kebebew, E., Linehan, W.M., Metwalli, A.R., Pacak, K., Pinto, P.A., Schiffman, M., Schmidt, L.S., Vocke, C.D., Wentzensen, N., Worrell, R., Yang, H., Moncrieff, M., Goparaju, C., Melamed, J., Pass, H., Botnariuc, N., Caraman, I., Cernat, M., Chemencedji, I., Clipca, A., Doruc, S., Gorincioi, G., Mura, S., Pirtac, M., Stancul, I., Tcaciuc, D., Albert, M., Alexopoulou, I., Arnaout, A., Bartlett, J., Engel, J., Gilbert, S., Parfitt, J., Sekhon, H., Thomas, G., Rassl, D.M., Rintoul, R.C., Bifulco, C., Tamakawa, R., Urba, W., Hayward, N., Timmers, H., Antenucci, A., Facciolo, F., Grazi, G., Marino, M., Merola, R., Krijger, R. de, Gimenez-Roqueplo, A.-P., Piché, A., Chevalier, S., McKercher, G., Birsoy, K., Barnett, G., Brewer, C., Farver, C., Naska, T., Pennell, N.A., Raymond, D., Schilero, C., Smolenski, K., Williams, F., Morrison, C., Borgia, J.A., Liptay, M.J., Pool, M., Seder, C.W., Junker, K., Omberg, L., Dinkin, M., Manikhas, G., Alvaro, D., Bragazzi, M.C., Cardinale, V., Carpino, G., Gaudio, E., Chesla, D., Cottingham, S., Dubina, M., Moiseenko, F., Dhanasekaran, R., Becker, K.-F., Janssen, K.-P., Slotta-Huspenina, J., Abdel-Rahman, M.H., Aziz, D., Bell, S., Cebulla, C.M., Davis, A., Duell, R., Elder, J.B., Hilty, J., Kumar, B., Lang, J., Lehman, N.L., Mandt, R., Nguyen, P., Pilarski, R., Rai, K., Schoenfield, L., Senecal, K., Wakely, P., Hansen, P., Lechan, R., Powers, J., Tischler, A., Grizzle, W.E., Sexton, K.C., Kastl, A., Henderson, J., Porten, S., Waldmann, J., Fassnacht, M., Asa, S.L., Schadendorf, D., Couce, M., Graefen, M., Huland, H., Sauter, G., Schlomm, T., Simon, R., Tennstedt, P., Olabode, O., Nelson, M., Bathe, O., Carroll, P.R., Chan, J.M., Disaia, P., Glenn, P., Kelley, R.K., Landen, C.N., Phillips, J., Prados, M., Simko, J., Smith-McCune, K., VandenBerg, S., Roggin, K., Fehrenbach, A., Kendler, A., Sifri, S., Steele, R., Jimeno, A., Carey, F., Forgie, I., Mannelli, M., Carney, M., Hernandez, B., Campos, B., Herold-Mende, C., Jungk, C., Unterberg, A., Deimling, A. von, Bossler, A., Galbraith, J., Jacobus, L., Knudson, M., Knutson, T., Ma, D., Milhem, M., Sigmund, R., Godwin, A.K., Madan, R., Rosenthal, H.G., Adebamowo, C., Adebamowo, S.N., Boussioutas, A., Beer, D., Giordano, T., Mes-Masson, A.-M., Saad, F., Bocklage, T., Landrum, L., Mannel, R., Moore, K., Moxley, K., Postier, R., Walker, J., Zuna, R., Feldman, M., Valdivieso, F., Dhir, R., Luketich, J., Pinero, E.M.M., Quintero-Aguilo, M., Carlotti, C.G., Santos, J.S.D., Kemp, R., Sankarankuty, A., Tirapelli, D., Catto, J., Agnew, K., Swisher, E., Creaney, J., Robinson, B., Shelley, C.S., Godwin, E.M., Kendall, S., Shipman, C., Bradford, C., Carey, T., Haddad, A., Moyer, J., Peterson, L., Prince, M., Rozek, L., Wolf, G., Bowman, R., Fong, K.M., Yang, I., Korst, R., Rathmell, W.K., Fantacone-Campbell, J.L., Hooke, J.A., Kovatich, A.J., Shriver, C.D., DiPersio, J., Drake, B., Govindan, R., Heath, S., Ley, T., Tine, B.V., Westervelt, P., Rubin, M.A., Lee, J.I., Aredes, N.D., Mariamidze, A., Chen, K., Lazar, A.J., Fields, R.C., Wendl, M.C., Tine, B.A.V., Vij, R., Chen, F., Nykter, M., Shmulevich, I., Ding, L., 2018. Driver Fusions and Their Implications in the Development and Treatment of Human Cancers. Cell Reports 23, 227-238.e3. https://doi.org/10.1016/j.celrep.2018.03.050

Garber, M.E., Troyanskaya, O.G., Schluens, K., Petersen, S., Thaesler, Z., Pacyna-Gengelbach, M., Rijn, M. van de, Rosen, G.D., Perou, C.M., Whyte,

R.I., Altman, R.B., Brown, P.O., Botstein, D., Petersen, I., 2001. Diversity of gene expression in adenocarcinoma of the lung. PNAS 98, 13784–13789. https://doi.org/10.1073/pnas.241500798

Garon, E.B., Rizvi, N.A., Hui, R., Leighl, N., Balmanoukian, A.S., Eder, J.P., Patnaik, A., Aggarwal, C., Gubens, M., Horn, L., Carcereny, E., Ahn, M.-J., Felip, E., Lee, J.-S., Hellmann, M.D., Hamid, O., Goldman, J.W., Soria, J.-C., Dolled-Filhart, M., Rutledge, R.Z., Zhang, J., Lunceford, J.K., Rangwala, R., Lubiniecki, G.M., Roach, C., Emancipator, K., Gandhi, L., 2015. Pembrolizumab for the Treatment of Non–Small-Cell Lung Cancer. New England Journal of Medicine 372, 2018–2028. https://doi.org/10.1056/NEJMoa1501824

Garraway, L.A., Lander, E.S., 2013. Lessons from the Cancer Genome. Cell 153, 17–37. https://doi.org/10.1016/j.cell.2013.03.002

Gentles, A.J., Newman, A.M., Liu, C.L., Bratman, S.V., Feng, W., Kim, D., Nair, V.S., Xu, Y., Khuong, A., Hoang, C.D., Diehn, M., West, R.B., Plevritis, S.K., Alizadeh, A.A., 2015. The prognostic landscape of genes and infiltrating immune cells across human cancers. Nat Med 21, 938–945. https://doi.org/10.1038/nm.3909

Gerhauser, C., Favero, F., Risch, T., Simon, R., Feuerbach, L., Assenov, Y., Heckmann, D., Sidiropoulos, N., Waszak, S.M., Hübschmann, D., Urbanucci, A., Girma, E.G., Kuryshev, V., Klimczak, L.J., Saini, N., Stütz, A.M., Weichenhan, D., Böttcher, L.-M., Toth, R., Hendriksen, J.D., Koop, C., Lutsik, P., Matzk, S., Warnatz, H.-J., Amstislavskiy, V., Feuerstein, C., Raeder, B., Bogatyrova, O., Schmitz, E.-M., Hube-Magg, C., Kluth, M., Huland, H., Graefen, M., Lawerenz, C., Henry, G.H., Yamaguchi, T.N., Malewska, A., Meiners, J., Schilling, D., Reisinger, E., Eils, R., Schlesner, M., Strand, D.W., Bristow, R.G., Boutros, P.C., Kalle, C. von, Gordenin, D., Sültmann, H., Brors, B., Sauter, G., Plass, C., Yaspo, M.-L., Korbel, J.O., Schlomm, T., Weischenfeldt, J., 2018. Molecular Evolution of Early-Onset Prostate Cancer Identifies Molecular Risk Markers and Clinical Trajectories. Cancer Cell 34, 996-1011.e8. https://doi.org/10.1016/j.ccell.2018.10.016

Gerlinger, M., Horswell, S., Larkin, J., Rowan, A.J., Salm, M.P., Varela, I., Fisher, R., McGranahan, N., Matthews, N., Santos, C.R., Martinez, P., Phillimore, B., Begum, S., Rabinowitz, A., Spencer-Dene, B., Gulati, S., Bates, P.A., Stamp, G., Pickering, L., Gore, M., Nicol, D.L., Hazell, S., Futreal, P.A., Stewart, A., Swanton, C., 2014. Genomic architecture and evolution of clear cell renal cell carcinomas defined by multiregion sequencing. Nat. Genet. 46, 225–233. https://doi.org/10.1038/ng.2891

Gerlinger, M., Rowan, A.J., Horswell, S., Larkin, J., Endesfelder, D., Gronroos, E., Martinez, P., Matthews, N., Stewart, A., Tarpey, P., Varela, I., Phillimore, B., Begum, S., McDonald, N.Q., Butler, A., Jones, D., Raine, K., Latimer, C., Santos, C.R., Nohadani, M., Eklund, A.C., Spencer-Dene, B., Clark, G., Pickering, L., Stamp, G., Gore, M., Szallasi, Z., Downward, J., Futreal, P.A., Swanton, C., 2012. Intratumor Heterogeneity and Branched Evolution Revealed by Multiregion Sequencing. New England Journal of Medicine 366, 883–892. https://doi.org/10.1056/NEJMoa1113205

Gerstung, M., Papaemmanuil, E., Martincorena, I., Bullinger, L., Gaidzik, V.I., Paschka, P., Heuser, M., Thol, F., Bolli, N., Ganly, P., Ganser, A., McDermott, U., Döhner, K., Schlenk, R.F., Döhner, H., Campbell, P.J., 2017. Precision oncology for acute myeloid leukemia using a knowledge

bank approach. Nature Genetics 49, 332–340. https://doi.org/10.1038/ng.3756

Goc, J., Germain, C., Vo-Bourgais, T.K.D., Lupo, A., Klein, C., Knockaert, S., Chaisemartin, L. de, Ouakrim, H., Becht, E., Alifano, M., Validire, P., Remark, R., Hammond, S.A., Cremer, I., Damotte, D., Fridman, W.-H., Sautès-Fridman, C., Dieu-Nosjean, M.-C., 2014. Dendritic Cells in Tumor-Associated Tertiary Lymphoid Structures Signal a Th1 Cytotoxic Immune Contexture and License the Positive Prognostic Value of Infiltrating CD8+ T Cells. Cancer Res 74, 705–715. https://doi.org/10.1158/0008-5472.CAN-13-1342

Goldstraw, P., Chansky, K., Crowley, J., Rami-Porta, Ramon, Asamura, H., Eberhardt, Wilfried E. E., Nicholson, A.G., Groome, P., Mitchell, A., Bolejack, V., Goldstraw, P., Rami-Porta, Ramón, Asamura, H., Ball, David, Beer, D.G., Beyruti, R., Bolejack, V., Chansky, K., Crowley, J., Detterbeck, F., Eberhardt, Wilfried Ernst Erich, Edwards, J., Galateau-Sallé, F., Giroux, D., Gleeson, F., Groome, P., Huang, J., Kennedy, Catherine, Kim, J., Kim, Y.T., Kingsbury, L., Kondo, H., Krasnik, M., Kubota, K., Lerut, A., Lyons, Gustavo, Marino, M., Marom, E.M., Meerbeeck, J. van, Mitchell, A., Nakano, T., Nicholson, A.G., Nowak, A., Peake, M., Rice, T., Rosenzweig, K., Ruffini, Enrico, Rusch, Valerie, Saijo, N., Schil, Paul Van, Sculier, J.-P., Shemanski, L., Stratton, K., Suzuki, K., Tachimori, Y., Thomas, C.F., Travis, W., Tsao, M.S., Turrisi, A., Vansteenkiste, J., Watanabe, H., Wu, Y.-L., Baas, P., Erasmus, J., Hasegawa, S., Inai, K., Kernstine, K., Kindler, H., Krug, L., Nackaerts, K., Pass, Harvey, Rice, D., Falkson, C., Filosso, P.L., Giaccone, G., Kondo, K., Lucchi, M., Okumura, M., Blackstone, E., Cavaco, F.A., Barrera, E.A., Arca, J.A., Lamelas, I.P., Obrer, A.A., Jorge, R.G., Ball, D., Bascom, G.K., Orozco, A.I.B., Castro, M.A.G., Blum, M.G., Chimondeguy, D., Cvijanovic, V., Defranchi, S., Navarro, B. de O., Campuzano, I.E., Vidueira, I.M., Araujo, E.F., García, F.A., Fong, K.M., Corral, G.F., González, S.C., Gilart, J.F., Arangüena, L.G., Barajas, S.G., Girard, P., Goksel, T., Budiño, M.T.G., Casaurrán, G.G., Blanco, J.A.G., Hernández, J.H., Rodríguez, H.H., Collantes, J.H., Heras, M.I., Elena, J.M.I., Jakobsen, E., Kostas, S., Atance, P.L., Ares, A.N., Liao, M., Losanovscky, M., Lyons, G., Magaroles, R., Júlvez, L.D.E., Gorospe, M.M., McCaughan, B., Kennedy, C., Íñiguez, R.M., Sorribes, L.M., Gozalo, S.N., Arriba, C.Á. de, Delgado, M.N., Alarcón, J.P., Cuesta, J.C.P., Park, J.S., Pass, H., Fernández, M.J.P., Rosenberg, M., Ruffini, E., Rusch, V., Escuín, J.S. de C., Vinuesa, A.S., Mitjans, M.S., Strand, T.E., Subotic, D., Swisher, S., Terra, R., Thomas, C., Tournoy, K., Schil, P. Van, Velasquez, M., Wu, Y.L., Yokoi, K., 2016. The IASLC Lung Cancer Staging Project: Proposals for Revision of the TNM Stage Groupings in the Forthcoming (Eighth) Edition of the TNM Classification for Lung Cancer. Journal of Thoracic Oncology 11, 39–51. https://doi.org/10.1016/j.jtho.2015.09.009

Goldstraw, P., Crowley, J., Chansky, K., Giroux, D.J., Groome, P.A., Rami-Porta, R., Postmus, P.E., Rusch, V., Sobin, L., 2007. The IASLC Lung Cancer Staging Project: Proposals for the Revision of the TNM Stage Groupings in the Forthcoming (Seventh) Edition of the TNM Classification of Malignant Tumours. Journal of Thoracic Oncology 2, 706–714. https://doi.org/10.1097/JTO.0b013e31812f3c1a

Golub, T.R., Slonim, D.K., Tamayo, P., Huard, C., Gaasenbeek, M., Mesirov, J.P., Coller, H., Loh, M.L., Downing, J.R., Caligiuri, M.A., Bloomfield, C.D., Lander, E.S., 1999. Molecular Classification of Cancer: Class Discovery and Class Prediction by Gene Expression Monitoring. Science 286, 531–537. https://doi.org/10.1126/science.286.5439.531

Gong, T., Szustakowski, J.D., 2013. DeconRNASeq: a statistical framework for deconvolution of heterogeneous tissue samples based on mRNA-Seq data. Bioinformatics 29, 1083–1085. https://doi.org/10.1093/bioinformatics/btt090

Gordon, S.R., Maute, R.L., Dulken, B.W., Hutter, G., George, B.M., McCracken, M.N., Gupta, R., Tsai, J.M., Sinha, R., Corey, D., Ring, A.M., Connolly, A.J., Weissman, I.L., 2017. PD-1 expression by tumour-associated macrophages inhibits phagocytosis and tumour immunity. Nature 545, 495–499. https://doi.org/10.1038/nature22396

Greaves, M., 2015. Evolutionary Determinants of Cancer. Cancer Discov 5, 806–820. https://doi.org/10.1158/2159-8290.CD-15-0439

Greenman, C., Stephens, P., Smith, R., Dalgliesh, G.L., Hunter, C., Bignell, G., Davies, H., Teague, J., Butler, A., Stevens, C., Edkins, S., O'Meara, S., Vastrik, I., Schmidt, E.E., Avis, T., Barthorpe, S., Bhamra, G., Buck, G., Choudhury, B., Clements, J., Cole, J., Dicks, E., Forbes, S., Gray, K., Halliday, K., Harrison, R., Hills, K., Hinton, J., Jenkinson, A., Jones, D., Menzies, A., Mironenko, T., Perry, J., Raine, K., Richardson, D., Shepherd, R., Small, A., Tofts, C., Varian, J., Webb, T., West, S., Widaa, S., Yates, A., Cahill, D.P., Louis, D.N., Goldstraw, P., Nicholson, A.G., Brasseur, F., Looijenga, L., Weber, B.L., Chiew, Y.-E., deFazio, A., Greaves, M.F., Green, A.R., Campbell, P., Birney, E., Easton, D.F., Chenevix-Trench, G., Tan, M.-H., Khoo, S.K., Teh, B.T., Yuen, S.T., Leung, S.Y., Wooster, R., Futreal, P.A., Stratton, M.R., 2007. Patterns of somatic mutation in human cancer genomes. Nature 446, 153–158. https://doi.org/10.1038/nature05610

Gubin, M.M., Zhang, X., Schuster, H., Caron, E., Ward, J.P., Noguchi, T., Ivanova, Y., Hundal, J., Arthur, C.D., Krebber, W.-J., Mulder, G.E., Toebes, M., Vesely, M.D., Lam, S.S.K., Korman, A.J., Allison, J.P., Freeman, G.J., Sharpe, A.H., Pearce, E.L., Schumacher, T.N., Aebersold, R., Rammensee, H.-G., Melief, C.J.M., Mardis, E.R., Gillanders, W.E., Artyomov, M.N., Schreiber, R.D., 2014. Checkpoint blockade cancer immunotherapy targets tumour-specific mutant antigens. Nature 515, 577–581. https://doi.org/10.1038/nature13988

Gulati, G.S., Sikandar, S.S., Wesche, D.J., Manjunath, A., Bharadwaj, A., Berger, M.J., Ilagan, F., Kuo, A.H., Hsieh, R.W., Cai, S., Zabala, M., Scheeren, F.A., Lobo, N.A., Qian, D., Yu, F.B., Dirbas, F.M., Clarke, M.F., Newman, A.M., 2020. Single-cell transcriptional diversity is a hallmark of developmental potential. Science 367, 405–411. https://doi.org/10.1126/science.aax0249

Gulati, S., Martinez, P., Joshi, T., Birkbak, N.J., Santos, C.R., Rowan, A.J., Pickering, L., Gore, M., Larkin, J., Szallasi, Z., Bates, P.A., Swanton, C., Gerlinger, M., 2014. Systematic Evaluation of the Prognostic Impact and Intratumour Heterogeneity of Clear Cell Renal Cell Carcinoma Biomarkers. European Urology 66, 936–948. https://doi.org/10.1016/j.eururo.2014.06.053

Gulati, S., Turajlic, S., Larkin, J., Bates, P.A., Swanton, C., 2015. Relapse models for clear cell renal carcinoma. The Lancet Oncology 16, e376–e378. https://doi.org/10.1016/S1470-2045(15)00090-X

Gyanchandani, R., Lin, Y., Lin, H.-M., Cooper, K., Normolle, D.P., Brufsky, A., Fastuca, M., Crosson, W., Oesterreich, S., Davidson, N.E., Bhargava, R., Dabbs, D.J., Lee, A.V., 2016. Intratumor Heterogeneity Affects Gene Expression Profile Test Prognostic Risk Stratification in Early Breast Cancer. Clin Cancer Res 22, 5362–5369. https://doi.org/10.1158/1078-0432.CCR-15-2889

Haar, J. van de, Canisius, S., Yu, M.K., Voest, E.E., Wessels, L.F.A., Ideker, T., 2019. Identifying Epistasis in Cancer Genomes: A Delicate Affair. Cell 177, 1375–1383. https://doi.org/10.1016/j.cell.2019.05.005

Hahn, W.C., Weinberg, R.A., 2002. Rules for Making Human Tumor Cells. New England Journal of Medicine 347, 1593–1603. https://doi.org/10.1056/NEJMra021902

Håkansson, L., Tropé, C., 1974. On the presence within tumours of clones that differ in sensitivity to cytostatic drugs. Acta Pathol Microbiol Scand A 82, 35–40.

Hanahan, D., Coussens, L.M., 2012. Accessories to the Crime: Functions of Cells Recruited to the Tumor Microenvironment. Cancer Cell 21, 309–322. https://doi.org/10.1016/j.ccr.2012.02.022

Hanahan, D., Weinberg, R.A., 2011. Hallmarks of cancer: the next generation. Cell 144, 646–674. https://doi.org/10.1016/j.cell.2011.02.013

Hänzelmann, S., Castelo, R., Guinney, J., 2013. GSVA: gene set variation analysis for microarray and RNA-Seq data. BMC Bioinformatics 14, 7. https://doi.org/10.1186/1471-2105-14-7

Harding, F.A., McArthur, J.G., Gross, J.A., Raulet, D.H., Allison, J.P., 1992. CD28-mediated signalling co-stimulates murine T cells and prevents induction of anergy in T-cell clones. Nature 356, 607–609. https://doi.org/10.1038/356607a0

Havel, J.J., Chowell, D., Chan, T.A., 2019. The evolving landscape of biomarkers for checkpoint inhibitor immunotherapy. Nature Reviews Cancer 1. https://doi.org/10.1038/s41568-019-0116-x

Heppner, G.H., 1984. Tumor heterogeneity. Cancer Res. 44, 2259–2265.

Herbst, R.S., Baas, P., Kim, D.-W., Felip, E., Pérez-Gracia, J.L., Han, J.-Y., Molina, J., Kim, J.-H., Arvis, C.D., Ahn, M.-J., Majem, M., Fidler, M.J., de Castro, G., Garrido, M., Lubiniecki, G.M., Shentu, Y., Im, E., Dolled-Filhart, M., Garon, E.B., 2016. Pembrolizumab versus docetaxel for previously treated, PD-L1-positive, advanced non-small-cell lung cancer (KEYNOTE-010): a randomised controlled trial. The Lancet 387, 1540–1550. https://doi.org/10.1016/S0140-6736(15)01281-7

Herbst, R.S., Soria, J.-C., Kowanetz, M., Fine, G.D., Hamid, O., Gordon, M.S., Sosman, J.A., McDermott, D.F., Powderly, J.D., Gettinger, S.N., Kohrt, H.E.K., Horn, L., Lawrence, D.P., Rost, S., Leabman, M., Xiao, Y., Mokatrin, A., Koeppen, H., Hegde, P.S., Mellman, I., Chen, D.S., Hodi, F.S., 2014. Predictive correlates of response to the anti-PD-L1 antibody MPDL3280A in cancer patients. Nature 515, 563–567. https://doi.org/10.1038/nature14011

Hirata, E., Sahai, E., 2017. Tumor Microenvironment and Differential Responses to Therapy. Cold Spring Harb Perspect Med 7, a026781. https://doi.org/10.1101/cshperspect.a026781

Hirayama, S., Ishii, G., Nagai, K., Ono, S., Kojima, M., Yamauchi, C., Aokage, K., Hishida, T., Yoshida, J., Suzuki, K., Ochiai, A., 2012. Prognostic Impact of CD204-Positive Macrophages in Lung Squamous Cell Carcinoma: Possible

Contribution of Cd204-Positive Macrophages to the Tumor-Promoting Microenvironment. Journal of Thoracic Oncology 7, 1790–1797. https://doi.org/10.1097/JTO.0b013e3182745968

Hoadley, K.A., Yau, C., Hinoue, T., Wolf, D.M., Lazar, A.J., Drill, E., Shen, R., Taylor, A.M., Cherniack, A.D., Thorsson, Vésteinn, Akbani, R., Bowlby, R., Wong, C.K., Wiznerowicz, M., Sanchez-Vega, F., Robertson, A.G., Schneider, B.G., Lawrence, M.S., Noushmehr, H., Malta, T.M., Caesar-Johnson, S.J., Demchok, J.A., Felau, I., Kasapi, M., Ferguson, M.L., Hutter, C.M., Sofia, H.J., Tarnuzzer, R., Wang, Z., Yang, L., Zenklusen, J.C., Zhang, J. (Julia), Chudamani, S., Liu, J., Lolla, L., Naresh, R., Pihl, T., Sun, Q., Wan, Y., Wu, Y., Cho, J., DeFreitas, T., Frazer, S., Gehlenborg, N., Getz, G., Heiman, D.I., Kim, J., Lawrence, M.S., Lin, P., Meier, S., Noble, M.S., Saksena, G., Voet, D., Zhang, Hailei, Bernard, B., Chambwe, N., Dhankani, V., Knijnenburg, T., Kramer, R., Leinonen, K., Liu, Y., Miller, M., Reynolds, S., Shmulevich, I., Thorsson, Vesteinn, Zhang, W., Akbani, R., Broom, B.M., Hegde, A.M., Ju, Z., Kanchi, R.S., Korkut, A., Li, J., Liang, H., Ling, S., Liu, W., Lu, Y., Mills, G.B., Ng, K.-S., Rao, A., Ryan, M., Wang, Jing, Weinstein, J.N., Zhang, J., Abeshouse, A., Armenia, J., Chakravarty, D., Chatila, W.K., Bruijn, I. de, Gao, J., Gross, B.E., Heins, Z.J., Kundra, R., La, K., Ladanyi, M., Luna, A., Nissan, M.G., Ochoa, A., Phillips, S.M., Reznik, E., Sanchez-Vega, F., Sander, C., Schultz, N., Sheridan, R., Sumer, S.O., Sun, Y., Taylor, B.S., Wang, Jioajiao, Zhang, Hongxin, Anur, P., Peto, M., Spellman, P., Benz, C., Stuart, J.M., Wong, C.K., Yau, C., Hayes, D.N., Parker, J.S., Wilkerson, M.D., Ally, A., Balasundaram, M., Bowlby, R., Brooks, D., Carlsen, R., Chuah, E., Dhalla, N., Holt, R., Jones, S.J.M., Kasaian, K., Lee, D., Ma, Y., Marra, M.A., Mayo, M., Moore, R.A., Mungall, A.J., Mungall, K., Robertson, A.G., Sadeghi, S., Schein, J.E., Sipahimalani, P., Tam, A., Thiessen, N., Tse, K., Wong, T., Berger, A.C., Beroukhim, R., Cherniack, A.D., Cibulskis, C., Gabriel, S.B., Gao, G.F., Ha, G., Meyerson, M., Schumacher, S.E., Shih, J., Kucherlapati, M.H., Kucherlapati, R.S., Baylin, S., Cope, L., Danilova, L., Bootwalla, M.S., Lai, P.H., Maglinte, D.T., Berg, D.J.V.D., Weisenberger, D.J., Auman, J.T., Balu, S., Bodenheimer, T., Fan, C., Hoadley, K.A., Hoyle, A.P., Jefferys, S.R., Jones, C.D., Meng, S., Mieczkowski, P.A., Mose, L.E., Perou, A.H., Perou, C.M., Roach, J., Shi, Y., Simons, J.V., Skelly, T., Soloway, M.G., Tan, D., Veluvolu, U., Fan, H., Hinoue, T., Laird, P.W., Shen, H., Zhou, W., Bellair, M., Chang, K., Covington, K., Creighton, C.J., Dinh, H., Doddapaneni, H., Donehower, L.A., Drummond, J., Gibbs, R.A., Glenn, R., Hale, W., Han, Y., Hu, J., Korchina, V., Lee, S., Lewis, L., Li, W., Liu, X., Morgan, M., Morton, D., Muzny, D., Santibanez, J., Sheth, M., Shinbrot, E., Wang, L., Wang, M., Wheeler, D.A., Xi, L., Zhao, F., Hess, J., Appelbaum, E.L., Bailey, M., Cordes, M.G., Ding, L., Fronick, C.C., Fulton, L.A., Fulton, R.S., Kandoth, C., Mardis, E.R., McLellan, M.D., Miller, C.A., Schmidt, H.K., Wilson, R.K., Crain, D., Curley, E., Gardner, J., Lau, K., Mallery, D., Morris, S., Paulauskis, J., Penny, R., Shelton, C., Shelton, T., Sherman, M., Thompson, E., Yena, P., Bowen, J., Gastier-Foster, J.M., Gerken, M., Leraas, K.M., Lichtenberg, T.M., Ramirez, N.C., Wise, L., Zmuda, E., Corcoran, N., Costello, T., Hovens, C., Carvalho, A.L., Carvalho, A.C. de, Fregnani, J.H., Longatto-Filho, A., Reis, R.M., Scapulatempo-Neto, C., Silveira, H.C.S., Vidal, D.O., Burnette, A., Eschbacher, J., Hermes, B., Noss, A., Singh, R., Anderson, M.L., Castro,

P.D., Ittmann, M., Huntsman, D., Kohl, B., Le, X., Thorp, R., Andry, C., Duffy, E.R., Lyadov, V., Paklina, O., Setdikova, G., Shabunin, A., Tavobilov, M., McPherson, C., Warnick, R., Berkowitz, R., Cramer, D., Feltmate, C., Horowitz, N., Kibel, A., Muto, M., Raut, C.P., Malykh, A., Barnholtz-Sloan, J.S., Barrett, W., Devine, K., Fulop, J., Ostrom, Q.T., Shimmel, K., Wolinsky, Y., Sloan, A.E., Rose, A.D., Giuliante, F., Goodman, M., Karlan, B.Y., Hagedorn, C.H., Eckman, J., Harr, J., Myers, J., Tucker, K., Zach, L.A., Deyarmin, B., Hu, H., Kvecher, L., Larson, C., Mural, R.J., Somiari, S., Vicha, A., Zelinka, T., Bennett, J., Iacocca, M., Rabeno, B., Swanson, P., Latour, M., Lacombe, L., Têtu, B., Bergeron, A., McGraw, M., Staugaitis, S.M., Chabot, J., Hibshoosh, H., Sepulveda, A., Su, T., Wang, T., Potapova, O., Voronina, O., Desjardins, L., Mariani, O., Roman-Roman, S., Sastre, X., Stern, M.-H., Cheng, F., Signoretti, S., Berchuck, A., Bigner, D., Lipp, E., Marks, J., McCall, S., McLendon, R., Secord, A., Sharp, A., Behera, M., Brat, D.J., Chen, A., Delman, K., Force, S., Khuri, F., Magliocca, K., Maithel, S., Olson, J.J., Owonikoko, T., Pickens, A., Ramalingam, S., Shin, D.M., Sica, G., Meir, E.G.V., Zhang, Hongzheng, Eijckenboom, W., Gillis, A., Korpershoek, E., Looijenga, L., Oosterhuis, W., Stoop, H., Kessel, K.E. van, Zwarthoff, E.C., Calatozzolo, C., Cuppini, L., Cuzzubbo, S., DiMeco, F., Finocchiaro, G., Mattei, L., Perin, A., Pollo, B., Chen, C., Houck, J., Lohavanichbutr, P., Hartmann, A., Stoehr, C., Stoehr, R., Taubert, H., Wach, S., Wullich, B., Kycler, W., Murawa, D., Wiznerowicz, M., Chung, K., Edenfield, W.J., Martin, J., Baudin, E., Bubley, G., Bueno, R., Rienzo, A.D., Richards, W.G., Kalkanis, S., Mikkelsen, T., Noushmehr, H., Scarpace, L., Girard, N., Aymerich, M., Campo, E., Giné, E., Guillermo, A.L., Bang, N.V., Hanh, P.T., Phu, B.D., Tang, Y., Colman, H., Evason, K., Dottino, P.R., Martignetti, J.A., Gabra, H., Juhl, H., Akeredolu, T., Stepa, S., Hoon, D., Ahn, K., Kang, K.J., Beuschlein, F., Breggia, A., Birrer, M., Bell, D., Borad, M., Bryce, A.H., Castle, E., Chandan, V., Cheville, J., Copland, J.A., Farnell, M., Flotte, T., Giama, N., Ho, T., Kendrick, M., Kocher, J.-P., Kopp, K., Moser, C., Nagorney, D., O'Brien, D., O'Neill, B.P., Patel, T., Petersen, G., Que, F., Rivera, M., Roberts, L., Smallridge, R., Smyrk, T., Stanton, M., Thompson, R.H., Torbenson, M., Yang, J.D., Zhang, L., Brimo, F., Ajani, J.A., Gonzalez, A.M.A., Behrens, C., Bondaruk, O., Broaddus, R., Czerniak, B., Esmaeli, B., Fujimoto, J., Gershenwald, J., Guo, C., Lazar, A.J., Logothetis, C., Meric-Bernstam, F., Moran, C., Ramondetta, L., Rice, D., Sood, A., Tamboli, P., Thompson, T., Troncoso, P., Tsao, A., Wistuba, I., Carter, C., Haydu, L., Hersey, P., Jakrot, V., Kakavand, H., Kefford, R., Lee, K., Long, G., Mann, G., Quinn, M., Saw, R., Scolyer, R., Shannon, K., Spillane, A., Stretch, J., Synott, M., Thompson, J., Wilmott, J., Al-Ahmadie, H., Chan, T.A., Ghossein, R., Gopalan, A., Levine, D.A., Reuter, V., Singer, S., Singh, B., Tien, N.V., Broudy, T., Mirsaidi, C., Nair, P., Drwiega, P., Miller, J., Smith, J., Zaren, H., Park, J.-W., Hung, N.P., Kebebew, E., Linehan, W.M., Metwalli, A.R., Pacak, K., Pinto, P.A., Schiffman, M., Schmidt, L.S., Vocke, C.D., Wentzensen, N., Worrell, R., Yang, H., Moncrieff, M., Goparaju, C., Melamed, J., Pass, H., Botnariuc, N., Caraman, I., Cernat, M., Chemencedji, I., Clipca, A., Doruc, S., Gorincioi, G., Mura, S., Pirtac, M., Stancul, I., Tcaciuc, D., Albert, M., Alexopoulou, I., Arnaout, A., Bartlett, J., Engel, J., Gilbert, S., Parfitt, J., Sekhon, H., Thomas, G., Rassl, D.M., Rintoul, R.C., Bifulco, C., Tamakawa, R., Urba, W., Hayward, N.,

Timmers, H., Antenucci, A., Facciolo, F., Grazi, G., Marino, M., Merola, R., Krijger, R. de, Gimenez-Roqueplo, A.-P., Piché, A., Chevalier, S., McKercher, G., Birsoy, K., Barnett, G., Brewer, C., Farver, C., Naska, T., Pennell, N.A., Raymond, D., Schilero, C., Smolenski, K., Williams, F., Morrison, C., Borgia, J.A., Liptay, M.J., Pool, M., Seder, C.W., Junker, K., Omberg, L., Dinkin, M., Manikhas, G., Alvaro, D., Bragazzi, M.C., Cardinale, V., Carpino, G., Gaudio, E., Chesla, D., Cottingham, S., Dubina, M., Moiseenko, F., Dhanasekaran, R., Becker, K.-F., Janssen, K.-P., Slotta-Huspenina, J., Abdel-Rahman, M.H., Aziz, D., Bell, S., Cebulla, C.M., Davis, A., Duell, R., Elder, J.B., Hilty, J., Kumar, B., Lang, J., Lehman, N.L., Mandt, R., Nguyen, P., Pilarski, R., Rai, K., Schoenfield, L., Senecal, K., Wakely, P., Hansen, P., Lechan, R., Powers, J., Tischler, A., Grizzle, W.E., Sexton, K.C., Kastl, A., Henderson, J., Porten, S., Waldmann, J., Fassnacht, M., Asa, S.L., Schadendorf, D., Couce, M., Graefen, M., Huland, H., Sauter, G., Schlomm, T., Simon, R., Tennstedt, P., Olabode, O., Nelson, M., Bathe, O., Carroll, P.R., Chan, J.M., Disaia, P., Glenn, P., Kelley, R.K., Landen, C.N., Phillips, J., Prados, M., Simko, J., Smith-McCune, K., VandenBerg, S., Roggin, K., Fehrenbach, A., Kendler, A., Sifri, S., Steele, R., Jimeno, A., Carey, F., Forgie, I., Mannelli, M., Carney, M., Hernandez, B., Campos, B., Herold-Mende, C., Jungk, C., Unterberg, A., Deimling, A. von, Bossler, A., Galbraith, J., Jacobus, L., Knudson, M., Knutson, T., Ma, D., Milhem, M., Sigmund, R., Godwin, A.K., Madan, R., Rosenthal, H.G., Adebamowo, C., Adebamowo, S.N., Boussioutas, A., Beer, D., Giordano, T., Mes-Masson, A.-M., Saad, F., Bocklage, T., Landrum, L., Mannel, R., Moore, K., Moxley, K., Postier, R., Walker, J., Zuna, R., Feldman, M., Valdivieso, F., Dhir, R., Luketich, J., Pinero, E.M.M., Quintero-Aguilo, M., Carlotti, C.G., Santos, J.S.D., Kemp, R., Sankarankuty, A., Tirapelli, D., Catto, J., Agnew, K., Swisher, E., Creaney, J., Robinson, B., Shelley, C.S., Godwin, E.M., Kendall, S., Shipman, C., Bradford, C., Carey, T., Haddad, A., Moyer, J., Peterson, L., Prince, M., Rozek, L., Wolf, G., Bowman, R., Fong, K.M., Yang, I., Korst, R., Rathmell, W.K., Fantacone-Campbell, J.L., Hooke, J.A., Kovatich, A.J., Shriver, C.D., DiPersio, J., Drake, B., Govindan, R., Heath, S., Ley, T., Tine, B.V., Westervelt, P., Rubin, M.A., Lee, J.I., Aredes, N.D., Mariamidze, A., Stuart, J.M., Benz, C.C., Laird, P.W., 2018. Cell-of-Origin Patterns Dominate the Molecular Classification of 10,000 Tumors from 33 Types of Cancer. Cell 173, 291-304.e6. https://doi.org/10.1016/j.cell.2018.03.022

Hodi, F.S., O'Day, S.J., McDermott, D.F., Weber, R.W., Sosman, J.A., Haanen, J.B., Gonzalez, R., Robert, C., Schadendorf, D., Hassel, J.C., Akerley, W., van den Eertwegh, A.J.M., Lutzky, J., Lorigan, P., Vaubel, J.M., Linette, G.P., Hogg, D., Ottensmeier, C.H., Lebbé, C., Peschel, C., Quirt, I., Clark, J.I., Wolchok, J.D., Weber, J.S., Tian, J., Yellin, M.J., Nichol, G.M., Hoos, A., Urba, W.J., 2010. Improved Survival with Ipilimumab in Patients with Metastatic Melanoma. New England Journal of Medicine 363, 711–723. https://doi.org/10.1056/NEJMoa1003466

Hu, X., Fujimoto, J., Ying, L., Fukuoka, J., Ashizawa, K., Sun, W., Reuben, A., Chow, C.-W., McGranahan, N., Chen, R., Hu, J., Godoy, M.C., Tabata, K., Kuroda, K., Shi, L., Li, J., Behrens, C., Parra, E.R., Little, L.D., Gumbs, C., Mao, X., Song, X., Tippen, S., Thornton, R.L., Kadara, H., Scheet, P., Roarty, E., Ostrin, E.J., Wang, X., Carter, B.W., Antonoff, M.B., Zhang,

Jianhua, Vaporciyan, A.A., Pass, H., Swisher, S.G., Heymach, J.V., Lee, J.J., Wistuba, I.I., Hong, W.K., Futreal, P.A., Su, D., Zhang, Jianjun, 2019. Multi-region exome sequencing reveals genomic evolution from preneoplasia to lung adenocarcinoma. Nat Commun 10, 2978. https://doi.org/10.1038/s41467-019-10877-8

Hu, Z., Ding, J., Ma, Z., Sun, R., Seoane, J.A., Shaffer, J.S., Suarez, C.J., Berghoff, A.S., Cremolini, C., Falcone, A., Loupakis, F., Birner, P., Preusser, M., Lenz, H.-J., Curtis, C., 2019. Quantitative evidence for early metastatic seeding in colorectal cancer. Nat Genet 51, 1113–1122. https://doi.org/10.1038/s41588-019-0423-x

Hua, X., Hyland, P.L., Huang, J., Song, L., Zhu, B., Caporaso, N.E., Landi, M.T., Chatterjee, N., Shi, J., 2016. MEGSA: A Powerful and Flexible Framework for Analyzing Mutual Exclusivity of Tumor Mutations. The American Journal of Human Genetics 98, 442–455. https://doi.org/10.1016/j.ajhg.2015.12.021

Hugo, W., Zaretsky, J.M., Sun, L., Song, C., Moreno, B.H., Hu-Lieskovan, S., Berent-Maoz, B., Pang, J., Chmielowski, B., Cherry, G., Seja, E., Lomeli, S., Kong, X., Kelley, M.C., Sosman, J.A., Johnson, D.B., Ribas, A., Lo, R.S., 2016. Genomic and Transcriptomic Features of Response to Anti-PD-1 Therapy in Metastatic Melanoma. Cell 165, 35–44. https://doi.org/10.1016/j.cell.2016.02.065

Hunter, C., Smith, R., Cahill, D.P., Stephens, P., Stevens, C., Teague, J., Greenman, C., Edkins, S., Bignell, G., Davies, H., O'Meara, S., Parker, A., Avis, T., Barthorpe, S., Brackenbury, L., Buck, G., Butler, A., Clements, J., Cole, J., Dicks, E., Forbes, S., Gorton, M., Gray, K., Halliday, K., Harrison, R., Hills, K., Hinton, J., Jenkinson, A., Jones, D., Kosmidou, V., Laman, R., Lugg, R., Menzies, A., Perry, J., Petty, R., Raine, K., Richardson, D., Shepherd, R., Small, A., Solomon, H., Tofts, C., Varian, J., West, S., Widaa, S., Yates, A., Easton, D.F., Riggins, G., Roy, J.E., Levine, K.K., Mueller, W., Batchelor, T.T., Louis, D.N., Stratton, M.R., Futreal, P.A., Wooster, R., 2006. A Hypermutation Phenotype and Somatic MSH6 Mutations in Recurrent Human Malignant Gliomas after Alkylator Chemotherapy. Cancer Res 66, 3987–3991. https://doi.org/10.1158/0008-5472.CAN-06-0127

Hyman, D.M., Piha-Paul, S.A., Won, H., Rodon, J., Saura, C., Shapiro, G.I., Juric, D., Quinn, D.I., Moreno, V., Doger, B., Mayer, I.A., Boni, V., Calvo, E., Loi, S., Lockhart, A.C., Erinjeri, J.P., Scaltriti, M., Ulaner, G.A., Patel, J., Tang, J., Beer, H., Selcuklu, S.D., Hanrahan, A.J., Bouvier, N., Melcer, M., Murali, R., Schram, A.M., Smyth, L.M., Jhaveri, K., Li, B.T., Drilon, A., Harding, J.J., Iyer, G., Taylor, B.S., Berger, M.F., Cutler Jr, R.E., Xu, F., Butturini, A., Eli, L.D., Mann, G., Farrell, C., Lalani, A.S., Bryce, R.P., Arteaga, C.L., Meric-Bernstam, F., Baselga, J., Solit, D.B., 2018. HER kinase inhibition in patients with HER2- and HER3-mutant cancers. Nature 554, 189–194. https://doi.org/10.1038/nature25475

Hyman, D.M., Taylor, B.S., Baselga, J., 2017. Implementing Genome-Driven Oncology. Cell 168, 584–599. https://doi.org/10.1016/j.cell.2016.12.015

Inukai, M., Toyooka, S., Ito, S., Asano, H., Ichihara, S., Soh, J., Suehisa, H., Ouchida, M., Aoe, K., Aoe, M., Kiura, K., Shimizu, N., Date, H., 2006. Presence of Epidermal Growth Factor Receptor Gene T790M Mutation as a Minor Clone in Non–Small Cell Lung Cancer. Cancer Res 66, 7854–7858. https://doi.org/10.1158/0008-5472.CAN-06-1951

Jamal-Hanjani, M., Hackshaw, A., Ngai, Y., Shaw, J., Dive, C., Quezada, S., Middleton, G., de Bruin, E., Le Quesne, J., Shafi, S., Falzon, M., Horswell, S., Blackhall, F., Khan, I., Janes, S., Nicolson, M., Lawrence, D., Forster, M., Fennell, D., Lee, S.-M., Lester, J., Kerr, K., Muller, S., Iles, N., Smith, S., Murugaesu, N., Mitter, R., Salm, M., Stuart, A., Matthews, N., Adams, H., Ahmad, T., Attanoos, R., Bennett, J., Birkbak, N.J., Booton, R., Brady, G., Buchan, K., Capitano, A., Chetty, M., Cobbold, M., Crosbie, P., Davies, H., Denison, A., Djearman, M., Goldman, J., Haswell, T., Joseph, L., Kornaszewska, M., Krebs, M., Langman, G., MacKenzie, M., Millar, J., Morgan, B., Naidu, B., Nonaka, D., Peggs, K., Pritchard, C., Remmen, H., Rowan, A., Shah, R., Smith, E., Summers, Y., Taylor, M., Veeriah, S., Waller, D., Wilcox, B., Wilcox, M., Woolhouse, I., McGranahan, N., Swanton, C., 2014. Tracking genomic cancer evolution for precision medicine: the lung TRACERx study. PLoS Biol. 12, e1001906. https://doi.org/10.1371/journal.pbio.1001906

Jamal-Hanjani, M., Wilson, G.A., McGranahan, N., Birkbak, N.J., Watkins, T.B.K., Veeriah, S., Shafi, S., Johnson, D.H., Mitter, R., Rosenthal, R., Salm, M., Horswell, S., Escudero, M., Matthews, N., Rowan, A., Chambers, T., Moore, D.A., Turajlic, S., Xu, H., Lee, S.-M., Forster, M.D., Ahmad, T., Hiley, C.T., Abbosh, C., Falzon, M., Borg, E., Marafioti, T., Lawrence, D., Hayward, M., Kolvekar, S., Panagiotopoulos, N., Janes, S.M., Thakrar, R., Ahmed, A., Blackhall, F., Summers, Y., Shah, R., Joseph, L., Quinn, A.M., Crosbie, P.A., Naidu, B., Middleton, G., Langman, G., Trotter, S., Nicolson, M., Remmen, H., Kerr, K., Chetty, M., Gomersall, L., Fennell, D.A., Nakas, A., Rathinam, S., Anand, G., Khan, S., Russell, P., Ezhil, V., Ismail, B., Irvin-Sellers, M., Prakash, V., Lester, J.F., Kornaszewska, M., Attanoos, R., Adams, H., Davies, H., Dentro, S., Taniere, P., O'Sullivan, B., Lowe, H.L., Hartley, J.A., Iles, N., Bell, H., Ngai, Y., Shaw, J.A., Herrero, J., Szallasi, Z., Schwarz, R.F., Stewart, A., Quezada, S.A., Le Quesne, J., Van Loo, P., Dive, C., Hackshaw, A., Swanton, C., 2017. Tracking the Evolution of Non–Small-Cell Lung Cancer. NEJM 376, 2109–2121. https://doi.org/10.1056/NEJMoa1616288

Jansen, C.S., Prokhnevska, N., Master, V.A., Sanda, M.G., Carlisle, J.W., Bilen, M.A., Cardenas, M., Wilkinson, S., Lake, R., Sowalsky, A.G., Valanparambil, R.M., Hudson, W.H., McGuire, D., Melnick, K., Khan, A.I., Kim, K., Chang, Y.M., Kim, A., Filson, C.P., Alemozaffar, M., Osunkoya, A.O., Mullane, P., Ellis, C., Akondy, R., Im, S.J., Kamphorst, A.O., Reyes, A., Liu, Y., Kissick, H., 2019. An intra-tumoral niche maintains and differentiates stem-like CD8 T cells. Nature 576, 465–470. https://doi.org/10.1038/s41586-019-1836-5

Jerby-Arnon, L., Pfetzer, N., Waldman, Y.Y., McGarry, L., James, D., Shanks, E., Seashore-Ludlow, B., Weinstock, A., Geiger, T., Clemons, P.A., Gottlieb, E., Ruppin, E., 2014. Predicting Cancer-Specific Vulnerability via Data-Driven Detection of Synthetic Lethality. Cell 158, 1199–1209. https://doi.org/10.1016/j.cell.2014.07.027

Jiang, P., Gu, S., Pan, D., Fu, J., Sahu, A., Hu, X., Li, Z., Traugh, N., Bu, X., Li, B., Liu, J., Freeman, G.J., Brown, M.A., Wucherpfennig, K.W., Liu, X.S., 2018. Signatures of T cell dysfunction and exclusion predict cancer immunotherapy response. Nature Medicine 1. https://doi.org/10.1038/s41591-018-0136-1

Johnson, B.E., Mazor, T., Hong, C., Barnes, M., Aihara, K., McLean, C.Y., Fouse, S.D., Yamamoto, S., Ueda, H., Tatsuno, K., Asthana, S., Jalbert, L.E., Nelson, S.J., Bollen, A.W., Gustafson, W.C., Charron, E., Weiss, W.A., Smirnov, I.V., Song, J.S., Olshen, A.B., Cha, S., Zhao, Y., Moore, R.A., Mungall, A.J., Jones, S.J.M., Hirst, M., Marra, M.A., Saito, N., Aburatani, H., Mukasa, A., Berger, M.S., Chang, S.M., Taylor, B.S., Costello, J.F., 2014. Mutational analysis reveals the origin and therapy-driven evolution of recurrent glioma. Science 343, 189–193. https://doi.org/10.1126/science.1239947

Johnson, D.B., Estrada, M.V., Salgado, R., Sanchez, V., Doxie, D.B., Opalenik, S.R., Vilgelm, A.E., Feld, E., Johnson, A.S., Greenplate, A.R., Sanders, M.E., Lovly, C.M., Frederick, D.T., Kelley, M.C., Richmond, A., Irish, J.M., Shyr, Y., Sullivan, R.J., Puzanov, I., Sosman, J.A., Balko, J.M., 2016. Melanoma-specific MHC-II expression represents a tumour-autonomous phenotype and predicts response to anti-PD-1/PD-L1 therapy. Nature Communications 7, 10582. https://doi.org/10.1038/ncomms10582

Jones, S., Zhang, X., Parsons, D.W., Lin, J.C.-H., Leary, R.J., Angenendt, P., Mankoo, P., Carter, H., Kamiyama, H., Jimeno, A., Hong, S.-M., Fu, B., Lin, M.-T., Calhoun, E.S., Kamiyama, M., Walter, K., Nikolskaya, T., Nikolsky, Y., Hartigan, J., Smith, D.R., Hidalgo, M., Leach, S.D., Klein, A.P., Jaffee, E.M., Goggins, M., Maitra, A., Iacobuzio-Donahue, C., Eshleman, J.R., Kern, S.E., Hruban, R.H., Karchin, R., Papadopoulos, N., Parmigiani, G., Vogelstein, B., Velculescu, V.E., Kinzler, K.W., 2008. Core Signaling Pathways in Human Pancreatic Cancers Revealed by Global Genomic Analyses. Science 321, 1801–1806. https://doi.org/10.1126/science.1164368

Joung, J.-G., Bae, J.S., Kim, S.C., Jung, H., Park, W.-Y., Song, S.-Y., 2016. Genomic Characterization and Comparison of Multi-Regional and Pooled Tumor Biopsy Specimens. PLOS ONE 11, e0152574. https://doi.org/10.1371/journal.pone.0152574

Kaelin, W.G., 2005. The Concept of Synthetic Lethality in the Context of Anticancer Therapy. Nat Rev Cancer 5, 689–698. https://doi.org/10.1038/nrc1691

Kahles, A., Lehmann, K.-V., Toussaint, N.C., Hüser, M., Stark, S.G., Sachsenberg, T., Stegle, O., Kohlbacher, O., Sander, C., Caesar-Johnson, S.J., Demchok, J.A., Felau, I., Kasapi, M., Ferguson, M.L., Hutter, C.M., Sofia, H.J., Tarnuzzer, R., Wang, Z., Yang, L., Zenklusen, J.C., Zhang, J. (Julia), Chudamani, S., Liu, J., Lolla, L., Naresh, R., Pihl, T., Sun, Q., Wan, Y., Wu, Y., Cho, J., DeFreitas, T., Frazer, S., Gehlenborg, N., Getz, G., Heiman, D.I., Kim, J., Lawrence, M.S., Lin, P., Meier, S., Noble, M.S., Saksena, G., Voet, D., Zhang, Hailei, Bernard, B., Chambwe, N., Dhankani, V., Knijnenburg, T., Kramer, R., Leinonen, K., Liu, Y., Miller, M., Reynolds, S., Shmulevich, I., Thorsson, V., Zhang, W., Akbani, R., Broom, B.M., Hegde, A.M., Ju, Z., Kanchi, R.S., Korkut, A., Li, J., Liang, H., Ling, S., Liu, W., Lu, Y., Mills, G.B., Ng, K.-S., Rao, A., Ryan, M., Wang, Jing, Weinstein, J.N., Zhang, J., Abeshouse, A., Armenia, J., Chakravarty, D., Chatila, W.K., Bruijn, I. de, Gao, J., Gross, B.E., Heins, Z.J., Kundra, R., La, K., Ladanyi, M., Luna, A., Nissan, M.G., Ochoa, A., Phillips, S.M., Reznik, E., Sanchez-Vega, F., Sander, C., Schultz, N., Sheridan, R., Sumer, S.O., Sun, Y., Taylor, B.S., Wang, Jioajiao, Zhang, Hongxin, Anur, P., Peto, M., Spellman, P., Benz, C., Stuart, J.M., Wong, C.K., Yau, C., Hayes, D.N., Parker, J.S.,

Wilkerson, M.D., Ally, A., Balasundaram, M., Bowlby, R., Brooks, D., Carlsen, R., Chuah, E., Dhalla, N., Holt, R., Jones, S.J.M., Kasaian, K., Lee, D., Ma, Y., Marra, M.A., Mayo, M., Moore, R.A., Mungall, A.J., Mungall, K., Robertson, A.G., Sadeghi, S., Schein, J.E., Sipahimalani, P., Tam, A., Thiessen, N., Tse, K., Wong, T., Berger, A.C., Beroukhim, R., Cherniack, A.D., Cibulskis, C., Gabriel, S.B., Gao, G.F., Ha, G., Meyerson, M., Schumacher, S.E., Shih, J., Kucherlapati, M.H., Kucherlapati, R.S., Baylin, S., Cope, L., Danilova, L., Bootwalla, M.S., Lai, P.H., Maglinte, D.T., Berg, D.J.V.D., Weisenberger, D.J., Auman, J.T., Balu, S., Bodenheimer, T., Fan, C., Hoadley, K.A., Hoyle, A.P., Jefferys, S.R., Jones, C.D., Meng, S., Mieczkowski, P.A., Mose, L.E., Perou, A.H., Perou, C.M., Roach, J., Shi, Y., Simons, J.V., Skelly, T., Soloway, M.G., Tan, D., Veluvolu, U., Fan, H., Hinoue, T., Laird, P.W., Shen, H., Zhou, W., Bellair, M., Chang, K., Covington, K., Creighton, C.J., Dinh, H., Doddapaneni, H., Donehower, L.A., Drummond, J., Gibbs, R.A., Glenn, R., Hale, W., Han, Y., Hu, J., Korchina, V., Lee, S., Lewis, L., Li, W., Liu, X., Morgan, M., Morton, D., Muzny, D., Santibanez, J., Sheth, M., Shinbrot, E., Wang, L., Wang, M., Wheeler, D.A., Xi, L., Zhao, F., Hess, J., Appelbaum, E.L., Bailey, M., Cordes, M.G., Ding, L., Fronick, C.C., Fulton, L.A., Fulton, R.S., Kandoth, C., Mardis, E.R., McLellan, M.D., Miller, C.A., Schmidt, H.K., Wilson, R.K., Crain, D., Curley, E., Gardner, J., Lau, K., Mallery, D., Morris, S., Paulauskis, J., Penny, R., Shelton, C., Shelton, T., Sherman, M., Thompson, E., Yena, P., Bowen, J., Gastier-Foster, J.M., Gerken, M., Leraas, K.M., Lichtenberg, T.M., Ramirez, N.C., Wise, L., Zmuda, E., Corcoran, N., Costello, T., Hovens, C., Carvalho, A.L., Carvalho, A.C. de, Fregnani, J.H., Longatto-Filho, A., Reis, R.M., Scapulatempo-Neto, C., Silveira, H.C.S., Vidal, D.O., Burnette, A., Eschbacher, J., Hermes, B., Noss, A., Singh, R., Anderson, M.L., Castro, P.D., Ittmann, M., Huntsman, D., Kohl, B., Le, X., Thorp, R., Andry, C., Duffy, E.R., Lyadov, V., Paklina, O., Setdikova, G., Shabunin, A., Tavobilov, M., McPherson, C., Warnick, R., Berkowitz, R., Cramer, D., Feltmate, C., Horowitz, N., Kibel, A., Muto, M., Raut, C.P., Malykh, A., Barnholtz-Sloan, J.S., Barrett, W., Devine, K., Fulop, J., Ostrom, Q.T., Shimmel, K., Wolinsky, Y., Sloan, A.E., Rose, A.D., Giuliante, F., Goodman, M., Karlan, B.Y., Hagedorn, C.H., Eckman, J., Harr, J., Myers, J., Tucker, K., Zach, L.A., Deyarmin, B., Hu, H., Kvecher, L., Larson, C., Mural, R.J., Somiari, S., Vicha, A., Zelinka, T., Bennett, J., Iacocca, M., Rabeno, B., Swanson, P., Latour, M., Lacombe, L., Têtu, B., Bergeron, A., McGraw, M., Staugaitis, S.M., Chabot, J., Hibshoosh, H., Sepulveda, A., Su, T., Wang, T., Potapova, O., Voronina, O., Desjardins, L., Mariani, O., Roman-Roman, S., Sastre, X., Stern, M.-H., Cheng, F., Signoretti, S., Berchuck, A., Bigner, D., Lipp, E., Marks, J., McCall, S., McLendon, R., Secord, A., Sharp, A., Behera, M., Brat, D.J., Chen, A., Delman, K., Force, S., Khuri, F., Magliocca, K., Maithel, S., Olson, J.J., Owonikoko, T., Pickens, A., Ramalingam, S., Shin, D.M., Sica, G., Meir, E.G.V., Zhang, Hongzheng, Eijckenboom, W., Gillis, A., Korpershoek, E., Looijenga, L., Oosterhuis, W., Stoop, H., Kessel, K.E. van, Zwarthoff, E.C., Calatozzolo, C., Cuppini, L., Cuzzubbo, S., DiMeco, F., Finocchiaro, G., Mattei, L., Perin, A., Pollo, B., Chen, C., Houck, J., Lohavanichbutr, P., Hartmann, A., Stoehr, C., Stoehr, R., Taubert, H., Wach, S., Wullich, B., Kycler, W., Murawa, D., Wiznerowicz, M., Chung, K., Edenfield, W.J., Martin, J., Baudin, E., Bubley, G., Bueno, R., Rienzo, A.D.,

Richards, W.G., Kalkanis, S., Mikkelsen, T., Noushmehr, H., Scarpace, L., Girard, N., Aymerich, M., Campo, E., Giné, E., Guillermo, A.L., Bang, N.V., Hanh, P.T., Phu, B.D., Tang, Y., Colman, H., Evason, K., Dottino, P.R., Martignetti, J.A., Gabra, H., Juhl, H., Akeredolu, T., Stepa, S., Hoon, D., Ahn, K., Kang, K.J., Beuschlein, F., Breggia, A., Birrer, M., Bell, D., Borad, M., Bryce, A.H., Castle, E., Chandan, V., Cheville, J., Copland, J.A., Farnell, M., Flotte, T., Giama, N., Ho, T., Kendrick, M., Kocher, J.-P., Kopp, K., Moser, C., Nagorney, D., O'Brien, D., O'Neill, B.P., Patel, T., Petersen, G., Que, F., Rivera, M., Roberts, L., Smallridge, R., Smyrk, T., Stanton, M., Thompson, R.H., Torbenson, M., Yang, J.D., Zhang, L., Brimo, F., Ajani, J.A., Gonzalez, A.M.A., Behrens, C., Bondaruk, J., Broaddus, R., Czerniak, B., Esmaeli, B., Fujimoto, J., Gershenwald, J., Guo, C., Lazar, A.J., Logothetis, C., Meric-Bernstam, F., Moran, C., Ramondetta, L., Rice, D., Sood, A., Tamboli, P., Thompson, T., Troncoso, P., Tsao, A., Wistuba, I., Carter, C., Haydu, L., Hersey, P., Jakrot, V., Kakavand, H., Kefford, R., Lee, K., Long, G., Mann, G., Quinn, M., Saw, R., Scolyer, R., Shannon, K., Spillane, A., Stretch, J., Synott, M., Thompson, J., Wilmott, J., Al-Ahmadie, H., Chan, T.A., Ghossein, R., Gopalan, A., Levine, D.A., Reuter, V., Singer, S., Singh, B., Tien, N.V., Broudy, T., Mirsaidi, C., Nair, P., Drwiega, P., Miller, J., Smith, J., Zaren, H., Park, J.-W., Hung, N.P., Kebebew, E., Linehan, W.M., Metwalli, A.R., Pacak, K., Pinto, P.A., Schiffman, M., Schmidt, L.S., Vocke, C.D., Wentzensen, N., Worrell, R., Yang, H., Moncrieff, M., Goparaju, C., Melamed, J., Pass, H., Botnariuc, N., Caraman, I., Cernat, M., Chemencedji, I., Clipca, A., Doruc, S., Gorincioi, G., Mura, S., Pirtac, M., Stancul, I., Tcaciuc, D., Albert, M., Alexopoulou, I., Arnaout, A., Bartlett, J., Engel, J., Gilbert, S., Parfitt, J., Sekhon, H., Thomas, G., Rassl, D.M., Rintoul, R.C., Bifulco, C., Tamakawa, R., Urba, W., Hayward, N., Timmers, H., Antenucci, A., Facciolo, F., Grazi, G., Marino, M., Merola, R., Krijger, R. de, Gimenez-Roqueplo, A.-P., Piché, A., Chevalier, S., McKercher, G., Birsoy, K., Barnett, G., Brewer, C., Farver, C., Naska, T., Pennell, N.A., Raymond, D., Schilero, C., Smolenski, K., Williams, F., Morrison, C., Borgia, J.A., Liptay, M.J., Pool, M., Seder, C.W., Junker, K., Omberg, L., Dinkin, M., Manikhas, G., Alvaro, D., Bragazzi, M.C., Cardinale, V., Carpino, G., Gaudio, E., Chesla, D., Cottingham, S., Dubina, M., Moiseenko, F., Dhanasekaran, R., Becker, K.-F., Janssen, K.-P., Slotta-Huspenina, J., Abdel-Rahman, M.H., Aziz, D., Bell, S., Cebulla, C.M., Davis, A., Duell, R., Elder, J.B., Hilty, J., Kumar, B., Lang, J., Lehman, N.L., Mandt, R., Nguyen, P., Pilarski, R., Rai, K., Schoenfield, L., Senecal, K., Wakely, P., Hansen, P., Lechan, R., Powers, J., Tischler, A., Grizzle, W.E., Sexton, K.C., Kastl, A., Henderson, J., Porten, S., Waldmann, J., Fassnacht, M., Asa, S.L., Schadendorf, D., Couce, M., Graefen, M., Huland, H., Sauter, G., Schlomm, T., Simon, R., Tennstedt, P., Olabode, O., Nelson, M., Bathe, O., Carroll, P.R., Chan, J.M., Disaia, P., Glenn, P., Kelley, R.K., Landen, C.N., Phillips, J., Prados, M., Simko, J., Smith-McCune, K., VandenBerg, S., Roggin, K., Fehrenbach, A., Kendler, A., Sifri, S., Steele, R., Jimeno, A., Carey, F., Forgie, I., Mannelli, M., Carney, M., Hernandez, B., Campos, B., Herold-Mende, C., Jungk, C., Unterberg, A., Deimling, A. von, Bossler, A., Galbraith, J., Jacobus, L., Knudson, M., Knutson, T., Ma, D., Milhem, M., Sigmund, R., Godwin, A.K., Madan, R., Rosenthal, H.G., Adebamowo, C., Adebamowo, S.N., Boussioutas, A., Beer, D., Giordano, T., Mes-Masson,

A.-M., Saad, F., Bocklage, T., Landrum, L., Mannel, R., Moore, K., Moxley, K., Postier, R., Walker, J., Zuna, R., Feldman, M., Valdivieso, F., Dhir, R., Luketich, J., Pinero, E.M.M., Quintero-Aguilo, M., Carlotti, C.G., Santos, J.S.D., Kemp, R., Sankarankuty, A., Tirapelli, D., Catto, J., Agnew, K., Swisher, E., Creaney, J., Robinson, B., Shelley, C.S., Godwin, E.M., Kendall, S., Shipman, C., Bradford, C., Carey, T., Haddad, A., Moyer, J., Peterson, L., Prince, M., Rozek, L., Wolf, G., Bowman, R., Fong, K.M., Yang, I., Korst, R., Rathmell, W.K., Fantacone-Campbell, J.L., Hooke, J.A., Kovatich, A.J., Shriver, C.D., DiPersio, J., Drake, B., Govindan, R., Heath, S., Ley, T., Tine, B.V., Westervelt, P., Rubin, M.A., Lee, J.I., Aredes, N.D., Mariamidze, A., Rätsch, G., 2018. Comprehensive Analysis of Alternative Splicing Across Tumors from 8,705 Patients. Cancer Cell 0. https://doi.org/10.1016/j.ccell.2018.07.001

Kandoth, C., McLellan, M.D., Vandin, F., Ye, K., Niu, B., Lu, C., Xie, M., Zhang, Q., McMichael, J.F., Wyczalkowski, M.A., Leiserson, M.D.M., Miller, C.A., Welch, J.S., Walter, M.J., Wendl, M.C., Ley, T.J., Wilson, R.K., Raphael, B.J., Ding, L., 2013. Mutational landscape and significance across 12 major cancer types. Nature 502, 333–339. https://doi.org/10.1038/nature12634

Kaplan, D.H., Shankaran, V., Dighe, A.S., Stockert, E., Aguet, M., Old, L.J., Schreiber, R.D., 1998. Demonstration of an interferon gamma-dependent tumor surveillance system in immunocompetent mice. Proc. Natl. Acad. Sci. U.S.A. 95, 7556–7561. https://doi.org/10.1073/pnas.95.13.7556

Katayama, R., Shaw, A.T., Khan, T.M., Mino-Kenudson, M., Solomon, B.J., Halmos, B., Jessop, N.A., Wain, J.C., Yeo, A.T., Benes, C., Drew, L., Saeh, J.C., Crosby, K., Sequist, L.V., Iafrate, A.J., Engelman, J.A., 2012. Mechanisms of Acquired Crizotinib Resistance in ALK-Rearranged Lung Cancers. Science Translational Medicine 4, 120ra17-120ra17. https://doi.org/10.1126/scitranslmed.3003316

Katz, S.J., Jagsi, R., Morrow, M., 2018. Reducing Overtreatment of Cancer With Precision Medicine: Just What the Doctor Ordered. JAMA. https://doi.org/10.1001/jama.2018.0018

Kaufman, B., Shapira-Frommer, R., Schmutzler, R.K., Audeh, M.W., Friedlander, M., Balmaña, J., Mitchell, G., Fried, G., Stemmer, S.M., Hubert, A., Rosengarten, O., Steiner, M., Loman, N., Bowen, K., Fielding, A., Domchek, S.M., 2015. Olaparib monotherapy in patients with advanced cancer and a germline BRCA1/2 mutation. J. Clin. Oncol. 33, 244–250. https://doi.org/10.1200/JCO.2014.56.2728

Kim, T.-M., Jung, S.-H., An, C.H., Lee, S.H., Baek, I.-P., Kim, M.S., Park, S.-W., Rhee, J.-K., Lee, S.-H., Chung, Y.-J., 2015. Subclonal Genomic Architectures of Primary and Metastatic Colorectal Cancer Based on Intratumoral Genetic Heterogeneity. Clin Cancer Res 21, 4461–4472. https://doi.org/10.1158/1078-0432.CCR-14-2413

Knudson, A.G., 1971. Mutation and cancer: statistical study of retinoblastoma. Proc. Natl Acad. Sci. USA 68, 820–823. https://doi.org/10.1073/pnas.68.4.820

Kobayashi, S., 2005. EGFR mutation and resistance of non-small-cell lung cancer to gefitinib. N. Engl. J. Med. 352, 786–792. https://doi.org/10.1056/NEJMoa044238

Koboldt, D.C., Zhang, Q., Larson, D.E., Shen, D., McLellan, M.D., Lin, L., Miller, C.A., Mardis, E.R., Ding, L., Wilson, R.K., 2012. VarScan 2: Somatic

mutation and copy number alteration discovery in cancer by exome sequencing. Genome Res. 22, 568–576. https://doi.org/10.1101/gr.129684.111

Kolodziejczyk, A.A., Kim, J.K., Svensson, V., Marioni, J.C., Teichmann, S.A., 2015. The Technology and Biology of Single-Cell RNA Sequencing. Molecular Cell 58, 610–620. https://doi.org/10.1016/j.molcel.2015.04.005

Kopetz, S., Grothey, A., Yaeger, R., Van Cutsem, E., Desai, J., Yoshino, T., Wasan, H., Ciardiello, F., Loupakis, F., Hong, Y.S., Steeghs, N., Guren, T.K., Arkenau, H.-T., Garcia-Alfonso, P., Pfeiffer, P., Orlov, S., Lonardi, S., Elez, E., Kim, T.-W., Schellens, J.H.M., Guo, C., Krishnan, A., Dekervel, J., Morris, V., Calvo Ferrandiz, A., Tarpgaard, L.S., Braun, M., Gollerkeri, A., Keir, C., Maharry, K., Pickard, M., Christy-Bittel, J., Anderson, L., Sandor, V., Tabernero, J., 2019. Encorafenib, Binimetinib, and Cetuximab in BRAF V600E–Mutated Colorectal Cancer. New England Journal of Medicine 381, 1632–1643. https://doi.org/10.1056/NEJMoa1908075

Kratz, J.R., Haro, G.J., Cook, N.R., He, J., Van Den Eeden, S.K., Woodard, G.A., Gubens, M.A., Jahan, T.M., Jones, K.D., Kim, I.-J., He, B., Jablons, D.M., Mann, M.J., 2019. Incorporation of a Molecular Prognostic Classifier Improves Conventional Non–Small Cell Lung Cancer Staging. Journal of Thoracic Oncology 14, 1223–1232. https://doi.org/10.1016/j.jtho.2019.03.015

Kratz, J.R., He, J., Van Den Eeden, S.K., Zhu, Z.-H., Gao, W., Pham, P.T., Mulvihill, M.S., Ziaei, F., Zhang, H., Su, B., Zhi, X., Quesenberry, C.P., Habel, L.A., Deng, Q., Wang, Z., Zhou, J., Li, H., Huang, M.-C., Yeh, C.-C., Segal, M.R., Ray, M.R., Jones, K.D., Raz, D.J., Xu, Z., Jahan, T.M., Berryman, D., He, B., Mann, M.J., Jablons, D.M., 2012. A practical molecular assay to predict survival in resected non-squamous, non-small-cell lung cancer: development and international validation studies. The Lancet 379, 823–832. https://doi.org/10.1016/S0140-6736(11)61941-7

Kratz, J.R., Tham, P.T., Mulvihill, M.S., Ziaei, F., Ray, M.R., Hurst, J.W., Segal, M.R., Berryman, D.M., Chu, W., He, B., Jablons, D.M., Mann, M.J., 2013. Analytical Validation of a Practical Molecular Assay Prognostic of Survival in Nonsquamous Non–Small Cell Lung Cancer. Diagnostic Molecular Pathology 22, 65–69. https://doi.org/10.1097/PDM.0b013e318273fb61

Krzystanek, M., Moldvay, J., Szüts, D., Szallasi, Z., Eklund, A.C., 2016. A robust prognostic gene expression signature for early stage lung adenocarcinoma. Biomark Res 4, 4. https://doi.org/10.1186/s40364-016-0058-3

Kucab, J.E., Zou, X., Morganella, S., Joel, M., Nanda, A.S., Nagy, E., Gomez, C., Degasperi, A., Harris, R., Jackson, S.P., Arlt, V.M., Phillips, D.H., Nik-Zainal, S., 2019. A Compendium of Mutational Signatures of Environmental Agents. Cell 177, 821-836.e16. https://doi.org/10.1016/j.cell.2019.03.001

Kumar-Sinha, C., Chinnaiyan, A.M., 2018. Precision oncology in the age of integrative genomics. Nature Biotechnology 36, 46–60. https://doi.org/10.1038/nbt.4017

Kurian, A.W., Bondarenko, I., Jagsi, R., Friese, C.R., McLeod, M.C., Hawley, S.T., Hamilton, A.S., Ward, K.C., Hofer, T.P., Katz, S.J., 2017. Recent Trends in Chemotherapy Use and Oncologists' Treatment Recommendations for Early-Stage Breast Cancer. J Natl Cancer Inst. https://doi.org/10.1093/jnci/djx239

LaFave, L.M., Kartha, V.K., Ma, S., Meli, K., Priore, I.D., Lareau, C., Naranjo, S., Westcott, P.M.K., Duarte, F.M., Sankar, V., Chiang, Z., Brack, A., Law, T., Hauck, H., Okimoto, A., Regev, A., Buenrostro, J.D., Jacks, T., 2020. Epigenomic State Transitions Characterize Tumor Progression in Mouse Lung Adenocarcinoma. Cancer Cell 38, 212-228.e13. https://doi.org/10.1016/j.ccell.2020.06.006

Lambrechts, D., Wauters, E., Boeckx, B., Aibar, S., Nittner, D., Burton, O., Bassez, A., Decaluwé, H., Pircher, A., Eynde, K.V. den, Weynand, B., Verbeken, E., Leyn, P.D., Liston, A., Vansteenkiste, J., Carmeliet, P., Aerts, S., Thienpont, B., 2018. Phenotype molding of stromal cells in the lung tumor microenvironment. Nature Medicine 1. https://doi.org/10.1038/s41591-018-0096-5

Landau, D.A., Carter, S.L., Stojanov, P., McKenna, A., Stevenson, K., Lawrence, M.S., Sougnez, C., Stewart, C., Sivachenko, A., Wang, L., Wan, Y., Zhang, W., Shukla, S.A., Vartanov, A., Fernandes, S.M., Saksena, G., Cibulskis, K., Tesar, B., Gabriel, S., Hacohen, N., Meyerson, M., Lander, E.S., Neuberg, D., Brown, J.R., Getz, G., Wu, C.J., 2013. Evolution and Impact of Subclonal Mutations in Chronic Lymphocytic Leukemia. Cell 152, 714–726. https://doi.org/10.1016/j.cell.2013.01.019

Lander, E.S., Linton, L.M., Birren, B., Nusbaum, C., Zody, M.C., Baldwin, J., Devon, K., Dewar, K., Doyle, M., FitzHugh, W., Funke, R., Gage, D., Harris, K., Heaford, A., Howland, J., Kann, L., Lehoczky, J., LeVine, R., McEwan, P., McKernan, K., Meldrim, J., Mesirov, J.P., Miranda, C., Morris, W., Naylor, J., Raymond, Christina, Rosetti, M., Santos, R., Sheridan, A., Sougnez, C., Stange-Thomann, N., Stojanovic, N., Subramanian, A., Wyman, D., Rogers, J., Sulston, J., Ainscough, R., Beck, S., Bentley, D., Burton, J., Clee, C., Carter, N., Coulson, A., Deadman, R., Deloukas, P., Dunham, A., Dunham, I., Durbin, R., French, L., Grafham, D., Gregory, S., Hubbard, T., Humphray, S., Hunt, A., Jones, M., Lloyd, C., McMurray, A., Matthews, L., Mercer, S., Milne, S., Mullikin, J.C., Mungall, A., Plumb, R., Ross, M., Shownkeen, R., Sims, S., Waterston, R.H., Wilson, R.K., Hillier, L.W., McPherson, J.D., Marra, M.A., Mardis, E.R., Fulton, L.A., Chinwalla, A.T., Pepin, K.H., Gish, W.R., Chissoe, S.L., Wendl, M.C., Delehaunty, K.D., Miner, T.L., Delehaunty, A., Kramer, J.B., Cook, L.L., Fulton, R.S., Johnson, D.L., Minx, P.J., Clifton, S.W., Hawkins, T., Branscomb, E., Predki, P., Richardson, P., Wenning, S., Slezak, T., Doggett, N., Cheng, J.-F., Olsen, A., Lucas, S., Elkin, C., Uberbacher, E., Frazier, M., Gibbs, R.A., Muzny, D.M., Scherer, S.E., Bouck, J.B., Sodergren, E.J., Worley, K.C., Rives, C.M., Gorrell, J.H., Metzker, M.L., Naylor, S.L., Kucherlapati, R.S., Nelson, D.L., Weinstock, G.M., Sakaki, Y., Fujiyama, A., Hattori, M., Yada, T., Toyoda, A., Itoh, T., Kawagoe, C., Watanabe, H., Totoki, Y., Taylor, T., Weissenbach, J., Heilig, R., Saurin, W., Artiguenave, F., Brottier, P., Bruls, T., Pelletier, E., Robert, C., Wincker, P., Rosenthal, A., Platzer, M., Nyakatura, G., Taudien, S., Rump, A., Smith, D.R., Doucette-Stamm, L., Rubenfield, M., Weinstock, K., Lee, H.M., Dubois, J., Yang, H., Yu, J., Wang, J., Huang, G., Gu, J., Hood, L., Rowen, L., Madan, A., Qin, S., Davis, R.W., Federspiel, N.A., Abola, A.P., Proctor, M.J., Roe, B.A., Chen, F., Pan, H., Ramser, J., Lehrach, H., Reinhardt, R., McCombie, W.R., Bastide, M. de la, Dedhia, N., Blöcker, H., Hornischer, K., Nordsiek, G., Agarwala, R., Aravind, L., Bailey, J.A., Bateman, A., Batzoglou, S., Birney, E., Bork, P.,

Brown, D.G., Burge, C.B., Cerutti, L., Chen, H.-C., Church, D., Clamp, M., Copley, R.R., Doerks, T., Eddy, S.R., Eichler, E.E., Furey, T.S., Galagan, J., Gilbert, J.G.R., Harmon, C., Hayashizaki, Y., Haussler, D., Hermjakob, H., Hokamp, K., Jang, W., Johnson, L.S., Jones, T.A., Kasif, S., Kaspryzk, A., Kennedy, S., Kent, W.J., Kitts, P., Koonin, E.V., Korf, I., Kulp, D., Lancet, D., Lowe, T.M., McLysaght, A., Mikkelsen, T., Moran, J.V., Mulder, N., Pollara, V.J., Ponting, C.P., Schuler, G., Schultz, J., Slater, G., Smit, A.F.A., Stupka, E., Szustakowki, J., Thierry-Mieg, D., Thierry-Mieg, J., Wagner, L., Wallis, J., Wheeler, R., Williams, A., Wolf, Y.I., Wolfe, K.H., Yang, S.-P., Yeh, R.-F., Collins, F., Guyer, M.S., Peterson, J., Felsenfeld, A., Wetterstrand, K.A., Myers, R.M., Schmutz, J., Dickson, M., Grimwood, J., Cox, D.R., Olson, M.V., Kaul, R., Raymond, Christopher, Shimizu, N., Kawasaki, K., Minoshima, S., Evans, G.A., Athanasiou, M., Schultz, R., Patrinos, A., Morgan, M.J., 2001. Initial sequencing and analysis of the human genome. Nature 409, 860–921. https://doi.org/10.1038/35057062

Lau, S.K., Boutros, P.C., Pintilie, M., Blackhall, F.H., Zhu, C.-Q., Strumpf, D., Johnston, M.R., Darling, G., Keshavjee, S., Waddell, T.K., Liu, N., Lau, D., Penn, L.Z., Shepherd, F.A., Jurisica, I., Der, S.D., Tsao, M.-S., 2007. Three-Gene Prognostic Classifier for Early-Stage Non–Small-Cell Lung Cancer. JCO 25, 5562–5569. https://doi.org/10.1200/JCO.2007.12.0352

Laughney, A.M., Elizalde, S., Genovese, G., Bakhoum, S.F., 2015. Dynamics of Tumor Heterogeneity Derived from Clonal Karyotypic Evolution. Cell Rep 12, 809–820. https://doi.org/10.1016/j.celrep.2015.06.065

Lawrence, M.S., Stojanov, P., Mermel, C.H., Robinson, J.T., Garraway, L.A., Golub, T.R., Meyerson, M., Gabriel, S.B., Lander, E.S., Getz, G., 2014. Discovery and saturation analysis of cancer genes across 21 tumour types. Nature 505, 495–501. https://doi.org/10.1038/nature12912

Lawrence, M.S., Stojanov, P., Polak, P., Kryukov, G.V., Cibulskis, K., Sivachenko, A., Carter, S.L., Stewart, C., Mermel, C.H., Roberts, S.A., Kiezun, A., Hammerman, P.S., McKenna, A., Drier, Y., Zou, L., Ramos, A.H., Pugh, T.J., Stransky, N., Helman, E., Kim, J., Sougnez, C., Ambrogio, L., Nickerson, E., Shefler, E., Cortés, M.L., Auclair, D., Saksena, G., Voet, D., Noble, M., DiCara, D., Lin, P., Lichtenstein, L., Heiman, D.I., Fennell, T., Imielinski, M., Hernandez, B., Hodis, E., Baca, S., Dulak, A.M., Lohr, J., Landau, D.-A., Wu, C.J., Melendez-Zajgla, J., Hidalgo-Miranda, A., Koren, A., McCarroll, S.A., Mora, J., Lee, R.S., Crompton, B., Onofrio, R., Parkin, M., Winckler, W., Ardlie, K., Gabriel, S.B., Roberts, C.W.M., Biegel, J.A., Stegmaier, K., Bass, A.J., Garraway, L.A., Meyerson, M., Golub, T.R., Gordenin, D.A., Sunyaev, S., Lander, E.S., Getz, G., 2013. Mutational heterogeneity in cancer and the search for new cancer-associated genes. Nature 499, 214–218. https://doi.org/10.1038/nature12213

Le, D.T., Durham, J.N., Smith, K.N., Wang, H., Bartlett, B.R., Aulakh, L.K., Lu, S., Kemberling, H., Wilt, C., Luber, B.S., Wong, F., Azad, N.S., Rucki, A.A., Laheru, D., Donehower, R., Zaheer, A., Fisher, G.A., Crocenzi, T.S., Lee, J.J., Greten, T.F., Duffy, A.G., Ciombor, K.K., Eyring, A.D., Lam, B.H., Joe, A., Kang, S.P., Holdhoff, M., Danilova, L., Cope, L., Meyer, C., Zhou, S., Goldberg, R.M., Armstrong, D.K., Bever, K.M., Fader, A.N., Taube, J., Housseau, F., Spetzler, D., Xiao, N., Pardoll, D.M., Papadopoulos, N., Kinzler, K.W., Eshleman, J.R., Vogelstein, B., Anders, R.A., Diaz, L.A.,

2017. Mismatch repair deficiency predicts response of solid tumors to PD-1 blockade. Science 357, 409–413. https://doi.org/10.1126/science.aan6733

Leach, D.R., Krummel, M.F., Allison, J.P., 1996. Enhancement of Antitumor Immunity by CTLA-4 Blockade. Science 271, 1734–1736. https://doi.org/10.1126/science.271.5256.1734

Lee, H.-O., Hong, Y., Etlioglu, H.E., Cho, Y.B., Pomella, V., Van den Bosch, B., Vanhecke, J., Verbandt, S., Hong, H., Min, J.-W., Kim, N., Eum, H.H., Qian, J., Boeckx, B., Lambrechts, D., Tsantoulis, P., De Hertogh, G., Chung, W., Lee, T., An, M., Shin, H.-T., Joung, J.-G., Jung, M.-H., Ko, G., Wirapati, P., Kim, S.H., Kim, H.C., Yun, S.H., Tan, I.B.H., Ranjan, B., Lee, W.Y., Kim, T.-Y., Choi, J.K., Kim, Y.-J., Prabhakar, S., Tejpar, S., Park, W.-Y., 2020. Lineage-dependent gene expression programs influence the immune landscape of colorectal cancer. Nature Genetics 1–10. https://doi.org/10.1038/s41588-020-0636-z

Lee, J.-K., Lee, J., Kim, Sehui, Kim, Soyeon, Youk, J., Park, S., An, Y., Keam, B., Kim, D.-W., Heo, D.S., Kim, Y.T., Kim, J.-S., Kim, S.H., Lee, J.S., Lee, S.-H., Park, K., Ku, J.-L., Jeon, Y.K., Chung, D.H., Park, P.J., Kim, J., Kim, T.M., Ju, Y.S., 2017. Clonal History and Genetic Predictors of Transformation Into Small-Cell Carcinomas From Lung Adenocarcinomas. JCO 35, 3065–3074. https://doi.org/10.1200/JCO.2016.71.9096

Lee, W.-C., Diao, L., Wang, J., Zhang, Jianhua, Roarty, E.B., Varghese, S., Chow, C.-W., Fujimoto, J., Behrens, C., Cascone, T., Peng, W., Kalhor, N., Moran, C.A., Weissferdt, A., Johnson, F.M., William, W.N., Swisher, S.G., Lee, J.J., Hong, W.K., Heymach, J.V., Wistuba, I.I., Futreal, P.A., Zhang, Jianjun, 2018. Multiregion gene expression profiling reveals heterogeneity in molecular subtypes and immunotherapy response signatures in lung cancer. Modern Pathology 1. https://doi.org/10.1038/s41379-018-0029-3

Lehman, J.A., Cross, F.S., Richey, D.G., 1966. Clinical study of forty-nine patients with malignant melanoma. Cancer 19, 611–619. https://doi.org/10.1002/1097-0142(196605)19:5<611::AID-CNCR2820190503>3.0.CO;2-M

Leiserson, M.D., Wu, H.-T., Vandin, F., Raphael, B.J., 2015. CoMEt: a statistical approach to identify combinations of mutually exclusive alterations in cancer. Genome Biology 16, 160. https://doi.org/10.1186/s13059-015-0700-7

Ley, T.J., Mardis, E.R., Ding, L., Fulton, B., McLellan, M.D., Chen, K., Dooling, D., Dunford-Shore, B.H., McGrath, S., Hickenbotham, M., Cook, L., Abbott, R., Larson, D.E., Koboldt, D.C., Pohl, C., Smith, S., Hawkins, A., Abbott, S., Locke, D., Hillier, L.W., Miner, T., Fulton, L., Magrini, V., Wylie, T., Glasscock, J., Conyers, J., Sander, N., Shi, X., Osborne, J.R., Minx, P., Gordon, D., Chinwalla, A., Zhao, Y., Ries, R.E., Payton, J.E., Westervelt, P., Tomasson, M.H., Watson, M., Baty, J., Ivanovich, J., Heath, S., Shannon, W.D., Nagarajan, R., Walter, M.J., Link, D.C., Graubert, T.A., DiPersio, J.F., Wilson, R.K., 2008. DNA sequencing of a cytogenetically normal acute myeloid leukaemia genome. Nature 456, 66–72. https://doi.org/10.1038/nature07485

Li, Bailiang, Cui, Y., Diehn, M., Li, R., 2017. Development and Validation of an Individualized Immune Prognostic Signature in Early-Stage Nonsquamous Non–Small Cell Lung Cancer. JAMA Oncol. https://doi.org/10.1001/jamaoncol.2017.1609

Li, B., Dewey, C.N., 2011. RSEM: accurate transcript quantification from RNA-Seq data with or without a reference genome. BMC Bioinformatics 12, 323. https://doi.org/10.1186/1471-2105-12-323

Li, Bo, Liu, J.S., Liu, X.S., 2017. Revisit linear regression-based deconvolution methods for tumor gene expression data. Genome Biology 18, 127. https://doi.org/10.1186/s13059-017-1256-5

Li, B., Severson, E., Pignon, J.-C., Zhao, H., Li, T., Novak, J., Jiang, P., Shen, H., Aster, J.C., Rodig, S., Signoretti, S., Liu, J.S., Liu, X.S., 2016. Comprehensive analyses of tumor immunity: implications for cancer immunotherapy. Genome Biology 17, 174. https://doi.org/10.1186/s13059-016-1028-7

Lindskrog, S.V., Prip, F.F., Lamy, P., Taber, A., Groeneveld, C.S., Birkenkamp-Demtroder, K., Jensen, J.B., Strandgaard, T., Nordentoft, I., Christensen, E., Sokac, M., Birkbak, N.J., Maretty, L., Hermann, G.H., Petersen, A.C., Weyerer, V., Grimm, M.-O., Horstmann, M., Sjodahl, G., Hoglund, M., Steiniche, T., Mogensen, K., Reynies, A. de, Nawroth, R., Jordan, B., Lin, X., Dragicevic, D., Ward, D.G., Goel, A., Hurst, C.D., Raman, J.D., Warrick, J.I., Segersten, U., Sikic, D., Kessel, K.E.M. van, Maurer, T., Meeks, J.J., Degraff, D.J., Bryan, R.T., Knowles, M.A., Simic, T., Hartmann, A., Zwarthoff, E.C., Malmstrom, P.-U., Malats, N., Real, F.X., Dyrskjot, L., 2020. An integrated multi-omics analysis identifies clinically relevant molecular subtypes of non-muscle-invasive bladder cancer. medRxiv 2020.06.19.20054809. https://doi.org/10.1101/2020.06.19.20054809

Lipinski, K.A., Barber, L.J., Davies, M.N., Ashenden, M., Sottoriva, A., Gerlinger, M., 2016. Cancer Evolution and the Limits of Predictability in Precision Cancer Medicine. Trends Cancer 2, 49–63. https://doi.org/10.1016/j.trecan.2015.11.003

Litchfield, K., Stanislaw, S., Spain, L., Gallegos, L.L., Rowan, A., Schnidrig, D., Rosenbaum, H., Harle, A., Au, L., Hill, S.M., Tippu, Z., Thomas, J., Thompson, L., Xu, H., Horswell, S., Barhoumi, A., Jones, C., Leith, K.F., Burgess, D.L., Watkins, T.B.K., Lim, E., Birkbak, N.J., Lamy, P., Nordentoft, I., Dyrskjøt, L., Pickering, L., Hazell, Stephen, Jamal-Hanjani, M., Abbosh, C., Shiu, K.-K., Bridgewater, J., Hochhauser, D., Forster, M., Lee, S.-M., Ahmad, T., Papadatos-Pastos, D., Janes, S., Loo, P.V., Enfield, K., McGranahan, N., Huebner, A., Quezada, S., Beck, S., Parker, P., Walczak, H., Enver, T., Hynds, R., Falzon, M., Proctor, I., Sinclair, R., Lok, C., Rhodes, Z., Moore, D., Marafioti, T., Borg, E., Mitchison, M., Khiroya, R., Trevisan, G., Ellery, P., Linch, M., Brandner, S., Hiley, C., Veeriah, S., Razaq, M., Shaw, H., Attard, G., Akther, M.A., Naceur-Lombardelli, C., Manzano, L., Al-Bakir, M., Summan, S., Kanu, N., Ward, S., Asghar, U., Lim, E., Gishen, F., Tookman, A., Stone, P., Stirling, C., Furness, A., Edmonds, K., Hunter, N., Sarker, S., Vaughan, S., Mangwende, M., Pearce, K., Spain, L., Shepherd, S., Yan, H., Shum, B., Carlyle, E., Hazell, Steve, Fendler, A., Byrne, F., Yousaf, N., Popat, S., Curtis, O., Stamp, G., Toncheva, A., Nye, E., Murra, A., Korteweg, J., Sheikh, N., Josephs, D., Chandra, A., Spicer, J., Mahadeva, U., Green, A., Stewart, R., Iredale, L.-R., Mackay, T., Deakin, B., Enting, D., Rudman, S., Ghosh, S., Karapagniotou, L., Pintus, E., Tutt, A., Howlett, S., Michalarea, V., Brenton, J., Caldas, C., Fitzgerald, R., Jimenez-Linan, M., Provenzano, E., Cluroe, A., Stewart, G., Watts, C., Gilbertson, R., McDermott, U., Tavare, S., Beddowes, E.,

Roxburgh, P., Biankin, A., Chalmers, A., Fraser, S., Oien, K., Kidd, A., Blyth, K., Krebs, M., Blackhall, F., Summers, Y., Dive, C., Marais, R., Gomes, F., Carter, M., Dransfield, J., Quesne, J.L., Fennell, D., Shaw, J., Naidu, B., Baijal, S., Tanchel, B., Langman, G., Robinson, A., Collard, M., Cockcroft, P., Ferris, C., Bancroft, H., Kerr, A., Middleton, G., Webb, J., Kadiri, S., Colloby, P., Olisemeke, B., Wilson, R., Tomlinson, I., Jogai, S., Ottensmeier, C., Harrison, D., Loda, M., Flanagan, A., McKenzie, M., Hackshaw, A., Ledermann, J., Sharp, A., Farrelly, L., Bridger, H., Larkin, J., Swanton, C., Alexander, N.R., Turajlic, S., 2020. Representative Sequencing: Unbiased Sampling of Solid Tumor Tissue. Cell Reports 31. https://doi.org/10.1016/j.celrep.2020.107550

Liu, David, Schilling, B., Liu, Derek, Sucker, A., Livingstone, E., Jerby-Amon, L., Zimmer, L., Gutzmer, R., Satzger, I., Loquai, C., Grabbe, S., Vokes, N., Margolis, C.A., Conway, J., He, M.X., Elmarakeby, H., Dietlein, F., Miao, D., Tracy, A., Gogas, H., Goldinger, S.M., Utikal, J., Blank, C.U., Rauschenberg, R., Bubnoff, D. von, Krackhardt, A., Weide, B., Haferkamp, S., Kiecker, F., Izar, B., Garraway, L., Regev, A., Flaherty, K., Paschen, A., Allen, E.M.V., Schadendorf, D., 2019. Integrative molecular and clinical modeling of clinical outcomes to PD1 blockade in patients with metastatic melanoma. Nat Med 25, 1916–1927. https://doi.org/10.1038/s41591-019-0654-5

Loo, P.V., Nordgard, S.H., Lingjærde, O.C., Russnes, H.G., Rye, I.H., Sun, W., Weigman, V.J., Marynen, P., Zetterberg, A., Naume, B., Perou, C.M., Børresen-Dale, A.-L., Kristensen, V.N., 2010. Allele-specific copy number analysis of tumors. PNAS 107, 16910–16915. https://doi.org/10.1073/pnas.1009843107

López, S., Lim, E.L., Horswell, S., Haase, K., Huebner, A., Dietzen, M., Mourikis, T.P., Watkins, T.B.K., Rowan, A., Dewhurst, S.M., Birkbak, N.J., Wilson, G.A., Loo, P.V., Jamal-Hanjani, M., Swanton, C., McGranahan, N., 2020. Interplay between whole-genome doubling and the accumulation of deleterious alterations in cancer evolution. Nat Genet 52, 283–293. https://doi.org/10.1038/s41588-020-0584-7

Lord, C.J., Ashworth, A., 2017. PARP inhibitors: Synthetic lethality in the clinic. Science 355, 1152–1158. https://doi.org/10.1126/science.aam7344

Lotti, F., Jarrar, A.M., Pai, R.K., Hitomi, M., Lathia, J., Mace, A., Gantt, G.A., Sukhdeo, K., DeVecchio, J., Vasanji, A., Leahy, P., Hjelmeland, A.B., Kalady, M.F., Rich, J.N., 2013. Chemotherapy activates cancer-associated fibroblasts to maintain colorectal cancer-initiating cells by IL-17A. Journal of Experimental Medicine 210, 2851–2872. https://doi.org/10.1084/jem.20131195

Love, M.I., Huber, W., Anders, S., 2014. Moderated estimation of fold change and dispersion for RNA-seq data with DESeq2. Genome Biology 15, 550. https://doi.org/10.1186/s13059-014-0550-8

Lynch, M., Bürger, R., Butcher, D., Gabriel, W., 1993. The Mutational Meltdown in Asexual Populations. J Hered 84, 339–344. https://doi.org/10.1093/oxfordjournals.jhered.a111354

Lynch, T.J., Bell, D.W., Sordella, R., Gurubhagavatula, S., Okimoto, R.A., Brannigan, B.W., Harris, P.L., Haserlat, S.M., Supko, J.G., Haluska, F.G., Louis, D.N., Christiani, D.C., Settleman, J., Haber, D.A., 2004. Activating mutations in the epidermal growth factor receptor underlying

responsiveness of non-small-cell lung cancer to gefitinib. N. Engl. J. Med. 350, 2129–2139. https://doi.org/10.1056/NEJMoa040938

Malanchi, I., Santamaria-Martínez, A., Susanto, E., Peng, H., Lehr, H.-A., Delaloye, J.-F., Huelsken, J., 2012. Interactions between cancer stem cells and their niche govern metastatic colonization. Nature 481, 85–89. https://doi.org/10.1038/nature10694

Maley, C.C., Aktipis, A., Graham, T.A., Sottoriva, A., Boddy, A.M., Janiszewska, M., Silva, A.S., Gerlinger, M., Yuan, Y., Pienta, K.J., Anderson, K.S., Gatenby, R., Swanton, C., Posada, D., Wu, C.-I., Schiffman, J.D., Hwang, E.S., Polyak, K., Anderson, A.R.A., Brown, J.S., Greaves, M., Shibata, D., 2017. Classifying the evolutionary and ecological features of neoplasms. Nat Rev Cancer 17, 605–619. https://doi.org/10.1038/nrc.2017.69

Mariathasan, S., Turley, S.J., Nickles, D., Castiglioni, A., Yuen, K., Wang, Y., Kadel Iii, E.E., Koeppen, H., Astarita, J.L., Cubas, R., Jhunjhunwala, S., Banchereau, R., Yang, Y., Guan, Y., Chalouni, C., Ziai, J., Şenbabaoğlu, Y., Santoro, S., Sheinson, D., Hung, J., Giltnane, J.M., Pierce, A.A., Mesh, K., Lianoglou, S., Riegler, J., Carano, R.A.D., Eriksson, P., Höglund, M., Somarriba, L., Halligan, D.L., van der Heijden, M.S., Loriot, Y., Rosenberg, J.E., Fong, L., Mellman, I., Chen, D.S., Green, M., Derleth, C., Fine, G.D., Hegde, P.S., Bourgon, R., Powles, T., 2018. TGFβ attenuates tumour response to PD-L1 blockade by contributing to exclusion of T cells. Nature 554, 544–548. https://doi.org/10.1038/nature25501

Marjanovic, N.D., Hofree, M., Chan, J.E., Canner, D., Wu, K., Trakala, M., Hartmann, G.G., Smith, O., Kim, J., Evans, K.V., Hudson, A., Ashenberg, O., Porter, C.B.M., Bejnood, A., Subramanian, A., Pitter, K., Yan, Y., Delroy, T., Phillips, D.R., Shah, N., Chaudhary, O., Tsankov, A., Hollmann, T., Rekhtman, N., Massion, P.P., Poirier, J.T., Mazutis, L., Li, R., Lee, J.-H., Amon, A., Rudin, C.M., Jacks, T., Regev, A., Tammela, T., 2020. Emergence of a High-Plasticity Cell State during Lung Cancer Evolution. Cancer Cell 0. https://doi.org/10.1016/j.ccell.2020.06.012

Marquart, J., Chen, E.Y., Prasad, V., 2018. Estimation of the Percentage of US Patients With Cancer Who Benefit From Genome-Driven Oncology. JAMA Oncol 4, 1093–1098. https://doi.org/10.1001/jamaoncol.2018.1660

Marusyk, A., Tabassum, D.P., Janiszewska, M., Place, A.E., Trinh, A., Rozhok, A.I., Pyne, S., Guerriero, J.L., Shu, S., Ekram, M., Ishkin, A., Cahill, D.P., Nikolsky, Y., Chan, T.A., Rimawi, M.F., Hilsenbeck, S., Schiff, R., Osborne, K.C., Letai, A., Polyak, K., 2016. Spatial Proximity to Fibroblasts Impacts Molecular Features and Therapeutic Sensitivity of Breast Cancer Cells Influencing Clinical Outcomes. Cancer Res 76, 6495–6506. https://doi.org/10.1158/0008-5472.CAN-16-1457

Mascaux, C., Angelova, M., Vasaturo, A., Beane, J., Hijazi, K., Anthoine, G., Buttard, B., Rothe, F., Willard-Gallo, K., Haller, A., Ninane, V., Burny, A., Sculier, J.-P., Spira, A., Galon, J., 2019. Immune evasion before tumour invasion in early lung squamous carcinogenesis. Nature 1. https://doi.org/10.1038/s41586-019-1330-0

Maser, R.S., DePinho, R.A., 2002. Connecting Chromosomes, Crisis, and Cancer. Science 297, 565–569. https://doi.org/10.1126/science.297.5581.565

McCall, S.J., Dry, S.M., 2019. Precision Pathology as Part of Precision Medicine: Are We Optimizing Patients' Interests in Prioritizing Use of Limited Tissue

Samples? JCO Precision Oncology 1–6. https://doi.org/10.1200/PO.18.00238

McGranahan, N., Burrell, R.A., Endesfelder, D., Novelli, M.R., Swanton, C., 2012. Cancer chromosomal instability: therapeutic and diagnostic challenges. EMBO reports 13, 528–538. https://doi.org/10.1038/embor.2012.61

McGranahan, N., Favero, F., de Bruin, E.C., Birkbak, N.J., Szallasi, Z., Swanton, C., 2015. Clonal status of actionable driver events and the timing of mutational processes in cancer evolution. Sci Transl Med 7, 283ra54. https://doi.org/10.1126/scitranslmed.aaa1408

McGranahan, N., Furness, A.J.S., Rosenthal, R., Ramskov, S., Lyngaa, R., Saini, S.K., Jamal-Hanjani, M., Wilson, G.A., Birkbak, N.J., Hiley, C.T., Watkins, T.B.K., Shafi, S., Murugaesu, N., Mitter, R., Akarca, A.U., Linares, J., Marafioti, T., Henry, J.Y., Van Allen, E.M., Miao, D., Schilling, B., Schadendorf, D., Garraway, L.A., Makarov, V., Rizvi, N.A., Snyder, A., Hellmann, M.D., Merghoub, T., Wolchok, J.D., Shukla, S.A., Wu, C.J., Peggs, K.S., Chan, T.A., Hadrup, S.R., Quezada, S.A., Swanton, C., 2016. Clonal neoantigens elicit T cell immunoreactivity and sensitivity to immune checkpoint blockade. Science 351, 1463–1469. https://doi.org/10.1126/science.aaf1490

McGranahan, N., Swanton, C., 2019. Neoantigen quality, not quantity. Science Translational Medicine 11, eaax7918. https://doi.org/10.1126/scitranslmed.aax7918

McGranahan, N., Swanton, C., 2017. Clonal Heterogeneity and Tumor Evolution: Past, Present, and the Future. Cell 168, 613–628. https://doi.org/10.1016/j.cell.2017.01.018

McInnes, L., Healy, J., Melville, J., 2018. UMAP: Uniform Manifold Approximation and Projection for Dimension Reduction. arXiv:1802.03426 [cs, stat].

McIntyre, B.W., Allison, J.P., 1983. The mouse T cell receptor: structural heterogeneity of molecules of normal T cells defined by xenoantiserum. Cell 34, 739–746. https://doi.org/10.1016/0092-8674(83)90530-5

Meads, M.B., Gatenby, R.A., Dalton, W.S., 2009. Environment-mediated drug resistance: a major contributor to minimal residual disease. Nat Rev Cancer 9, 665–674. https://doi.org/10.1038/nrc2714

Merritt, C.R., Ong, G.T., Church, S.E., Barker, K., Danaher, P., Geiss, G., Hoang, M., Jung, J., Liang, Y., McKay-Fleisch, J., Nguyen, K., Norgaard, Z., Sorg, K., Sprague, I., Warren, C., Warren, S., Webster, P.J., Zhou, Z., Zollinger, D.R., Dunaway, D.L., Mills, G.B., Beechem, J.M., 2020. Multiplex digital spatial profiling of proteins and RNA in fixed tissue. Nat Biotechnol 38, 586–599. https://doi.org/10.1038/s41587-020-0472-9

Middleton, G., Fletcher, P., Popat, S., Savage, J., Summers, Y., Greystoke, A., Gilligan, D., Cave, J., O'Rourke, N., Brewster, A., Toy, E., Spicer, J., Jain, P., Dangoor, A., Mackean, M., Forster, M., Farley, A., Wherton, D., Mehmi, M., Sharpe, R., Mills, T.C., Cerone, M.A., Yap, T.A., Watkins, T.B.K., Lim, E., Swanton, C., Billingham, L., 2020. The National Lung Matrix Trial of personalized therapy in lung cancer. Nature 1–6. https://doi.org/10.1038/s41586-020-2481-8

Mikulak, J., Oriolo, F., Bruni, E., Roberto, A., Colombo, F.S., Villa, A., Bosticardo, M., Bortolomai, I., Lo Presti, E., Meraviglia, S., Dieli, F., Vetrano, S., Danese, S., Della Bella, S., Carvello, M.M., Sacchi, M., Cugini, G., Colombo, G., Klinger, M., Spaggiari, P., Roncalli, M., Prinz, I., Ravens, S., di

Lorenzo, B., Marcenaro, E., Silva-Santos, B., Spinelli, A., Mavilio, D., 2019. NKp46-expressing human gut-resident intraepithelial Vδ1 T cell subpopulation exhibits high antitumor activity against colorectal cancer. JCI Insight 4. https://doi.org/10.1172/jci.insight.125884

Miller, C.A., Settle, S.H., Sulman, E.P., Aldape, K.D., Milosavljevic, A., 2011. Discovering functional modules by identifying recurrent and mutually exclusive mutational patterns in tumors. BMC Med Genomics 4, 34. https://doi.org/10.1186/1755-8794-4-34

Mina, M., Raynaud, F., Tavernari, D., Battistello, E., Sungalee, S., Saghafinia, S., Laessle, T., Sanchez-Vega, F., Schultz, N., Oricchio, E., Ciriello, G., 2017. Conditional Selection of Genomic Alterations Dictates Cancer Evolution and Oncogenic Dependencies. Cancer Cell 32, 155-168.e6. https://doi.org/10.1016/j.ccell.2017.06.010

Misale, S., Yaeger, R., Hobor, S., Scala, E., Janakiraman, M., Liska, D., Valtorta, E., Schiavo, R., Buscarino, M., Siravegna, G., Bencardino, K., Cercek, A., Chen, C.-T., Veronese, S., Zanon, C., Sartore-Bianchi, A., Gambacorta, M., Gallicchio, M., Vakiani, E., Boscaro, V., Medico, E., Weiser, M., Siena, S., Di Nicolantonio, F., Solit, D., Bardelli, A., 2012. Emergence of KRAS mutations and acquired resistance to anti-EGFR therapy in colorectal cancer. Nature 486, 532–536. https://doi.org/10.1038/nature11156

Mitchell, T.J., Turajlic, S., Rowan, A., Nicol, D., Farmery, J.H.R., O'Brien, T., Martincorena, I., Tarpey, P., Angelopoulos, N., Yates, L.R., Butler, A.P., Raine, K., Stewart, G.D., Challacombe, B., Fernando, A., Lopez, J.I., Hazell, S., Chandra, A., Chowdhury, S., Rudman, S., Soultati, A., Stamp, G., Fotiadis, N., Pickering, L., Au, L., Spain, L., Lynch, J., Stares, M., Teague, J., Maura, F., Wedge, D.C., Horswell, S., Chambers, T., Litchfield, K., Xu, H., Stewart, A., Elaidi, R., Oudard, S., McGranahan, N., Csabai, I., Gore, M., Futreal, P.A., Larkin, J., Lynch, A.G., Szallasi, Z., Swanton, C., Campbell, P.J., 2018. Timing the Landmark Events in the Evolution of Clear Cell Renal Cell Cancer: TRACERx Renal. Cell 173, 611-623.e17. https://doi.org/10.1016/j.cell.2018.02.020

Mlecnik, B., Van den Eynde, M., Bindea, G., Church, S.E., Vasaturo, A., Fredriksen, T., Lafontaine, L., Haicheur, N., Marliot, F., Debetancourt, D., Pairet, G., Jouret-Mourin, A., Gigot, J.-F., Hubert, C., Danse, E., Dragean, C., Carrasco, J., Humblet, Y., Valge-Archer, V., Berger, A., Pagès, F., Machiels, J.-P., Galon, J., 2018. Comprehensive Intrametastatic Immune Quantification and Major Impact of Immunoscore on Survival. J Natl Cancer Inst 110, 97–108. https://doi.org/10.1093/jnci/djx123

Mok, T.S., Wu, Y.-L., Ahn, M.-J., Garassino, M.C., Kim, H.R., Ramalingam, S.S., Shepherd, F.A., He, Y., Akamatsu, H., Theelen, W.S.M.E., Lee, C.K., Sebastian, M., Templeton, A., Mann, H., Marotti, M., Ghiorghiu, S., Papadimitrakopoulou, V.A., AURA3 Investigators, 2017. Osimertinib or Platinum-Pemetrexed in EGFR T790M-Positive Lung Cancer. N. Engl. J. Med. 376, 629–640. https://doi.org/10.1056/NEJMoa1612674

Monach, P.A., Meredith, S.C., Siegel, C.T., Schreiber, H., 1995. A unique tumor antigen produced by a single amino acid substitution. Immunity 2, 45–59.

Moore, A.L., Kuipers, J., Singer, J., Burcklen, E., Schraml, P., Beisel, C., Moch, H., Beerenwinkel, N., 2018. Intra-tumor heterogeneity and clonal exclusivity in renal cell carcinoma. bioRxiv 305623. https://doi.org/10.1101/305623

Morris, L.G.T., Riaz, N., Desrichard, A., Şenbabaoğlu, Y., Hakimi, A.A., Makarov, V., Reis-Filho, J.S., Chan, T.A., Morris, L.G.T., Riaz, N., Desrichard, A., Şenbabaoğlu, Y., Hakimi, A.A., Makarov, V., Reis-Filho, J.S., Chan, T.A., 2016. Pan-cancer analysis of intratumor heterogeneity as a prognostic determinant of survival. Oncotarget 7, 10051–10063. https://doi.org/10.18632/oncotarget.7067

Morrissy, A.S., Cavalli, F.M.G., Remke, M., Ramaswamy, V., Shih, D.J.H., Holgado, B.L., Farooq, H., Donovan, L.K., Garzia, L., Agnihotri, S., Kiehna, E.N., Mercier, E., Mayoh, C., Papillon-Cavanagh, S., Nikbakht, H., Gayden, T., Torchia, J., Picard, D., Merino, D.M., Vladoiu, M., Luu, B., Wu, X., Daniels, C., Horswell, S., Thompson, Y.Y., Hovestadt, V., Northcott, P.A., Jones, D.T.W., Peacock, J., Wang, X., Mack, S.C., Reimand, J., Albrecht, S., Fontebasso, A.M., Thiessen, N., Li, Y., Schein, J.E., Lee, D., Carlsen, R., Mayo, M., Tse, K., Tam, A., Dhalla, N., Ally, A., Chuah, E., Cheng, Y., Plettner, P., Li, H.I., Corbett, R.D., Wong, T., Long, W., Loukides, J., Buczkowicz, P., Hawkins, C.E., Tabori, U., Rood, B.R., Myseros, J.S., Packer, R.J., Korshunov, A., Lichter, P., Kool, M., Pfister, S.M., Schüller, U., Dirks, P., Huang, A., Bouffet, E., Rutka, J.T., Bader, G.D., Swanton, C., Ma, Y., Moore, R.A., Mungall, A.J., Majewski, J., Jones, S.J.M., Das, S., Malkin, D., Jabado, N., Marra, M.A., Taylor, M.D., 2017. Spatial heterogeneity in medulloblastoma. Nat Genet 49, 780–788. https://doi.org/10.1038/ng.3838

Morrissy, A.S., Garzia, L., Shih, D.J.H., Zuyderduyn, S., Huang, X., Skowron, P., Remke, M., Cavalli, F.M.G., Ramaswamy, V., Lindsay, P.E., Jelveh, S., Donovan, L.K., Wang, X., Luu, B., Zayne, K., Li, Y., Mayoh, C., Thiessen, N., Mercier, E., Mungall, K.L., Ma, Y., Tse, K., Zeng, T., Shumansky, K., Roth, A.J.L., Shah, S., Farooq, H., Kijima, N., Holgado, B.L., Lee, J.J.Y., Matan-Lithwick, S., Liu, J., Mack, S.C., Manno, A., Michealraj, K.A., Nor, C., Peacock, J., Qin, L., Reimand, J., Rolider, A., Thompson, Y.Y., Wu, X., Pugh, T., Ally, A., Bilenky, M., Butterfield, Y.S.N., Carlsen, R., Cheng, Y., Chuah, E., Corbett, R.D., Dhalla, N., He, A., Lee, D., Li, H.I., Long, W., Mayo, M., Plettner, P., Qian, J.Q., Schein, J.E., Tam, A., Wong, T., Birol, I., Zhao, Y., Faria, C.C., Pimentel, J., Nunes, S., Shalaby, T., Grotzer, M., Pollack, I.F., Hamilton, R.L., Li, X.-N., Bendel, A.E., Fults, D.W., Walter, A.W., Kumabe, T., Tominaga, T., Collins, V.P., Cho, Y.-J., Hoffman, C., Lyden, D., Wisoff, J.H., Garvin, J.H., Stearns, D.S., Massimi, L., Schüller, U., Sterba, J., Zitterbart, K., Puget, S., Ayrault, O., Dunn, S.E., Tirapelli, D.P.C., Carlotti, C.G., Wheeler, H., Hallahan, A.R., Ingram, W., MacDonald, T.J., Olson, J.J., Van Meir, E.G., Lee, J.-Y., Wang, K.-C., Kim, S.-K., Cho, B.-K., Pietsch, T., Fleischhack, G., Tippelt, S., Ra, Y.S., Bailey, S., Lindsey, J.C., Clifford, S.C., Eberhart, C.G., Cooper, M.K., Packer, R.J., Massimino, M., Garre, M.L., Bartels, U., Tabori, U., Hawkins, C.E., Dirks, P., Bouffet, E., Rutka, J.T., Wechsler-Reya, R.J., Weiss, W.A., Collier, L.S., Dupuy, A.J., Korshunov, A., Jones, D.T.W., Kool, M., Northcott, P.A., Pfister, S.M., Largaespada, D.A., Mungall, A.J., Moore, R.A., Jabado, N., Bader, G.D., Jones, S.J.M., Malkin, D., Marra, M.A., Taylor, M.D., 2016. Divergent clonal selection dominates medulloblastoma at recurrence. Nature 529, 351–357. https://doi.org/10.1038/nature16478

Mountain, C.F., Carr, D.T., Anderson, W.A., 1974. A system for the clinical staging of lung cancer. Am J Roentgenol Radium Ther Nucl Med 120, 130–138.

Murugaesu, N., Wilson, G.A., Birkbak, N.J., Watkins, T.B.K., McGranahan, N., Kumar, S., Abbassi-Ghadi, N., Salm, M., Mitter, R., Horswell, S., Rowan, A., Phillimore, B., Biggs, J., Begum, S., Matthews, N., Hochhauser, D., Hanna, G.B., Swanton, C., 2015. Tracking the Genomic Evolution of Esophageal Adenocarcinoma through Neoadjuvant Chemotherapy. Cancer Discov 5, 821–831. https://doi.org/10.1158/2159-8290.CD-15-0412

Nangalia, J., Campbell, P.J., 2019. Genome Sequencing during a Patient's Journey through Cancer. New England Journal of Medicine 381, 2145–2156. https://doi.org/10.1056/NEJMra1910138

Neou, M., Villa, C., Armignacco, R., Jouinot, A., Raffin-Sanson, M.-L., Septier, A., Letourneur, F., Diry, S., Diedisheim, M., Izac, B., Gaspar, C., Perlemoine, K., Verjus, V., Bernier, M., Boulin, A., Emile, J.-F., Bertagna, X., Jaffrezic, F., Laloe, D., Baussart, B., Bertherat, J., Gaillard, S., Assié, G., 2020. Pangenomic Classification of Pituitary Neuroendocrine Tumors. Cancer Cell 37, 123-134.e5. https://doi.org/10.1016/j.ccell.2019.11.002

Newman, A.M., Alizadeh, A.A., 2016. High-throughput genomic profiling of tumor-infiltrating leukocytes. Current Opinion in Immunology, Vaccines * Special section: Cancer immunology: Genomics & biomarkers 41, 77–84. https://doi.org/10.1016/j.coi.2016.06.006

Newman, A.M., Gentles, A.J., Liu, C.L., Diehn, M., Alizadeh, A.A., 2017. Data normalization considerations for digital tumor dissection. Genome Biology 18, 128. https://doi.org/10.1186/s13059-017-1257-4

Newman, A.M., Liu, C.L., Green, M.R., Gentles, A.J., Feng, W., Xu, Y., Hoang, C.D., Diehn, M., Alizadeh, A.A., 2015. Robust enumeration of cell subsets from tissue expression profiles. Nat Meth 12, 453–457. https://doi.org/10.1038/nmeth.3337

Newman, A.M., Steen, C.B., Liu, C.L., Gentles, A.J., Chaudhuri, A.A., Scherer, F., Khodadoust, M.S., Esfahani, M.S., Luca, B.A., Steiner, D., Diehn, M., Alizadeh, A.A., 2019. Determining cell type abundance and expression from bulk tissues with digital cytometry. Nature Biotechnology 1. https://doi.org/10.1038/s41587-019-0114-2

Nishino, M., Ramaiya, N.H., Hatabu, H., Hodi, F.S., 2017. Monitoring immune-checkpoint blockade: response evaluation and biomarker development. Nature Reviews Clinical Oncology 14, 655. https://doi.org/10.1038/nrclinonc.2017.88

Noorbakhsh, J., Kim, H., Namburi, S., Chuang, J.H., 2018. Distribution-based measures of tumor heterogeneity are sensitive to mutation calling and lack strong clinical predictive power. Scientific Reports 8, 11445. https://doi.org/10.1038/s41598-018-29154-7

Nowell, P.C., 1976. The clonal evolution of tumor cell populations. Science 194, 23–28. https://doi.org/10.1126/science.959840

O'Callaghan, D.S., Rexhepaj, E., Gately, K., Coate, L., Delaney, D., O'Donnell, D.M., Kay, E., O'Connell, F., Gallagher, W.M., O'Byrne, K.J., 2015. Tumour islet Foxp3+ T-cell infiltration predicts poor outcome in nonsmall cell lung cancer. European Respiratory Journal 46, 1762–1772. https://doi.org/10.1183/13993003.00176-2014

Ohri, C.M., Shikotra, A., Green, R.H., Waller, D.A., Bradding, P., 2009. Macrophages within NSCLC tumour islets are predominantly of a cytotoxic M1 phenotype associated with extended survival. European Respiratory Journal 33, 118–126. https://doi.org/10.1183/09031936.00065708

Okayama, H., Kohno, T., Ishii, Y., Shimada, Y., Shiraishi, K., Iwakawa, R., Furuta, K., Tsuta, K., Shibata, T., Yamamoto, S., Watanabe, S., Sakamoto, H., Kumamoto, K., Takenoshita, S., Gotoh, N., Mizuno, H., Sarai, A., Kawano, S., Yamaguchi, R., Miyano, S., Yokota, J., 2012. Identification of Genes Upregulated in ALK-Positive and EGFR/KRAS/ALK-Negative Lung Adenocarcinomas. Cancer Res 72, 100–111. https://doi.org/10.1158/0008-5472.CAN-11-1403

Opasic, L., Zhou, D., Werner, B., Dingli, D., Traulsen, A., 2019. How many samples are needed to infer truly clonal mutations from heterogenous tumours? BMC Cancer 19, 403. https://doi.org/10.1186/s12885-019-5597-1

Ortmann, C.A., Kent, D.G., Nangalia, J., Silber, Y., Wedge, D.C., Grinfeld, J., Baxter, E.J., Massie, C.E., Papaemmanuil, E., Menon, S., Godfrey, A.L., Dimitropoulou, D., Guglielmelli, P., Bellosillo, B., Besses, C., Döhner, K., Harrison, C.N., Vassiliou, G.S., Vannucchi, A., Campbell, P.J., Green, A.R., 2015. Effect of Mutation Order on Myeloproliferative Neoplasms. New England Journal of Medicine 372, 601–612. https://doi.org/10.1056/NEJMoa1412098

Paez, J.G., Jänne, P.A., Lee, J.C., Tracy, S., Greulich, H., Gabriel, S., Herman, P., Kaye, F.J., Lindeman, N., Boggon, T.J., Naoki, K., Sasaki, H., Fujii, Y., Eck, M.J., Sellers, W.R., Johnson, B.E., Meyerson, M., 2004. EGFR Mutations in Lung Cancer: Correlation with Clinical Response to Gefitinib Therapy. Science 304, 1497–1500. https://doi.org/10.1126/science.1099314

Pagès, F., Berger, A., Camus, M., Sanchez-Cabo, F., Costes, A., Molidor, R., Mlecnik, B., Kirilovsky, A., Nilsson, M., Damotte, D., Meatchi, T., Bruneval, P., Cugnenc, P.-H., Trajanoski, Z., Fridman, W.-H., Galon, J., 2005. Effector memory T cells, early metastasis, and survival in colorectal cancer. N. Engl. J. Med. 353, 2654–2666. https://doi.org/10.1056/NEJMoa051424

Paik, S., Shak, S., Tang, G., Kim, C., Baker, J., Cronin, M., Baehner, F.L., Walker, M.G., Watson, D., Park, T., Hiller, W., Fisher, E.R., Wickerham, D.L., Bryant, J., Wolmark, N., 2004. A Multigene Assay to Predict Recurrence of Tamoxifen-Treated, Node-Negative Breast Cancer. New England Journal of Medicine 351, 2817–2826. https://doi.org/10.1056/NEJMoa041588

Pao, W., Miller, V., Zakowski, M., Doherty, J., Politi, K., Sarkaria, I., Singh, B., Heelan, R., Rusch, V., Fulton, L., Mardis, E., Kupfer, D., Wilson, R., Kris, M., Varmus, H., 2004. EGF receptor gene mutations are common in lung cancers from “never smokers” and are associated with sensitivity of tumors to gefitinib and erlotinib. PNAS 101, 13306–13311. https://doi.org/10.1073/pnas.0405220101

Paradis, E., Claude, J., Strimmer, K., 2004. APE: Analyses of Phylogenetics and Evolution in R language. Bioinformatics 20, 289–290. https://doi.org/10.1093/bioinformatics/btg412

Park, S., Lehner, B., 2015. Cancer type-dependent genetic interactions between cancer driver alterations indicate plasticity of epistasis across cell types. Molecular Systems Biology 11, 824. https://doi.org/10.15252/msb.20156102

Parker, J.S., Mullins, M., Cheang, M.C.U., Leung, S., Voduc, D., Vickery, T., Davies, S., Fauron, C., He, X., Hu, Z., Quackenbush, J.F., Stijleman, I.J., Palazzo, J., Marron, J. s., Nobel, A.B., Mardis, E., Nielsen, T.O., Ellis, M.J., Perou, C.M., Bernard, P.S., 2009. Supervised Risk Predictor of Breast Cancer Based on Intrinsic Subtypes. JCO 27, 1160–1167. https://doi.org/10.1200/JCO.2008.18.1370

Patel, A.P., Tirosh, I., Trombetta, J.J., Shalek, A.K., Gillespie, S.M., Wakimoto, H., Cahill, D.P., Nahed, B.V., Curry, W.T., Martuza, R.L., Louis, D.N., Rozenblatt-Rosen, O., Suvà, M.L., Regev, A., Bernstein, B.E., 2014. Single-cell RNA-seq highlights intratumoral heterogeneity in primary glioblastoma. Science 344, 1396–1401. https://doi.org/10.1126/science.1254257

Pennycuick, A., Teixeira, V.H., AbdulJabbar, K., Raza, S.E.A., Lund, T., Akarca, A.U., Rosenthal, R., Kalinke, L., Chandrasekharan, D.P., Pipinikas, C.P., Lee-Six, H., Hynds, R.E., Gowers, K.H.C., Henry, J.Y., Millar, F.R., Hagos, Y.B., Denais, C., Falzon, M., Moore, D.A., Antoniou, S., Durrenberger, P.F., Furness, A.J.S., Carroll, B., Marceaux, C., Asselin-Labat, M.-L., Larson, W., Betts, C., Coussens, L.M., Thakrar, R.M., George, J., Swanton, C., Thirlwell, C., Campbell, P.J., Marafioti, T., Yuan, Y., Quezada, S.A., McGranahan, N., Janes, S.M., 2020. Immune surveillance in clinical regression of pre-invasive squamous cell lung cancer. Cancer Discov. https://doi.org/10.1158/2159-8290.CD-19-1366

Perou, C.M., Sørlie, T., Eisen, M.B., Rijn, M. van de, Jeffrey, S.S., Rees, C.A., Pollack, J.R., Ross, D.T., Johnsen, H., Akslen, L.A., Fluge, Ø., Pergamenschikov, A., Williams, C., Zhu, S.X., Lønning, P.E., Børresen-Dale, A.-L., Brown, P.O., Botstein, D., 2000. Molecular portraits of human breast tumours. Nature 406, 747–752. https://doi.org/10.1038/35021093

Petersen, S.E., Bichel, P., Lorentzen, M., 1979. Flow-cytometric demonstration of tumour-cell subpopulations with different DNA content in human colo-rectal carcinoma. European Journal of Cancer (1965) 15, 383–386. https://doi.org/10.1016/0014-2964(79)90072-0

Philip, M., Fairchild, L., Sun, L., Horste, E.L., Camara, S., Shakiba, M., Scott, A.C., Viale, A., Lauer, P., Merghoub, T., Hellmann, M.D., Wolchok, J.D., Leslie, C.S., Schietinger, A., 2017. Chromatin states define tumour-specific T cell dysfunction and reprogramming. Nature 545, 452–456. https://doi.org/10.1038/nature22367

Picelli, S., Faridani, O.R., Björklund, A.K., Winberg, G., Sagasser, S., Sandberg, R., 2014. Full-length RNA-seq from single cells using Smart-seq2. Nat Protoc 9, 171–181. https://doi.org/10.1038/nprot.2014.006

Pignon, J.-P., Tribodet, H., Scagliotti, G.V., Douillard, J.-Y., Shepherd, F.A., Stephens, R.J., Dunant, A., Torri, V., Rosell, R., Seymour, L., Spiro, S.G., Rolland, E., Fossati, R., Aubert, D., Ding, K., Waller, D., Le Chevalier, T., 2008. Lung Adjuvant Cisplatin Evaluation: A Pooled Analysis by the LACE Collaborative Group. JCO 26, 3552–3559. https://doi.org/10.1200/JCO.2007.13.9030

Pleasance, E.D., Stephens, P.J., O'Meara, S., McBride, D.J., Meynert, A., Jones, D., Lin, M.-L., Beare, D., Lau, K.W., Greenman, C., Varela, I., Nik-Zainal, S., Davies, H.R., Ordoñez, G.R., Mudie, L.J., Latimer, C., Edkins, S., Stebbings, L., Chen, L., Jia, M., Leroy, C., Marshall, J., Menzies, A., Butler, A., Teague, J.W., Mangion, J., Sun, Y.A., McLaughlin, S.F., Peckham, H.E., Tsung, E.F., Costa, G.L., Lee, C.C., Minna, J.D., Gazdar, A., Birney, E., Rhodes, M.D., McKernan, K.J., Stratton, M.R., Futreal, P.A., Campbell, P.J., 2010. A small-cell lung cancer genome with complex signatures of tobacco exposure. Nature 463, 184–190. https://doi.org/10.1038/nature08629

Pollack, J.R., Sørlie, T., Perou, C.M., Rees, C.A., Jeffrey, S.S., Lonning, P.E., Tibshirani, R., Botstein, D., Børresen-Dale, A.-L., Brown, P.O., 2002. Microarray analysis reveals a major direct role of DNA copy number

alteration in the transcriptional program of human breast tumors. PNAS 99, 12963–12968. https://doi.org/10.1073/pnas.162471999

Priestley, P., Baber, J., Lolkema, M.P., Steeghs, N., Bruijn, E. de, Shale, C., Duyvesteyn, K., Haidari, S., Hoeck, A. van, Onstenk, W., Roepman, P., Voda, M., Bloemendal, H.J., Tjan-Heijnen, V.C.G., Herpen, C.M.L. van, Labots, M., Witteveen, P.O., Smit, E.F., Sleijfer, S., Voest, E.E., Cuppen, E., 2019. Pan-cancer whole-genome analyses of metastatic solid tumours. Nature 575, 210–216. https://doi.org/10.1038/s41586-019-1689-y

Puchalski, R.B., Shah, N., Miller, J., Dalley, R., Nomura, S.R., Yoon, J.-G., Smith, K.A., Lankerovich, M., Bertagnolli, D., Bickley, K., Boe, A.F., Brouner, K., Butler, S., Caldejon, S., Chapin, M., Datta, S., Dee, N., Desta, T., Dolbeare, T., Dotson, N., Ebbert, A., Feng, D., Feng, X., Fisher, M., Gee, G., Goldy, J., Gourley, L., Gregor, B.W., Gu, G., Hejazinia, N., Hohmann, J., Hothi, P., Howard, R., Joines, K., Kriedberg, A., Kuan, L., Lau, C., Lee, F., Lee, H., Lemon, T., Long, F., Mastan, N., Mott, E., Murthy, C., Ngo, K., Olson, E., Reding, M., Riley, Z., Rosen, D., Sandman, D., Shapovalova, N., Slaughterbeck, C.R., Sodt, A., Stockdale, G., Szafer, A., Wakeman, W., Wohnoutka, P.E., White, S.J., Marsh, D., Rostomily, R.C., Ng, L., Dang, C., Jones, A., Keogh, B., Gittleman, H.R., Barnholtz-Sloan, J.S., Cimino, P.J., Uppin, M.S., Keene, C.D., Farrokhi, F.R., Lathia, J.D., Berens, M.E., Iavarone, A., Bernard, A., Lein, E., Phillips, J.W., Rostad, S.W., Cobbs, C., Hawrylycz, M.J., Foltz, G.D., 2018. An anatomic transcriptional atlas of human glioblastoma. Science 360, 660–663. https://doi.org/10.1126/science.aaf2666

Quezada, S.A., Peggs, K.S., 2013. Exploiting CTLA-4, PD-1 and PD-L1 to reactivate the host immune response against cancer. Br J Cancer 108, 1560–1565. https://doi.org/10.1038/bjc.2013.117

Racle, J., Jonge, K. de, Baumgaertner, P., Speiser, D.E., Gfeller, D., 2017. Simultaneous enumeration of cancer and immune cell types from bulk tumor gene expression data. eLife Sciences 6, e26476. https://doi.org/10.7554/eLife.26476

Ramalingam, S.S., Vansteenkiste, J., Planchard, D., Cho, B.C., Gray, J.E., Ohe, Y., Zhou, C., Reungwetwattana, T., Cheng, Y., Chewaskulyong, B., Shah, R., Cobo, M., Lee, K.H., Cheema, P., Tiseo, M., John, T., Lin, M.-C., Imamura, F., Kurata, T., Todd, A., Hodge, R., Saggese, M., Rukazenkov, Y., Soria, J.-C., 2020. Overall Survival with Osimertinib in Untreated, EGFR-Mutated Advanced NSCLC. New England Journal of Medicine 382, 41–50. https://doi.org/10.1056/NEJMoa1913662

Raz, D.J., Ray, M.R., Kim, J.Y., He, B., Taron, M., Skrzypski, M., Segal, M., Gandara, D.R., Rosell, R., Jablons, D.M., 2008. A Multigene Assay Is Prognostic of Survival in Patients with Early-Stage Lung Adenocarcinoma. Clin Cancer Res 14, 5565–5570. https://doi.org/10.1158/1078-0432.CCR-08-0544

Reddy, E.P., Reynolds, R.K., Santos, E., Barbacid, M., 1982. A point mutation is responsible for the acquisition of transforming properties by the T24 human bladder carcinoma oncogene. Nature 300, 149–152. https://doi.org/10.1038/300149a0

Reiter, J.G., Baretti, M., Gerold, J.M., Makohon-Moore, A.P., Daud, A., Iacobuzio-Donahue, C.A., Azad, N.S., Kinzler, K.W., Nowak, M.A., Vogelstein, B.,

2019. An analysis of genetic heterogeneity in untreated cancers. Nat. Rev. Cancer. https://doi.org/10.1038/s41568-019-0185-x

Reka, A.K., Chen, G., Jones, R.C., Amunugama, R., Kim, S., Karnovsky, A., Standiford, T.J., Beer, D.G., Omenn, G.S., Keshamouni, V.G., 2014. Epithelial–mesenchymal transition-associated secretory phenotype predicts survival in lung cancer patients. Carcinogenesis 35, 1292–1300. https://doi.org/10.1093/carcin/bgu041

Rheinbay, E., Nielsen, M.M., Abascal, F., Wala, J.A., Shapira, O., Tiao, G., Hornshøj, H., Hess, J.M., Juul, R.I., Lin, Z., Feuerbach, L., Sabarinathan, R., Madsen, T., Kim, J., Mularoni, L., Shuai, S., Lanzós, A., Herrmann, C., Maruvka, Y.E., Shen, C., Amin, S.B., Bandopadhayay, P., Bertl, J., Boroevich, K.A., Busanovich, J., Carlevaro-Fita, J., Chakravarty, D., Chan, C.W.Y., Craft, D., Dhingra, P., Diamanti, K., Fonseca, N.A., Gonzalez-Perez, A., Guo, Q., Hamilton, M.P., Haradhvala, N.J., Hong, C., Isaev, K., Johnson, T.A., Juul, M., Kahles, A., Kahraman, A., Kim, Y., Komorowski, J., Kumar, K., Kumar, S., Lee, D., Lehmann, K.-V., Li, Y., Liu, E.M., Lochovsky, L., Park, K., Pich, O., Roberts, N.D., Saksena, G., Schumacher, S.E., Sidiropoulos, N., Sieverling, L., Sinnott-Armstrong, N., Stewart, C., Tamborero, D., Tubio, J.M.C., Umer, H.M., Uusküla-Reimand, L., Wadelius, C., Wadi, L., Yao, X., Zhang, C.-Z., Zhang, J., Haber, J.E., Hobolth, A., Imielinski, M., Kellis, M., Lawrence, M.S., Mering, C. von, Nakagawa, H., Raphael, B.J., Rubin, M.A., Sander, C., Stein, L.D., Stuart, J.M., Tsunoda, T., Wheeler, D.A., Johnson, R., Reimand, J., Gerstein, M., Khurana, E., Campbell, P.J., López-Bigas, N., Weischenfeldt, J., Beroukhim, R., Martincorena, I., Pedersen, J.S., Getz, G., 2020. Analyses of non-coding somatic drivers in 2,658 cancer whole genomes. Nature 578, 102–111. https://doi.org/10.1038/s41586-020-1965-x

Riaz, N., Havel, J.J., Makarov, V., Desrichard, A., Urba, W.J., Sims, J.S., Hodi, F.S., Martín-Algarra, S., Mandal, R., Sharfman, W.H., Bhatia, S., Hwu, W.-J., Gajewski, T.F., Slingluff, C.L., Chowell, D., Kendall, S.M., Chang, H., Shah, R., Kuo, F., Morris, L.G.T., Sidhom, J.-W., Schneck, J.P., Horak, C.E., Weinhold, N., Chan, T.A., 2017. Tumor and Microenvironment Evolution during Immunotherapy with Nivolumab. Cell 0. https://doi.org/10.1016/j.cell.2017.09.028

Ribas, A., Hu-Lieskovan, S., 2016. What does PD-L1 positive or negative mean? Journal of Experimental Medicine 213, 2835–2840. https://doi.org/10.1084/jem.20161462

Rice, C.M., Davies, L.C., Subleski, J.J., Maio, N., Gonzalez-Cotto, M., Andrews, C., Patel, N.L., Palmieri, E.M., Weiss, J.M., Lee, J.-M., Annunziata, C.M., Rouault, T.A., Durum, S.K., McVicar, D.W., 2018. Tumour-elicited neutrophils engage mitochondrial metabolism to circumvent nutrient limitations and maintain immune suppression. Nature Communications 9, 5099. https://doi.org/10.1038/s41467-018-07505-2

Rimmer, A., Phan, H., Mathieson, I., Iqbal, Z., Twigg, S.R.F., Wilkie, A.O.M., McVean, G., Lunter, G., 2014. Integrating mapping-, assembly- and haplotype-based approaches for calling variants in clinical sequencing applications. Nature Genetics 46, 912–918. https://doi.org/10.1038/ng.3036

Rizvi, N.A., Hellmann, M.D., Snyder, A., Kvistborg, P., Makarov, V., Havel, J.J., Lee, W., Yuan, J., Wong, P., Ho, T.S., Miller, M.L., Rekhtman, N., Moreira, A.L., Ibrahim, F., Bruggeman, C., Gasmi, B., Zappasodi, R., Maeda, Y.,

Sander, C., Garon, E.B., Merghoub, T., Wolchok, J.D., Schumacher, T.N., Chan, T.A., 2015. Mutational landscape determines sensitivity to PD-1 blockade in non–small cell lung cancer. Science 348, 124–128. https://doi.org/10.1126/science.aaa1348

Robinson, D.R., Wu, Y.-M., Lonigro, R.J., Vats, P., Cobain, E., Everett, J., Cao, X., Rabban, E., Kumar-Sinha, C., Raymond, V., Schuetze, S., Alva, A., Siddiqui, J., Chugh, R., Worden, F., Zalupski, M.M., Innis, J., Mody, R.J., Tomlins, S.A., Lucas, D., Baker, L.H., Ramnath, N., Schott, A.F., Hayes, D.F., Vijai, J., Offit, K., Stoffel, E.M., Roberts, J.S., Smith, D.C., Kunju, L.P., Talpaz, M., Cieślik, M., Chinnaiyan, A.M., 2017. Integrative clinical genomics of metastatic cancer. Nature advance online publication. https://doi.org/10.1038/nature23306

Roche-Lestienne, C., Laï, J.-L., Darré, S., Facon, T., Preudhomme, C., 2003. A Mutation Conferring Resistance to Imatinib at the Time of Diagnosis of Chronic Myelogenous Leukemia. New England Journal of Medicine 348, 2265–2266. https://doi.org/10.1056/NEJMc035089

Rooney, M.S., Shukla, S.A., Wu, C.J., Getz, G., Hacohen, N., 2015. Molecular and Genetic Properties of Tumors Associated with Local Immune Cytolytic Activity. Cell 160, 48–61. https://doi.org/10.1016/j.cell.2014.12.033

Rosenthal, R., Cadieux, E.L., Salgado, R., Bakir, M.A., Moore, D.A., Hiley, C.T., Lund, T., Tanić, M., Reading, J.L., Joshi, K., Henry, J.Y., Ghorani, E., Wilson, G.A., Birkbak, N.J., Jamal-Hanjani, M., Veeriah, S., Szallasi, Z., Loi, S., Hellmann, M.D., Feber, A., Chain, B., Herrero, J., Quezada, S.A., Demeulemeester, J., Loo, P.V., Beck, S., McGranahan, N., Swanton, C., 2019. Neoantigen-directed immune escape in lung cancer evolution. Nature 1. https://doi.org/10.1038/s41586-019-1032-7

Roth, A., Khattra, J., Yap, D., Wan, A., Laks, E., Biele, J., Ha, G., Aparicio, S., Bouchard-Côté, A., Shah, S.P., 2014. PyClone: statistical inference of clonal population structure in cancer. Nat Methods 11, 396–398. https://doi.org/10.1038/nmeth.2883

Rous, P., 1967. The challenge to man of the neoplastic cell. Science 157, 24–28. https://doi.org/10.1126/science.157.3784.24

Rousseaux, S., Debernardi, A., Jacquiau, B., Vitte, A.-L., Vesin, A., Nagy-Mignotte, H., Moro-Sibilot, D., Brichon, P.-Y., Lantuejoul, S., Hainaut, P., Laffaire, J., Reyniès, A. de, Beer, D.G., Timsit, J.-F., Brambilla, C., Brambilla, E., Khochbin, S., 2013. Ectopic Activation of Germline and Placental Genes Identifies Aggressive Metastasis-Prone Lung Cancers. Science Translational Medicine 5, 186ra66-186ra66. https://doi.org/10.1126/scitranslmed.3005723

Rueda, O.M., Sammut, S.-J., Seoane, J.A., Chin, S.-F., Caswell-Jin, J.L., Callari, M., Batra, R., Pereira, B., Bruna, A., Ali, H.R., Provenzano, E., Liu, B., Parisien, M., Gillett, C., McKinney, S., Green, A.R., Murphy, L., Purushotham, A., Ellis, I.O., Pharoah, P.D., Rueda, C., Aparicio, S., Caldas, C., Curtis, C., 2019. Dynamics of breast-cancer relapse reveal late-recurring ER-positive genomic subgroups. Nature 1. https://doi.org/10.1038/s41586-019-1007-8

Sacher, A.G., Gandhi, L., 2016. Biomarkers for the Clinical Use of PD-1/PD-L1 Inhibitors in Non–Small-Cell Lung Cancer: A Review. JAMA Oncol 2, 1217–1222. https://doi.org/10.1001/jamaoncol.2016.0639

Sack, L.M., Davoli, T., Li, M.Z., Li, Y., Xu, Q., Naxerova, K., Wooten, E.C., Bernardi, R.J., Martin, T.D., Chen, T., Leng, Y., Liang, A.C., Scorsone, K.A., Westbrook, T.F., Wong, K.-K., Elledge, S.J., 2018. Profound Tissue Specificity in Proliferation Control Underlies Cancer Drivers and Aneuploidy Patterns. Cell 173, 499-514.e23. https://doi.org/10.1016/j.cell.2018.02.037

Sakurada, A., Lara-Guerra, H., Liu, N., Shepherd, F.A., Tsao, M.-S., 2008. Tissue heterogeneity of EGFR mutation in lung adenocarcinoma. J Thorac Oncol 3, 527–529. https://doi.org/10.1097/JTO.0b013e318168be93

Salcedo, A., Tarabichi, M., Espiritu, S.M.G., Deshwar, A.G., David, M., Wilson, N.M., Dentro, S., Wintersinger, J.A., Liu, L.Y., Ko, M., Sivanandan, S., Zhang, H., Zhu, K., Yang, T.-H.O., Chilton, J.M., Buchanan, A., Lalansingh, C.M., P'ng, C., Anghel, C.V., Umar, I., Lo, B., Zou, W., Simpson, J.T., Stuart, J.M., Anastassiou, D., Guan, Y., Ewing, A.D., Ellrott, K., Wedge, D.C., Morris, Q., Loo, P.V., Boutros, P.C., 2020. A community effort to create standards for evaluating tumor subclonal reconstruction. Nat Biotechnol 38, 97–107. https://doi.org/10.1038/s41587-019-0364-z

Samstein, R.M., Lee, C.-H., Shoushtari, A.N., Hellmann, M.D., Shen, R., Janjigian, Y.Y., Barron, D.A., Zehir, A., Jordan, E.J., Omuro, A., Kaley, T.J., Kendall, S.M., Motzer, R.J., Hakimi, A.A., Voss, M.H., Russo, P., Rosenberg, J., Iyer, G., Bochner, B.H., Bajorin, D.F., Al-Ahmadie, H.A., Chaft, J.E., Rudin, C.M., Riely, G.J., Baxi, S., Ho, A.L., Wong, R.J., Pfister, D.G., Wolchok, J.D., Barker, C.A., Gutin, P.H., Brennan, C.W., Tabar, V., Mellinghoff, I.K., DeAngelis, L.M., Ariyan, C.E., Lee, N., Tap, W.D., Gounder, M.M., D'Angelo, S.P., Saltz, L., Stadler, Z.K., Scher, H.I., Baselga, J., Razavi, P., Klebanoff, C.A., Yaeger, R., Segal, N.H., Ku, G.Y., DeMatteo, R.P., Ladanyi, M., Rizvi, N.A., Berger, M.F., Riaz, N., Solit, D.B., Chan, T.A., Morris, L.G.T., 2019. Tumor mutational load predicts survival after immunotherapy across multiple cancer types. Nature Genetics 1. https://doi.org/10.1038/s41588-018-0312-8

Samuels, Y., Wang, Z., Bardelli, A., Silliman, N., Ptak, J., Szabo, S., Yan, H., Gazdar, A., Powell, S.M., Riggins, G.J., Willson, J.K.V., Markowitz, S., Kinzler, K.W., Vogelstein, B., Velculescu, V.E., 2004. High Frequency of Mutations of the PIK3CA Gene in Human Cancers. Science 304, 554–554. https://doi.org/10.1126/science.1096502

Sangha, R., Price, J., Butts, C.A., 2010. Adjuvant Therapy in Non-Small Cell Lung Cancer: Current and Future Directions. The Oncologist 15, 862–872. https://doi.org/10.1634/theoncologist.2009-0186

Sato, E., Olson, S.H., Ahn, J., Bundy, B., Nishikawa, H., Qian, F., Jungbluth, A.A., Frosina, D., Gnjatic, S., Ambrosone, C., Kepner, J., Odunsi, T., Ritter, G., Lele, S., Chen, Y.-T., Ohtani, H., Old, L.J., Odunsi, K., 2005. Intraepithelial CD8+ tumor-infiltrating lymphocytes and a high CD8+/regulatory T cell ratio are associated with favorable prognosis in ovarian cancer. PNAS 102, 18538–18543. https://doi.org/10.1073/pnas.0509182102

Savas, P., Virassamy, B., Ye, C., Salim, A., Mintoff, C.P., Caramia, F., Salgado, R., Byrne, D.J., Teo, Z.L., Dushyanthen, S., Byrne, A., Wein, L., Luen, S.J., Poliness, C., Nightingale, S.S., Skandarajah, A.S., Gyorki, D.E., Thornton, C.M., Beavis, P.A., Fox, S.B., Darcy, P.K., Speed, T.P., Mackay, L.K., Neeson, P.J., Loi, S., 2018. Single-cell profiling of breast cancer T cells reveals a tissue-resident memory subset associated with improved

prognosis. Nature Medicine 24, 986–993. https://doi.org/10.1038/s41591-018-0078-7

Sawyers, C.L., 2008. The cancer biomarker problem. Nature 452, 548–552. https://doi.org/10.1038/nature06913

Schafer, J.M., Lehmann, B.D., Gonzalez-Ericsson, P.I., Marshall, C.B., Beeler, J.S., Redman, L.N., Jin, H., Sanchez, V., Stubbs, M.C., Scherle, P., Johnson, K.N., Sheng, Q., Roland, J.T., Bauer, J.A., Shyr, Y., Chakravarthy, B., Mobley, B.C., Hiebert, S.W., Balko, J.M., Sanders, M.E., Liu, P.C.C., Pietenpol, J.A., 2020. Targeting MYCN-expressing triple-negative breast cancer with BET and MEK inhibitors. Science Translational Medicine 12. https://doi.org/10.1126/scitranslmed.aaw8275

Schreiber, R.D., Old, L.J., Smyth, M.J., 2011. Cancer immunoediting: integrating immunity's roles in cancer suppression and promotion. Science 331, 1565–1570. https://doi.org/10.1126/science.1203486

Schumacher, K., Haensch, W., Röefzaad, C., Schlag, P.M., 2001. Prognostic Significance of Activated CD8+ T Cell Infiltrations within Esophageal Carcinomas. Cancer Res 61, 3932–3936.

Schumacher, T.N., Hacohen, N., 2016. Neoantigens encoded in the cancer genome. Current Opinion in Immunology, Vaccines * Special section: Cancer immunology: Genomics & biomarkers 41, 98–103. https://doi.org/10.1016/j.coi.2016.07.005

Schumacher, T.N., Schreiber, R.D., 2015. Neoantigens in cancer immunotherapy. Science 348, 69–74. https://doi.org/10.1126/science.aaa4971

Sensi, M., Nicolini, G., Petti, C., Bersani, I., Lozupone, F., Molla, A., Vegetti, C., Nonaka, D., Mortarini, R., Parmiani, G., Fais, S., Anichini, A., 2006. Mutually exclusive NRAS Q61R and BRAF V600E mutations at the single-cell level in the same human melanoma. Oncogene 25, 3357–3364. https://doi.org/10.1038/sj.onc.1209379

Sethi, T., Rintoul, R.C., Moore, S.M., MacKinnon, A.C., Salter, D., Choo, C., Chilvers, E.R., Dransfield, I., Donnelly, S.C., Strieter, R., Haslett, C., 1999. Extracellular matrix proteins protect small cell lung cancer cells against apoptosis: A mechanism for small cell lung cancer growth and drug resistance in vivo. Nature Medicine 5, 662–668. https://doi.org/10.1038/9511

Shah, S.P., Roth, A., Goya, R., Oloumi, A., Ha, G., Zhao, Y., Turashvili, G., Ding, J., Tse, K., Haffari, G., Bashashati, A., Prentice, L.M., Khattra, J., Burleigh, A., Yap, D., Bernard, V., McPherson, A., Shumansky, K., Crisan, A., Giuliany, R., Heravi-Moussavi, A., Rosner, J., Lai, D., Birol, I., Varhol, R., Tam, A., Dhalla, N., Zeng, T., Ma, K., Chan, S.K., Griffith, M., Moradian, A., Cheng, S.-W.G., Morin, G.B., Watson, P., Gelmon, K., Chia, S., Chin, S.-F., Curtis, C., Rueda, O.M., Pharoah, P.D., Damaraju, S., Mackey, J., Hoon, K., Harkins, T., Tadigotla, V., Sigaroudinia, M., Gascard, P., Tlsty, T., Costello, J.F., Meyer, I.M., Eaves, C.J., Wasserman, W.W., Jones, S., Huntsman, D., Hirst, M., Caldas, C., Marra, M.A., Aparicio, S., 2012. The clonal and mutational evolution spectrum of primary triple-negative breast cancers. Nature 486, 395–399. https://doi.org/10.1038/nature10933

Shankaran, V., Ikeda, H., Bruce, A.T., White, J.M., Swanson, P.E., Old, L.J., Schreiber, R.D., 2001. IFNgamma and lymphocytes prevent primary tumour development and shape tumour immunogenicity. Nature 410, 1107–1111. https://doi.org/10.1038/35074122

Sharma, P., Hu-Lieskovan, S., Wargo, J.A., Ribas, A., 2017. Primary, Adaptive, and Acquired Resistance to Cancer Immunotherapy. Cell 168, 707–723. https://doi.org/10.1016/j.cell.2017.01.017

Shedden, K., Taylor, J.M.G., Enkemann, S.A., Tsao, M.-S., Yeatman, T.J., Gerald, W.L., Eschrich, S., Jurisica, I., Giordano, T.J., Misek, D.E., Chang, A.C., Zhu, C.Q., Strumpf, D., Hanash, S., Shepherd, F.A., Ding, K., Seymour, L., Naoki, K., Pennell, N., Weir, B., Verhaak, R., Ladd-Acosta, C., Golub, T., Gruidl, M., Sharma, A., Szoke, J., Zakowski, M., Rusch, V., Kris, M., Viale, A., Motoi, N., Travis, W., Conley, B., Seshan, V.E., Meyerson, M., Kuick, R., Dobbin, K.K., Lively, T., Jacobson, J.W., Beer, D.G., 2008. Gene expression–based survival prediction in lung adenocarcinoma: a multi-site, blinded validation study. Nat Med 14, 822–827. https://doi.org/10.1038/nm.1790

Shen-Orr, S.S., Gaujoux, R., 2013. Computational deconvolution: extracting cell type-specific information from heterogeneous samples. Current Opinion in Immunology, Special section: Systems biology and bioinformatics / Immunogenetics and transplantation 25, 571–578. https://doi.org/10.1016/j.coi.2013.09.015

Sherman-Baust, C.A., Weeraratna, A.T., Rangel, L.B.A., Pizer, E.S., Cho, K.R., Schwartz, D.R., Shock, T., Morin, P.J., 2003. Remodeling of the extracellular matrix through overexpression of collagen VI contributes to cisplatin resistance in ovarian cancer cells. Cancer Cell 3, 377–386. https://doi.org/10.1016/S1535-6108(03)00058-8

Shukla, S., Evans, J.R., Malik, R., Feng, F.Y., Dhanasekaran, S.M., Cao, X., Chen, G., Beer, D.G., Jiang, H., Chinnaiyan, A.M., 2017. Development of a RNA-Seq Based Prognostic Signature in Lung Adenocarcinoma. J Natl Cancer Inst 109. https://doi.org/10.1093/jnci/djw200

Sidow, A., Spies, N., 2015. Concepts in solid tumor evolution. Trends in Genetics 31, 208–214. https://doi.org/10.1016/j.tig.2015.02.001

Siegel, R.L., Miller, K.D., Jemal, A., 2019. Cancer statistics, 2019. CA: A Cancer Journal for Clinicians 69, 7–34. https://doi.org/10.3322/caac.21551

Sinha, A., Huang, V., Livingstone, J., Wang, J., Fox, N.S., Kurganovs, N., Ignatchenko, V., Fritsch, K., Donmez, N., Heisler, L.E., Shiah, Y.-J., Yao, C.Q., Alfaro, J.A., Volik, S., Lapuk, A., Fraser, M., Kron, K., Murison, A., Lupien, M., Sahinalp, C., Collins, C.C., Tetu, B., Masoomian, M., Berman, D.M., Kwast, T. van der, Bristow, R.G., Kislinger, T., Boutros, P.C., 2019. The Proteogenomic Landscape of Curable Prostate Cancer. Cancer Cell 35, 414-427.e6. https://doi.org/10.1016/j.ccell.2019.02.005

Sjöblom, T., Jones, S., Wood, L.D., Parsons, D.W., Lin, J., Barber, T.D., Mandelker, D., Leary, R.J., Ptak, J., Silliman, N., Szabo, S., Buckhaults, P., Farrell, C., Meeh, P., Markowitz, S.D., Willis, J., Dawson, D., Willson, J.K.V., Gazdar, A.F., Hartigan, J., Wu, L., Liu, C., Parmigiani, G., Park, B.H., Bachman, K.E., Papadopoulos, N., Vogelstein, B., Kinzler, K.W., Velculescu, V.E., 2006. The Consensus Coding Sequences of Human Breast and Colorectal Cancers. Science 314, 268–274. https://doi.org/10.1126/science.1133427

Slamon, D.J., Leyland-Jones, B., Shak, S., Fuchs, H., Paton, V., Bajamonde, A., Fleming, T., Eiermann, W., Wolter, J., Pegram, M., Baselga, J., Norton, L., 2009. Use of Chemotherapy plus a Monoclonal Antibody against HER2 for

Metastatic Breast Cancer That Overexpresses HER2. The New England Journal of Medicine. https://doi.org/10.1056/NEJM200103153441101

Smith, M.P., Sanchez-Laorden, B., O'Brien, K., Brunton, H., Ferguson, J., Young, H., Dhomen, N., Flaherty, K.T., Frederick, D.T., Cooper, Z.A., Wargo, J.A., Marais, R., Wellbrock, C., 2014. The Immune Microenvironment Confers Resistance to MAPK Pathway Inhibitors through Macrophage-Derived TNFα. Cancer Discov 4, 1214–1229. https://doi.org/10.1158/2159-8290.CD-13-1007

Smyth, M.J., Ngiow, S.F., Ribas, A., Teng, M.W.L., 2016. Combination cancer immunotherapies tailored to the tumour microenvironment. Nat Rev Clin Oncol 13, 143–158. https://doi.org/10.1038/nrclinonc.2015.209

Snyder, A., Makarov, V., Merghoub, T., Yuan, J., Zaretsky, J.M., Desrichard, A., Walsh, L.A., Postow, M.A., Wong, P., Ho, T.S., Hollmann, T.J., Bruggeman, C., Kannan, K., Li, Y., Elipenahli, C., Liu, C., Harbison, C.T., Wang, L., Ribas, A., Wolchok, J.D., Chan, T.A., 2014. Genetic Basis for Clinical Response to CTLA-4 Blockade in Melanoma. New England Journal of Medicine 371, 2189–2199. https://doi.org/10.1056/NEJMoa1406498

Sottoriva, A., Kang, H., Ma, Z., Graham, T.A., Salomon, M.P., Zhao, J., Marjoram, P., Siegmund, K., Press, M.F., Shibata, D., Curtis, C., 2015. A Big Bang model of human colorectal tumor growth. Nat. Genet. 47, 209–216. https://doi.org/10.1038/ng.3214

Sparano, J.A., Gray, R.J., Makower, D.F., Pritchard, K.I., Albain, K.S., Hayes, D.F., Geyer, C.E., Dees, E.C., Goetz, M.P., Olson, J.A., Lively, T., Badve, S.S., Saphner, T.J., Wagner, L.I., Whelan, T.J., Ellis, M.J., Paik, S., Wood, W.C., Ravdin, P.M., Keane, M.M., Gomez Moreno, H.L., Reddy, P.S., Goggins, T.F., Mayer, I.A., Brufsky, A.M., Toppmeyer, D.L., Kaklamani, V.G., Berenberg, J.L., Abrams, J., Sledge, G.W., 2018. Adjuvant Chemotherapy Guided by a 21-Gene Expression Assay in Breast Cancer. New England Journal of Medicine 0, null. https://doi.org/10.1056/NEJMoa1804710

Sparks, A.B., Morin, P.J., Vogelstein, B., Kinzler, K.W., 1998. Mutational analysis of the APC/beta-catenin/Tcf pathway in colorectal cancer. Cancer Res. 58, 1130–1134.

Ståhl, P.L., Salmén, F., Vickovic, S., Lundmark, A., Navarro, J.F., Magnusson, J., Giacomello, S., Asp, M., Westholm, J.O., Huss, M., Mollbrink, A., Linnarsson, S., Codeluppi, S., Borg, Å., Pontén, F., Costea, P.I., Sahlén, P., Mulder, J., Bergmann, O., Lundeberg, J., Frisén, J., 2016. Visualization and analysis of gene expression in tissue sections by spatial transcriptomics. Science 353, 78–82. https://doi.org/10.1126/science.aaf2403

Stratton, M.R., Campbell, P.J., Futreal, P.A., 2009. The cancer genome. Nature 458, 719–724. https://doi.org/10.1038/nature07943

Strauss, G.M., Herndon, J.E., Maddaus, M.A., Johnstone, D.W., Johnson, E.A., Harpole, D.H., Gillenwater, H.H., Watson, D.M., Sugarbaker, D.J., Schilsky, R.L., Vokes, E.E., Green, M.R., 2008. Adjuvant Paclitaxel Plus Carboplatin Compared With Observation in Stage IB Non–Small-Cell Lung Cancer: CALGB 9633 With the Cancer and Leukemia Group B, Radiation Therapy Oncology Group, and North Central Cancer Treatment Group Study Groups. JCO 26, 5043–5051. https://doi.org/10.1200/JCO.2008.16.4855

Straussman, R., Morikawa, T., Shee, K., Barzily-Rokni, M., Qian, Z.R., Du, J., Davis, A., Mongare, M.M., Gould, J., Frederick, D.T., Cooper, Z.A., Chapman, P.B., Solit, D.B., Ribas, A., Lo, R.S., Flaherty, K.T., Ogino, S.,

Wargo, J.A., Golub, T.R., 2012. Tumour micro-environment elicits innate resistance to RAF inhibitors through HGF secretion. Nature 487, 500–504. https://doi.org/10.1038/nature11183

Sturm, G., Finotello, F., Petitprez, F., Zhang, J.D., Baumbach, J., Fridman, W.H., List, M., Aneichyk, T., 2019. Comprehensive evaluation of transcriptome-based cell-type quantification methods for immuno-oncology. Bioinformatics 35, i436–i445. https://doi.org/10.1093/bioinformatics/btz363

Subramanian, A., Tamayo, P., Mootha, V.K., Mukherjee, S., Ebert, B.L., Gillette, M.A., Paulovich, A., Pomeroy, S.L., Golub, T.R., Lander, E.S., Mesirov, J.P., 2005. Gene set enrichment analysis: A knowledge-based approach for interpreting genome-wide expression profiles. PNAS 102, 15545–15550. https://doi.org/10.1073/pnas.0506580102

Subramanian, J., Simon, R., 2010a. Gene Expression–Based Prognostic Signatures in Lung Cancer: Ready for Clinical Use? J Natl Cancer Inst 102, 464–474. https://doi.org/10.1093/jnci/djq025

Subramanian, J., Simon, R., 2010b. What should physicians look for in evaluating prognostic gene-expression signatures? Nat Rev Clin Oncol 7, 327–334. https://doi.org/10.1038/nrclinonc.2010.60

Suda, K., 2020. Personalized post-surgical care?—possible strategies for NSCLCs with EGFR mutation. Transl Lung Cancer Res 9, 441–445. https://doi.org/10.21037/tlcr.2020.03.32

Suda, K., Kim, J., Murakami, I., Rozeboom, L., Shimoji, M., Shimizu, S., Rivard, C.J., Mitsudomi, T., Tan, A.-C., Hirsch, F.R., 2018. Innate Genetic Evolution of Lung Cancers and Spatial Heterogeneity: Analysis of Treatment-Naïve Lesions. Journal of Thoracic Oncology 0. https://doi.org/10.1016/j.jtho.2018.05.039

Suda, K., Mitsudomi, T., 2020. Inter-tumor heterogeneity of PD-L1 status: is it important in clinical decision making? J Thorac Dis 12, 1770–1775. https://doi.org/10.21037/jtd-20-1661

Sun, Y., Campisi, J., Higano, C., Beer, T.M., Porter, P., Coleman, I., True, L., Nelson, P.S., 2012. Treatment-induced damage to the tumor microenvironment promotes prostate cancer therapy resistance through WNT16B. Nat Med 18, 1359–1368. https://doi.org/10.1038/nm.2890

Sun, Z., Wigle, D.A., Yang, P., 2008. Non-Overlapping and Non–Cell-Type–Specific Gene Expression Signatures Predict Lung Cancer Survival. JCO 26, 877–883. https://doi.org/10.1200/JCO.2007.13.1516

Svensson, V., Teichmann, S.A., Stegle, O., 2018. SpatialDE: identification of spatially variable genes. Nature Methods. https://doi.org/10.1038/nmeth.4636

Swanton, C., 2012. Intratumor Heterogeneity: Evolution through Space and Time. Cancer Res 72, 4875–4882. https://doi.org/10.1158/0008-5472.CAN-12-2217

Szczurek, E., Beerenwinkel, N., 2014. Modeling Mutual Exclusivity of Cancer Mutations. PLOS Computational Biology 10, e1003503. https://doi.org/10.1371/journal.pcbi.1003503

Tabin, C.J., Bradley, S.M., Bargmann, C.I., Weinberg, R.A., Papageorge, A.G., Scolnick, E.M., Dhar, R., Lowy, D.R., Chang, E.H., 1982. Mechanism of activation of a human oncogene. Nature 300, 143–149. https://doi.org/10.1038/300143a0

Takeuchi, T., Tomida, S., Yatabe, Y., Kosaka, T., Osada, H., Yanagisawa, K., Mitsudomi, T., Takahashi, T., 2006. Expression Profile–Defined Classification of Lung Adenocarcinoma Shows Close Relationship With Underlying Major Genetic Changes and Clinicopathologic Behaviors. JCO 24, 1679–1688. https://doi.org/10.1200/JCO.2005.03.8224

Tang, H., Wang, S., Xiao, G., Schiller, J., Papadimitrakopoulou, V., Minna, J., Wistuba, I.I., Xie, Y., 2017. Comprehensive evaluation of published gene expression prognostic signatures for biomarker-based lung cancer clinical studies. Ann Oncol 28, 733–740. https://doi.org/10.1093/annonc/mdw683

Tang, H., Xiao, G., Behrens, C., Schiller, J., Allen, J., Chow, C.-W., Suraokar, M., Corvalan, A., Mao, J., White, M.A., Wistuba, I.I., Minna, J.D., Xie, Y., 2013. A 12-Gene Set Predicts Survival Benefits from Adjuvant Chemotherapy in Non–Small Cell Lung Cancer Patients. Clin Cancer Res 19, 1577–1586. https://doi.org/10.1158/1078-0432.CCR-12-2321

Tannock, I.F., Hickman, J.A., 2016. Limits to Personalized Cancer Medicine. New England Journal of Medicine 375, 1289–1294. https://doi.org/10.1056/NEJMsb1607705

Taube, J.M., Anders, R.A., Young, G.D., Xu, H., Sharma, R., McMiller, T.L., Chen, S., Klein, A.P., Pardoll, D.M., Topalian, S.L., Chen, L., 2012. Colocalization of inflammatory response with B7-h1 expression in human melanocytic lesions supports an adaptive resistance mechanism of immune escape. Sci Transl Med 4, 127ra37. https://doi.org/10.1126/scitranslmed.3003689

Teng, M.W.L., Ngiow, S.F., Ribas, A., Smyth, M.J., 2015. Classifying Cancers Based on T-cell Infiltration and PD-L1. Cancer Res 75, 2139–2145. https://doi.org/10.1158/0008-5472.CAN-15-0255

The Cancer Genome Atlas Network, 2012. Comprehensive molecular characterization of human colon and rectal cancer. Nature 487, 330–337. https://doi.org/10.1038/nature11252

The Cancer Genome Atlas Research Network, 2017. Integrated genomic characterization of oesophageal carcinoma. Nature 541, 169–175. https://doi.org/10.1038/nature20805

The Cancer Genome Atlas Research Network, 2014. Comprehensive molecular profiling of lung adenocarcinoma. Nature 511, 543–550. https://doi.org/10.1038/nature13385

The Cancer Genome Atlas Research Network, 2012. Comprehensive genomic characterization of squamous cell lung cancers. Nature 489, 519–525. https://doi.org/10.1038/nature11404

The Cancer Genome Atlas Research Network, 2011. Integrated genomic analyses of ovarian carcinoma. Nature 474, 609–615. https://doi.org/10.1038/nature10166

The ICGC/TCGA Pan-Cancer Analysis of Whole Genomes Consortium, 2020. Pan-cancer analysis of whole genomes. Nature 578, 82–93. https://doi.org/10.1038/s41586-020-1969-6

The International Cancer Genome Consortium, 2010. International network of cancer genome projects. Nature 464, 993–998. https://doi.org/10.1038/nature08987

Thomas, L., 1982. On immunosurveillance in human cancer. Yale J Biol Med 55, 329–333.

Thommen, D.S., Koelzer, V.H., Herzig, P., Roller, A., Trefny, M., Dimeloe, S., Kiialainen, A., Hanhart, J., Schill, C., Hess, C., Prince, S.S., Wiese, M.,

Lardinois, D., Ho, P.-C., Klein, C., Karanikas, V., Mertz, K.D., Schumacher, T.N., Zippelius, A., 2018. A transcriptionally and functionally distinct PD-1 + CD8 + T cell pool with predictive potential in non-small-cell lung cancer treated with PD-1 blockade. Nature Medicine 1. https://doi.org/10.1038/s41591-018-0057-z

Tirosh, I., Izar, B., Prakadan, S.M., Wadsworth, M.H., Treacy, D., Trombetta, J.J., Rotem, A., Rodman, C., Lian, C., Murphy, G., Fallahi-Sichani, M., Dutton-Regester, K., Lin, J.-R., Cohen, O., Shah, P., Lu, D., Genshaft, A.S., Hughes, T.K., Ziegler, C.G.K., Kazer, S.W., Gaillard, A., Kolb, K.E., Villani, A.-C., Johannessen, C.M., Andreev, A.Y., Van Allen, E.M., Bertagnolli, M., Sorger, P.K., Sullivan, R.J., Flaherty, K.T., Frederick, D.T., Jané-Valbuena, J., Yoon, C.H., Rozenblatt-Rosen, O., Shalek, A.K., Regev, A., Garraway, L.A., 2016. Dissecting the multicellular ecosystem of metastatic melanoma by single-cell RNA-seq. Science 352, 189–196. https://doi.org/10.1126/science.aad0501

Tofigh, A., Suderman, M., Paquet, E.R., Livingstone, J., Bertos, N., Saleh, S.M., Zhao, H., Souleimanova, M., Cory, S., Lesurf, R., Shahalizadeh, S., Garcia Lopez, N., Riazalhosseini, Y., Omeroglu, A., Ursini-Siegel, J., Park, M., Dumeaux, V., Hallett, M., 2014. The Prognostic Ease and Difficulty of Invasive Breast Carcinoma. Cell Reports 9, 129–142. https://doi.org/10.1016/j.celrep.2014.08.073

Tonon, G., Wong, K.-K., Maulik, G., Brennan, C., Feng, B., Zhang, Y., Khatry, D.B., Protopopov, A., You, M.J., Aguirre, A.J., Martin, E.S., Yang, Z., Ji, H., Chin, L., DePinho, R.A., 2005. High-resolution genomic profiles of human lung cancer. PNAS 102, 9625–9630. https://doi.org/10.1073/pnas.0504126102

Topalian, S.L., Hodi, F.S., Brahmer, J.R., Gettinger, S.N., Smith, D.C., McDermott, D.F., Powderly, J.D., Carvajal, R.D., Sosman, J.A., Atkins, M.B., Leming, P.D., Spigel, D.R., Antonia, S.J., Horn, L., Drake, C.G., Pardoll, D.M., Chen, L., Sharfman, W.H., Anders, R.A., Taube, J.M., McMiller, T.L., Xu, H., Korman, A.J., Jure-Kunkel, M., Agrawal, S., McDonald, D., Kollia, G.D., Gupta, A., Wigginton, J.M., Sznol, M., 2012. Safety, Activity, and Immune Correlates of Anti–PD-1 Antibody in Cancer. New England Journal of Medicine 366, 2443–2454. https://doi.org/10.1056/NEJMoa1200690

Topalian, S.L., Hom, S.S., Kawakami, Y., Mancini, M., Schwartzentruber, D.J., Zakut, R., Rosenberg, S.A., 1992. Recognition of shared melanoma antigens by human tumor-infiltrating lymphocytes. J. Immunother. 12, 203–206.

Topalian, S.L., Taube, J.M., Anders, R.A., Pardoll, D.M., 2016. Mechanism-driven biomarkers to guide immune checkpoint blockade in cancer therapy. Nature Reviews Cancer 16, 275. https://doi.org/10.1038/nrc.2016.36

Torre-Amione, G., Beauchamp, R.D., Koeppen, H., Park, B.H., Schreiber, H., Moses, H.L., Rowley, D.A., 1990. A highly immunogenic tumor transfected with a murine transforming growth factor type beta 1 cDNA escapes immune surveillance. PNAS 87, 1486–1490. https://doi.org/10.1073/pnas.87.4.1486

Turajlic, S., Xu, H., Litchfield, K., Rowan, A., Horswell, S., Chambers, T., O'Brien, T., Lopez, J.I., Watkins, T.B.K., Nicol, D., Stares, M., Challacombe, B., Hazell, S., Chandra, A., Mitchell, T.J., Au, L., Eichler-Jonsson, C., Jabbar, F., Soultati, A., Chowdhury, S., Rudman, S., Lynch, J., Fernando, A., Stamp, G., Nye, E., Stewart, A., Xing, W., Smith, J.C., Escudero, M., Huffman, A., Matthews, N., Elgar, G., Phillimore, B., Costa, M., Begum, S.,

Ward, S., Salm, M., Boeing, S., Fisher, R., Spain, L., Navas, C., Grönroos, E., Hobor, S., Sharma, S., Aurangzeb, I., Lall, S., Polson, A., Varia, M., Horsfield, C., Fotiadis, N., Pickering, L., Schwarz, R.F., Silva, B., Herrero, J., Luscombe, N.M., Jamal-Hanjani, M., Rosenthal, R., Birkbak, N.J., Wilson, G.A., Pipek, O., Ribli, D., Krzystanek, M., Csabai, I., Szallasi, Z., Gore, M., McGranahan, N., Loo, P.V., Campbell, P., Larkin, J., Swanton, C., 2018. Deterministic Evolutionary Trajectories Influence Primary Tumor Growth: TRACERx Renal. Cell 173, 595-610.e11. https://doi.org/10.1016/j.cell.2018.03.043

Turke, A.B., Zejnullahu, K., Wu, Y.-L., Song, Y., Dias-Santagata, D., Lifshits, E., Toschi, L., Rogers, A., Mok, T., Sequist, L., Lindeman, N.I., Murphy, C., Akhavanfard, S., Yeap, B.Y., Xiao, Y., Capelletti, M., Iafrate, A.J., Lee, C., Christensen, J.G., Engelman, J.A., Jänne, P.A., 2010. Preexistence and Clonal Selection of MET Amplification in EGFR Mutant NSCLC. Cancer Cell 17, 77–88. https://doi.org/10.1016/j.ccr.2009.11.022

Tutt, A., Robson, M., Garber, J.E., Domchek, S.M., Audeh, M.W., Weitzel, J.N., Friedlander, M., Arun, B., Loman, N., Schmutzler, R.K., Wardley, A., Mitchell, G., Earl, H., Wickens, M., Carmichael, J., 2010. Oral poly(ADP-ribose) polymerase inhibitor olaparib in patients with BRCA1 or BRCA2 mutations and advanced breast cancer: a proof-of-concept trial. Lancet 376, 235–244. https://doi.org/10.1016/S0140-6736(10)60892-6

Uhlen, M., Karlsson, M.J., Zhong, W., Tebani, A., Pou, C., Mikes, J., Lakshmikanth, T., Forsström, B., Edfors, F., Odeberg, J., Mardinoglu, A., Zhang, C., Feilitzen, K. von, Mulder, J., Sjöstedt, E., Hober, A., Oksvold, P., Zwahlen, M., Ponten, F., Lindskog, C., Sivertsson, Å., Fagerberg, L., Brodin, P., 2019. A genome-wide transcriptomic analysis of protein-coding genes in human blood cells. Science 366. https://doi.org/10.1126/science.aax9198

Uhlen, M., Zhang, C., Lee, S., Sjöstedt, E., Fagerberg, L., Bidkhori, G., Benfeitas, R., Arif, M., Liu, Z., Edfors, F., Sanli, K., Feilitzen, K. von, Oksvold, P., Lundberg, E., Hober, S., Nilsson, P., Mattsson, J., Schwenk, J.M., Brunnström, H., Glimelius, B., Sjöblom, T., Edqvist, P.-H., Djureinovic, D., Micke, P., Lindskog, C., Mardinoglu, A., Ponten, F., 2017. A pathology atlas of the human cancer transcriptome. Science 357, eaan2507. https://doi.org/10.1126/science.aan2507

van der Bruggen, P., Traversari, C., Chomez, P., Lurquin, C., Plaen, E.D., Eynde, B.V. den, Knuth, A., Boon, T., 1991. A gene encoding an antigen recognized by cytolytic T lymphocytes on a human melanoma. Science 254, 1643–1647. https://doi.org/10.1126/science.1840703

van ’t Veer, L.J., Dai, H., Vijver, M.J. van de, He, Y.D., Hart, A.A.M., Mao, M., Peterse, H.L., Kooy, K. van der, Marton, M.J., Witteveen, A.T., Schreiber, G.J., Kerkhoven, R.M., Roberts, C., Linsley, P.S., Bernards, R., Friend, S.H., 2002. Gene expression profiling predicts clinical outcome of breast cancer. Nature 415, 530. https://doi.org/10.1038/415530a

Vandin, F., Upfal, E., Raphael, B.J., 2012. De novo discovery of mutated driver pathways in cancer. Genome Res. 22, 375–385. https://doi.org/10.1101/gr.120477.111

van’t Veer, L.J., Bernards, R., 2008. Enabling personalized cancer medicine through analysis of gene-expression patterns. Nature 452, 564–570. https://doi.org/10.1038/nature06915

Varela, I., Tarpey, P., Raine, K., Huang, D., Ong, C.K., Stephens, P., Davies, H., Jones, D., Lin, M.-L., Teague, J., Bignell, G., Butler, A., Cho, J., Dalgliesh, G.L., Galappaththige, D., Greenman, C., Hardy, C., Jia, M., Latimer, C., Lau, K.W., Marshall, J., McLaren, S., Menzies, A., Mudie, L., Stebbings, L., Largaespada, D.A., Wessels, L.F.A., Richard, S., Kahnoski, R.J., Anema, J., A.Tuveson, D., Perez-Mancera, P.A., Mustonen, V., Fischer, A., Adams, D.J., Rust, A., Chan-on, W., Subimerb, C., Dykema, K., Furge, K., Campbell, P.J., Teh, B.T., Stratton, M.R., Futreal, P.A., 2011. Exome sequencing identifies frequent mutation of the SWI/SNF complex gene PBRM1 in renal carcinoma. Nature 469, 539–542. https://doi.org/10.1038/nature09639

Vargas, A.J., Harris, C.C., 2016. Biomarker development in the precision medicine era: lung cancer as a case study. Nat Rev Cancer 16, 525–537. https://doi.org/10.1038/nrc.2016.56

Vasaikar, S., Huang, C., Wang, X., Petyuk, V.A., Savage, S.R., Wen, B., Dou, Y., Zhang, Y., Shi, Z., Arshad, O.A., Gritsenko, M.A., Zimmerman, L.J., McDermott, J.E., Clauss, T.R., Moore, R.J., Zhao, R., Monroe, M.E., Wang, Y.-T., Chambers, M.C., Slebos, Robbert J. C., Lau, K.S., Mo, Q., Ding, L., Ellis, M., Thiagarajan, M., Kinsinger, C.R., Rodriguez, H., Smith, R.D., Rodland, K.D., Liebler, D.C., Liu, T., Zhang, B., Ellis, M.J.C., Shi, Z., Zhang, B., Bavarva, J., Borucki, M., Elburn, K., Hannick, L., Thiagarajan, M., Vatanian, N., Payne, S.H., Carr, S.A., Clauser, K.R., Gillette, M.A., Kuhn, E., Mani, D.R., Cai, S., Ketchum, K.A., Thangudu, R.R., Whiteley, G.A., Paulovich, A., Whiteaker, J., Edward, N.J., Madhavan, S., McGarvey, P.B., Chan, D.W., Shih, I.-M., Zhang, H., Zhang, Z., Zhu, H., Skates, S.J., White, F.M., Mertins, P., Pandey, A., Slebos, Robert J. C., Boja, E., Hiltke, T., Kinsinger, C.R., Mesri, M., Rivers, R.C., Rodriguez, H., Stein, S.E., Fenyo, D., Ruggles, K., Levine, D.A., Oberti, M., Liu, T., McDermott, J.E., Rodland, K.D., Smith, R.D., Zimmerman, L.J., Rudnick, P.A., Snyder, M., Tabb, D.L., Zhao, Y., Chen, X., Ransohoff, D.F., Hoofnagle, A., Liebler, D.C., Sanders, M.E., Wang, Y., Davies, S.R., Ding, L., Townsend, R.R., Watson, M., 2019. Proteogenomic Analysis of Human Colon Cancer Reveals New Therapeutic Opportunities. Cell 0. https://doi.org/10.1016/j.cell.2019.03.030

Venet, D., Dumont, J.E., Detours, V., 2011. Most Random Gene Expression Signatures Are Significantly Associated with Breast Cancer Outcome. PLOS Computational Biology 7, e1002240. https://doi.org/10.1371/journal.pcbi.1002240

Venter, J.C., Adams, M.D., Myers, E.W., Li, P.W., Mural, R.J., Sutton, G.G., Smith, H.O., Yandell, M., Evans, C.A., Holt, R.A., Gocayne, J.D., Amanatides, P., Ballew, R.M., Huson, D.H., Wortman, J.R., Zhang, Q., Kodira, C.D., Zheng, X.H., Chen, L., Skupski, M., Subramanian, G., Thomas, P.D., Zhang, J., Miklos, G.L.G., Nelson, C., Broder, S., Clark, A.G., Nadeau, J., McKusick, V.A., Zinder, N., Levine, A.J., Roberts, R.J., Simon, M., Slayman, C., Hunkapiller, M., Bolanos, R., Delcher, A., Dew, I., Fasulo, D., Flanigan, M., Florea, L., Halpern, A., Hannenhalli, S., Kravitz, S., Levy, S., Mobarry, C., Reinert, K., Remington, K., Abu-Threideh, J., Beasley, E., Biddick, K., Bonazzi, V., Brandon, R., Cargill, M., Chandramouliswaran, I., Charlab, R., Chaturvedi, K., Deng, Z., Francesco, V.D., Dunn, P., Eilbeck, K., Evangelista, C., Gabrielian, A.E., Gan, W., Ge, W., Gong, F., Gu, Z., Guan, P., Heiman, T.J., Higgins, M.E., Ji, R.-R., Ke, Z., Ketchum, K.A., Lai, Z., Lei,

Y., Li, Z., Li, J., Liang, Y., Lin, X., Lu, F., Merkulov, G.V., Milshina, N., Moore, H.M., Naik, A.K., Narayan, V.A., Neelam, B., Nusskern, D., Rusch, D.B., Salzberg, S., Shao, W., Shue, B., Sun, J., Wang, Z.Y., Wang, A., Wang, X., Wang, J., Wei, M.-H., Wides, R., Xiao, C., Yan, C., Yao, A., Ye, J., Zhan, M., Zhang, W., Zhang, H., Zhao, Q., Zheng, L., Zhong, F., Zhong, W., Zhu, S.C., Zhao, S., Gilbert, D., Baumhueter, S., Spier, G., Carter, C., Cravchik, A., Woodage, T., Ali, F., An, H., Awe, A., Baldwin, D., Baden, H., Barnstead, M., Barrow, I., Beeson, K., Busam, D., Carver, A., Center, A., Cheng, M.L., Curry, L., Danaher, S., Davenport, L., Desilets, R., Dietz, S., Dodson, K., Doup, L., Ferriera, S., Garg, N., Gluecksmann, A., Hart, B., Haynes, J., Haynes, C., Heiner, C., Hladun, S., Hostin, D., Houck, J., Howland, T., Ibegwam, C., Johnson, J., Kalush, F., Kline, L., Koduru, S., Love, A., Mann, F., May, D., McCawley, S., McIntosh, T., McMullen, I., Moy, M., Moy, L., Murphy, B., Nelson, K., Pfannkoch, C., Pratts, E., Puri, V., Qureshi, H., Reardon, M., Rodriguez, R., Rogers, Y.-H., Romblad, D., Ruhfel, B., Scott, R., Sitter, C., Smallwood, M., Stewart, E., Strong, R., Suh, E., Thomas, R., Tint, N.N., Tse, S., Vech, C., Wang, G., Wetter, J., Williams, S., Williams, M., Windsor, S., Winn-Deen, E., Wolfe, K., Zaveri, J., Zaveri, K., Abril, J.F., Guigó, R., Campbell, M.J., Sjolander, K.V., Karlak, B., Kejariwal, A., Mi, H., Lazareva, B., Hatton, T., Narechania, A., Diemer, K., Muruganujan, A., Guo, N., Sato, S., Bafna, V., Istrail, S., Lippert, R., Schwartz, R., Walenz, B., Yooseph, S., Allen, D., Basu, A., Baxendale, J., Blick, L., Caminha, M., Carnes-Stine, J., Caulk, P., Chiang, Y.-H., Coyne, M., Dahlke, C., Mays, A.D., Dombroski, M., Donnelly, M., Ely, D., Esparham, S., Fosler, C., Gire, H., Glanowski, S., Glasser, K., Glodek, A., Gorokhov, M., Graham, K., Gropman, B., Harris, M., Heil, J., Henderson, S., Hoover, J., Jennings, D., Jordan, C., Jordan, J., Kasha, J., Kagan, L., Kraft, C., Levitsky, A., Lewis, M., Liu, X., Lopez, J., Ma, D., Majoros, W., McDaniel, J., Murphy, S., Newman, M., Nguyen, T., Nguyen, N., Nodell, M., Pan, S., Peck, J., Peterson, M., Rowe, W., Sanders, R., Scott, J., Simpson, M., Smith, T., Sprague, A., Stockwell, T., Turner, R., Venter, E., Wang, M., Wen, M., Wu, D., Wu, M., Xia, A., Zandieh, A., Zhu, X., 2001. The Sequence of the Human Genome. Science 291, 1304–1351. https://doi.org/10.1126/science.1058040

Verdegaal, E.M.E., de Miranda, N.F.C.C., Visser, M., Harryvan, T., van Buuren, M.M., Andersen, R.S., Hadrup, S.R., van der Minne, C.E., Schotte, R., Spits, H., Haanen, J.B.A.G., Kapiteijn, E.H.W., Schumacher, T.N., van der Burg, S.H., 2016. Neoantigen landscape dynamics during human melanoma-T cell interactions. Nature 536, 91–95. https://doi.org/10.1038/nature18945

Vogelstein, B., Fearon, E.R., Hamilton, S.R., Kern, S.E., Preisinger, A.C., Leppert, M., Smits, A.M.M., Bos, J.L., 1988. Genetic Alterations during Colorectal-Tumor Development. New England Journal of Medicine 319, 525–532. https://doi.org/10.1056/NEJM198809013190901

Vogelstein, B., Kinzler, K.W., 2004. Cancer genes and the pathways they control. Nat Med 10, 789–799. https://doi.org/10.1038/nm1087

von Hansemann, D., 1890. Ueber asymmetrische Zelltheilung in epithel Krebsen und deren biologische Bedeutung. Virchow's Arch. Path. Anat.

Wan, Y.-W., Allen, G.I., Liu, Z., 2016. TCGA2STAT: simple TCGA data access for integrated statistical analysis in R. Bioinformatics 32, 952–954. https://doi.org/10.1093/bioinformatics/btv677

Wang, F., Zhang, S., Kim, T.-B., Lin, Y., Iqbal, R., Wang, Z., Mohanty, V., Sircar, K., Karam, J.A., Wendl, M.C., Meric-Bernstam, F., Weinstein, J.N., Ding, L., Mills, G.B., Chen, K., 2019. Integrated transcriptomic–genomic tool Texomer profiles cancer tissues. Nature Methods 16, 401–404. https://doi.org/10.1038/s41592-019-0388-9

Wang, K., Li, M., Hakonarson, H., 2010. ANNOVAR: functional annotation of genetic variants from high-throughput sequencing data. Nucleic Acids Res 38, e164–e164. https://doi.org/10.1093/nar/gkq603

Wang, W., Li, Q., Yamada, T., Matsumoto, K., Matsumoto, I., Oda, M., Watanabe, G., Kayano, Y., Nishioka, Y., Sone, S., Yano, S., 2009. Crosstalk to Stromal Fibroblasts Induces Resistance of Lung Cancer to Epidermal Growth Factor Receptor Tyrosine Kinase Inhibitors. Clin Cancer Res 15, 6630–6638. https://doi.org/10.1158/1078-0432.CCR-09-1001

Wang, X., Allen, W.E., Wright, M.A., Sylwestrak, E.L., Samusik, N., Vesuna, S., Evans, K., Liu, C., Ramakrishnan, C., Liu, J., Nolan, G.P., Bava, F.-A., Deisseroth, K., 2018. Three-dimensional intact-tissue sequencing of single-cell transcriptional states. Science eaat5691. https://doi.org/10.1126/science.aat5691

Wang, Z., Gerstein, M., Snyder, M., 2009. RNA-Seq: a revolutionary tool for transcriptomics. Nat Rev Genet 10, 57–63. https://doi.org/10.1038/nrg2484

Wigle, D.A., Jurisica, I., Radulovich, N., Pintilie, M., Rossant, J., Liu, N., Lu, C., Woodgett, J., Seiden, I., Johnston, M., Keshavjee, S., Darling, G., Winton, T., Breitkreutz, B.-J., Jorgenson, P., Tyers, M., Shepherd, F.A., Tsao, M.S., 2002. Molecular Profiling of Non-Small Cell Lung Cancer and Correlation with Disease-free Survival. Cancer Res 62, 3005–3008.

Williams, M.J., Werner, B., Barnes, C.P., Graham, T.A., Sottoriva, A., 2016. Identification of neutral tumor evolution across cancer types. Nat. Genet. 48, 238–244. https://doi.org/10.1038/ng.3489

Wilson, T.R., Fridlyand, J., Yan, Y., Penuel, E., Burton, L., Chan, E., Peng, J., Lin, E., Wang, Y., Sosman, J., Ribas, A., Li, J., Moffat, J., Sutherlin, D.P., Koeppen, H., Merchant, M., Neve, R., Settleman, J., 2012. Widespread potential for growth-factor-driven resistance to anticancer kinase inhibitors. Nature 487, 505–509. https://doi.org/10.1038/nature11249

Wistuba, I.I., Behrens, C., Lombardi, F., Wagner, S., Fujimoto, J., Raso, M.G., Spaggiari, L., Galetta, D., Riley, R., Hughes, E., Reid, J., Sangale, Z., Swisher, S.G., Kalhor, N., Moran, C.A., Gutin, A., Lanchbury, J.S., Barberis, M., Kim, E.S., 2013. Validation of a Proliferation-Based Expression Signature as Prognostic Marker in Early Stage Lung Adenocarcinoma. Clin Cancer Res. https://doi.org/10.1158/1078-0432.CCR-13-0596

Wood, L.D., Parsons, D.W., Jones, S., Lin, J., Sjöblom, T., Leary, R.J., Shen, D., Boca, S.M., Barber, T., Ptak, J., Silliman, N., Szabo, S., Dezso, Z., Ustyanksky, V., Nikolskaya, T., Nikolsky, Y., Karchin, R., Wilson, P.A., Kaminker, J.S., Zhang, Z., Croshaw, R., Willis, J., Dawson, D., Shipitsin, M., Willson, J.K.V., Sukumar, S., Polyak, K., Park, B.H., Pethiyagoda, C.L., Pant, P.V.K., Ballinger, D.G., Sparks, A.B., Hartigan, J., Smith, D.R., Suh, E., Papadopoulos, N., Buckhaults, P., Markowitz, S.D., Parmigiani, G., Kinzler, K.W., Velculescu, V.E., Vogelstein, B., 2007. The Genomic

Landscapes of Human Breast and Colorectal Cancers. Science 318, 1108–1113. https://doi.org/10.1126/science.1145720

Woodard, G.A., Wang, S.X., Kratz, J.R., Zoon-Besselink, C.T., Chiang, C.-Y., Gubens, M.A., Jahan, T.M., Blakely, C.M., Jones, K.D., Mann, M.J., Jablons, D.M., 2018. Adjuvant Chemotherapy Guided by Molecular Profiling and Improved Outcomes in Early Stage, Non–Small-Cell Lung Cancer. Clinical Lung Cancer 19, 58–64. https://doi.org/10.1016/j.cllc.2017.05.015

Wu, Y., Kyle-Cezar, F., Woolf, R.T., Naceur-Lombardelli, C., Owen, J., Biswas, D., Lorenc, A., Vantourout, P., Gazinska, P., Grigoriadis, A., Tutt, A., Hayday, A., 2019. An innate-like Vδ1+ γδ T cell compartment in the human breast is associated with remission in triple-negative breast cancer. Science Translational Medicine 11, eaax9364. https://doi.org/10.1126/scitranslmed.aax9364

Yachida, S., Jones, S., Bozic, I., Antal, T., Leary, R., Fu, B., Kamiyama, M., Hruban, R.H., Eshleman, J.R., Nowak, M.A., Velculescu, V.E., Kinzler, K.W., Vogelstein, B., Iacobuzio-Donahue, C.A., 2010. Distant metastasis occurs late during the genetic evolution of pancreatic cancer. Nature 467, 1114–1117. https://doi.org/10.1038/nature09515

Yap, T.A., Gerlinger, M., Futreal, P.A., Pusztai, L., Swanton, C., 2012. Intratumor Heterogeneity: Seeing the Wood for the Trees. Science Translational Medicine 4, 127ps10-127ps10. https://doi.org/10.1126/scitranslmed.3003854

Yates, L.R., Gerstung, M., Knappskog, S., Desmedt, C., Gundem, G., Van Loo, P., Aas, T., Alexandrov, L.B., Larsimont, D., Davies, H., Li, Y., Ju, Y.S., Ramakrishna, M., Haugland, H.K., Lilleng, P.K., Nik-Zainal, S., McLaren, S., Butler, A., Martin, S., Glodzik, D., Menzies, A., Raine, K., Hinton, J., Jones, D., Mudie, L.J., Jiang, B., Vincent, D., Greene-Colozzi, A., Adnet, P.-Y., Fatima, A., Maetens, M., Ignatiadis, M., Stratton, M.R., Sotiriou, C., Richardson, A.L., Lønning, P.E., Wedge, D.C., Campbell, P.J., 2015. Subclonal diversification of primary breast cancer revealed by multiregion sequencing. Nat Med 21, 751–759. https://doi.org/10.1038/nm.3886

Yeang, C.-H., McCormick, F., Levine, A., 2008. Combinatorial patterns of somatic gene mutations in cancer. FASEB J 22, 2605–2622. https://doi.org/10.1096/fj.08-108985

Yeh, P., Hunter, T., Sinha, D., Ftouni, S., Wallach, E., Jiang, D., Chan, Y.-C., Wong, S.Q., Silva, M.J., Vedururu, R., Doig, K., Lam, E., Arnau, G.M., Semple, T., Wall, M., Zivanovic, A., Agarwal, R., Petrone, P., Jones, K., Westerman, D., Blombery, P., Seymour, J.F., Papenfuss, A.T., Dawson, M.A., Tam, C.S., Dawson, S.-J., 2017. Circulating tumour DNA reflects treatment response and clonal evolution in chronic lymphocytic leukaemia. Nature Communications 8, 14756. https://doi.org/10.1038/ncomms14756

Yoshihara, K., Shahmoradgoli, M., Martínez, E., Vegesna, R., Kim, H., Torres-Garcia, W., Treviño, V., Shen, H., Laird, P.W., Levine, D.A., Carter, S.L., Getz, G., Stemke-Hale, K., Mills, G.B., Verhaak, R.G.W., 2013. Inferring tumour purity and stromal and immune cell admixture from expression data. Nature Communications 4, ncomms3612. https://doi.org/10.1038/ncomms3612

Yu, G., He, Q.-Y., 2016. ReactomePA: an R/Bioconductor package for reactome pathway analysis and visualization. Mol. BioSyst. 12, 477–479. https://doi.org/10.1039/C5MB00663E

Zahir, N., Sun, R., Gallahan, D., Gatenby, R.A., Curtis, C., 2020. Characterizing the ecological and evolutionary dynamics of cancer. Nature Genetics 52, 759–767. https://doi.org/10.1038/s41588-020-0668-4

Zaromytidou, A.-I., 2020. Shaping the future of cancer research at NCI. Nat Cancer 1, 7–11. https://doi.org/10.1038/s43018-019-0017-7

Zhang, A.W., McPherson, A., Milne, K., Kroeger, D.R., Hamilton, P.T., Miranda, A., Funnell, T., Little, N., Souza, C.P.E. de, Laan, S., LeDoux, S., Cochrane, D.R., Lim, J.L.P., Yang, W., Roth, A., Smith, M.A., Ho, J., Tse, K., Zeng, T., Shlafman, I., Mayo, M.R., Moore, R., Failmezger, H., Heindl, A., Wang, Y.K., Bashashati, A., Grewal, D.S., Brown, S.D., Lai, D., Wan, A.N.C., Nielsen, C.B., Huebner, C., Tessier-Cloutier, B., Anglesio, M.S., Bouchard-Côté, A., Yuan, Y., Wasserman, W.W., Gilks, C.B., Karnezis, A.N., Aparicio, S., McAlpine, J.N., Huntsman, D.G., Holt, R.A., Nelson, B.H., Shah, S.P., 2018. Interfaces of Malignant and Immunologic Clonal Dynamics in Ovarian Cancer. Cell 0. https://doi.org/10.1016/j.cell.2018.03.073

Zhang, L., Conejo-Garcia, J.R., Katsaros, D., Gimotty, P.A., Massobrio, M., Regnani, G., Makrigiannakis, A., Gray, H., Schlienger, K., Liebman, M.N., Rubin, S.C., Coukos, G., 2003. Intratumoral T cells, recurrence, and survival in epithelial ovarian cancer. N. Engl. J. Med. 348, 203–213. https://doi.org/10.1056/NEJMoa020177

Zhang, Y., Chen, L., 2016. Classification of Advanced Human Cancers Based on Tumor Immunity in the MicroEnvironment (TIME) for Cancer Immunotherapy. JAMA Oncol 2, 1403–1404. https://doi.org/10.1001/jamaoncol.2016.2450

Zhao, J., Chen, A.X., Gartrell, R.D., Silverman, A.M., Aparicio, L., Chu, T., Bordbar, D., Shan, D., Samanamud, J., Mahajan, A., Filip, I., Orenbuch, R., Goetz, M., Yamaguchi, J.T., Cloney, M., Horbinski, C., Lukas, R.V., Raizer, J., Rae, A.I., Yuan, J., Canoll, P., Bruce, J.N., Saenger, Y.M., Sims, P., Iwamoto, F.M., Sonabend, A.M., Rabadan, R., 2019. Immune and genomic correlates of response to anti-PD-1 immunotherapy in glioblastoma. Nature Medicine 25, 462–469. https://doi.org/10.1038/s41591-019-0349-y

Zhao, J., Zhang, S., Wu, L.-Y., Zhang, X.-S., 2012. Efficient methods for identifying mutated driver pathways in cancer. Bioinformatics 28, 2940–2947. https://doi.org/10.1093/bioinformatics/bts564

Zheng, Y., Bueno, R., 2015. Commercially available prognostic molecular models in early-stage lung cancer: a review of the Pervenio Lung RS and Myriad myPlan Lung Cancer tests. Expert Review of Molecular Diagnostics 15, 589–596. https://doi.org/10.1586/14737159.2015.1028371

Zhu, C.-Q., Ding, K., Strumpf, D., Weir, B.A., Meyerson, M., Pennell, N., Thomas, R.K., Naoki, K., Ladd-Acosta, C., Liu, N., Pintilie, M., Der, S., Seymour, L., Jurisica, I., Shepherd, F.A., Tsao, M.-S., 2010. Prognostic and Predictive Gene Signature for Adjuvant Chemotherapy in Resected Non–Small-Cell Lung Cancer. JCO 28, 4417–4424. https://doi.org/10.1200/JCO.2009.26.4325

Zhu, C.-Q., Pintilie, M., John, T., Strumpf, D., Shepherd, F.A., Der, S.D., Jurisica, I., Tsao, M.-S., 2009. Understanding Prognostic Gene Expression Signatures in Lung Cancer. Clinical Lung Cancer 10, 331–340. https://doi.org/10.3816/CLC.2009.n.045

Zhu, C.-Q., Tsao, M.-S., 2014. Prognostic markers in lung cancer: is it ready for prime time? Transl Lung Cancer Res 3, 149–158. https://doi.org/10.3978/j.issn.2218-6751.2014.06.09